STABLE AND RADIOISOTOPIC CONSTRAINTS ON THE EVOLUTION OF MESOZOIC CARBONATITE-ALKALINE COMPLEXES OF INDIA

A Thesis Submitted to
THE MAHARAJA SAYAJIRAO UNIVERSITY OF BARODA

for

THE DEGREE OF DOCTOR OF PHILOSOPHY

in

GEOLOGY

by

Jyotiranjan Srichandan Ray

PHYSICAL RESEARCH LABORATORY
AHMEDABAD 380 009
INDIA

AUGUST 1997

With Love

To

All Those

Who Care For Me

CERTIFICATE

I hereby declare that the work presented in this thesis is original and has not formed the basis for the award of any degree or diploma by any University or Institution.

Jyotiranjan S. Ray.

Jyotiranjan Srichandan Ray

(Candidate)

Certified by:

Dr. R. Ramesh
(Guide)
Physical Research Laboratory
Ahmedabad 380 009, India.

Dr. P. P. Patel
(Co-Guide)
M. S. University of Boroda
Baroda 390 002, India.

Head, Deptt. of Geology
M. S. University of Boroda
Boroda 390 002, India.

CONTENTS

List of Tables

List of Figures

ACKNOWLEDGMENTS

India is celebrating its fiftieth year of independence, three governments have changed in last five years, Sri Lankans are new world champions in cricket, fossil life form (?) has been found in a Martian meteorite, many of my friends have married and have started populating the country, and I have several grey hairs -it must be time to finish up! What I have been able to achieve in this project has been due to a large part to the support, advice, assistance and encouragement of advisers, colleagues, collaborators and friends. I finally have an opportunity to express my deep sense of gratitude to them all.

I have had the honour and pleasure to be guided by one of the most brilliant, highly dedicated young scientists of India. Dr. R. Ramesh initiated my research career at Physical Research Laboratory and has continued to be supportive. He has provided appropriate advice on a range of subjects and has always been a motivating influence in my work. He taught me more about enquiry and scientific pursuit than any other person in my life. He has tolerated my sloppiness, my sports activities and has been a foundation to my studies throughout. I express my considerable debt of gratitude to him for all he has done for me.

My introduction to isotope techniques was provided, in addition to Dr. Ramesh, by Dr. J. R. Trivedi, Dr. Kanchan Pande, Dr. P. N. Shukla, and Dr. T. R. Venkatesan. Their help, advice, and patience are gratefully acknowledged. I am extremely grateful to Prof. S. Krishnaswami for his constant encouragement and criticism.

I express my sincere thanks to Dr. P. P. Patel of M.S. University, Baroda for his advice on academic and technical matters. I thank Dr. N. Sharma for assistance in field work. I also thank Dr. L. S. Chamyal, Anirudha Khadikar, and other members of the Geology Department of M.S. University for their constant help throughout.

I am grateful to Dr. P. Krishnamurthy, Late Dr. R. K. Srivastava and Mr. S. K. Sengupta for providing me samples from Sung Valley, Samu-Dandali, Mundwara and Samchampi complexes. I sincerely thank Prof. K. Gopalan for allowing me to get a part of my strontium measurements done at NGRI. I also thank Dr. Krishnan Unni and Mr. N. P. Choudhary of GSI, Shillong for their help during my field trip to Meghalaya.

I am thankful to Dr. S. G. Viladkar for giving me a chance to attend the international workshop on carbonatites.

I have had opportunity to work with many other colleagues at PRL who have helped me in numerous ways. Academic advice by Prof. N. Bhandari, Dr. M. M. Sarin, Prof. S. K. Bhattacharya, Dr. S. V. S. Murty, Dr. Sheela Kusumgar and Prof. A. K. Singhvi is gratefully acknowledged. Other technical advice and assistance have been provided by J. T. Padia, R. A. Jani, Rashmi Jadeja, R. Rengarajan, V. G. Shah, A. R. Pandian, P. K. Kurup and K. K. Sivasankaran and library staff. I wish to thank them all. I also thank R. Nambiar for helping me in typing the thesis. Thanks are due to Ratan, Anil, Thomas, Sunil and Mayank for many stimulating scientific discussions and their help during the last stages of the project.

I was lucky to enjoy the friendship of a new spectrum of people during my five years of life at PRL. Ravi, Shravani, Navin, Ramani, Madhusudan, Deshpande, Pranav, Ban, Tarun, Prabir, Manish, Santh, Siva, Shikha, Ghosh, Nandu, Kunu and a whole host of others too numerous to mention, have helped me in several ways in the course of my study.

My parents continue to be an anchor of stability and support in my studies and my life. I am deeply grateful to them.

ABSTRACT

In this thesis I present the stable and radioisotopic study of six Mesozoic carbonatite-alkaline complexes of India. (Amba Dongar, Mundwara and Sarnu-Dandali complexes of Deccan Flood Basalt Province, and Sung Valley, Samchampi and Swangkre of Assam-Meghalaya Plateau). This work is aimed at understanding the nature of mantle source regions, origin and evolution of carbonatites in general and the Mesozoic Indian complexes in particular. The geochemical tracers used for this purpose are stable carbon and oxygen isotopes, strontium isotopes and trace elements. In order to find out the emplacement ages of two of these complexes (Amba Dongar and Sung Valley), I have used ^{40}Ar-^{39}Ar method of dating. Theoretical models have also been developed to understand the isotopic and trace element effects generated by different magmatic and postmagmatic processes such as liquid immiscibility, crustal contamination, fractional crystallization and secondary alteration in carbonatites and associate alkaline rocks.

The results of this study revealed some important facts about the carbonatite-alkaline magmatism in general. I got an evidence for incorporation of recycled crystal carbon in carbonatites. Such a conclusive evidence was not available before because of the difficulty in deciphering the primary carbon isotopic composition of the carbonatite magma. Spatial and temporal relationship, and Sr isotopic ratios suggest that carbonatites and alkaline rocks are genetically related. This work also revealed that liquid immiscibility is probably the underlying process in generating carbonatites and associated silicate rocks. Modelling the effects of combined liquid immiscibility, fractional crystallization and crustal contamination, on strontium isotope systematics, I found that the carbonatites do not preserve the effects of crustal contamination, whereas alkaline rocks do. Rare earth element study in Amba Dongar complex also supports the generation of carbonatites and associated alkaline rocks by liquid immiscibility. Stable carbon and oxygen isotopic study of carbonatites revealed that the $\delta^{13}C$ and $\delta^{18}O$ variations of uncontaminated and unaltered carbonatites are a result of fractional crystallization of these rocks from fluid rich magmas. A theoretical model

has been developed in this work to treat C and O isotopic fractionation during such a process.

Amba Dongar and Sung Valley complexes have been dated to 65.0 Ma and 107.0 Ma, respectively These ages along with their Sr isotopic ratios suggest their derivation from Reunion and Kerguelen plumes, respectively. Stable isotopic studies in the three carbonatite-alkaline complexes of Deccan province suggest that these complexes were derived from isotopically average mantle except a particular group of calcite carbonatites of Amba Dongar, which shows evidence of incorporation of recycled crustal carbon. The strongest evidence of this kind of incorporation comes from the $\delta^{13}C$ and $\delta^{18}O$ values of the primary magmas for the complexes of Assam-Meghalaya Plateau. Extreme variations of $\delta^{13}C$ and $\delta^{18}O$ of carbonatites in all the complexes have been found to be a result of low temperature alteration processes involving CO_2 bearing aqueous fluids.

CHAPTER I

INTRODUCTION

Rocks derived from Earth's mantle and exposed on the crust allow us to learn about the mantle, its properties, physico-chemical processes occurring therein and its evolution thorough time. Carbonatites are such mantle derived rocks. Though carbonatites represent <1% of all the magmatic rocks, they have attracted much attention because of their unusual physical and chemical properties. These are carbonate rich (>50 wt%) rocks characterized by high abundances of Sr, Ba, Zr, Nb, Th and rare-earth elements (Barker, 1996). These have been observed both in continental and oceanic plates, and occur in various types of tectonic settings. Continental carbonatites are commonly associated with alkaline (nephelinitic/kimberlitic) igneous provinces. Except the Na-rich carbonatites of Oldoinyo Lengai (an active carbonatite volcano, Tanzania), all the carbonatites of the world are Ca-rich carbonatites.

Being rich in carbonates, carbonatites are probably the best samples to study the mantle carbon inventory. Apart from this, the study of carbonatites and associated alkaline rocks can give important clues to many mantle and crustal processes such as melt extraction, recycling of crustal material, mantle metasomatism, mantle degassing, and silicate-carbonate liquid immiscibility. The present work focuses on six Mesozoic carbonatite-alkaline complexes of India. Specifically, the results obtained from stable and radioisotopic studies carried out in these complexes are presented and discussed with an aim to contribute to a better understanding of their mantle source regions and the evolution of the rocks present in these complexes through time.

1.1. CARBONATITES AND ALKALINE ROCKS

1.1.1. General Features

Carbonatites rarely occur in isolation and except a few cases, where these are associated with kimberlites (e.g., Saltpetre Kop and Premier Mine, South Africa), are almost always associated with silica-undersaturated nephelinitic rocks (LeBas, 1984). Carbonatite-alkaline complexes usually occur in continents and rarely in oceanic plates

(e.g., Cape Verde and Canary Islands; LeBas, 1984) and have been observed in association with rift valleys, major faults, fold belts and plate margins (Woolley, 1989). Most of the carbonatite-alkaline complexes display oval or semicircular outline in a plan view, alkaline rocks constituting more than eighty percent of the total volume. Different lithological units in these complexes may be related either to their erosion level or their emplacement level within the crust (Santos and Clayton, 1995). Hence, carbonatite alkaline complexes may show characteristics of deep-seated plutons or subvolcanic intrusions or volcanic provinces. Fenitization of country rocks is a common feature around the carbonatites in all carbonatite complexes.

Carbonatites, by definition, are igneous rocks, which contain more than 50% by weight of carbonate minerals. If the carbonate is calcite, the rock is a calcite-carbonatite. Dolomite-carbonatite or beforsite is a carbonatite with dolomite as the major carbonate mineral. Ferrocarbonatite is essentially composed of iron-rich carbonate minerals (ankerite, siderite etc.). Natrocarbonatite, only found as an extrusive product, is composed of sodium-potassium, calcium carbonates. Carbonatites which have mixtures of different carbonate minerals are commonly named according to the established rules for quantitative composition of rocks at the 10-50-90% boundaries (Woolley and Kempe, 1989). In absence of modal analysis, chemical analysis can be used to name a carbonatite. If [CaO] : [CaO + MgO + FeO + Fe_2O_3 + MnO] is greater than 0.8, then the rock is a calciocarbonatite; if it is less than 0.8 and [MgO] > [FeO + Fe_2O_3 + MnO] it is a magnesiocarbonatite, but if [MgO] < [FeO + Fe_2O_3 + MnO] it is a ferrocarbonatite (Woolley and Kempe, 1989).

The alkaline rocks of carbonatite complexes are generally olivine-poor nephelinites and phonolites or their plutonic equivalents. Sometimes these rocks can be very diverse in their composition in a given complex and may show effects of fenitization as a result of carbonatite emplacement.

1.1.2. Origin of Carbonatites

The origin of carbonatite-alkaline complexes is still a matter of debate. Several scenarios have been proposed to explain this. In general, these hypotheses attribute the

formation of carbonatites to: (1) direct partial melting of mantle (Green and Wallace, 1988; Dalton and Wood, 1993; Sweeney, 1994); (2) fractional crystallization of carbonated silicate melts (Wyllie, 1987); or (3) carbonatite-silicate liquid immiscibility (LeBas, 1977; Kjarsgaard and Hamilton, 1989). Studies (field as well as experimental) have shown that none of the scenarios can uniquely explain the formation of carbonatites observed in nature. The hypothesis of direct melt, although explains many usual properties of carbonatites, fails to explain the observed association of alkaline silicate rocks with the carbonatites. Liquid immiscibility may be the most important mechanism for the evolution of carbonatites and alkaline rocks but laboratory experiments to test this hypothesis although demonstrate that the carbonatite and silicate magmas are immiscible, do not necessarily prove that they are of a common parentage (Gittins, 1989).

1.1.3. Mantle Source Regions

The question regarding the nature of mantle source regions of carbonatites has been mainly addressed by the study of radiogenic isotope systematics (Rb-Sr, Sm-Nd and U-Th-Pb). As the carbonatites are highly enriched in Sr, Nd and Pb relative to the crust, the isotopic ratios involving these elements are relatively insensitive to the crustal contamination and hence the isotopic ratios must reflect those of the mantle source regions. Most isotopic studies of Sr, Nd and Pb in carbonatites younger than 200 Ma have shown that the data generally plot in the fields of ocean island basalts (OIB) in isotope correlation diagrams. (Fig.1.1 and Fig.1.2) (Bell et al., 1982; Bell and Blenkinsop, 1987; Nelson et al., 1988; Kwon et al., 1989; Tilton and Bell, 1994) and carbonatites older than 2.0 Ga show signatures of a much more depleted mantle (Barker, 1996) (Fig.1.2). In particular, Tilton and Bell (1994) showed that younger carbonatites (< 200 Ma), in a plot of initial $^{87}Sr/^{86}Sr$ versus $^{206}Pb/^{204}Pb$ (Fig.1.3) fall in an array between EMI and HIMU mantle end-members reflecting the enriched nature of their source regions and older carbonatites (between 0.2 Ga and 2.0 Ga) show trends of increasing diversity and more highly radiogenic sources (Barker, 1996) (Fig.1.3). In an earlier study Bell and Blenkinsop (1987) had proposed lithospheric origin for the carbonatites and later Barreiro and Cooper (1987) proposed a metasomatized lithospheric mantle as the source region of carbonatites.

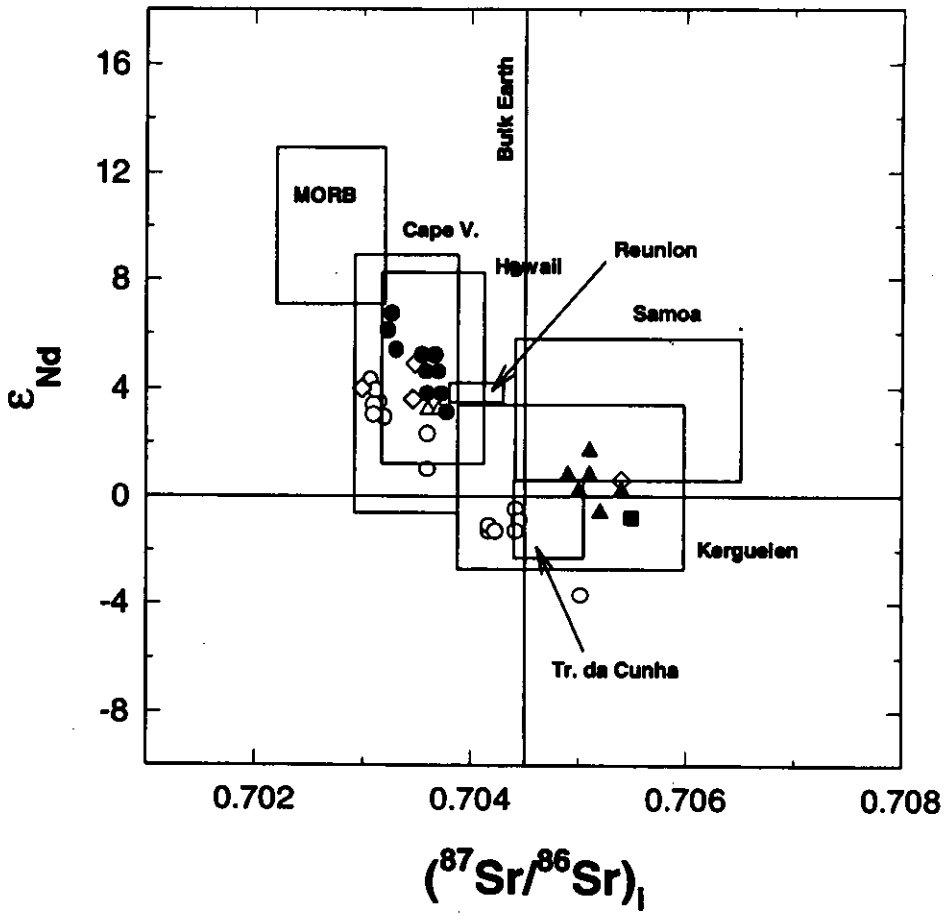

Fig. 1.1. *ε_{Nd} (T) versus initial $^{87}Sr/^{86}Sr$ for young (<200 Ma) carbonatites compared with the fields of MORB and OIBs. The ε_{Nd} (T) values were calculated using: $^{143}Nd/^{144}Nd$ = 0.512638, and $^{147}Sm/^{144}Nd$ = 0.1967. MORB and OIB data are from Rollinson, (1993) -a compilation. Carbonatite data are from Bell and Blenkinsop (1989) and Simonetti et al. (1995). Symbols: open circles = African carbonatites; open diamonds = Australian and New Zealandian carbonatites; open triangle = European carbonatites; filled square = Amba Dongar carbonatite, India; and filled triangle = South American carbonatites.*

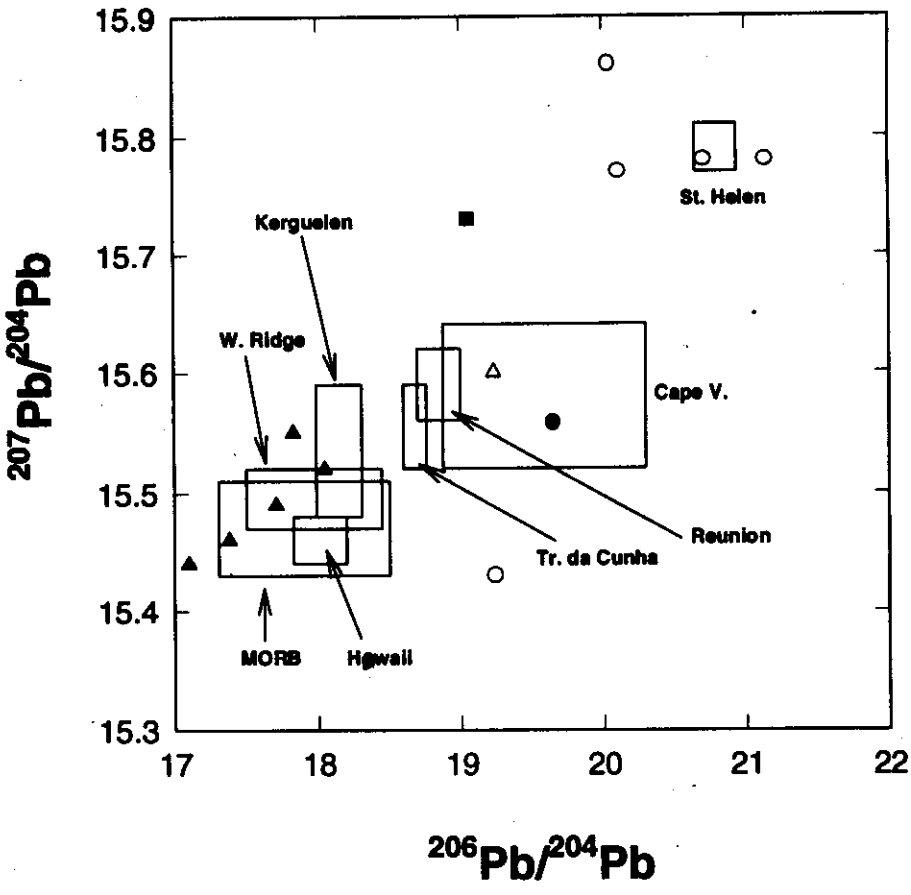

Fig. 1.2. *$^{206}Pb/^{204}Pb$ - $^{207}Pb/^{204}Pb$ correlation diagram for carbonatites with ages less than 200 Ma from different continents compared with fields of MORB and OIBs. Each datum point represents a single complex. Symbols are same as in Fig. 1.1. MORB and OIB data from Sun (1980); Richardson et al. (1982); and Rollinson (1993) -a compilation. Carbonatite data sources: Nelson et al. (1988); Toyoda et al. (1994); and Simonetti et al. (1995).*

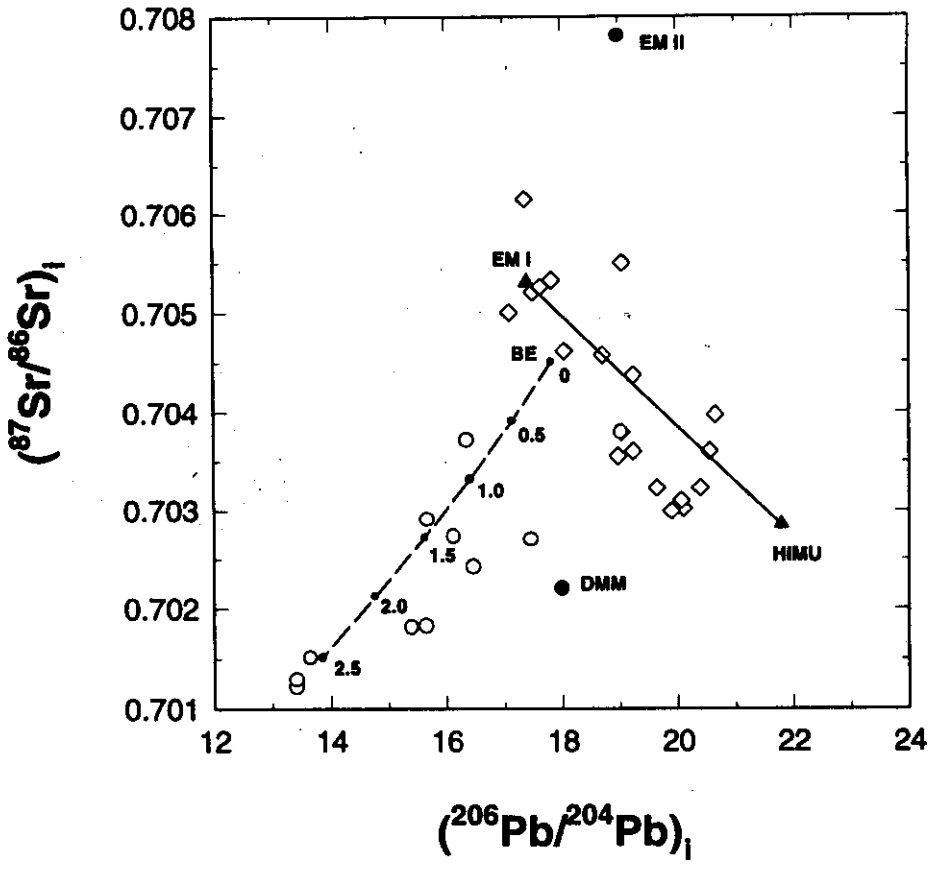

Fig. 1.3. *Initial $^{87}Sr/^{86}Sr$ versus initial $^{206}Pb/^{207}Pb$ for carbonatites plotted with different mantle-source end-members (EM I = Enriched Mantle I, EM II = Enriched Mantle II, HIMU = High μ mantle, and DMM = Depleted MORB Mantle) as defined by Hart et al. (1992). Symbols: open diamond = carbonatites with ages < 200 Ma; and open circle = carbonatites with ages between 200 Ma and 2.7 Ga. Solid curve is a hypothetical mixing curve between EM I and HIMU and dashed curve is the Bulk Earth (BE) evolution curve of Kwon et al. (1989) which is labeled with age in Ga. Data Source: Barker (1996).*

However, increasing evidence from younger carbonatites, particularly from Pb isotope systematics, suggests an asthenospheric origin for these rocks (Nelson et al., 1988; Kwon et al., 1989). At this juncture, with the available data, it is difficult to decipher exactly whether carbonatites are lithospheric melts or asthenospheric melts.

Earlier it was believed that carbonatites remove the juvenile carbon that is locked inside the earth's mantle. However, more and more evidence has been accumulating that the crustal carbon is recycled into the mantle through subduction and this recycled carbon may feed the carbonatite magmas (Nelson et al., 1988; Hauri et al. 1993; Barker, 1996). The process by which mantle carbon gets incorporated into the carbonatite is not clearly understood. Stable carbon and oxygen isotopic compositions have been used to understand such processes and to characterize the source regions of carbonatite magma. The observed variation of $\delta^{13}C$ in carbonatites does not clearly indicate the involvement of recycled material in the formation of carbonatite magma (Barker, 1996). This is probably because the initial mantle isotopic signature gets modified during and after the emplacement of carbonatite magma by 'magmatic' and 'secondary alteration' processes. Barker (1996) suggests that the observed $\delta^{13}C$ variation is a result of a multi-step process involved (from subducted crust to solidified carbonatite) in the generation of carbonatite magma. However, most authors believe that with proper identification of the isotopic effects generated by different processes, one can find out the isotopic composition of the source region and the signatures (if any) of the recycled carbon.

1.2. INDIAN CARBONATITE-ALKALINE COMPLEXES

The carbonatite complexes of India have been reviewed by Sukheswala and Viladkar (1978) and Krishnamurthy (1988). These complexes (about 18 in number) occur in five distinct structural regimes (Fig. 1.4) associated with major rift systems and fold belts (Krishnamurthy, 1988). With the present chronological status, these complexes can be broadly grouped into two: (1) Precambrian carbonatites, all of which, except Newania, are present in the southern Indian Craton (Fig. 1.4); (2) Mesozoic carbonatites, which are present in the Deccan flood basalt province in the west and in the Assam-Meghalaya plateau in the east. Apart from the established carbonatite complexes (those shown in Fig. 1.4), there have been reports of small carbonatite occurrences (Ghosh Roy and Sengupta, 1993; Ramaswamy, 1996) from different parts of the country, but these have not yet been rigorously proved to be carbonatites.

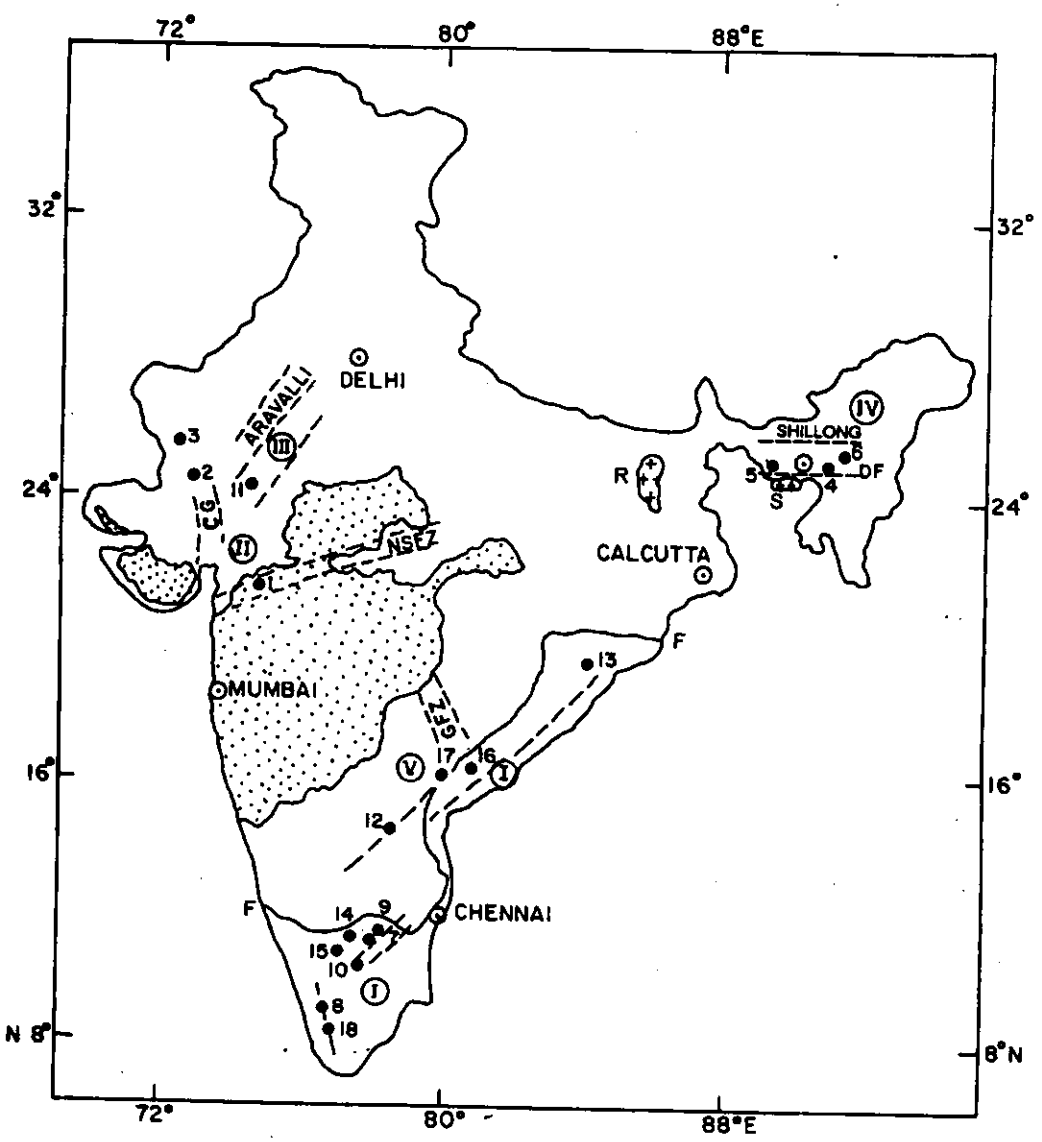

Fig. 1.4. *Map of India showing the approximate locations of carbonatite-alkaline complexes (solid circles) and the extent of Deccan Traps (dotted region); Rajmahal (R) and Sylhet Traps (S) (area marked with crosses). The five structural regimes of Krishnamurthy (1988) are : (I) Eastern Ghat Belt; (II) Narmada-Son Fracture Zone (NSFZ) and Cambey Graben (CG); (III) Aravalli; (IV) Dauki Fault System (DF); and (V) Godavari Fracture Zone (GFZ). F-F : charnokite- non charnokite boundary. Carbonatite complexes are numbered in the sequence as they appear in Table 1.1. (Figure modified from Krishnamurthy, 1988).*

Except Newania carbonatite of Rajasthan and Khambamettu carbonatite of Tamil Nadu, all other carbonatites of India are associated with alkaline silicate rocks. Chelima carbonatite of Andhra Pradesh is the only Indian carbonatite which is associated with Kimberlite (Sen and Rao, 1967). The nature of magmatism in Indian carbonatites varies from volcanic to plutonic. Most of the Mesozoic carbonatite alkaline complexes have volcanic to subvolcanic rock associations, whereas all the Precambrian complexes show plutonic rock associations. Calcite carbonatite is the major variety of carbonatite in all the Indian complexes except the Newania complex, where dolomite carbonatite is the major variety. Ferrocarbonatites and dolomite carbonatite are minor in many of these complexes. The nature of fenitization, like other carbonatite complexes of the world, varies from potassic to sodic depending on the depth of intrusion of these complexes. Table 1.1 gives a list of all the carbonatite complexes of India, their emplacement ages, types of carbonatite found in them, associated alkaline rocks and types of fenites observed along with the references from which these information have been taken.

Table 1.1. Indian Carbonatite Alkaline Complexes

Locality	Age (Ma)	Type of Carbonatite	Associated Alkaline Rocks	Type of fenite	References
Amba Dongar, Gujarat (1)	65[1]*	Calciocarbonatite and Ferrocarbonatite	Tinguaite, Nephelinite, and Phonolitic-Nephelinite	Sodic and Potassic	Viladkar, 1981; Srivastava, 1994
Mundwara, Rajasthan (2)	68.5[1]	Calcio-carbonatite	Pyroxenite, Alkaline Gabbro, and Syenite	Potassic	Subrahmanyam and Leelanandam, 1989, 1991; Basu et al., 1993
Sarnu-Dandali, Rajasthan (3)	68.5[1]	Calciocarbonatite and Ferrocarbonatite	Pyroxenite, Syenite, Ijolite, and Nephelinite	Sodic	Chandrasekaran et al., 1990; Basu et al., 1993

contd.

Sung Valley, Meghalaya (4)	107[1]*	Calciocarbonatite and Magnesio-carbonatite	Alkali peridotite, Pyroxenite, Ijolite, and Uncompahgrite	Sodic and Potassic	Krishnamurthy, 1985
Swangkre, Meghalaya (5)	equival-ent of Sung Valley	Calciocarbonatite	Ijolite and Lamprophyre	---	Nambiar and Golani, 1985
Samchampi, Assam (6)	,,	Calciocarbonatite, Magnesio-carbonatite	Pyroxenite, Melteigite, and Syenite	Potassic	Kumar et al., 1989
Samalpatti, Tamil Nadu (7)	700[3]	Calciocarbonatite, Magnesio-carbonatite	Dunite, Pyroxenite, and Syenite	Sodic and Potassic	Moralev et al., 1975; Viladkar and Upendran, 1978
Munnar, Kerala (8)	740[2]	Calciocarbonatite	Alkali granite and syenite	----	Santosh et al., 1987
Sevattur, Tamil Nadu (9)	770[2]	Calciocarbonatite, Magnesio-carbonatite	Pyroxenite and Syenite	Soda-potassic	Kumar & Gopalan, 1991
Pakkanadu, Tamil Nadu (10)	771[3]	Calcio-carbonatite	Dunite, Pyroxenite, and Syenite	Sodic	Moralev et al., 1975; Krishnamurthy, 1988
Newania, Rajasthan (11)	959[3]	Magnesio-carbonatite and Ferrocarbonatite	None	Sodic	Deans and Powell, 1968
Chelima, Andhra Pradesh (12)	1340[2]	Calcio-carbonatite	Kimberlite	----	Crawford, 1969; Sen and Rao, 1967
Hogra, Andhra Pradesh (13)	1490[2]	Calcio-carbonatite	Pyroxenite and Syenite	----	Raman and Viswanathan, 1977

contd.

Hogenakal, Tamil Nadu (14)	1990[2]	Calcio-carbonatite	Pyroxenite and Syenite	Sodic	Srinivasan, 1978; Natrajan et al., 1994
Kollegal, Karnataka (15)	----	Calcio-carbonatite	Pyroxenite and Syenite	----	Krishnamurthy, 1988
Kunavaram, Andhra Pradesh (16)	----	----	Syenite	----	Bose et al., 1976
Elchuru, Andra Pradesh (17)	----	----	Syenite	----	Bose et al., 1976
Khambamettu, Tamil Nadu (18)	----	Calcio-carbonatite	None	----	Balakrishanan et al., 1985

1= ^{40}Ar-^{39}Ar plateau ages; 2= Rb-Sr isochron ages; 3= K- Ar ages; and *= this work

Like many other carbonatites of the world, the origin of Indian carbonatites is also not clearly understood. In most complexes, fractional crystallization of a carbonated silicate magma or silicate-carbonate liquid immiscibility was believed to be responsible for the generation of carbonate magma (Krishnamurthy, 1988). In the case of Newania, absence of associated alkaline rocks led to the proposal of a dolomitic primary melt hypothesis for this complex (Krishnamurthy, 1988). Most of the carbonatites of Eastern Ghat mobile belt are suspected to have been affected by metamorphism, hence are not believed to bear the original magmatic signatures (Krishnamurthy, 1988).

Isotopic investigations on Indian carbonatite alkaline complexes are preliminary in nature and are available only for seven complexes; Amba Dongar (Simonetti et a., 1995), Sarnu-Dandali and Mundwara (Sarkar and Bhattacharya, 1992; Basu et al., 1993), Sung Valley (Krishna et al., 1991), Hogenakal (Natarajan et al., 1994), Sevettur (Kumar and Gopalan, 1991) and Newania (Deans and Powell, 1968). None of the above papers reports detailed study of stable carbon and oxygen isotopes in

carbonatites and associated rocks. In the case of Sarnu-Dandali and Mundwara, the radioisotopic studies (Sr and He) are confined only to the alkaline rocks (Basu et al., 1993). Amba Dongar is the only complex whose Sr, Nd and Pb isotopes (only for carbonatites) have been studied in detail by Simonetti et al. (1995). Stable carbon and oxygen isotopic data from Sarnu-Dandali, Mundwara and Amba Dongar (Sarkar and Bhattacharya, 1992; Simonetti et al., 1995) essentially show magmatic nature of these carbonatites and the extreme variation of $\delta^{13}C$ and $\delta^{18}O$ observed in these complexes has been attributed to low temperature alteration processes. In a Sr-evolution diagram (Fig. 1.5; initial $^{87}Sr/^{86}Sr$ versus age plot), it can be seen that the initial $^{87}Sr/^{86}Sr$ in Indian carbonatites becomes increasingly radiogenic towards younger ages, an observation true for most carbonatites of the world in general (Nelson et al., 1988; Tilton and Bell, 1994; Barker, 1996). Two Precambrian carbonatites (Newania and Hogenakal) have lower initial $^{87}Sr/^{86}Sr$ than that of the bulk-earth, which probably suggests that these complexes were derived from depleted mantle sources. The Mesozoic carbonatites (Sung Valley, Sarnu-Dandali, Mundwara and Amba Dongar) have higher initial $^{87}Sr/^{86}Sr$ than that of the bulk earth indicating their derivation from enriched mantle sources. This observation is consistent with the hypothesis of plume origin of the complexes (Basu et al., 1993; Sen, 1995; Ghose et al., 1996), which will be discussed in detail in the next chapter. The initial $^{87}Sr/^{86}Sr$ of Sevattur complex has also been interpreted as a signature of an enriched mantle (Kumar and Gopalan, 1991). By studying Sr, Nd and Pb isotope systematics of Amba Dongar carbonatites Simonetti et al. (1995) suggested an LREE enriched mantle source for this complex (possibly an EMII type of mantle) and speculated that probably this complex was genetically related to the Reunion-Deccan plume, which was responsible for Deccan flood basalt eruption. In a preliminary study of Sr-Nd-Pb isotopes in Sung valley carbonatites, Krishna et al., (1991) found signatures of DUPAL anomaly in carbonatites, a property of present day Indian Ocean OIBs. This possibly indicates a OIB source derivation for this complex.

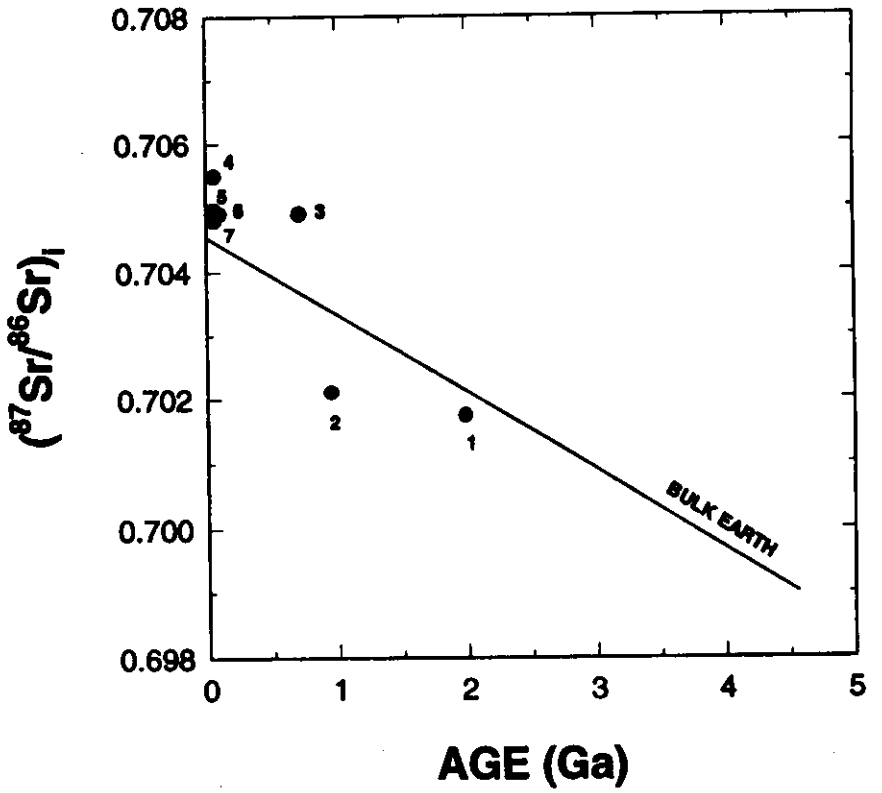

Fig. 1.5. Plot of minimum initial $^{87}Sr/^{86}Sr$ versus age for Indian carbonatites. 1 = Hogenakal, Natarajan et al. (1994); 2 = Newania, Deans and Powell (1968); 3 = Sevattur, Kumar and Gopalan (1991); 4 = Amba Dongar, Simonetti et al. (1995); 5 = Sarnu-Dandali and 6 = Mundwara, Basu et al. (1993); and 7 = Sung Valley, this study. Straight line is Bulk-Earth evolution line from Bell and Blenkinsop (1989).

1.3. PURPOSE OF THIS STUDY

In the geologic history of India, Cretaceous period had remained eventful. In the Early Cretaceous India got separated from Australia and Antarctica with the initiation of Kerguelen hot spot, which generated Rajmahal Traps in eastern India. Towards the end of Cretaceous, Reunion hot spot got activated and generated the voluminous flood basalts of Deccan. Deccan and Rajmahal Traps are major constituents of two Large Igneous Provinces (LIP), which also include numerous minor acidic, alkaline and carbonatitic igneous complexes (Coffin and Eldholm, 1994). The Mesozoic carbonatite-alkaline complexes of India, which are present in these LIPs, are also

hypothesized to have been generated by Kerguelen-Rajmahal and Reunion-Deccan plumes (Kent et al., 1992; Basu et al., 1993; Sen, 1995). This hypothesis of plume origin makes the study of the Mesozoic carbonatite complexes very important. I took up the study of six of these complexes (Amba Dongar, Mundwara and Sarnu-Dandali of Deccan Province and Sung Valley, Samchampi and Swangkre of Assam-Meghalaya Plateau).

In an attempt to characterize the source regions of the carbonatite alkaline complexes and to understand the origin and evolution of these, I used different tracers such as stable carbon and oxygen isotopes, strontium isotopes and trace elements. To find out the emplacement age of some of the complexes, I used ^{40}Ar-^{39}Ar method of dating. The main objectives of this work were to:

1. Establish the temporal relationship of these complexes with the plume originated Deccan and Rajmahal flood basalts.
2. Characterize the source regions on the basis of stable carbon and oxygen and strontium isotopes and confirm the hypothesized link between the Reunion and Kerguelen hotspots and the generation of these complexes.
3. Assess the role of different magmatic processes like partial melting, liquid immiscibility, crustal contamination and fractional crystallization in the generation of these complexes.
4. Distinguish primary (magmatic) and secondary stable carbon and oxygen isotopic variations in carbonatites by theoretically modelling them and apply these models to the observed data from Indian complexes in order to test the models and to understand the isotopic evolution of these complexes.

From the experimental point of view, analysis of C and O isotopes in the various carbonate constituents of carbonatites was difficult (as physical separation was almost impossible). In order to make this possible, I developed an appropriate experimental procedure by which CO_2 from different carbonate minerals could be chemically separated without significant mixing.

For this work, three major field trips to the study areas were undertaken and samples of carbonatites, alkaline rocks, metasomatic rocks and country rocks were collected, details of which are given in Chapter-III.

1.4. OUTLINE OF THE THESIS

This thesis is divided into five chapters. Chapter-I gives an introduction to carbonatites and a brief discussion about their origin and the nature of their mantle source regions, based on earlier studies. It also introduces the carbonatite-alkaline complexes of India. The objectives and the outline of the thesis are also given in this chapter. Chapter-II gives an overview of the geology of Mesozoic carbonatite-alkaline complexes of India on which the present work is based. It also briefly reviews the existing studies on these complexes. Chapter-III describes the experimental techniques used to study the isotopic ratios and trace elemental abundances in samples of carbonatites, alkaline rocks and other country rocks from the above mentioned complexes. These techniques include stable carbon and oxygen isotope analysis; strontium isotope ratio measurements by thermal ionization mass spectrometry (TIMS) ^{40}Ar-^{39}Ar dating technique; and trace elemental abundance measurements by instrumental neutron activation analysis (INAA). In this chapter the step-wise CO_2 extraction procedures developed for carbonate mixtures are also discussed. Following these procedures CO_2 from pure carbonate end-members was collected for C and O isotope ratio determinations. In Chapter-IV, I present and discuss the results of this work. Finally in Chapter-V, I summarize the ideas developed, from the present work, on the formation and evolution of carbonatites in general and the Mesozoic carbonatite-alkaline complexes of India in particular.

CHAPTER II

GEOLOGY AND EARLIER WORK

The Mesozoic carbonatite-alkaline complexes taken up for this study include Amba Dongar, Mundwara and Sarnu-Dandali of Deccan flood basalt province, western India and Sung Valley, Samchampi, and Swangkre of Assam-Meghalaya plateau, eastern India (Fig. 1.4). In this chapter, the geology of these regions is described and the earlier work is reviewed.

2.1. GENERAL FEATURES OF MESOZOIC INDIAN CARBONATITE -ALKALINE COMPLEXES

A brief review of the geology of the carbonatite-alkaline complexes mentioned above is available in Krishnamurthy (1988). The emplacement ages of these complexes were estimated to be falling in the range 65 Ma to 156 Ma (Basu et al., 1993; Deans et al., 1973; Chattopadhyay and Hashimi, 1984; Krishna et al., 1991) prior to the present work. The origin of Amba Dongar, Mundwara and Sarnu-Dandali complexes, which are present within the Deccan Flood Basalt Province, has been linked to the Reunion-Deccan plume which generated the massive flood basalts over Indian subcontinent (Basu et al., 1993; Sen, 1995). Eastern Indian carbonatite complexes (Sung Valley; Samchampi; Swangkre) are thought to be related to the Kerguelen plume activity, which caused the volcanism of Rajmahal Traps, Bengal basin basalts and Sylhet traps on the eastern margin of Indian subcontinent (Kent et al., 1992). All these Mesozoic complexes are associated with major fracture zones (Fig. 1.4).

Most of the complexes, discussed here, display oval or semicircular outlines in plan view. They usually intrude into Precambrian gneisses, granites, metasedimentary rocks and in Amba Dongar into Deccan basalts as well. Rocks of many complexes, eastern region carbonatites in particular, are poorly exposed because of thick soil/alluvium cover in these regions. The alkaline silicate rocks comprise the major part in all these complexes. These consist of dominantly alkali pyroxenites, ijolites, and syenites except in Amba Dongar, where tinguaites, nephelinites and phonolites are predominant. Carbonatites comprise only a minor part of these complexes, barring the Amba Dongar

where they form ~20% of the whole complex. Calcite-carbonatites are the major carbonatites in all these complexes, whereas ferrocarbonatites and dolomite-carbonatites are minor in occurrence. Carbonatites show a variety of intrusive forms like ring dykes, dykes, sills, cone sheets and veins. Fenitization of country rocks is a common feature in all these complexes and both potassic and sodic fenites have been observed.

2.2. THE AMBA DONGAR COMPLEX

2.2.1. Regional Geology and Field Relations

The Amba Dongar carbonatite-alkaline complex is the first carbonatite complex to be identified in India (Sukheswala and Udas, 1963). This complex is located 2 km north of Narmada river in Baroda district of Gujarat state and is a part of a large carbonatite-alkaline province of Chhota Udaipur (Sukheswala and Viladkar, 1978). The rocks of this complex intrude into the 955 Ma old gneisses (Gopalan et al., 1979), Cretaceous Bagh sediments (sandstones and limestones) and some earlier flows of Deccan tholeiites. It was believed that this complex intruded late in the Deccan trap magmatism (Deans and Powell, 1968), however, there was no accurate age data available in support of this hypothesis.

This complex is present within the Narmada-Son rift zone (Fig. 1.4) and inside the complex the magmatic activity seems to have followed the local fault patterns as majority of dykes are aligned along these (Viladkar, 1984). The complex is characterized by concentric ring dykes of calcite-carbonatite (sovite of Viladkar, 1981) and carbonatite breccia with tholeiitic basalt in the central depression. The alkaline rocks are present as plugs and dykes in the low surrounding areas of the main carbonatite dome and are exposed at places inside the ring dyke (Fig. 2.1). Ferrocarbonatites (ankerite-carbonatites of Viladkar, 1981) occur as small plugs in the ring dyke in the southern part of the complex (Fig. 2.1). The carbonatites of this complex host a massive fluorite deposit. Extensive fenitization of the country rock sandstones is the most striking feature of this complex.

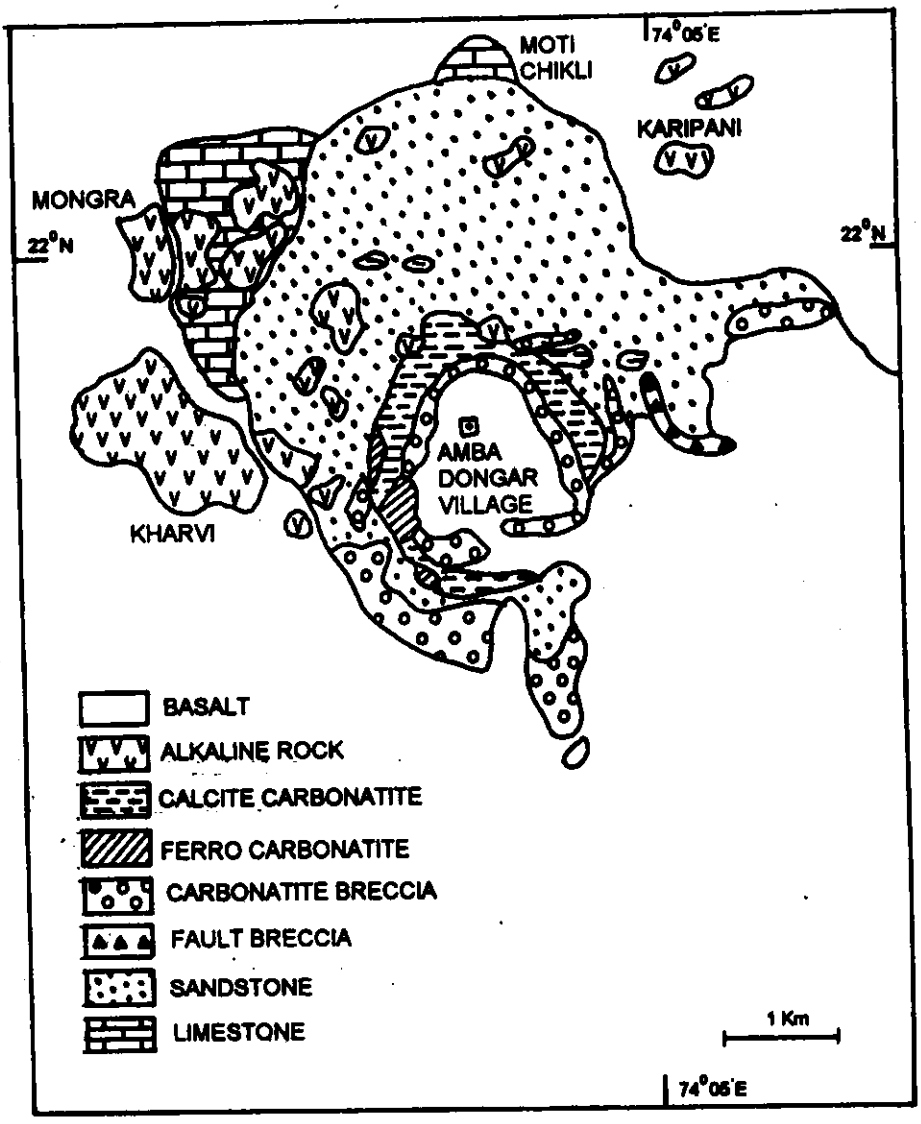

***Fig. 2.1.** Geological map of Amba Dongar carbonatite-alkaline complex modified from Viladkar, 1981.*

2.2.2. Alkaline Silicate Rocks

Alkaline silicate rocks of Amba Dongar have been identified as tinguaite, phonolite/phono-nephelinite and syenite/nepheline-syenite (Viladkar, 1984; Srivastava, 1994). These rocks occupy most of the hill tops surrounding the carbonatite ring dyke. Mineralogically, these rocks have nepheline, aegirine-augite and melanite-garnet as phenocrysts while ground mass contains analcite and calcite (Srivastava, 1994). Phonolitic nephelinities have, apart from above minerals, alkali feldspars as phenocrysts (Viladkar, 1984). Chemically, most of these rocks have been classified as foidites and basanites (Srivastava, 1994). From trace and rare earth elemental studies it was found that Sr and REE content in alkaline rocks are smaller compared to the associated carbonatites (Viladkar, 1984; Viladkar and Dulski, 1986). By studying trace elements in growth zones of pyroxenes from these rocks, Rock et al. (1994) found that the pyroxenes reflect disequilibrium effect, which according to them, is due to rapid growth or fast cooling of these minerals. There is no report of isotopic data on these rocks.

2.2.3. Carbonatites

Carbonatites of this complex are mainly of two types, calcite-carbonatites and ferrocarbonatites. As mentioned earlier, calcite-carbonatites form a large ring dyke into which ferrocarbonatites intrude as small plugs (Fig. 2.1). The carbonatite breccia, which forms the innermost ring of the dyke, contains xenoliths of older rocks (gneisses; basalts; sandstones). Apart from dykes and plugs, numerous calcite carbonatite and ferrocarbonatite veins are present within the massive calcite carbonatites all over the complex. Calcite carbonatites of Amba Dongar are coarse to fine grained rocks, in which the most common minerals are calcites (>70%), magnetites and apatites. Accessory minerals include fluorites, barites, pyrochlores and zircons. Sometimes they also contain phlogopites, particularly the carbonatite veins. It has been observed that there are two generations of calcite-carbonatites, an early coarse grained variety and a late medium to fine grained variety which usually carries the earlier phase as xenoliths (Viladkar and Wimmenauer, 1992). Ferrocarbonatites are fine grained dark red coloured carbonatites in which ankerite is the major carbonate mineral. In many instances, ankerites were found to have been oxidized giving rise to

iron oxides. Calcite in ferrocarbonatites is present up to 40%. Other minerals include apatite, barite, magnetite, pyrochlore, bastenite, cerite, monazite and some sulphides. These rocks are invariably altered and have lots of microcrystalline silica and in many instances, are affected by fluorite mineralization.

Major elemental analyses of these rocks by Viladkar and Wimmenauer (1992) show that the calcite carbonatites have ~50% CaO and ~2% MgO on an average, whereas ferrocarbonatites have ~35% CaO, >10% Fe_2O_3, ~8% MgO, and ~2% MnO. Among the trace elements Sr and Ba are the most abundant elements in both the types of carbonatite. In calcite-carbonatites Sr concentration is generally more than the Ba concentration while in ferrocarbonatites it is just the reverse (Viladkar and Wimmenauer, 1992). These carbonatites are highly enriched in REE and it has been observed that the REE content increases from coarse grained calcite carbonatites to ferrocarbonatites through medium to fine grained calcite carbonatites suggesting extreme differentiation of the parent carbonate magma (Viladkar and Dulski, 1986).

The first ever isotopic work in this complex were reported by Deans and Powell (1968). This study showed that the carbonatites have an average $^{87}Sr/^{86}Sr$ of 0.706, which is higher than the observed ratio in most of the carbonatites of the world. The authors also ruled out any possible genetic relationship between the carbonatites and country rock limestones owing to their widely different $^{87}Sr/^{86}Sr$. In a recent isotopic study Simonetti et al. (1995) have observed that the Nd and Sr isotopic results from this complex indicate derivation from a Rb/Sr and Nd/Sm enriched mantle source region, which is very different from many carbonatite complexes of the world. They also suggested that, the carbonatites do not show any kind of contamination/assimilation of the country rock sandstones. A few numbers of $\delta^{13}C$ and $\delta^{18}O$ values of carbonatites, reported by Simonetti et al. (1995), have been interpreted as primary or results of low temperature meteoric water alteration.

2.2.4. Metasomatic Rocks

Metasomatic features (fenitization) are inherent to carbonatite complexes and these are generally produced during the emplacement of the carbonatites. At Amba Dongar

fenitization is widespread in the host rocks, in sandstones particularly. These fenites have been extensively studied, both from mineralogical and chemical point of view by Shukeswala and Viladkar (1981) and Viladkar (1996). The chemistry of fenites revealed two trends of fenitization, an earlier and deeper sodic fenitization and a later predominantly potassic fenitization confined to shallower levels (Viladkar, 1996). Some alkaline rocks are also thought to have been fenitized by the carbonatite related metasomatic activity (Viladkar, 1996). In this variety of rocks, we also include the rocks which show fluorite mineralization. The carbonate content of these rocks vary from 0 to 10%. The fluorite mineralized rocks also contain large amounts of micro crystalline silica.

2.2.5. The Fluorite Deposit

The Amba Dongar fluorite deposit, the largest in India, is believed to be a hydrothermal deposit, formed much later to the carbonatite emplacement (Deans and Powell, 1968; Simonetti and Bell, 1995). Chemical and isotopic studies of fluorites do not indicate any direct genetic relationship of the mineralization with the carbonatite magmatism (Simonetti and Bell, 1995). Fluid inclusion studies revealed that these fluorite deposits were formed from a low-salinity, CO_2- bearing aqueous fluid at low temperatures (100-150°C) [Roedder (1973); Sharma (1991)].

2.2.6. The Geologic Evolution of the Complex

The general belief is that the Amba Dongar alkaline complex, like Phenai Mata of the same alkalic province (Chhota Udaipur), represents one of the late magmatic pulses of the Deccan Flood Basalts (Basu et al., 1993). However there is no unambiguous age data in support of this hypothesis. Very early attempts by Deans et al. (1973) to date the pyroxenes from nephelinites and two feldspars from potassic fenites, using K-Ar method of dating, yielded varying ages of 37.5±2.5 Ma, 61±2 Ma and 76±2 Ma, respectively. Basu et al. (1993) reported an ^{40}Ar-^{39}Ar age of 65 Ma for the Phenai Mata alkaline-carbonatite complex, which is geographically close to Amba Dongar complex, and hypothesized it to be contemporaneous with Amba Dongar. However, it is so far not clearly established whether Phenai Mata and Amba Dongar are temporally related.

Viladkar (1981, 1984) suggested, on basis of major and trace elemental chemistry, that this complex is not genetically related to the Deccan tholeiites. He also suggested that the alkaline silicate rocks and carbonatites of this complex were derived as a result of liquid immiscibility of a parent melanephelinitic magma. The only combined isotopic study on this complex based on Nd, Sr and Pb isotopes, by Simonetti et al. (1995), suggested an LREE enriched mantle source for the carbonatites (possibly an EM-II type of mantle) and indicated a possible relationship with the Reunion-Deccan plume activity. In a recent experimental phase equilibria study, Sen (1995) suggested that the tholeiites, carbonatites and alkaline silicate rocks, all are generated from the Deccan-Reunion plume. According to him carbonatites and alkaline lavas were generated by very low degree of melting (~1%) from the cooler, volatile rich apron of the plume head.

2.3. THE MUNDWARA COMPLEX

2.3.1. Regional Geology and Field Relations

The Mundwara alkaline-carbonatite complex is present 400 km northwest of Amba Dongar complex (Fig. 1.4) in the Sirohi District of Rajasthan. The complex occurs as ring shaped and plug like intrusions within the Precambrian Erinpura granites. This complex is composed of three plutons namely, Musala, Mer and Toa, which are laccolith type of bodies fringed by basalts (Fig. 2.2). Mer is the largest plug, which is composed mostly of alkaline mafic rocks. Carbonatites form a very minor part of the complex and are also present as dykes and veins in the basement rocks, east of Mer plug. Ultramafic and mafic rocks are dominant in Toa complex, whereas in Musala some minor felsic rocks are present along with the major mafic rocks. The Mundwara complex is present within the northward extension of Cambay Graben (Fig. 1.4) and is believed to be an early alkalic pulse of the Deccan Flood Basalt volcanism (Basu et al., 1993).

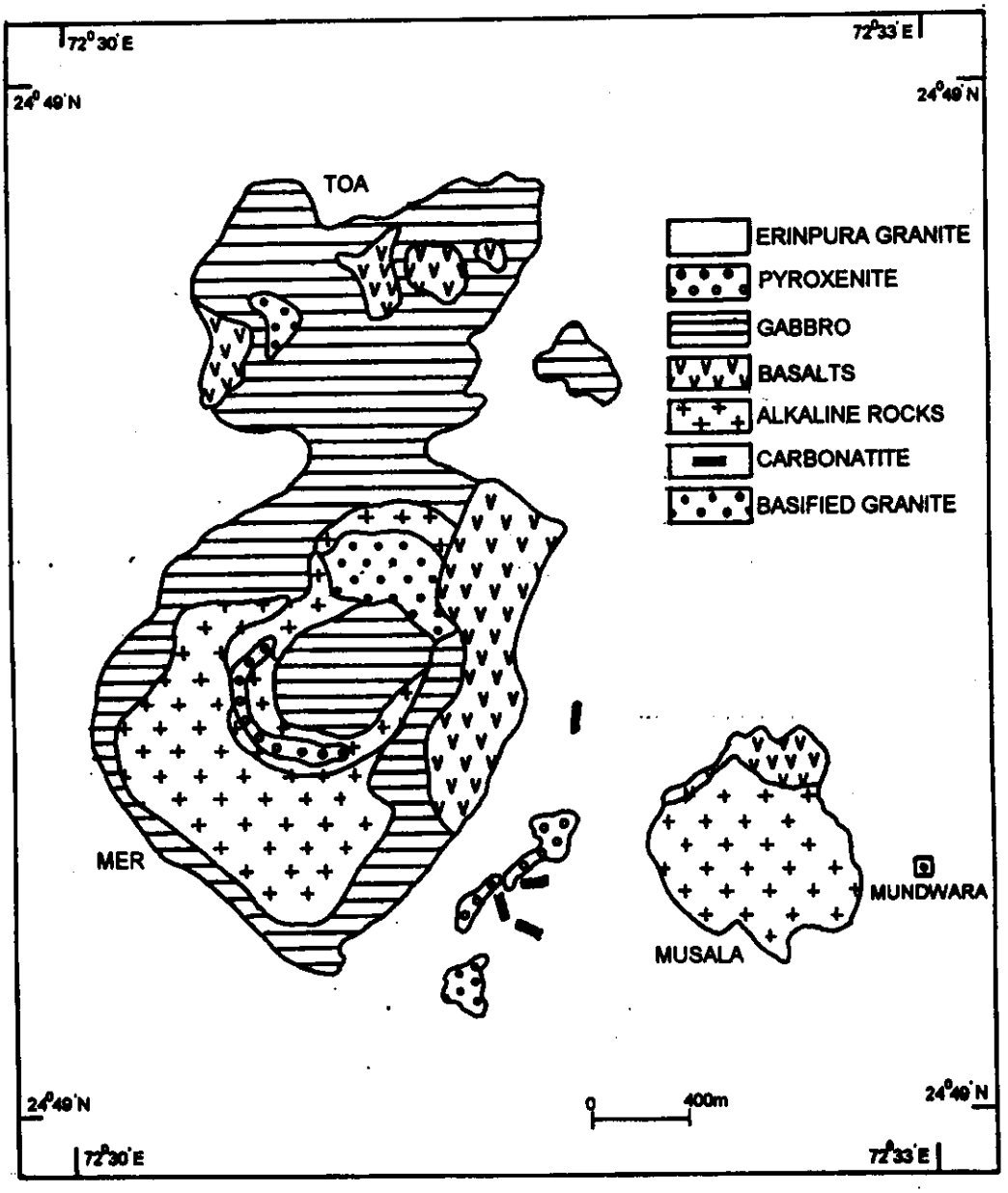

Fig. 2.2. *Geological map of Mundwara carbonatite-alkaline complex modified from Rathore et al.(1995).*

2.3.2. Alkaline Silicate Rocks

The alkaline end members of this complex include alkali pyroxenites, alkali gabbros, theralites, essexites, melteigites, and syenites (Subrahmanyam and Leelanandam, 1989). Extensive studies on petrology and geochemistry of these rocks and other silicate rocks of this complex have been carried out by various workers viz. Sharma (1967); Bose and Das Gupta (1973); Das Gupta (1974, 1975); Chakraborty and Bose (1978); LeBas and Srivastava (1989); and Subrahmanyam and Leelanandam (1989, 1991). These authors suggested that the alkali olivine basalt (which occurs as flows in Toa) was the parent magma for this complex, which generated the whole sequence of rocks through fractional crystallization. Sr and He isotopic study by Basu et al. (1993) favours a lower mantle source (possibly plume related) for these rocks.

2.3.3. Carbonatites

Mundwara carbonatites occur as dykes and veins. They intrude into the Erinpura granite (Fig. 2.2) and comprise <1% of the complex. Compositionally all these carbonatites are calcite carbonatites (LeBas and Srivastava, 1989). Calcite is the only carbonate mineral present in all these. Other minerals include amphiboles, magnetites, apatites, phlogopites and some times minor pyroxenes. Some calcite carbonatites show considerable secondary alteration. Chemically, CaO content of Mundwara calcite carbonatites is ~50%, MgO content is ~0.5% and SrO content is 1.5%. These also show very high enrichment of rare earth elements (LeBas and Srivastava, 1989).

Radioisotopic measurements in carbonatites is lacking. Based on only three analyses of $\delta^{13}C$ and $\delta^{18}O$ of these carbonatites LeBas and Srivastava (1989) suggested that these indeed show mantle values, which proves their magmatic nature.

2.3.4. Fenitization

Fenitization in this complex is observed only on a small scale. Contact granites are fenitized from a few millimeters up to 3 cm (Subrahmanyam and Rao, 1977). Both potassic and sodic fenitization effects have been observed by LeBas and Srivastava (1989).

2.3.5. The Geologic Evolution of the Complex

The Mundwara alkaline magmatism, like Amba Dongar, is also believed to be a variation of the Deccan flood basalt volcanism. In a recent work, Basu et al. (1993) showed that this complex is 68.53±0.16 Ma old and high $^{3}He/^{4}He$ ratio in olivine gabbro and olivine pyroxenite (~13.9 times atmospheric) suggested a lower mantle origin. Using He isotopes and Sr isotopes, they suggested a plume origin of this complex. Being present north of the Deccan Traps and older in age (by 3.5 Ma), Mundwara alkaline magmatism fits well into the plume model of Reunion-Deccan, which generated the traps and represents an early alkalic pulse.

As mentioned earlier, it is now believed the wide variety of alkaline rocks may have formed, from a parental alkali olivine basaltic magma by fractional crystallization. However, the evolution of carbonatites of this complex is not understood clearly. Subrahmanyam and Rao (1977) suggested that the fractional crystallization of primary carbonated-silicate magma was probably responsible for the formation of carbonatites of this complex.

2.4. THE SARNU-DANDALI COMPLEX

2.4.1. Regional Geology and Field Relations

The Sarnu-Dandali alkaline-carbonatite complex is located 150 km northwest of Mundwara in the Barmer district of Rajasthan and falls within the Malani Igneous Province which forms a part of the Thar desert. Although the complex was recognized earlier by Udas et al. (1974), the work of Chandrasekaran (1987) revealed the alkaline silicate rocks and carbonatite association in it. It comprises a variety of acidic, intermediate, and alkalic rocks, including plugs of ijolites, foidal syenites, and dykes of carbonatites and is intrusive into the Malani rhyolites and Cretaceous sediments (sandstones and siltstones). Fenitization here is predominantly sodic in nature. Fig.2.3 gives the distribution of different rock types in the complex.

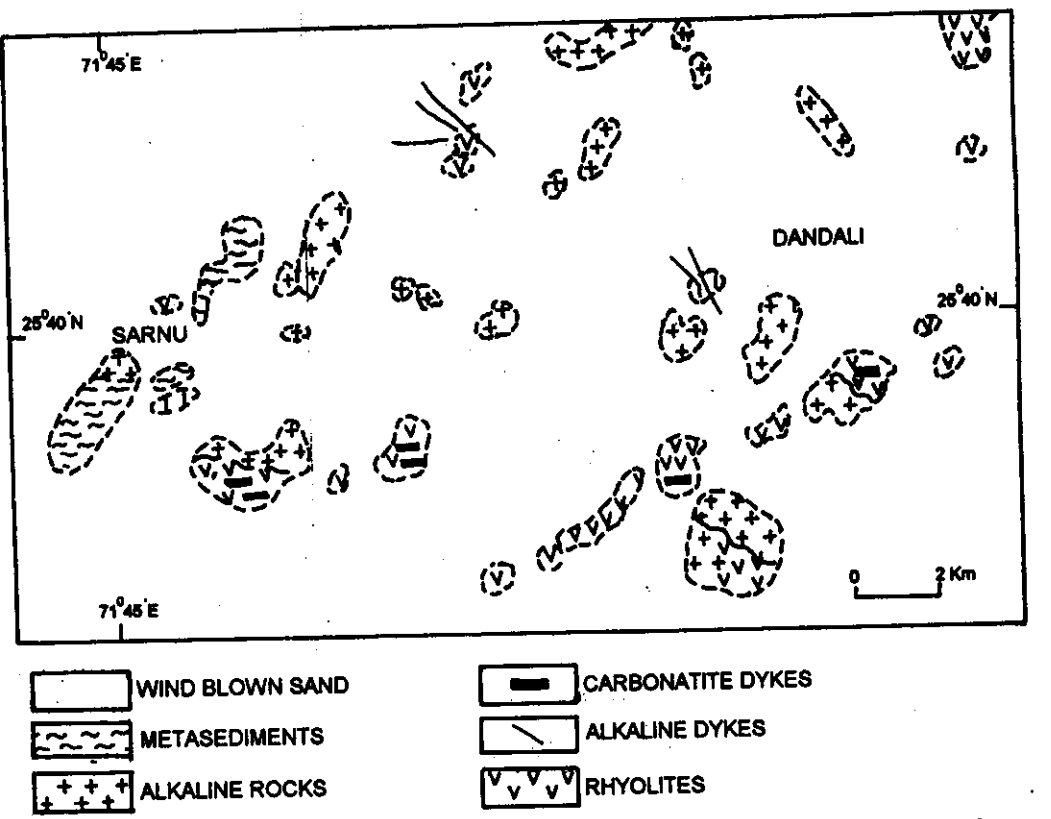

Fig. 2.3. *Geological map of Sarnu-Dandali carbonatite-alkaline complex modified from Chandrasekaran et al.(1990).*

2.4.2. Alkaline Silicate Rocks

The alkaline suite ranges in composition from alkali pyroxenites to foidal syenites through melteigite and ijolite, besides nephelinite and phonolite (Chandrasekaran et al., 1990). The mineral constituents of these rocks, in general, are titano-augite and nepheline in various proportions besides orthoclase, aegirine augite, aegirine, biotite, melanite, carncrinite etc.(Chandrasekaran et al., 1990). The whole suite of alkaline rocks here have been interpreted as the product of extreme differentiation of a primary alkali pyroxenite or a carbonated alkali peridotite magma (Chandrasekaran et al., 1990). Like the Mundwara complex, $^{3}He/^{4}He$ ratio and $^{87}Sr/^{86}Sr$ ratio of these rocks indicate a plume origin for the complex (Basu et al., 1993).

2.4.3. Carbonatites

Like Mundwara, carbonatites here too comprise a very minor part of the complex. They occur as dykes and veins scattered all over the complex. These dykes and veins vary in length from a few cm to ~12 m and in width from a few mm to ~30 cm. They cut across the mafic alkaline members and contain angular xenoliths of various country rocks. Chemically two types of carbonatites, calcite carbonatites and ferrocarbonatites, are observed in this complex (Chandrasekaran and Srivastava, 1992). Calcite carbonatites are medium to fine grained rocks containing more than 50% of calcite (the only carbonate mineral). The accessory minerals include magnetite, biotite, barite and apatite. Ferrocarbonatite is yellow to yellowish-brown in colour and rich in iron-oxide. Some of the calcite carbonatites and ferrocarbonatites are highly altered and show the presence of microcrystalline silica in them. Radioisotopic studies in carbonatites do not exist. Very preliminary studies of carbon and oxygen isotopes revealed the magmatic nature of these carbonatites (Sarkar and Bhattacharya, 1992; Chandrasekaran and Srivastava, 1992).

2.4.4. Metasomatic Rocks

Most of the suspected calcite bearing carbonatites of Barmer town proper are actually metasomatic rocks as they contain <50% carbonates in them. These rocks are highly altered. Apart from calcites they also contain siderite, orthoclase and microcrystalline

silica. Fenitization is confined only to the associated alkaline rocks and is predominantly sodic in nature (Chandrasekaran and Srivastava, 1992).

2.4.5. The Geologic Evolution of the Complex

Basu et al. (1993) reported an ^{40}Ar-^{39}Ar age of 68.57±0.08 Ma for the biotites from alkali pyroxenite, which has been interpreted as the emplacement age of the complex. Based on this age data, $^{3}He/^{4}He$ ratio of 12.8 times atmospheric value and initial $^{87}Sr/^{86}Sr$ ratio of 0.70499, Basu et al. (1993) suggested a lower mantle source these rocks and linked their origin to the Deccan-Reunion plume activity. They also suggested that this complex is probably the earliest manifestation of the Deccan volcanism on the Indian subcontinent.

The genesis of wide variety of alkaline silicate rocks have been explained by extreme differentiation of a parent alkaline pyroxenitic magma. However, so far no attempts have been made to link the alkaline rocks to the carbonatites of this complex, except that they are thought to be genetically related.

2.5. THE SUNG VALLEY COMPLEX

2.5.1. Regional Geology and Field Relations

The Sung Valley carbonatite-alkaline complex is the largest of all eastern Indian carbonatite complexes. It is located 49 km south of Shillong, in the state of Meghalaya. The complex intrudes into the Precambrian Shillong series metasedimentary rocks (quartzites, phyllites and quartz-sericite schists). The Assam-Meghalaya plateau in which Sung Valley is located, is considered to be an uplifted horst bordered by Dauki fault to the south and the Brahmaputra trough zone to the north (Fig. 1.4) (Krishnamurthy, 1985). The Sung Valley complex is an oval shaped pluton with the core occupied by serpentinized peridotite and rimmed by pyroxenite (Fig. 2.4). It is composed of a variety of alkaline silicate rocks like uncompahgrite, ijolite and syenite, which occur as small bodies within the pyroxenite. The carbonatites occur as small stocks, lenses, dykes and veins within the pyroxenites and are confined to the southern part of the complex (Fig. 2.4). Preliminary studies indicate the presence of both sodic and potassic fenites in this complex (Krishnamurthy, 1985).

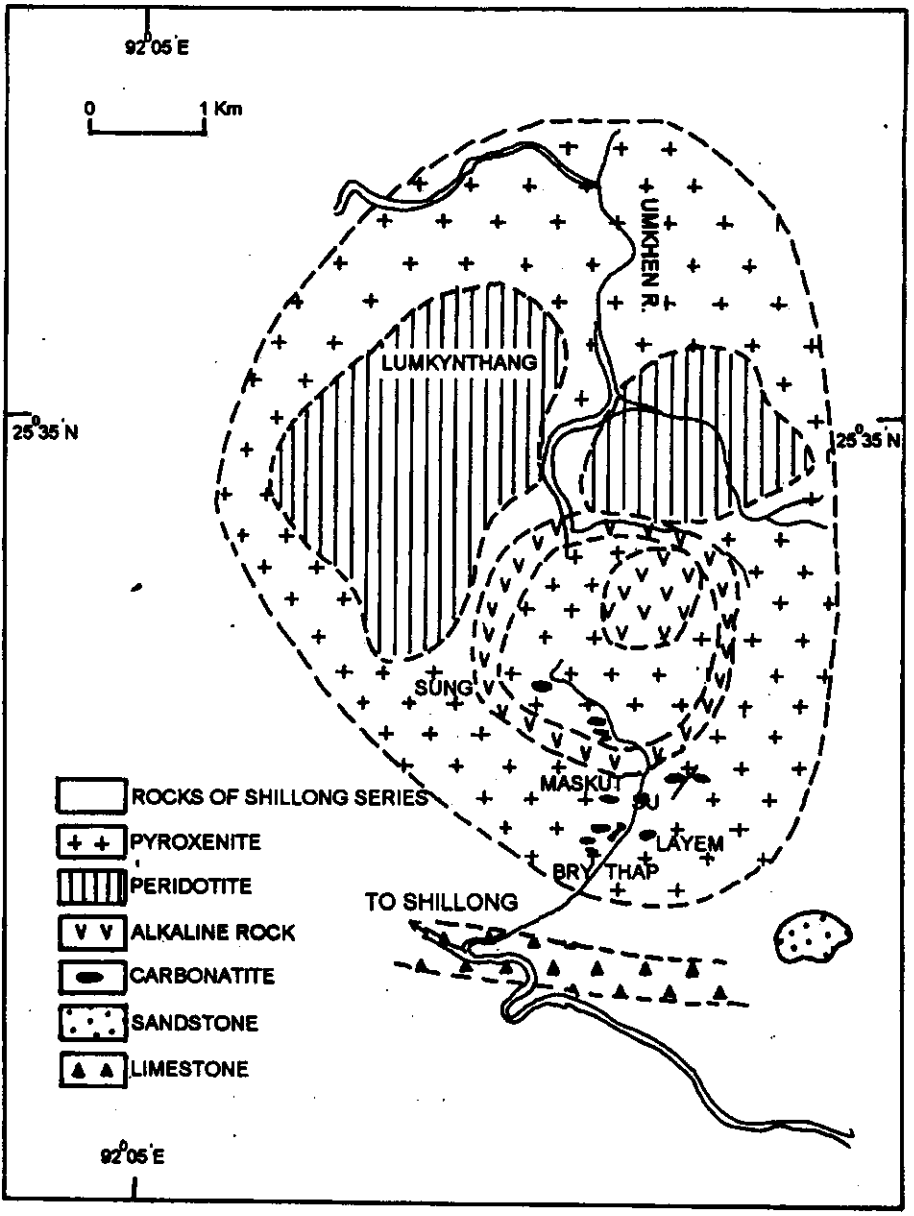

Fig. 2.4. *Geological map of Sung valley carbonatite-alkaline complex modified from Krishnamurthy et al. (1985).*

2.5.2. Alkaline Silicate Rocks

Alkaline silicate rocks of Sung Valley complex include alkali pyroxenites, uncompahgrites, ijolites and syenites. Pyroxenites appear to be the earliest member and constitute the bulk of the complex. Two types of pyroxenites, coarse grained and medium to fine grained, have been reported (Krishnamurthy, 1985). Diopsidic augite is the major mineral of these rocks with minor phlogopite. Ijolite occurs as a ring dyke and a central plug, whereas syenite occurs as minor dykes. At places all the silicate rocks have been affected by fenitization due to carbonatite activity.

2.5.3. Carbonatites

Carbonatites comprise a minor part of the complex and are present as small stocks, dykes and veins in the pyroxenite. Calcite carbonatite is the major carbonatite variety, however, magnesiocarbonatite is also present (Krishnamurthy, 1985). Apart from calcite and dolomite, these rocks also contain a substantial amount of magnetite and apatite. Other accessory minerals include phlogopite, fluorite, pyrochlore, perovskite and olivine. Like other carbonatites of the world, Sung Valley carbonatites also show high enrichment of Sr, Ba, Nb and REE (Krishnamurthy, 1985).

A combined Pb, Sr and Nd isotopic study on these carbonatites (Krishna et al.; 1991) indicated a DUPAL mantle source for this complex and the isotopic ratios are found to be broadly similar to those of ninety degree east ridge basalts.

2.5.4. The Geologic Evolution of the Complex

The age of Sung Valley complex is not known unambiguously. The available age data show two widely different values; 90±10 Ma (Fission track age, Chattopadhay and Hashimi, 1984) and 150±26 Ma (Pb-Pb, whole rock isochron age, Krishna et al., 1991). In a recent development different workers have tried to link this carbonatite magmatism with the Rajmahal trap volcanism (Kent et al., 1992; Ghose et al., 1996 and references therein). The isotopic evidence for similar source regions for Ninety East Ridge Basalts and Sung Valley carbonatites (Krishna et al., 1991) indicates that probably the Kerguelen plume was responsible for this carbonatite magmatism. If so, then one would expect an age close to the 116 Ma (age of Rajmahal Traps, Baksi,

1986). However, accurate age data and detailed isotopic study are required to prove this hypothesis.

It is believed that both liquid immiscibility and fractional crystallization have played a major role in generating alkaline silicate rocks and carbonatites (Krishnamurthy, 1985). It is also suggested that a melanephelinitic parent magma was responsible for the generation of the whole complex (Krishnamurthy, 1985).

2.6. THE SAMCHAMPI COMPLEX

The Samchampi alkaline-carbonatite complex was first reported by Kumar et al. (1989). This complex is in Karbi Anglong district of Assam and located ~100 km to the east of Sung Valley complex (Fig. 1.4). It intrudes into the Precambrian Gneissic Complex of Karbi Hill Massif (Sengupta et al. 1997). Apart from carbonatites, this complex comprises of alkali pyroxenites, melteigites, ijolites, nephelinites and syenites. Carbonatites, which occur as dykes and veins, are mainly calcite-carbonatites. Only syenitic fenites have been reported from this complex (Sengupta et al. 1997). Detailed petrological or geochemical work in this complex is lacking.

2.7. THE SWANGKRE COMPLEX

The Swangkre complex of,West Khasi Hill of Meghalaya (Fig. 1.4) was first reported by Nambiar and Golani (1985). After its discovery, to our knowledge, no further work on this complex has been done. Carbonatites of this complex occur as small dykes which intrude into Precambrian gneisses and granites and are calcite-carbonatites. The carbonatites of this complex are associated with lamprophyres, ijolites and tinguaites (Nambiar and Golani, 1985).

2.8. RELATIVE EROSION LEVELS OF THESE COMPLEXES

The relative erosion levels of the carbonatite complexes are estimated based on rock association, nature of carbonatites, degree of fenitization and type of fenites. Fig. 2.5 shows an idealized vertical profile of an alkaline-carbonatite complex (LeBas, 1977) with the estimated relative erosion levels of the complexes studied here. Except Amba Dongar complex, all other complexes show plutonic to subvolcanic associations.

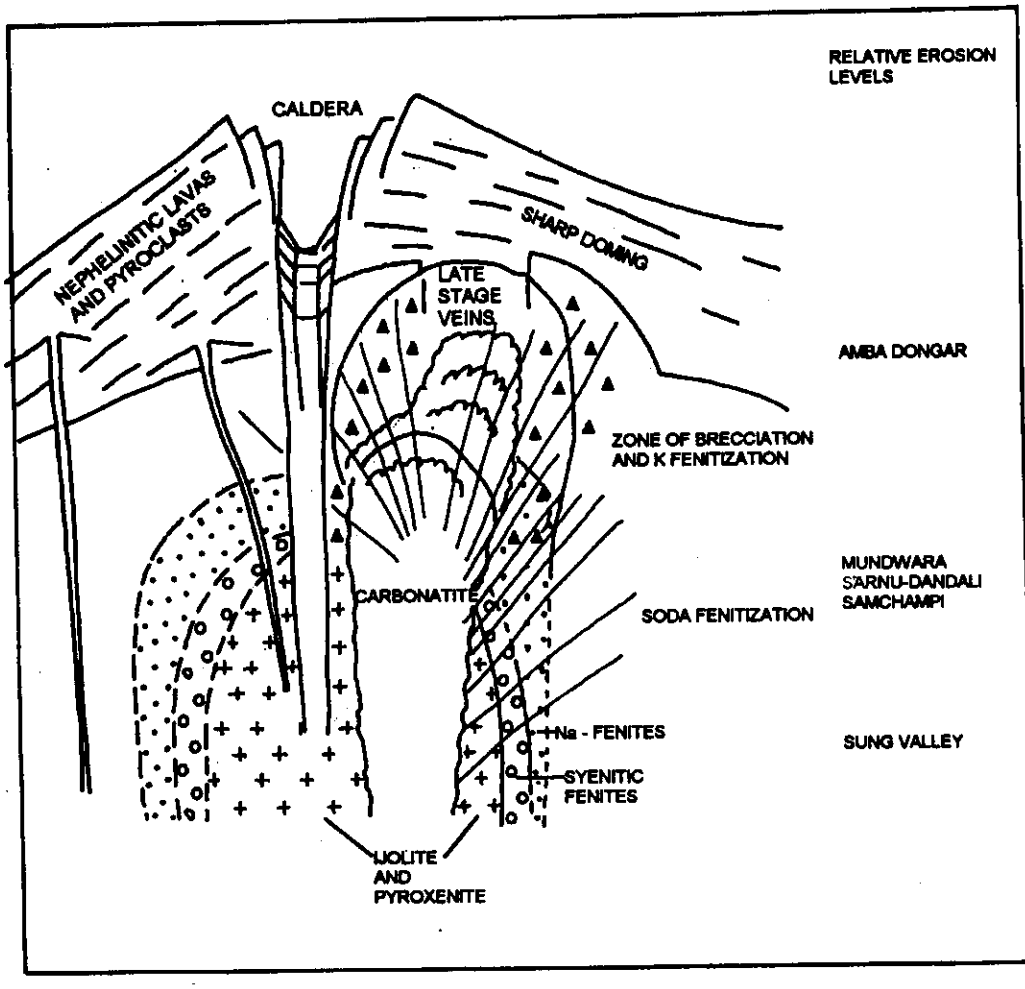

Fig. 2.5. *Schematic cross-section of an idealized carbonatite-alkaline volcanic complex showing the normal structure, sequence of intrusion and zones of Na & K fenitization. It also shows the estimated erosion levels of the six complexes studied in the present work. Figure is modified from LeBas (1977).*

The subvolcanic to volcanic association, extensive brecciation, late stage carbonatite veining and predominant feldspathic fenitization, indicate a very shallow level of emplacement for Amba Dongar complex (Fig. 2.5). The plutonic association, the presence of sodic and syenitic fenites, and the very coarse grained nature of carbonatites put Sung Valley complex at the deepest emplacement level. The rock association and fenites of Mundwara, Sarnu Dandali and Samchampi indicate that the erosion level of these complexes is between those of Amba Dongar and Sung Valley complexes (Fig. 2.5). The emplacement/erosion levels estimated here are highly schematic, however, these probably have greater implications towards understanding the stable carbon and oxygen isotopic evolution of these complexes.

In summary, it was found that the following questions remained unanswered, which are addressed in the present work:

1. What is the exact relationship between the carbonatites and the associated alkaline rocks present in these complexes?
2. Where is the source region of carbonatite located, in the lower mantle or in the subcontinental mantle?
3. Is there any genetic relationship between the Cretaceous plume activities (Reunion-Deccan and Kerguelen-Rajmahal) with the above described contemporaneous carbonatite-alkaline magamtisms?
4. What is the nature of carbon in these carbonatites, juvenile or recycled?

CHAPTER III

EXPERIMENTAL TECHNIQUES

This chapter describes the experimental techniques used in the present work to study the isotopic and trace elemental characteristics of different samples from the Mesozoic carbonatite complexes of India. The chapter is divided into six sections. The first section (3.1) describes the samples collected for this work. The technique of stable carbon and oxygen isotope analysis in carbonatites and other carbonate bearing rocks are described in the section 3.2 with a detailed discussion on the CO_2 extraction procedure, developed during this work, to analyze oxygen and carbon isotopic compositions in individual carbonate phases present in natural multicarbonate mixtures. The section 3.3 describes the ^{40}Ar-^{39}Ar dating technique and details of the experimental procedures followed in our laboratory. Brief descriptions of Sr isotope analysis by thermal ionization mass-spectrometry, trace elemental analysis by instrumental neutron activation analysis, mineral identification by X-ray diffractometry, and Rb and Sr concentration measurements by atomic absorption spectrophotometry are given in sections 3.4, 3.5, 3.6 and 3.7, respectively.

3.1. SAMPLES FOR THIS WORK

Three field trips were undertaken, two to Amba Dongar (November, 1993 and June, 1995) and one to Sung Valley (December, 1994), to collect samples for this work. Samples of various carbonatites, alkaline rocks, metasomatic rocks and country rocks were collected. The main criteria for selection of samples were freshness in hand specimen and the collection of samples which fairly represented a particular exposure. Samples of carbonatites and metasomatic rocks from Mundwara and Sarnu-Dandali complexes were kindly provided by late Dr. R. K. Srivastava of M. S. University, Udaipur; samples of Samchampi complex were given by Mr. S. K. Sengupta of Geological Survey of India, Guwahati. Five carbonatite samples from Sung Valley complex and a carbonatite sample of Swangkre complex were given by Dr. P. Krishnamurthy of Atomic Mineral Division, Hyderabad.

Petrographic studies (thin section and X-ray diffractometry) were carried out to identify different minerals and to classify the rock types. Carbonatite samples, by definition, had more than 50% modal carbonate and they displayed magmatic features. Metasomatic rocks contained <10% carbonate. Alkaline rocks of Amba Dongar and Sung Valley were sampled particularly for dating and Sr-isotopic studies. Amba Dongar alkaline rocks had ~ 7% carbonate (mostly calcite) in them. Country rocks and hydrothermal calcite veins, which were associated with the fluorite deposits of Amba Dongar complex were also sampled. Table 3.1 gives a brief description of samples used in different studies.

Table 3.1. Description of the samples analysed in the present work

Sample	Description
Amba Dongar	
AD-1	Medium grained calcite carbonatite. Collected from a small dyke which intrudes into coarse grained calcite carbonatites. (90 % carbonate).
AD-2	Medium grained calcite carbonatite. Apart from carbonates (~80%), the rock has secondary minerals like fluorite, micro crystalline silica and hematite.
AD-3	Fine grained calcite carbonatite. It contains secondary veinlets of Fe-rich carbonates and shows replacement texture. (~70% carbonate).
AD-4	Limestone (Bagh beds). A micrite, has no fossils. A lot of microcrystalline silica is present. Collected from a road side exposure near Moti Chikli.
AD-6	Sandstone (Bagh beds). Quartz is the dominant mineral.
AD-8	Medium grained calcite carbonatite collected from the fluorite mine from a dyke that intrudes into coarse grained calcite carbonatite. (90 % carbonate).
AD-9/2	Medium grained calcite carbonatite. (92% carbonate).
AD-10/1	Very coarse grained monomineralic calcite carbonatite collected from the fluorite mine. A deeper level carbonatite.
AD-10/2	Very coarse grained monomineralic calcite carbonatite like AD-10/1.
AD-12	Very fine grained ferrocarbonatite collected from the southern-most ferrocarbonatite plug. Ankerite is the major carbonate, calcite to ankerite ratio is 24:76. Shows signs of hydrothermal alteration. (52 % carbonate).
AD-13/1	Fine grained calcite carbonatite collected from a vein in the southern part of the eastern limb of the ring dyke. (75 % carbonate).
AD-13/2	Medium grained calcite carbonatite collected close to AD-13/1. (85 % carbonate.

AD-14	Nephelinite from the base of main dome. It has phenocrysts of nepheline, aegirine augite and melanite garnet. Groundmass contains calcite and analcite. Collected from an exposure at the base of rig dyke (Western margin).
AD-16	Nephelinite. Groundmass does not contain calcite. Collected from a site close to AD-14.
AD-17	Nephelinite for Khadla village. Groundmass contains calcite.
AD-18	Nephelinitic tuff. Groundmass contains carbonates (Khadla).
AD-19	Dark brown coloured ferrocarbonatite, contains a lot of iron oxide. Calcite to ankerite ratio is 60:40. Collected from a small exposure within the calcite carbonatite main dyke.
AD-20	Jasper rich vein. (~7 % carbonate).
AD-21	Banded (gray and red) calcite carbonatite. (88 % carbonate).
AD-24	Fluoritized carbonatite. (2 % carbonate).
AD-25	Fine grained ferrocarbonatite. Calcite : Ankerite = 8:92.
AD-26	K-feldspar rich rock (fenite). (2 % carbonate).
AD-27	Medium grained calcite carbonatite. From a small dyke that intrudes into coarse grained calcite carbonatite. (90 % carbonate).
AD-28	Sodic fenite. (4 % carbonate).
AD-29	Brownish yellow coloured, fine grained calcite carbonatite vein. The vein intrudes, into the coarse grained calcite carbonatites. (65 % carbonate).
AD-30	Highly altered calcite carbonatite vein. (51% carbonate).
AD-31	Coarse grained calcite carbonatite. (85 % carbonate).
AD-32	Coarse grained monomineralic calcite carbonatite.
AD-33	Fine grained ferrocarbonatite from the main ferrocarbonatite plug. Ankerites in these have been altered to calcite and iron oxides. Calcite to ankerite ratio = 40:60.
AD-34	Ferrocarbonatite, collected from the same exposure as AD-33. Ankerite is the only carbonate present in this.
AD-35	Highly altered ferrocarbonatite, calcite:ankerite = 20:80.
AD-38	Monomineralic coarse grained calcite carbonatite.
AD-39	Fine grained calcite carbonatite from a vein that cuts across course grained calcite carbonatite.
AD-40	Medium grained calcite carbonatite. (95 % carbonate).
AD-41	Fine grained, brownish yellow, calcite carbonatite vein. (75 % carbonate).
AD-42	Medium grained calcite carbonatite, shows recrystallization of calcites. (79 % carbonate).
AD-43	Highly altered calcite carbonatite vein from east part of the ring dyke. (66 % carbonate).

AD-44/1	Highly altered, fluoritized, red coloured calcite carbonatite. (55 % carbonate).
AD-45	Calcite bearing tinguaite. Minerals present are; nepheline, aegirine augite, melanite and calcite. (7 % carbonate).
AD-46	Phlogopite bearing calcite carbonatite from a vein that intrudes into sodic fenites and alkaline rocks. Such veins are numerous inside the mine.
AD-47	Calcite bearing tinguaite. Minerals present; nepheline, aegirine-augite, K-feldspar and magnetite. Calcite constitutes 8 % of the total rock. Collected from an exposure close to the fluorite mine.
AD-49	Medium grained calcite carbonatite. A common carbonatite on the western benches of the mine. (~ 80 % carbonate).
AD-50	Silicified carbonatite. Contains very little carbonate. At places original carbonatite texture is preserved.
AD-51	Calcite carbonatite from a vein. (93 % carbonate).
AD-52	Phlogopite bearing calcite carbonatite vein that intrudes into an alkaline rock. (91 % carbonate).
AD-54	Coarse grained calcite carbonatite. (95 % carbonate).
AD-55	Fine grained, highly altered ferrocarbonatite. (calcite:ankerite = 15:85).
AD-58	Calcite vein associated with fluorite deposits.
AD-59/1	Micritic limestone similar to AD-4.
AD-61	A calcareous sand stone. (25 % carbonate).
AD-62	Fine grained, fossiliferous limestone. (80 % carbonate).
AD-64	Calcite carbonatite (90 % carbonate).
AD-65	Phonolite
AD-66	Nephelinite
AD-67	Nephelinitic tuff
AD-69	Phonolite
AD-70	Calcite bearing nephelinite (6 % carbonate).
AD-71	Calcite bearing tinguaite (7 % carbonate).
NS-20/2	Very coarse grained monomineralic calcite carbonatite.
NS-20/O/2	Very coarse grained monomineralic calcite carbonatite.
NS-20/O/3	Very coarse grained monomineralic calcite carbonatite.
NS-20/O/4	Coarse grained calcite carbonatite. (85 % carbonate).
NS-20/6	Coarse grained calcite carbonatite. (93 % carbonate).
NS-20/8	Coarse grained calcite carbonatite. (88 % carbonate).
NS-20/9	Coarse grained calcite carbonatite. (87 % carbonate).
NS-20/10	Coarse grained calcite carbonatite. (92 % carbonate).
NS-20/11	Phlogopite bearing medium grained calcite carbonatite. From a vein that intrudes into coarse grained calcite carbonatite. (87 % carbonate).

NS-20/13	Coarse grained calcite carbonatite. (85 % carbonate).
Mundwara	
M-1	Coarse grained calcite carbonatite (93 % carbonate).
M-2	Na-amphibole bearing calcite carbonate (83 % carbonate).
M-3	Yellowish brown fine grained calcite carbonatite. Shows signs of alteration.
M-15	Coarse grained calcite carbonatite. (88 % carbonate).
M-39	Medium grained calcite carbonatite. (87 % carbonate).
M-40	Highly altered calcite carbonatite. (76 % carbonate).
M-121	Highly altered calcite carbonatite. (62 % carbonate).
Sarnu-Dandali	
C-94	Fine grained calcite carbonatite. (77 % carbonate).
C-119	Coarse grained calcite carbonatite. (86 % carbonate).
C-142	Fine grained calcite carbonatite. (73 % carbonate).
C-143	Coarse grained calcite carbonatite. (90 % carbonate).
C-149	Brownish red, fine grained ferrocarbonatite. (58 % carbonate).
C-177	Brownish red, fine grained ferrocarbonatite. (69 % carbonate).
C-245	Coarse grained calcite carbonatite.
C-290	Medium grained calcite carbonatite.
C-291	Calcite carbonatite, shows signs of recrystallization.
A-18	Carbonate bearing K-feldspar rich rock. (8 % carbonate).
A-161	Fine grained ferrocarbonatite.
A-800	Carbonate bearing potash fenite (~10 % carbonate).
A-805	Ferrocarbonatite
A-807	Ferrocarbonatite
A-808	Ferrocarbonatite
A-841	Highly altered calcite carbonatite.
Sung Valley	
SV-1	Medium grained dolomite bearing calcite carbonatite, contains olivine and phlogopite apart from other characteristic minerals. (calcite:dolomite = 83:17).
SV-2	Dolomite carbonatite. Collected from a vein that intrudes coarse grained pyroxenite.
SV-3	Very coarse grained pyroxenite. Apart from pyroxene (mainly augite), it contains phlogopite.
SV-4	Very coarse grained pyroxenite.
SV-5	Phlogopite bearing calcite carbonatite.
SV-6	Apatite rich calcite carbonatite.
SV-7	Phlogopite bearing calcite carbonatite.
SV-10	Apatite rich calcite carbonatite.

SV-11	Calcite carbonatite. Olivine and Phlogopite bearing.
SV-12	Phlogopite bearing calcite carbonatite.
SV-13	Dolomite bearing calcite carbonatite. (calcite:dolomite = 92:08).
SV-15	Magnetite rich calcite carbonatite.
SV-18	Dolomite bearing calcite carbonatite. (calcite:dolomite = 80:20).
SV-19	Olivine-rich, dolomite bearing calcite carbonatite. (calcite:dolomite = 87:17).
SV-20	Dolomite bearing calcite carbonatite. (calcite:dolomite = 88:12).
PKS-145	Coarse grained magnetite-rich calcite carbonatite. (88 % carbonate).
PKS-164	Calcite Carbonatite (85 % carbonate).
PKS-270	Olivine bearing calcite carbonatite. (82 % carbonate).
PKS-241	Dolomite bearing calcite carbonatite. (88% carbonate).
PKS-279	Calcite carbonatite, contains olivine and amphiboles. (87 % carbonate).
Samchampi	
71	Calcite carbonatite.
C1/93	Coarse grained calcite carbonatite.
165	Calcite carbonatite.
177	Dolomite bearing calcite carbonatite (calcite:dolomite = 89:11).
179	Dolomite bearing calcite carbonatite (calcite:dolomite = 90:10).
Swangkre	
WKS-1	Medium grained calcite carbonatite.

Note: Like most of the carbonatites of the world, the carbonatite samples described above contain accessory minerals like magnetite, apatite, phlogopite, barite, pyrochlore, fluorite, monazite etc. (determined from thin section study). Carbonate percentage and the type of carbonate mineral(s) present in a sample were determined respectively from, the CO_2 yield during the acid reaction performed for stable isotope analysis and X-ray diffractometry. The samples of fenites, fluoritized carbonatites, silicified carbonatites and some highly altered rocks (as described in the above table), which contain < 50 % carbonate, have been termed as metasomatic rocks in this work.

3.2. STABLE ISOTOPIC STUDIES

3.2.1. Principle

Most naturally occurring elements consist of more than one stable isotope. In elements of lower atomic masses, it is possible for the isotope to get fractionated through physico-chemical processes as a result of the mass difference between the isotopes. The stable isotopes of light elements H, C, N, O and S have been used extensively as important tracers for many geological processes. The extent of fractionation of the isotopes of these elements helps us in finding the temperature of a process, source of

an element, extent of alteration and nature of diffusion processes. In the case of igneous rocks, study of isotopes of carbon (^{12}C and ^{13}C) and oxygen (^{16}O and ^{18}O) tells about the nature of the source regions of these rocks and the isotopic effects generated during magmatic and post-magmatic-alteration processes.

I measured carbon and oxygen isotopic compositions of the carbonates present in carbonatites and alkaline rocks. The stable isotopic ratios are generally measured relative to a standard or reference and are expressed as a δ value in per mill (‰) units. For carbon and oxygen, the δ values respectively are :

$$\delta^{13}C = [(^{13}C/^{12}C)_{sample} - (^{13}C/^{12}C)_{V\text{-}PDB}] / [(^{13}C/^{12}C)_{V\text{-}PDB}] \times 10^3$$

and

$$\delta^{18}O = [(^{18}O/^{16}O)_{sample} - (^{18}O/^{16}O)_{V\text{-}SMOW}] / [(^{18}O/^{16}O)_{V\text{-}SMOW}] \times 10^3$$

where V-PDB (Vienna Pee Dee Belemnite) is the standard used for carbon isotopic ratio and V-SMOW (Vienna Standard Mean Ocean Water) is the standard for oxygen isotopic ratio (Gonfiantini, 1981).

3.2.2 Experimental Details

3.2.2a. Sample Preparation

Fresh samples were powdered using a stainless steel mortar and pestle. Homogenized powders of grain size < 200 mesh (75μm) were taken. Sample powders were then dried at 110°C for 10-12 hours in an oven to remove moisture from them. Then 10 - 20 mg of each sample powder was taken for isotopic analysis.

3.2.2b. Extraction of CO_2 from carbonates of carbonatites and other rocks.

Carbonatite carbonates are either pure calcites or mixtures of calcites and dolomites/ankerites. For measurements of carbon and oxygen isotopic ratios mass-spectrometrically we need to extract CO_2 from them. For pure calcite bearing samples the standard CO_2 extraction procedure, suggested by McCrea (1950), was followed. ~10 mg of each sample was taken in glass bottles with side-arms which contained ~2 ml of 100% orthophosphoric acid (H_3PO_4) in the side arms. These bottles were evacuated and kept in a 25°C constant temperature water bath for 6 hours to allow them to attain the temperature of 25°C. Then the bottles were tilted inside water to

react the sample with H_3PO_4. The reaction was allowed to continue for 24 hours at 25°C and the liberated CO_2 was cleaned of water vapour and collected in glass bottles after measuring the pressure with a pre-calibrated Hg-manometer. The yield of CO_2 was 100% for pure calcite samples. The gas was then allowed into a mass-spectrometer after another round of cleaning for carbon and oxygen isotopic ratio measurements.

For carbonatites which have different proportions of calcites, dolomites and ankerite, the above procedure is likely to generate CO_2 which will have contamination from different carbonates. Hence, to get CO_2 from pure physically inseparable end-members during the acid reaction, a selective step-wise CO_2 extraction (chemical separation) procedure was developed which is discussed in detail in the following paragraphs.

Chemical separation techniques, to separate coexisting carbonate minerals for accurate determination of the oxygen and carbon isotope compositions, have been based on differential reaction rates of various carbonate minerals with phosphoric acid under variable temperatures. Fig.3.1 shows the reaction rates of pure carbonate minerals with phosphoric acid at 25°C and 50°C. Most of the earlier studies tried to separate calcite-CO_2 from dolomite-CO_2 (Epstein et al., 1964; Walters et al., 1972; Wada and Suzuki, 1983) and some studies separated CO_2 from mixtures of calcite and other carbonate minerals such as siderite, ankerite and magnesite (Fritz et al. 1971; Rosenbaum and Sheppard, 1986; Al-aasm et al., 1990). However, so far extraction protocols have not been proposed for multiple-carbonate samples. An attempt was made to develop an extraction procedure for calcite and dolomite/ankerite mixed samples with the following specific aims to:

- reduce the grain size effect on the reaction rates
- reduce the reaction time to a reasonable interval
- avoid using multiple temperature steps as proposed by many earlier workers
- efficiently separate pure end-members without any significant mixing
- propose the exact procedure(s) to be followed for samples having varying proportions of calcite and dolomites

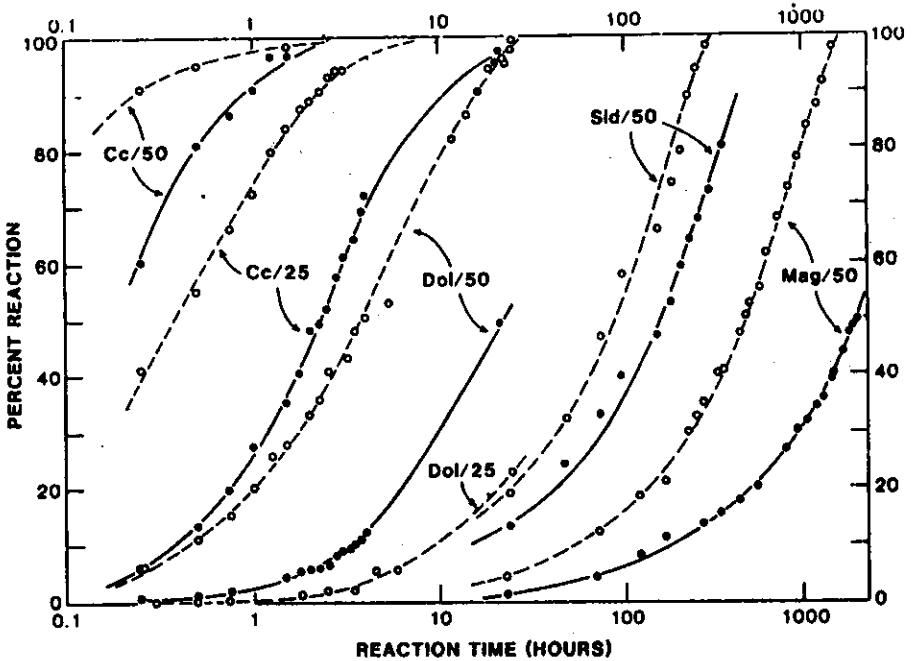

Fig.3.1. *Reaction rates of pure carbonate minerals (expressed in cumulative percent of theoretical yield) with phosphoric acid vs. reaction time (in hours) at 25°C and 50°C, respectively. The open circles denote the < 200 mesh grain size fraction and the filled circles represent the 100-140 mesh size fraction (from Al-aasm et al., 1990)*

For this experiment, pure calcite and dolomite (verified by X-ray diffractometry) standards were selected, powdered and sieved to <325 and >400 mesh size (between 37 to 45 μm size) and then dried in oven at 110°C. Such uniform fine grained powders were used to enhance the reaction rate as well as to reduce the grain size effect on the reaction. When these pure calcite and dolomites were reacted with H_3PO_4 at 25°C, it was found that for calcite 100% CO_2 comes out after 10 hours reaction time and for dolomite 100% CO_2 comes out after 120 hours of reaction. However, ~ 50 to 55% of the total gas from calcite (also dolomite), collected before the completion of the reaction, was found to give $\delta^{13}C$ and $\delta^{18}O$ values of pure calcite (dolomite) (within experimental uncertainty), i.e. 50 to 55% of the total gas amount appears to be good enough to measure the isotopic compositions of calcite or dolomite. This confirms the observations made by Epstein et al. (1964), Al-aasm et al. (1990) and Knudsen and Buchardt (1991). Our results are presented in tables 3.2 and 3.3. It was found that for pure dolomites 72 hours of reaction time is sufficient to give the true representative CO_2 of the whole sample and for pure calcite 15 min. reaction time is sufficient. Pure calcite and pure dolomite isotopic compositions (averages of eight measurements each) were found to be:

Calcite: $\delta^{13}C_{V\text{-}PDB} = -2.8 \pm 0.1$ ‰

$\delta^{18}O_{V\text{-}PDB} = -10.9 \pm 0.2$ ‰

Dolomite: $\delta^{13}C_{V\text{-}PDB} = +0.6 \pm 0.1$ ‰

$\delta^{18}O_{V\text{-}PDB} = -9.1 \pm 0.2$ ‰

$\delta^{13}C$ and $\delta^{18}O$ of dolomite are 3.4 ‰ and 1.8 ‰ higher than those of calcite, respectively.

Table 3.2. Yield and isotopic composition of calcite-CO_2 from various mixtures

Sample	Calcite:Dolomite	% Yield of Calcite-CO_2	Reaction Time (min.)	$\delta^{13}C$ (‰)	$\delta^{18}O$ (‰)
MX-15	22:78	54	5	-2.6	-10.8
MX-18	32:68	49	15	-2.7	-10.8
MX-22	36:64	67	15	-2.7	-10.7
MX-26	21:79	73	15	-2.7	-11.1
MX-19	80:20	78	30	-2.8	-10.8

MX-28	62:38	78	30	-2.8	-10.8
MX-34	100:00	63	30	-2.9	-10.8
MX-30	91:09	77	60	-2.8	-10.8
MX-1	80:20	84	120	-2.8	-11.0
MEAN				-2.8±0.1	-10.8±0.1
Pure calcite (av of 8)	100:00	100	600	-2.8 ± 0.1	-10.9 ± 0.2

Table 3.3. Yield and Isotopic composition of dolomite-CO_2 from various mixture

Sample	Calcite:Dolomite	% Yield of Dolomite-CO_2	Reaction Time (hours)	$\delta^{13}C$ (‰)	$\delta^{18}O$ (‰)
MX-5	20:80	57	78	0.7	-9.1
MX-9	19:81	56	72	0.7	-9.2
MX-11	21:79	55	72	0.6	-9.0
MX-17	20:80	56	72	0.6	-9.0
MX-19	80:20	59	72	0.5	-9.2
MX-20	64:36	56	72	0.6	-9.1
MX-25	32:68	57	72	0.6	-9.0
MX-26	21:79	55	72	0.7	-9.1
MX-27	43:57	58	72	0.6	-9.2
MX-30	91:09	70	120	0.6	-9.1
MX-32	10:90	64	120	0.6	-9.3
MX-33	11:89	64	120	0.6	-9.1
MEAN				0.6±0.1	-9.1±0.1
Pure dolomite (av of 8)	0:100	100	120	0.6 ± 0.1	-9.1 ± 0.2

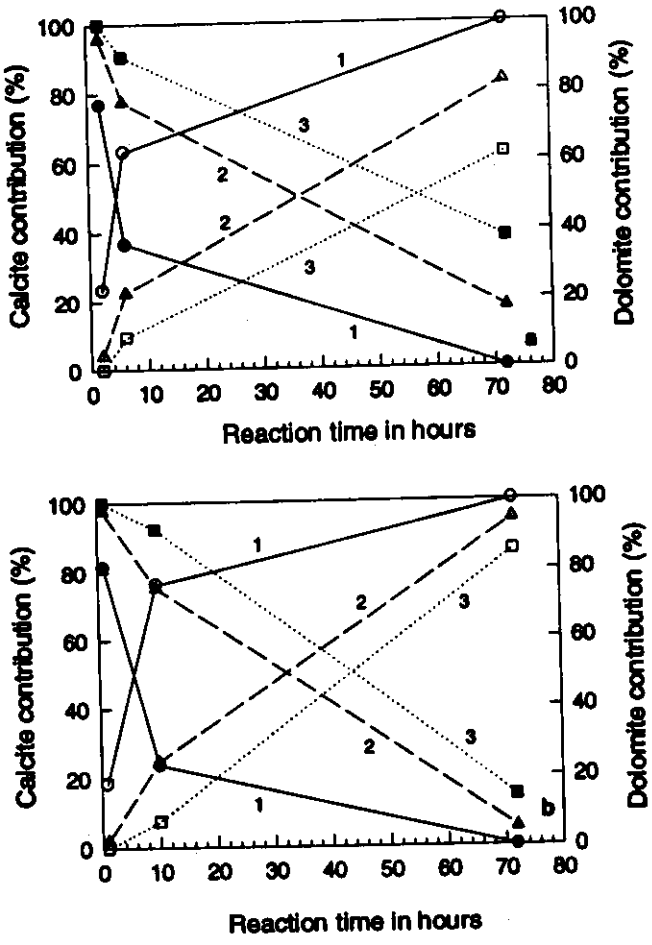

Fig. 3.2. Calcite and dolomite contributions to CO_2 extracted at different steps versus reaction time for three different mixtures (1 for calcite:dolomite = 20:80; 2 for calcite:dolomite = 60:40; 3 for calcite:dolomite = 80:20). (a) plots the results from procedure-I and (b) from procedure-II (see section 3.2.2b). Filled symbols (represent calcite contributions and corresponding dolomite contributions are represented by open symbols. The contributions of the calcite and dolomite were calculated knowing the $\delta^{13}C$ of the end-members and the $\delta^{13}C$ of the extracted gas. $\delta^{13}C$ was preferred to $\delta^{18}O$ because the analytical uncertainty of the former is less.

Different weight proportions of these calcite and dolomite powders were physically mixed to prepare samples having wide ranges of calcite:dolomite ratios. Then the samples were taken in side-arm reaction vessels (35 cc) with the side arms filled with ~2 ml of 100% H_3PO_4 acid. After evacuation samples were reacted at 25°C. CO_2 was extracted following stepwise extraction procedures advocated by earlier workers (Walters et al., 1972; Al-aasm et al., 1990). Many different combinations of

intermediate extraction were also tried out. Results of two such procedures are shown in Fig.3.2 for three different mixtures (calcite:dolomite in Mix-1 = 20:80, in Mix-2 = 40:60 and in Mix-3 = 80:20). In procedure-1, first 2 hours reaction time was given for calcite CO_2 to evolve which was then extracted out of the bottle, then after 6 hours the CO_2 was extracted and rejected as it contained mixed CO_2 and then after 72 hours the CO_2 was collected for dolomite-CO_2 . In this procedure each time an aliquot of CO_2 was taken out in a particular volume (46.7 cc) in the extraction line. In procedure-2, only 1 hour was given for calcite-CO_2 while dolomite-CO_2 was collected from the reaction of the sample from 10 hours to 72 hours time with an in between (1 to 10h) CO_2-rejection. In this procedure, except for the calcite fraction (i.e. 1 hour extraction), each time all CO_2 was extracted out of the bottle. Then the gases collected at different steps were measured for $\delta^{13}C$ and $\delta^{18}O$ compositions. In Fig.3.2, dolomite-CO_2 and calcite-CO_2 contributions are plotted (calculated from $\delta^{13}C$ of CO_2 collected in different steps) against the reaction time. It was observed that in all mixtures except the mixtures having calcite > 80% (curve-3, Fig.3.2), the CO_2 extracted in the first step (which was expected to contain only calcite-CO_2) had contributions from dolomite (curves-1 and 2, Fig.3.2). Similarly in the last step, the CO_2 extracted (which was expected to contain only dolomite-CO_2) had contributions from calcite except for mixtures having >80% dolomite. It was also observed that the extent of contamination of calcite-CO_2 by dolomite-CO_2 in mixtures increased with the increase in the dolomite content in the sample and vice-versa. High CO_2 pressure inside the reaction bottles found to reduce the reaction rate resulting in low yield of dolomite-CO_2.

Different other combinations of reaction durations were tried out but all failed to give pure end-member values following a single extraction procedure for various mixtures. Finally, I came out with two different procedures for two different kinds of mixtures using which it was possible to get the isotopic compositions of the pure end-members. The proposed two procedures for calcite enriched mixtures (calcite >50%) and dolomite enriched mixtures (dolomite >50%) are given below:

For mixtures having Calcite >50% (25°C):

1. CO_2 to be collected after first 30 minutes of reaction: Calcite-CO_2.
2. 30 min. to 1 hour of reaction: Mixed CO_2, to be pumped.
3. 1 hour to 4 hours of reaction: Mixed CO_2, to be pumped.
4. 4 hours to 10 hours of reaction: Mixed CO_2, to be pumped.
5. 10 hours to 72 hours of reaction: To be collected for Dolomite-CO_2.

For mixtures having Dolomite >50% (25°C):

1. CO_2 to be collected after 15 minutes of reaction: Calcite-CO_2.
2. 15 min. to 10 hours of reaction: Mixed-CO_2, to be pumped.
3. 10 hours to 72 hours of reaction: To be collected for Dolomite-CO_2.

In between pumping steps are required to reduce the overlying CO_2 pressure on the reactants to make the reaction faster (law of mass action) and also to reduce the chance of intermixing of dolomite-CO_2 with calcite-CO_2. In the case of calcite enriched mixtures, three intermediate steps of pumping are required to remove mixed CO_2 and to reduce the overlying CO_2 pressure, while in dolomite enriched mixtures we need only one such intermediate pumping. These procedures found to work satisfactorily for various mixtures except for the mixtures having <10% calcite (or dolomite) (Table 3.4). From such mixtures it was extremely difficult to take out the pure CO_2 of the minor carbonate. Hence such mixtures may be treated as pure carbonates of the major carbonate mineral. In such a case isotopic compositions of the major carbonate would be affected only if the isotopic compositions of the minor mineral are very different from those of the major. Table 3.4 gives the results of $\delta^{13}C$ and $\delta^{18}O$ measurements of calcite and dolomite fractions from different mixtures from which CO_2 was extracted following the above described selective extraction procedures. In Fig.3.3, cumulative yields are plotted against the reaction time. For calcite dominant mixtures almost 100% total yield could be achieved in 72 hours (Fig.3.3a), whereas for dolomite dominant samples the cumulative yield was around ~85% after 72 hours (Fig.3.3b). Though all CO_2 from dolomite did not evolve in 72 hours of reaction in the case of dolomite dominant mixtures, the CO_2 from the last extraction (~55% of the total expected CO_2 from dolomite fraction) when analyzed for $\delta^{13}C$ and $\delta^{18}O$, gave the pure dolomite values.

Table 3.4. $\delta^{13}C$ and $\delta^{18}O$ of calcite and dolomite of various carbonate mixtures.

I. Results of mixtures having calcite >50% by weight

Calcite:Dolomite	30 min. CO_2		72 hours CO_2	
	$\delta^{13}C_{V\text{-}PDB}$ (‰)	$\delta^{18}O_{V\text{-}PDB}$ (‰)	$\delta^{13}C_{V\text{-}PDB}$ (‰)	$\delta^{18}O_{V\text{-}PDB}$ (‰)
91:09	-2.8	-10.7	0.4	-9.4
80:20	-2.8	-10.8	0.6	-9.2
74:26	-2.8	-10.8	0.6	-9.2
66:34	-2.8	-11.0	--	--
64:36	--	--	0.6	-9.1
62:38	-2.8	-10.8	--	--

II. Results of mixtures having dolomite >50% by weight

Calcite:Dolomite	15 min. CO_2		72 hours CO_2	
	$\delta^{13}C_{V\text{-}PDB}$ (‰)	$\delta^{18}O_{V\text{-}PDB}$ (‰)	$\delta^{13}C_{V\text{-}PDB}$ (‰)	$\delta^{18}O_{V\text{-}PDB}$ (‰)
09:91	-2.1	-10.2	0.6	-9.3
10:90	-2.1	-10.5	0.6	-9.1
18:82	-2.4	-10.6	--	--
20:80	--	--	0.6	-9.1
21:79	-2.7	-11.1	0.7	-9.1
22:78	-2.6	-11.0	0.7	-9.1
32:68	-2.7	-10.6	0.6	-9.1
36:64	-2.7	-10.7	--	--
43:57	-2.7	-10.6	0.6	-9.2

Note: Reproducibility of $\delta^{13}C$ and $\delta^{18}O$ measurements is 0.1 ‰ for standards (see section 3.2.2c). End-members compositions are calcite: $\delta^{13}C = -2.8 \pm 0.1$ ‰ & $\delta^{18}O = -10.9 \pm 0.2$ ‰, dolomite: $\delta^{13}C = 0.6 \pm 0.1$ ‰ & $\delta^{18}O = -9.1 \pm 0.2$ ‰ (average of eight measurements). All the above $\delta^{18}O$ values for dolomite-CO_2 are uncorrected for the difference in acid fractionation between dolomite and calcite.

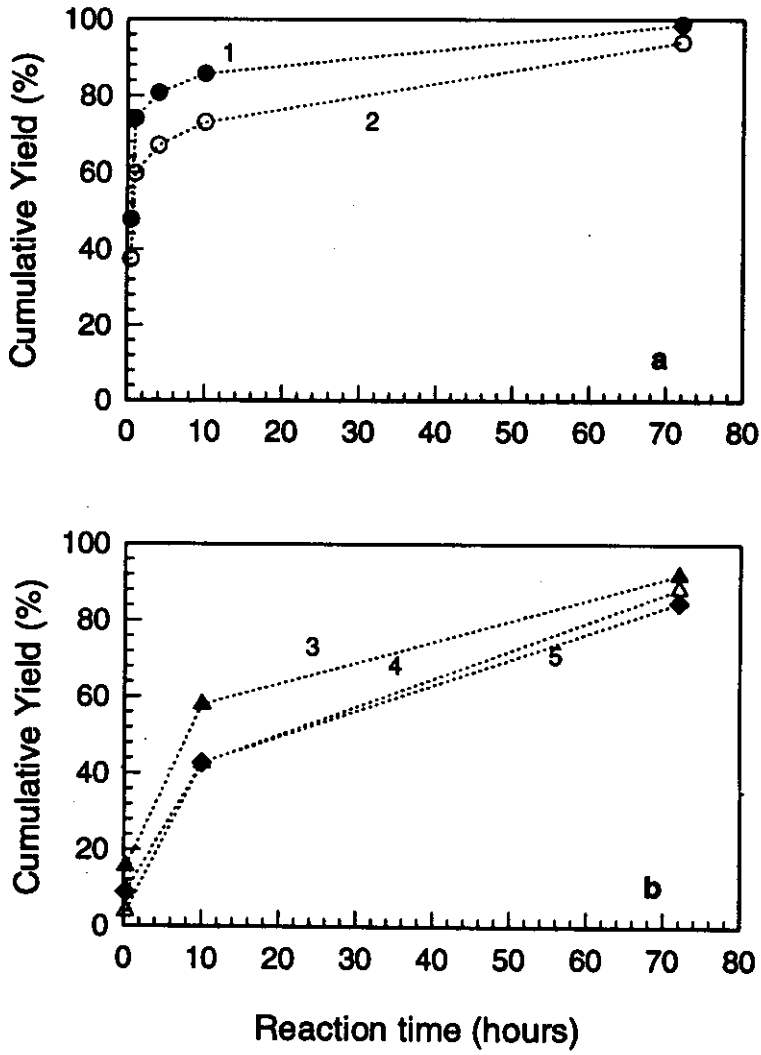

Fig.3.3. *Plot of cumulative CO_2 yield vs. reaction time for different carbonate mixtures when, (a) calcite is > 50 % and (b) dolomite is > 50 %, in the mixture. CO_2 was extracted following the selective extraction procedures (see section 3.2.2b). Calcite: Dolomite in 1 = 80:20; 2 = 62:38; 3 = 43:57; 4 = 32:68; and 5 = 20:80. (From sample weight, weight proportions of calcite and dolomite, manometric pressure of CO_2 collected, the yield was calculated as observed number of micromoles/ expected number of micromoles of CO_2).*

Following the selective CO_2 extraction procedures, CO_2 from calcites, dolomite/ankerites of dolomite bearing calcite-carbonatites, dolomite carbonatite and ferrocarbonatites were extracted for isotopic measurements. This is because the time taken to evolve CO_2 from ankerite is similar to that from dolomite (Rosenbaum and Sheppard, 1986).

3.2.2c. Mass Spectrometry

$\delta^{13}C$ and $\delta^{18}O$ of CO_2 were measured using a triple collector VG Micromass 903 mass-spectrometer with respect to a pre-calibrated internal laboratory standard CO_2 (Foram-Standard CO_2) and then converted to V-PDB and V-SMOW respectively. The acid fractionation factors used for $\delta^{18}O$ measurements of calcite, dolomite and ankerite were 1.01025 (Friedman and O'Neil, 1977), 1.01186 and 1.01177 (Rosenbaum and Sheppard, 1986), respectively. The whole process of data collection and reduction was automated. For this SIRA software (VG Isotech) was used.

(i) Calibration of laboratory standard CO_2

The Foram- CO_2 laboratory standard (Lab Std) was calibrated against V-PDB using an international standard NBS-19 (Toilet Seat limestone). For NBS-19, IAEA recommended values ($\delta^{13}C_{V\text{-}PDB}$ = -1.95 and $\delta^{18}O_{V\text{-}PDB}$ = -2.2) were used. The calibration procedure involved the following steps.

1. $\delta^{45\ NBS\text{-}19}{}_{V\text{-}PDB}$ and $\delta^{46\ NBS\text{-}19}{}_{V\text{-}PDB}$ were calculated from the recommended $\delta^{13}C$ and $\delta^{18}O$ values using Craig equations, (Craig, 1957) modified for a triple collector machine (Gonfiantini, 1981).
2. Ten samples of NBS-19 were analyzed following McCrea (1950)'s CO_2 extraction procedure and mean values of $\delta^{45\ NBS\text{-}19}{}_{Lab\ Std}$ and $\delta^{46\ NBS\text{-}19}{}_{Lab\ Std}$ were taken.
3. $\delta^{45\ Lab\ Std}{}_{NBS\text{-}19}$ and $\delta^{46\ Lab\ Std}{}_{NBS\text{-}19}$ were calculated using the equation: $\delta^{Lab\ Std}{}_{NBS\text{-}19} = (-\delta^{NBS\text{-}19}{}_{Lab\ Std})/(1+10^{-3}\ \delta^{NBS\text{-}19}{}_{Lab\ Std})$
4. The $\delta^{45\ Lab\ Std}{}_{V\text{-}PDB}$ and $\delta^{46\ Lab\ Std}{}_{V\text{-}PDB}$ values which were required (called offsets) for calibration were found out using the relations:

$$\delta^{45\ Lab\ Std}{}_{V\text{-}PDB} = \delta^{45\ Lab\ Std}{}_{NBS\text{-}19} + \delta^{45\ NBS\text{-}19}{}_{V\text{-}PDB} + 10^{-3}\ \delta^{45\ Lab\ Std}{}_{NBS\text{-}19}\ \delta^{45\ NBS\text{-}19}{}_{V\text{-}PDB}$$

$$\delta^{46\ Lab\ Std}{}_{V\text{-}PDB} = \delta^{46\ Lab\ Std}{}_{NBS\text{-}19} + \delta^{46\ NBS\text{-}19}{}_{V\text{-}PDB} + 10^{-3}\ \delta^{46\ Lab\ Std}{}_{NBS\text{-}19}\ \delta^{46\ NBS\text{-}19}{}_{V\text{-}PDB}$$

(ii) Precision and Reproducibility

The mass spectrometric precision (1σ) for a single sample (12 sets of ratios) was better than ±0.01 ‰ for $\delta^{13}C$ and ±0.02 ‰ for $\delta^{18}O$. When the same gas was run several times the reproducibility of the measurements remained same as the precision of individual runs given above.

An international carbonatite standard NBS-18 was run at regular intervals of time (Table 3.5), whose long term average matches well with the IAEA (1995) values within 1σ level of error. For inter-laboratory comparison an internal standard (MAKMARB; a homogenized powder of pure marble) was sent to Godwin Laboratory (Cambridge), whose $\delta^{13}C$ and $\delta^{18}O$ values agree well with our long term averages within the 1σ level of error (see Table 3.6).

Table 3.5. International carbonatite standard (NBS-18)

Date	$\delta^{13}C_{V\text{-}PDB}$ (‰)	$\delta^{18}O_{V\text{-}PDB}$ (‰)
6.8.93	-5.11	-23.08
16.8.93	-5.13	-23.15
8.4.94	-4.92	-22.98
15.4.94	-4.96	-22.85
14.6.94	-5.12	-22.99
25.5.95	-5.05	-22.97
27.12.96	-5.06	-22.88
30.1.96	-5.04	-22.83
8.3.96	-5.11	-23.02
22.8.96	-5.13	-23.09
28.8.96	-5.02	-23.05
18.8.96	-5.04	-23.09
Mean	-5.058 ± 0.068 (1σ)	-22.998 ± 0.102 (1σ)
IAEA Recommended Values (1995)	-5.029 ± 0.049 (1σ)	-23.035 ± 0.172 (1σ)

Table 3.6. MAKMARB (Makrana Marble - an internal calcite standard)

Date	$\delta^{13}C_{V\text{-}PDB}$ (‰)	$\delta^{18}O_{V\text{-}PDB}$ (‰)
30.6.93	3.72	-10.83
19.7.94	3.69	-10.79
9.9.94	3.86	-10.54
7.10.94	3.86	-10.67
14.4.95	3.77	-10.69
25.5.95	3.88	-10.71
3.8.95	3.76	-10.70
2.9.95	3.86	-10.33

4.9.95	3.74	-10.59
18.9.95	3.77	-10.74
27.12.95	3.78	-10.90
1.1.96	3.90	-10.63
Mean	3.81 ± 0.08 (1σ)	-10.69 ± 0.12 (1σ)
Cambridge Values (1983)	3.81 ± 0.03 (1σ)	-10.63 ± 0.05 (1σ)

3.2.2d. Inter-laboratory Comparisons

To check our measurements for systematic errors, inter-laboratory comparison was done by comparing our results on one of our internal carbonate standards (MAKMARB) with the results obtained by Godwin Laboratory (Cambridge). As already discussed, Table 3.6 gives this comparison and it can be seen that the results agree among themselves within the experimental uncertainties (1σ). In addition to this, I also measured some carbonatite samples (Qaqarssuk carbonatites) provided by Dr. Christian Knudsen of the Geological Survey of Greenland, Denmark on our request. These samples include pure calcite bearing calciocarbonatites, carbonatites containing different proportions of calcite and dolomite and beforsites (pure dolomite bearing carbonatites). For pure calcite samples the CO_2 extraction procedures followed in both the laboratories were similar (25°C reaction and total CO_2 extraction after 24 hours but the H_3PO_4 used by them was 98 %), whereas for samples having calcite and dolomite mixtures the extraction procedures were slightly different. In their case (Knudsen and Buchardt, 1991), calcite-CO_2 was extracted after 2 hours and dolomite-CO_2 was extracted from the acid reaction between 4 to 18 hours of time with an in-between pumping (2 to 4 hours). I extended the reaction for the rejection interval from 2 hours to 4 hours (2 to 6 hours) and dolomite-CO_2 was collected from the reaction interval 6 hours to 24 hours. For pure dolomite bearing samples, again, similar procedures were followed (24 hours reaction and complete extraction). The comparison of results is given in Table 3.7. It was found that in the case of pure calcites (320536,7), there is a systematic difference between $\delta^{13}C$ (also $\delta^{18}O$) values measured by Knudsen and Buchardt (1991) and results of this work (Table 3.7 and Fig.3.4a). My $\delta^{13}C$ values are ~0.31 ‰ more negative. This is also seen in the calcite-CO_2 of the calcite-dolomite mixtures. Similarly my $\delta^{18}O$ values for pure calcites are more positive by ~0.35 ‰. The other samples show an enrichment of 0.3 to 0.7 ‰ in calcite-CO_2. Likewise, for

pure dolomite (320488) my $\delta^{13}C$ value is 0.51 ‰ more negative and $\delta^{18}O$ value is 1.37 ‰ more negative, whereas the dolomite-CO_2 from mixtures show difference ranging between +0.33 to -0.42 ‰ in $\delta^{13}C$ and +1.62 to -0.62 ‰ in $\delta^{18}O$. I have already eliminated systematic errors by the analyses of international carbonatite standard (NBS-18) and inter-laboratory comparison of internal standard (MAKMARB) of our laboratory measurements. Such an exercise was probably not done by Knudsen and Buchardt (1991). Hence, the observed systematic difference in the δ values of Greenland samples measured by us and them could be due to the inter-laboratory differences in the analytical conditions (choice of mass spectrometric reference material; instrumental drift effects; percentage of H_3PO_4 in the acid used etc.). $\delta^{13}C$ and $\delta^{18}O$ values of dolomites from mixed carbonates and dolomite carbonatites showed random differences (Table 3.7 and Fig.3.4b) which could be attributed to the differences in the extraction procedures. As I have increased the pumping interval for the mixed-CO_2, it is possible that my dolomite-CO_2 is less contaminated with calcite-CO_2.

Table 3.7. Inter-laboratory comparison for Qaqarssuk carbonatite samples*

Sample	Mineral	Modal % carbonate	Knudsen & Buchardt (1991)		This Study	
			$\delta^{13}C_{V\text{-}PDB}$ (‰)	$\delta^{18}O_{V\text{-}SMOW}$ (‰)	$\delta^{13}C_{V\text{-}PDB}$ (‰)	$\delta^{18}O_{V\text{-}SMOW}$ (‰)
252540	calcite	47	-1.04	16.39	-1.37	16.72
	dolomite	53	-2.73	10.58	-2.40	12.20
320411	calcite	30	-3.27	7.32	-3.58	8.02
	dolomite	70	-3.21	7.50	-3.47	6.96
320430	calcite	59	-3.9	7.93	-4.28	8.42
	dolomite	41	-3.35	8.84	-3.77	8.22
320488	dolomite	100	-2.74	10.39	-3.25	9.02
320536	calcite	100	-4.60	7.50	-4.87	7.76
320537	calcite	100	-4.68	7.11	-5.03	7.56
320522	ankerite	100	-2.52	9.93	-2.83	10.52

* dolomite $\delta^{18}O$ values were corrected in both cases using acid fractionation factor of 1.01109 (Knudsen and Buchardt, 1991).

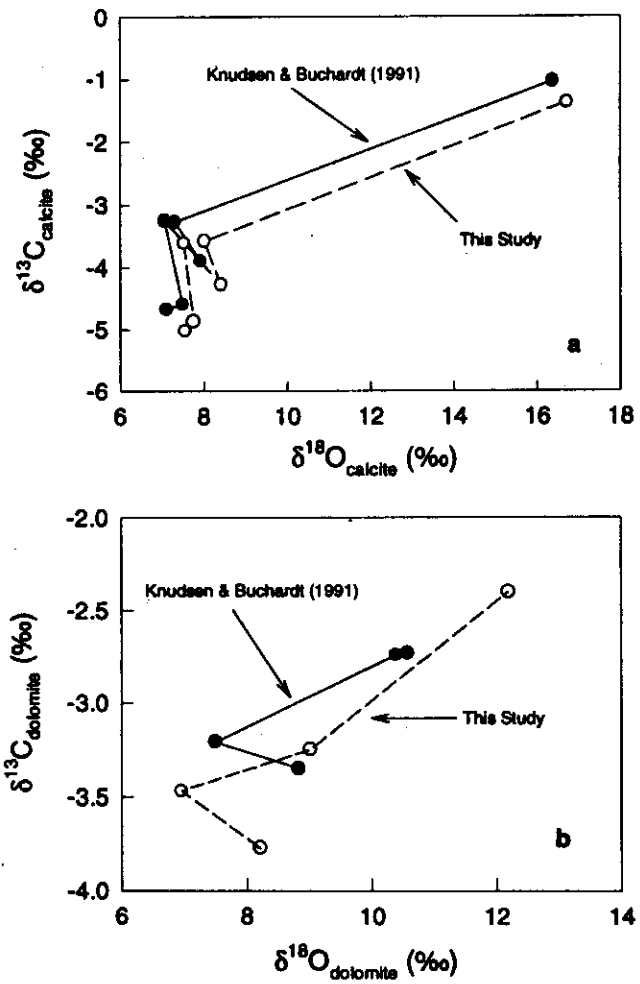

Fig. 3.4. Plots of $\delta^{13}C$ and $\delta^{18}O$ of calcites (a) and dolomites (b) from Qaqarssuk carbonatite samples. Filled circles are results from Knudsen and Buchardt (1991) and open circles represent values from this study on the same samples. Solid lines join values of Knudsen and Buchardt (1991) and dashed line join values of the present study.

3.3 ^{40}Ar-^{39}Ar METHOD OF DATING

3.3.1a Principle

Potassium (Z=19), an alkali metal, has three naturally occurring isotopes ^{39}K, ^{40}K and ^{41}K. Out of these ^{40}K is radioactive, 11.2 % of which decays to stable ^{40}Ar by electron capture (decay constant = 0.581×10^{-10} y^{-1}) and 88.8 % decays to ^{40}Ca by beta decay (decay constant = 4.962×10^{-10} y^{-1}). The growth of radiogenic ^{40}Ar in a K-bearing

system closed with respect to K and Ar during its life time is used to determine the age of the system by the K-Ar method of dating. The details of this dating technique have been provided by McDougall (1966), Damon (1970) and Hunziker (1979). As discussed by these authors this method has major limitations such as (i) difficulty in knowing the loss or excess of Ar in the sample, which can lead to uncertainty in the age of the sample; (ii) sample heterogeneity can cause erroneous K and Ar estimations as these analyses are done in two different aliquots of a sample; (iii) quantity of sample required is large, hence, small samples cannot be dated using this method. The ^{40}Ar-^{39}Ar method of dating is a variant of K-Ar method, which overcomes these limitations.

The basis of ^{40}Ar-^{39}Ar method of dating is the formation of ^{39}Ar by irradiation of the samples with fast neutrons (threshold energy = 1.2 MeV) following the reaction $^{39}K_{19}(n,p)^{39}Ar_{18}$. This reaction permits the K determination for a K-Ar age as a part of the argon isotope analysis in a single aliquot of the sample. The ^{39}Ar thus produced is radioactive, however, because of its large half life (269±3 years), it can be treated as a stable isotope during the short time involved in the analysis. After irradiation, the sample is either fused or incrementally heated until fusion and argon released during this process is measured for isotopic ratios mass-spectrometrically.

The number of atoms of ^{39}Ar produced, due to irradiation with fast neutrons, is given by:

$$^{39}Ar_K = {}^{39}K\, \Delta T \int \Phi(\varepsilon)\, \sigma(\varepsilon)\, d\varepsilon \qquad (1)$$

where ^{39}K is the number of atoms of this isotope in the irradiated sample, ΔT is the length of irradiation, $\Phi(\varepsilon)$ is the neutron flux density at energy ε and $\sigma(\varepsilon)$ is the neutron capture cross section at energy ε for the $^{39}K_{19}(n,p)^{39}Ar_{18}$ reaction. The integration is over all energies of the incident neutrons. The equation for the number of radiogenic ^{40}Ar atoms in the sample is

$$^{40}Ar^* = (\lambda_e/\lambda)\, {}^{40}K\, (e^{\lambda t}-1) \qquad (2)$$

where λ_e is the decay constant for electron capture and λ is the total decay constant of ^{40}K (= $\lambda_e + \lambda_\beta$; where λ_β is the decay constant for the β^- decay of ^{40}K to ^{40}Ca). Hence combining (1) and (2) we get an expression for $^{40}Ar^*/^{39}Ar_K$ which is

$$^{40}Ar^*/^{39}Ar_K = (\lambda_e/\lambda)\, [{}^{40}K\, (e^{\lambda t}-1)] \,/\, [{}^{39}K\, \Delta T \int \Phi(\varepsilon)\, \sigma(\varepsilon)\, d\varepsilon] \qquad (3)$$

To simplify, it is conventional to define the quantity

$$J = (\lambda/\lambda_e)\ {}^{39}K/{}^{40}K\ \Delta T \int \Phi(\varepsilon)\ \sigma(\varepsilon)\ d\varepsilon \quad (4)$$

then rewrite equation (3) as

$${}^{40}Ar^*/{}^{39}Ar_K = (e^{\lambda t}-1)/J \quad (5)$$

which gives the age equation upon rearrangement:

$$t = (1/\lambda)\ \ln\ [({}^{40}Ar^*/{}^{39}Ar_K)\ J + 1] \quad (6)$$

The equation (6) can give us the age of the sample provided the quantity J is known. J depends on neutron flux density and capture cross section that are difficult to determine. However, J can be determined by irradiating a sample of known age (called a monitor) together with samples whose ages are unknown. After measuring ${}^{40}Ar^*/{}^{39}Ar$ of the monitor, the equation (5) is used to find J :

$$J = (e^{\lambda t_m} - 1)\ /({}^{40}Ar^*/{}^{39}Ar)_m \quad (7)$$

where subscript m denotes monitor; t_m is the age of the monitor.

This value of J is then used in equation (6), together with the ${}^{40}Ar^*/{}^{39}Ar_K$ of the samples irradiated at the same time, to calculate the ages of these samples. The dates obtained by complete fusion are called as "total argon release dates" which have similar limitations as K-Ar dating method but avoid problems arising from sample heterogeneity.

3.3.1b. Correction for Interfering Isotopes

If the only contaminant present in the irradiated sample were atmospheric argon, then ${}^{40}Ar^*/{}^{39}Ar_K$ could be calculated from measured ${}^{40}Ar/{}^{39}Ar$ and ${}^{36}Ar/{}^{39}Ar$ ratios using

$${}^{40}Ar^*/{}^{39}Ar_K = ({}^{40}Ar/{}^{39}Ar)_{meas} - ({}^{40}Ar/{}^{36}Ar)_{atm}({}^{36}Ar/{}^{39}Ar)_{meas} \quad (8)$$

where "meas" is used for measured and "atm" is used for atmospheric. $({}^{40}Ar/{}^{36}Ar)_{atm}$ is normally taken as 295.5. However, when a rock is irradiated, many undesirable neutron reactions with different elements produce interfering argon isotopes. These reactions have been discussed in detail by Mitchell (1968), Brereton (1970), Dalrymple and Lanphere (1971), Turner (1971), Tetley et al. (1980) and Dalrymple et al. (1981).

The most important interfering reactions are those involving Ca and K: $^{40}Ca(n,n\alpha)^{36}Ar$, $^{42}Ca(n,\alpha)^{39}Ar$, and $^{40}K(n,p)^{40}Ar$. Therefore, to determine the actual $^{40}Ar^*/^{39}Ar_K$ ratio of the sample, the $^{40}Ar/^{39}Ar$ ratio measured needs to be corrected for atmospheric, calcium and potassium derived interfering isotopes. Another isotope of Ar, ^{37}Ar, which is primarily derived from ^{40}Ca by the reaction $^{40}Ca(n,\alpha)^{37}Ar$, is used in correction of both reactor induced ^{36}Ar and ^{39}Ar (Brereton, 1970). The correction factors $(^{36}Ar/^{37}Ar)_{Ca}$ and $(^{39}Ar/^{37}Ar)_{Ca}$ are determined by measuring the relative production rates of these isotopes in a pure calcium salt (CaF_2) irradiated along with the samples. The correction factor $(^{40}Ar/^{39}Ar)_K$ is determined by measuring the relative production rates of these isotopes in an irradiated pure potassium salt (K_2SO_4). Incorporating these corrections the expression for $(^{40}Ar^*/^{39}Ar)_K$ becomes

$$^{40}Ar^*/^{39}Ar_K=\{(^{40}Ar/^{39}Ar)_{meas}-295.5[(^{36}Ar/^{39}Ar)_{meas}-(^{36}Ar/^{37}Ar)_{Ca}(^{37}Ar/^{39}Ar)_{meas}]\}/\{1-(^{39}Ar/^{37}Ar)_{Ca}(^{37}Ar/^{39}Ar)_{meas}\}-\{(^{40}Ar/^{39}Ar)_K\} \quad (9)$$

where $(^{40}Ar/^{39}Ar)_{meas}$, $(^{36}Ar/^{39}Ar)_{meas}$ and $(^{37}Ar/^{39}Ar)_{meas}$ are measured ratios and $(^{36}Ar/^{37}Ar)_{Ca}$, $(^{39}Ar/^{37}Ar)_{Ca}$ and $(^{40}Ar/^{39}Ar)_K$ are the correction factors determined for a given reactor.

3.3.1c. Decay correction

^{37}Ar and ^{39}Ar produced by irradiation are radioactive, so it is important to correct for their decays in the total time involved in analysis. Fortunately, the larger half life of ^{39}Ar (269±3 years) enables us to neglect the correction involved for its decay. However, ^{37}Ar has a half life of only 35.1 days, therefore, significant decay of it will occur during the time involved in the whole process of analysis. Therefore, proper corrections must be made for this. The general equation for the decay factor given by Brereton (1970) and Dalrymple et al. (1981) is :

$$\text{Decay factor} = \lambda t\, e^{\lambda t'}/(1-e^{-\lambda t}) \quad (10)$$

where t is the irradiation time, t' is the time elapsed since the end of the irradiation and analysis and λ is the decay constant for ^{37}Ar. If the irradiation was done in a number of discrete intervals or segments then the decay factor is calculated using the following equation (Wijbrans, 1985 and Pande et al., 1988).

$$\text{Decay factor} = \lambda\sum_1^n t_i \,/\, \sum_1^n[(1-e^{-\lambda t_i})/e^{-\lambda t'_i}] \quad (11)$$

where t_i is the duration of irradiation of segment I, t_i' is the time elapsed between the end of the irradiation segment I and analysis of the sample, n is the total number of irradiation segments and λ is the decay constant for ^{37}Ar.

3.3.1d. The Incremental Heating Technique

A series of dates (apparent ages) can be obtained for a single sample by releasing argon from it in steps at increasing temperatures. If the sample has remained undisturbed (i.e. closed with respect to argon and potassium) since its formation then the apparent ages calculated at each step should be constant. However, if radiogenic argon was lost from some crystallographic sites after its initial cooling, then the $^{40}Ar/^{39}Ar$ ratios of the gas released at different steps may vary so also the apparent ages. Customarily, the apparent ages calculated for different steps are plotted against cumulative ^{39}Ar percentage, which is called an age spectrum. In the case, when apparent ages of different steps (more than four) are constant (within experimental errors), an age called plateau age for the sample is calculated taking the weighted mean of all plateau step ages. Samples affected by metamorphism or other secondary processes show disturbed age spectra and in such cases no plateau age can be calculated. However, a disturbed spectrum may give many other useful information, which are discussed in detail by McDougall and Harrison (1988).

The ^{40}Ar-^{39}Ar method of dating requires a correction for the presence of trapped ^{40}Ar (as discussed in the section 3.3.1b). This component is normally taken to be atmospheric so that $^{40}Ar/^{36}Ar = 295.5$. However, this assumption may not be valid always because there are possibilities when $^{40}Ar/^{36}Ar$ of non-radiogenic component is inherited (incorporation of a non-atmospheric component during crystallization). To evaluate such possibilities argon isotope correlation diagrams ($^{40}Ar/^{36}Ar$ vs. $^{39}Ar/^{36}Ar$ and $^{36}Ar/^{40}Ar$ vs. $^{39}Ar/^{40}Ar$) are useful. In a $^{40}Ar/^{36}Ar$ vs. $^{39}Ar/^{36}Ar$ plot (popularly known as isochron diagram) the plateau steps are plotted and fitted with straight lines, whose intercepts give the non-radiogenic (or trapped) $^{40}Ar/^{36}Ar$. The $^{36}Ar/^{40}Ar$ vs. $^{39}Ar/^{40}Ar$ plot (known as inverse isochron diagram) also helps in a similar manner.

3.3.2. Experimental Details

3.3.2a. Sample Preparation for Irradiation

Whole rock samples of alkaline silicates and phlogopite mineral separates from carbonatites were analyzed. For whole rocks, fresh samples were powdered in a stainless steel mortar and pestle to 100-150 μm size. About 600-700 mg aliquot of homogenized powders were used. For mineral separates (phlogopite), minerals were hand picked from whole rock powders and about 100-200 mg of pure mineral separates were taken for analysis. Whole rock powders and mineral separates were ultrasonicated with 0.05N HCl (to remove unwanted carbonates) and water several times and dried before being packed for irradiation. The 520.4±1.7 Ma old Minnesota Hornblende (MMhb-1) (Samson and Alexander, 1987) was used as a monitor.

The samples and monitor along with pure CaF_2 and K_2SO_4 were packed in aluminum foils and filled in flat-bottomed quartz vials. Two type of vials were used, one 6-7 mm diameter for rock/mineral samples and the other 2-3 mm diameter type for CaF_2, K_2SO_4 and monitor. To minimize the effect vertical neutron flux gradient, all the samples were filled to the same height. To monitor the fluence variation, high purity Ni wire, of the same height as the sample, was placed in each vial. These vials were then sealed and packed in an aluminum reactor can. The reactor can was then sealed and sent for irradiation.

3.3.2b. Irradiation of samples

The samples were irradiated in two batches in APSARA reactor of BARC, Mubmai. APSARA is a light-water moderated reactor with total neutron flux of about 10^{12} n cm^{-2} s^{-2} with the fast neutron flux representing about 50-60% of the total. The samples were irradiated in D4 (core) position of the reactor which receives maximum flux with minimum variation. The irradiation was done for 98 and 100 hours at 1 MW power level in 19 and 22 discrete steps spreading over 19 to 22 days, respectively for two batches. The maximum and minimum duration of the irradiation in a step was 7 and 0.05 hour, respectively. The maximum neutron fluence variation as determined by ^{58}Co activity, which was generated by the same neutron reaction that produces ^{39}K, $^{58}Ni(n,p)^{58}Co$, was found to be 6.0 and 5.0%, respectively in vertical and horizontal

directions. The irradiated samples were allowed to cool for a few weeks to reduce the activity of the samples for safe handling. Samples were then wrapped in aluminum foils and stored in the sample holder of the extraction system.

3.3.2c. Argon Extraction and Purification

Argon extraction and purification was carried in an compact UHV furnace and purification system indigenously developed (Venkatesan et al., 1986). Fig.3.5 shows the schematic of the complete system. It essentially consists of a high vacuum line with appropriate pumping facilities, a furnace assembly in which a sample can be heated in a controlled manner to release argon, getter systems for purification of the released gas, isolation valves and activated charcoal trap cooled at -196°C for moving gas from one part of the system to another.

The furnace consists of a molybdenum crucible electrically heated by a concentric, tantalum mesh filaments surrounded by tantalum radiation shields in a stainless steel vacuum chamber. The temperature of the crucible is measured with a 95 % Pt + 5 % Rh - 80 % Pt + 20 % Rh thermocouple, which has been calibrated earlier by optical pyrometry. The temperatures are estimated with a ± 10°C precision. The outer SS jacket of furnace is connected to chilled water supply for cooling purpose. Samples are dropped into the crucible from a glass sample holder connected to the top flange.

The gas purification system consists of four valves (V_1 to V_4) and three getters, all interconnected and fitted into a single rectangular stainless steel block. The sample gas released from the crucible, first comes in contact with Ti-Zr getter connected between valves V_2 and V_3. The Ti-Zr is kept hot at around 800°C when most of the active gases will either chemically combine with or get absorbed by the getter. Further, on cooling to room temperature this getter absorbs the hydrogen present in the sample gas. Then this cleaned gas, accumulated for about 50 minutes (typical duration given for a temperature step) is allowed to react with another Ti-Zr getter and with SAES getter by opening valve V_2 for further purification. The purified gas is then adsorbed on the charcoal cooled at liquid nitrogen temperature. It is then admitted into the mass-spectrometer, after removing water vapour by passing the gas through the cold finger

kept at liquid nitrogen temperature, by opening V_4. After the gas is equilibrated in the mass-spectrometer, V_4 is closed and remaining gas along with other unwanted gases adsorbed to different units are pumped by opening V_1.

In step-wise extraction (incremental heating) procedure, the samples were degassed in steps, normally nineteen steps of successively higher temperature, starting from 450°C until fusion at about 1400°C with an interval of 50°C. The K_2SO_4, CaF_2 and the monitor sample were, however, degassed in a single (1400°C) temperature step. The gas in each step was purified following the procedure described earlier and then admitted into an AEI MS10 (180° deflection, 5 cm radius) mass-spectrometer having a permanent magnet of 1.8 kilogauss. The mass-spectrometer was operated in the static mode. By voltage scanning, the ions of masses 40, 39, 38, 37 and 36 were collected on a Faraday cup. The acquisition of ion currents (measured sequentially in pico amperes) was done by a computer. Peak heights and relative timing of peak measurement from the time of sample introduction (T_o), which were acquired by a "peakjump" routine, were fed to a curve-fit routine (Bevington, 1969) to compute required isotopic ratios and abundance corresponding to zero time.

Each sample was preceded and followed by several steps of system blank measurements. System-blank estimation consists of measuring the argon concentration for a particular temperature step by following the same procedure as for samples but without any sample in the crucible. 10 to 12 steps of blank measurement were normally done and blank contribution for all temperature steps were calculated by interpolation. The ^{40}Ar blank contributions to the sample gas, in the present work, varied from 0.5 to 10% of the sample-gas for temperature steps up to about 1200°C and increases up to 20% and occasionally to 30% in the fusion step. Table 3.8 gives a typical blank variation in different temperature steps for a sample.

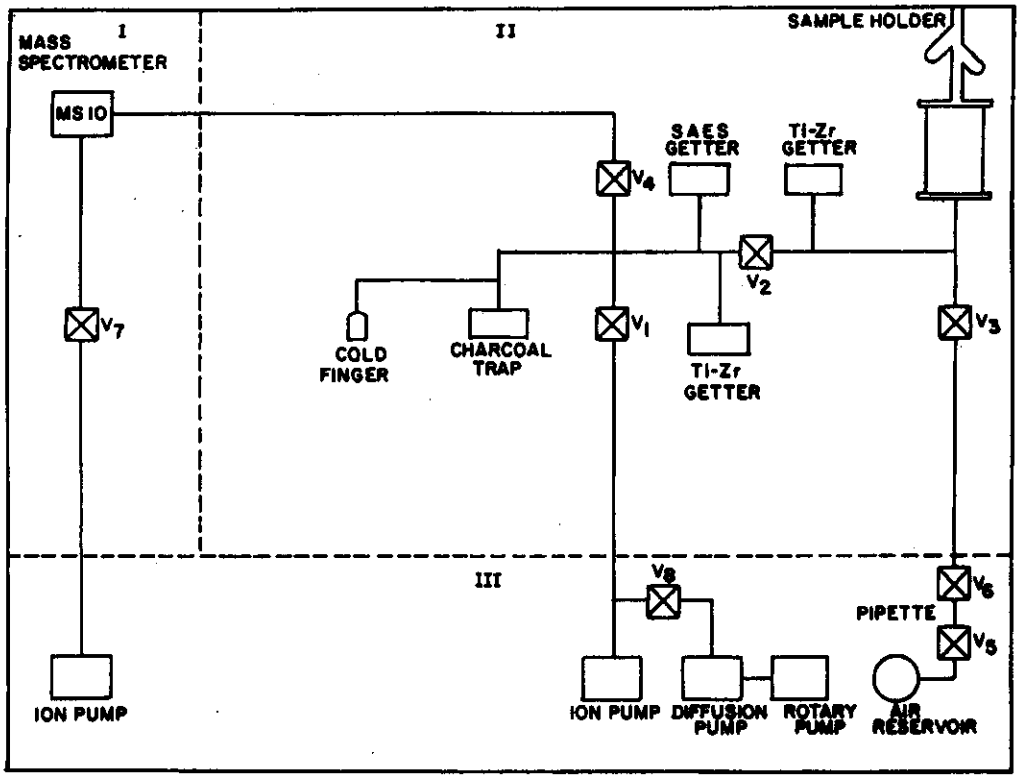

Fig. 3.5. Schematic of the complete Argon Gas Extraction - Purification system. I = Mass Spectrometer, II = Extraction System and III = Pumping System.

Table 3.8. Typical percentage of system blanks for sample AD-16

Temperature	^{40}Ar (%)
450	2.3
500	7.8
550	5.8
650	3.3
700	2.7
750	4.3
800	4.8
850	6.3
900	4.5
950	4.3
1000	2.5
1050	0.67
1100	1.02
1150	4.99
1200	16.56
1250	24.98
1300	26.6
1400	22.4

Mass discrimination (MD) corrections were determined based on analysis of atmospheric argon (AIR SPIKE) introduced from a pipette system connected to the extraction line. Each sample was preceded and followed by an AIR SPIKE analyses and average MD values were found out for corrections in sample ratios. Mass-spectrometer sensitivity was estimated from repeated measurements of the monitor

sample (MMhb-1) and was found to be typically in the range of 0.94 - 2.58 x 10^{-7} cc STP/mv. Errors were computed by quadratically propagating the errors in the measured ratios, blanks and interfering isotopes. The error quoted on the apparent and integrated ages include the error in J but the error boxes in age spectra do not include the error in J. All the errors are quoted at 2σ level. The plateau ages are weighted means of the apparent ages of steps forming the plateaus. A plateau is defined when four of more temperature steps, representing more than 60% of the total ^{39}Ar of the sample, give constant apparent ages (within 2σ levels of error). Weighted means of apparent ages are calculated using the method of Bevington (1969) where $1/\sigma^2_i$(σ_i is the standard deviation for step i) is taken as the weight. Isochron ages have been computed using the two error regression method outlined by York (1969) of data points corresponding to the plateau steps.

3.4. STRONTIUM ISOTOPIC STUDIES

3.4.1. Principle

Rubidium (Z=37) is an alkali metal. It has two naturally occurring isotopes ^{85}Rb and ^{87}Rb of which ^{87}Rb is radioactive. ^{87}Rb decays to stable ^{87}Sr by β^- decay (decay constant = 1.42 $\times$ 10^{-11} y^{-1}). Strontium is an alkaline earth element and normally replaces calcium in crystal lattices. Strontium has four naturally occurring isotopes (^{88}Sr, ^{87}Sr, ^{86}Sr and ^{84}Sr) all of which are stable. The decay scheme of ^{87}Rb to ^{87}Sr is generally used to date rocks which have remained closed to Rb and Sr since their formation. Because of the difference in the geochemical properties of Rb and Sr the Rb/Sr ratio acquires widely different values in rocks and minerals and hence, $^{87}Sr/^{86}Sr$ ratios also vary widely. The Sr isotopic evolution of a system gets affected by complex geological processes; however, evidence for these phenomena is normally preserved in the "initial $^{87}Sr/^{86}Sr$ ratio" of the system. It is this property of Rb-Sr isotope systematics which is used to understand the petrogenetic aspects of the igneous rocks.

3.4.2. Sample Preparation

Fresh samples (each about 4 or 5 kg) were cleaned and broken into small pieces using a hammer. Then these were crushed to <3-5 mm size using a jaw crusher (Fritz pulverizer). The crushing surfaces of the pulverizer were cleaned before and after each

sample and preconditioned with a small amount of the sample to be processed. Crushed sample pieces were mixed thoroughly to ensure homogenization. Then about 300 gm coarse fraction of the each sample was selected by coning and quartering for powdering. This sample fraction was then powdered to <200 mesh size (i.e. <0.074 mm) using a TEMA swing mill and stored in a pre-cleaned and pre-conditioned polythene bottles. This fraction, which is a homogeneous representative of the whole rock sample, was used for Sr-isotopic measurements. Phlogopites were hand picked from whole rock powders for Sr-isotopic measurements. Most of the measurements were carried at our laboratory and part of the measurements were carried out at National Geophysical Research Institute, Hyderabad.

Sr-isotopic analyses were carried out for whole rock samples of alkaline silicate rocks, carbonatites, sandstones, limestones and mineral separates of phlogopite. For dissolution of silicates, about 100-150 mg of representative powder sample was taken in a 25 ml teflon beaker. Mixture of acids (6 ml HF + 2 ml HNO_3) was added in the samples and kept at 150°C in closed cap condition for 6 to 8 hours and then evaporated to dryness at ~100°C. Then a few drops of HNO_3 and 2 ml of 2.5N HCl were added to ensure complete digestion. If samples were not completely dissolved another cycle of acid treatment was given. The final solution was taken in 2.5N HCl. Carbonatites being mixtures of carbonates, oxides and silicates needed a different dissolution procedure for complete dissolution. First a HNO_3 + HCl treatment was given to carbonatites and then to dissolve the silicates and oxide minerals HNO_3 + HF treatment was given. HF amount was decided by the amount of silicates/oxides present in a particular sample. Care was taken to avoid calcium/strontium fluoride precipitation (this was done by HNO_3 + HCl treatments). Again the final solution upon complete dissolution was taken in 2.5N HCl. The solutions were spiked with ^{87}Rb and ^{84}Sr enriched solutions for Rb and Sr concentration measurements.

3.4.3. Isotope Dilution

To measure the Rb and Sr concentrations in the sample, isotope dilution technique was followed (Long, 1966). For this, high purity ^{87}Rb and ^{84}Sr spikes were used. The isotopic ratios of the spikes are given in Table 3.9. Concentrations of the spikes were

calibrated against standard solutions of normal Rb and Sr (NBS984 and NBS987). Dilute Rb and Sr solutions (concentrations about 17.59 ppm and 1.59 ppm respectively) were prepared from concentrated spike solutions for our experimental purpose. The spikes were periodically checked for concentrations to guard against evaporation losses. The spike solutions were added to sample solutions and mixed thoroughly by means of several cycles of evaporation and HCl addition.

Table 3.9. Isotopic ratios of spikes

^{87}Rb SPIKE

$^{85}Rb/^{87}Rb = 0.008$

^{84}Sr SPIKE

$^{88}Sr/^{84}Sr = 0.0009$

$^{86}Sr/^{84}Sr = 0.0011$

$^{87}Sr/^{84}Sr = 0.0002$

3.4.4. Ion Exchange Chromatography

Ion exchange chromatography was employed to separate pure Rb and Sr fractions from the sample solutions. The ion exchange columns were made from quartz tubes (I.D. = 0.8 cm) and filled with Dowex 50W X8 (200 to 400 mesh size) cation exchange resin to a height of 19 cm. Elution was done using 2.5N HCl. The columns were frequently calibrated to ensure optimum collection of Rb and Sr fractions. Sample solutions were centrifuged for about five minutes in clean 3 ml quartz centrifuge tubes and then loaded gently onto the resin bed using pipettes. The Rb and Sr fractions were collected in separate teflon beakers, evaporated to dryness. The columns were cleaned between samples with at least 200 ml of 6N HCl and 10 ml of distilled water and conditioned with 25 ml of 2.5 N HCl.

3.4.5. Mass Spectrometry

At our laboratory, Rb and Sr isotopic measurements were carried out on a 23 cm radius, 60^{o} sector magnetic field and single focusing mass-spectrometer fabricated in-house (Trivedi et al., 1982). The mass-spectrometer is fitted with a thin lens ion source

and a Faraday cup for collection of ions. The filament holder with first source slit is removable so that a new filament could be fitted with a new sample. For our study Tantalum filaments (0.030" x 0.001") of more than 99.9% purity were used. Filaments were spot welded on the sample holders and degassed in a separate vacuum system at a temperature (>1800°C) higher than the Sr ionization temperature. Dried sample was added with a drop or two of high purity phosphoric acid and loaded onto a precleaned filament using a disposable quartz pipette and evaporated. Then the filament was loaded in the source. A working pressure of $\sim 10^{-7}$ torr in the source chamber was obtained in an hour after loading a new sample. The ion acceleration potential used was usually 4500V. The filament was heated with a highly stable DC current supply. Ion currents were measured on a semi automated data acquisition system using an IBM PC. This system controls the mass-spectrometer in the peak switching mode, measures the ion currents digitally and computes the isotopic ratios. It was ensured that no cross contamination of Rb occurs in Sr separates. At National Geophysical Research Institute (NGRI), Hyderabad, Sr isotopic measurements were carried out on a VG 354 thermal ionization mass-spectrometer.

Errors in the mass spectrometric determinations of ^{87}Rb and ^{86}Sr, at our laboratory, estimated to be within ±0.5% leading to a random error of not more than ±1% for their ratios. ^{87}Rb and ^{86}Sr concentrations were calculated by isotope dilution technique. The $^{87}Sr/^{88}Sr$ ratios were corrected for mass fractionation (linear) assuming $^{86}Sr/^{87}Sr = 0.1194$. The long term average of $^{87}Sr/^{86}Sr$ for NBS987, measured in our laboratory, is 0.71025±0.00007 (at 2σ). Typical 2σ errors in $^{87}Sr/^{86}Sr$ measurements of my samples were 0.0002 (for those measured at our laboratory) and 0.00004 (for those measured at NGRI).

3.5 TRACE ELEMENTAL STUDIES

Trace and rare earth elemental analyses were done by instrumental neutron-activation analysis (INAA). The samples were crushed, dried at 110°C and packed in small aluminum foils and sealed in a quartz vial. This quartz vial was then put in a container suitable for irradiation at the CIRUS reactor of the Bhabha Atomic Research Center, Bombay. The neutron flux in this reactor is $\sim 10^{13}$n $cm^{-2}s^{-2}$. The samples were irradiated

for 15 days together with USGS basalt standard BCR-1. After the irradiation, the gamma-ray spectra of the samples were obtained using a coaxial germanium detector (148-cm^3, high purity Ge-detector having a resolution of 2.2 keV for 1333 keV gamma rays of ^{60}Co). Counting of samples and the standard was done and concentration of several trace elements including nine rare earth elements (La, Ce, Nd, Sm, Eu, Gd, Tb, Yb and Lu) were measured following the standard procedures as outlined by Laul (1979).

Concentration of these elements in BCR-1 were taken from Laul (1979). Typical errors of counting (1σ) are as follows:

Elements	1σ Error (%) in BCR-1	1σ Error (%) in samples
(i) La, Ce, Sm, Eu and Tb	0.6	0.5 - 1.5
(ii) Nd, Yb, Lu, Hf and Ba	1.2	1.0 - 4.0
(iii) Gd	3.0	4.0 - 6.0
(iv) Zr and Cr	5.0	7.0 - 17.0

3.6 X-RAY DIFFRACTOMETRY

X-ray diffractometry (XRD) was done on carbonatite samples at our laboratory to find out the type of carbonates present in them. For this purpose a Philips PW1730, manually operated, X-ray diffractometer was used. CuK_α X-ray was used for my samples. A semi-quantitative calculation was performed using the peak areas of different carbonates (calcite, dolomite and ankerite) to find out their modal ratios (Cal:Dol, Cal:Ank) in the samples. This information was required for the stable isotopic measurements already discussed in Section 3.2.2.

3.7. ATOMIC ABSORPTION SPECTROPHOTOMETRY

Sr and Rb concentration in some samples were also measured by Atomic Absorption Spectrophotometry (AAS). ~0.5 g dry powder of the sample was dissolved in acid following the procedure described in section 3.4.2 and made to 25 ml in 1N HCl. Rb concentration was directly measured in this solution, whereas Sr concentration was measured after 1000 times dilution. The measurements were done in a Perkin Elmer

AAS (model 305A), following the procedures described by Sarin et al. (1979). The precision of measurements was ≤ 4 % (2σ) for both Rb and Sr. To check the accuracy of the measurements an alkaline rock sample (AD-47) was used, whose Rb and Sr concentrations (Rb=95 ppm & Sr=93 ppm) were pre-determined by isotope dilution technique and it was found that the concentrations measured by AAS (Rb=98 ppm & Sr=94 ppm) are indistinguishable from those measured by isotope dilution within 2σ level of error.

CHAPTER IV

RESULTS AND DISCUSSION

Results of various measurements carried out in the present work on samples of carbonatites, alkaline rocks, metasomatic rocks and country rocks from different Mesozoic carbonatite-alkaline complexes of India are presented in this chapter and their implications are discussed. This chapter consists of two parts. The first part discusses the results of different studies on the complexes of Deccan Province (Western India) and the second part discusses the results from complexes of Assam-Meghalaya plateau (Eastern India). For the sake of convenience each part is divided into several sections and each section deals with a particular method of investigation.

PART-A: CARBONATITE-ALKALINE COMPLEXES OF DECCAN PROVINCE

In this part, the results of different studies on the rocks of the three carbonatite alkaline complexes (Amba Dongar, Mundwara and Sarnu-Dandali) are presented and discussed in light of the evolution of these complexes. This part is again divided into five sections describing the results of ^{40}Ar-^{39}Ar chronology, strontium isotopic studies, trace and rare earth elements studies of Amba Dongar complex and stable isotopic studies of all the three complexes, respectively.

4.1. ^{40}Ar-^{39}Ar CHRONOLOGY OF AMBA DONGAR COMPLEX

4.1.1. Results

The Amba Dongar alkaline complex is one of the several alkaline complexes that are spatially associated with the Deccan Traps. According to the present notion these complexes represent magmatic activity either older or younger than the main tholeiitic volcanism (Basu et al., 1993; Sen, 1995) of the Deccan Province. As discussed in Chapter II the only chronological study by Deans et al. (1973) of the Amba Dongar complex failed to provide a reliable age for this complex, as the K-Ar dates given by these authors varied from 37.5 Ma to 76 Ma.

To establish the temporal relationship between the Amba Dongar alkaline complex and the Deccan Traps, precise ^{40}Ar-^{39}Ar dating of samples from Amba Dongar was undertaken following the procedures described in Chapter III. Three fresh alkaline rock samples (AD-16, AD-45 and AD-47) and a phlogopite separate from a carbonatite (AD-46) were dated. The description of these samples are given in Table 3.1 of Chapter-III. The argon isotopic compositions, fractions of ^{39}Ar released, apparent ages and percent of radiogenic argon ($^{40}Ar^*$) released, for each temperature step are given in Tables 4.1 - 4.4. The tables also give modified J factors, determined from horizontal neutron fluence variation in the irradiation can.

Table 4.1. Step heating argon isotopic compositions and apparent ages of sample AD-16 (Amba Dongar Nephelinite). Errors on age are without and with (bracketed) error on J. Errors quoted are at 1σ.

(J = 0.00218 ± 0.00002)

Temp. (°C)	$^{36}Ar/^{39}Ar$ ±1σ	$^{37}Ar/^{39}Ar$ ±1σ	$^{40}Ar/^{39}Ar$ ±1σ	AGE (Ma) ±1σ	^{39}Ar (%)	$^{40}Ar^*$ (%)
450	2.201	0.0362	654.0	16	0.02	0.61
	0.099	0.003	21.0	81 (81)		
500	0.2513	0.0362	91.48	67	0.14	18.82
	0.0093	0.0036	0.93	11 (11)		
550	0.0383	0.0363	27.90	64.1	1.56	59.47
	0.0012	0.0036	0.26	1.6 (1.7)		
650	0.02081	4.740	22.79	64.33	5.27	73.02
	0.00038	0.074	0.15	0.67 (0.95)		
700	0.03599	4.35	27.46	65.04	5.0	61.27
	0.00059	0.22	0.18	0.88 (1.11)		
750	0.01950	3.74	22.54	64.9	4.07	74.43
	0.00059	0.11	0.16	1.1 (1.3)		
800	0.01567	5.63	21.25	64.26	4.78	78.21
	0.00066	0.83	0.16	0.89 (1.11)		

850	0.02445	11.02	23.91	64.5	3.60	69.78
	0.00074	0.11	0.21	1.1 (1.3)		
900	0.04381	1.89	29.79	65.1	3.67	56.54
	0.00081	0.16	0.22	1.2 (1.4)		
950	0.01782	3.57	21.93	64.44	5.67	75.99
	0.00047	0.11	0.16	0.77 (1.02)		
1000	0.00962	3.58	19.71	65.22	11.34	85.58
	0.00045	0.40	0.12	0.65 (0.93)		
1050	0.00531	3.442	18.34	64.82	26.0	91.44
	0.00040	0.060	0.12	0.57 (0.88)		
1100	0.00329	1.75	17.86	65.27	17.51	94.56
	0.0006	0.15	0.10	0.75 (1.01)		
1150	0.00817	4.941	19.26	65.11	7.61	87.46
	0.00062	0.062	0.15	0.88 (1.11)		
1200	0.0416	8.32	28.77	63.8	1.8	57.32
	0.0019	0.81	0.60	3.1 (3.2)		
1250	0.0924	10.6	45.7	70.9	0.72	40.23
	0.0055	1.1	1.5	8.4 (8.5)		
1300	0.219	0.416	94.7	114.0	0.41	31.51
	0.017	0.042	3.5	23.0 (23.0)		
1400	0.317	0.417	103.7	39	0.82	9.59
	0.010	0.042	3.3	16 (16)		
Integrated Values	0.01784	3.774	22.061	64.91	100.0	76.11
	0.00022	0.072	0.058	0.31 (0.74)		

Table 4.2. Step heating argon isotopic compositions and apparent ages of sample AD-45 (Amba Dongar Tinguaite). Errors on age are without and with (bracketed) error on J. Errors quoted are at 1σ.

(J = 0.00218 ± 0.00002)

Temp. (°C)	$^{36}Ar/^{39}Ar$ ±1σ	$^{40}Ar/^{39}Ar$ ±1σ	$^{40}Ar/^{39}Ar$ ±1σ	AGE (Ma) ±1σ	^{39}Ar (%)	$^{40}Ar^*$ (%)
450	0.643	0.259	221.2	119	0.02	14.14
	0.021	0.026	2.9	25 (25)		
500	0.1240	0.519	52.9	62.8	0.34	30.74
	0.0038	0.052	1.2	4.2 (4.2)		
550	0.05598	0.550	33.71	66.2	0.82	50.94
	0.00055	0.055	0.36	1.4 (1.5)		
600	0.01252	0.551	20.69	65.54	3.26	82.12
	0.00015	0.055	0.17	0.90 (1.13)		
650	0.005673	0.551	18.66	65.51	6.59	91.02
	0.000076	0.055	0.17	0.60 (0.91)		
700	0.01151	0.552	20.25	64.98	8.45	83.20
	0.00011	0.055	0.17	0.63 (0.92)		
750	0.0046	0.841	18.18	64.39	11.20	92.52
	0.0001	0.084	0.14	0.50 (0.84)		
800	0.00166	0.842	17.18	64.39	10.33	97.15
	0.00013	0.084	0.12	0.43 (0.43)		
850	0.00142	1.12	17.15	64.56	7.11	97.56
	0.00021	0.11	0.12	0.49 (0.83)		
900	0.00126	0.281	17.01	64.20	4.24	97.81
	0.00054	0.028	0.17	0.88 (1.10)		
950	0.00229	0.286	17.35	64.34	3.07	96.10
	0.00067	0.028	0.14	0.89 (1.11)		

1000	0.00173	0.893	17.43	65.2	3.21	97.07
	0.00074	0.089	0.35	1.3 (1.4)		
1050	0.00078	2.518	16.91	64.37	7.58	98.63
	0.00038	0.051	0.11	0.57 (0.87)		
1100	0.00105	3.58	16.94	64.18	15.69	98.17
	0.00026	0.11	0.11	0.47 (0.87)		
1150	0.00245	2.553	17.50	64.71	14.30	95.86
	0.00024	0.050	0.13	0.52 (0.85)		
1200	0.00188	1.58	17.32	64.7	2.42	96.80
	0.00096	0.16	0.30	1.5 (1.7)		
1250	0.0183	1.58	22.88	67.3	0.75	76.34
	0.0031	0.16	0.78	4.5 (4.6)		
1300	0.226	0.0316	74.2	29.0	0.40	10.09
	0.012	0.0032	4.2	16 (16)		
1400	4.463	0.0316	1327	33.0	0.22	0.64
	0.084	0.0032	24	55 (55)		
Integrated Values	0.01502	1.586	21.153	64.49	100.00	79.02
	0.00012	0.026	0.051	22 (70)		

Table 4.3. Step heating argon isotopic compositions and apparent ages of sample AD-46 (Phlogopite from Amba Dongar Carbonatite). Errors on age are without and with (bracketed) error on J. Errors quoted are at 1σ.

J = 0.00239 ± 0.00002

Temp. (°C)	$^{36}Ar/^{39}Ar$ ±1σ	$^{40}Ar/^{39}Ar$ ±1σ	$^{40}Ar/^{39}Ar$ ±1σ	AGE (Ma) ±1σ	^{39}Ar (%)	$^{40}Ar^*$ (%)
500	2.565	0.00686	804	189	0.01	5.75
	0.097	0.00069	32	57 (57)		
550	0.9362	0.00687	279.8	14	0.05	1.14
	0.0076	0.00069	2.4	13 (13)		

600	0.2930	0.00688	106.91	85.5	0.22	19.01
	0.0027	0.00069	0.88	4.4 (4.5)		
650	0.3897	0.00688	128.71	57.5	2.07	10.54
	0.0034	0.00069	0.80	4.7 (4.8)		
700	0.1902	0.00689	71.65	65.4	4.24	21.58
	0.0011	0.00069	0.44	2.0 (2.0)		
750	0.05629	0.00699	31.86	64.5	3.87	47.79
	0.00029	0.0007	0.26	1.0 (1.2)		
800	0.04732	0.00701	29.67	66.38	7.73	52.87
	0.00017	0.0007	0.23	0.91 (1.1)		
850	0.03839	0.00702	26.84	65.59	7.73	57.74
	0.00018	0.00018	0.21	0.82 (1.02)		
900	0.04767	0.00702	29.60	65.65	7.85	52.41
	0.00019	0.0007	0.25	0.96 (1.14)		
950	0.04702	0.00714	29.28	65.1	6.49	52.54
	0.0002	0.00071	0.26	1.0 (1.2)		
1000	0.036651	0.00715	26.46	66.32	27.34	59.23
	0.00022	0.00072	0.25	1.0 (1.18)		
1050	0.0390	0.00742	27.2	66.2	17.85	57.62
	0.0028	0.00074	2.0	1.5 (1.6)		
1100	0.021954	0.00743	21.71	64.45	10.52	70.12
	0.000097	0.00074	0.24	0.95 (1.13)		
1150	0.01666	0.00744	20.30	65.1	2.21	75.75
	0.00027	0.00074	0.59	2.3 (2.4)		
1200	0.00113	0.00745	13.72	56.8	1.28	97.57
	0.00074	0.00075	0.48	2.2 (2.3)		
1250	0.0094	0.00747	12.7	42.4	0.49	78.14
	0.0022	0.00075	1.2	5.9 (5.9)		

1300	0.0669	0.00757	37.5	75.0	0.06	47.31
	0.0099	0.00076	2.8	17 (17)		
Integrated Values	0.05274	0.00719	31.04	65.4	100.0	49.79
	0.00068	0.00027	0.41	0.45 (0.76)		

Table 4.4. Step heating argon isotopic compositions and apparent ages of sample AD-47 (Amba Dongar Tinguaite). Errors on age are without and with (bracketed) error on J. Errors quoted are at 1σ.

(J = 0.00232 ± 0.00002)

Temp. (°C)	$^{36}Ar/^{39}Ar$ ±1σ	$^{40}Ar/^{39}Ar$ ±1σ	$^{40}Ar/^{39}Ar$ ±1σ	AGE (Ma) ±1σ	^{39}Ar (%)	$^{40}Ar^{*}$ (%)
450	0.03744	0.0461	28.39	70.95	3.22	61.03
	0.00018	0.0021	0.17	0.64 (0.92)		
500	0.01877	0.13644	22.61	69.90	19.46	92.96
	0.00009	0.00027	0.13	0.47 (0.80)		
600	0.01004	0.34765	18.99	65.72	11.12	84.38
	0.00011	0.0007	0.11	0.41 (0.74)		
650	0.00146	0.0916	16.261	64.94	10.87	97.34
	0.00033	0.0026	0.094	0.52 (0.80)		
700	0.00312	0.0426	16.84	65.29	5.31	94.53
	0.00033	0.0010	0.10	0.73 (0.95)		
750	0.00255	0.03771	16.55	64.81	3.99	95.45
	0.00049	0.00062	0.11	0.70(0.93)		
800	0.01162	0.0520	19.40	65.49	4.26	82.30
	0.00053	0.0023	0.13	0.77 (0.99)		
850	0.00956	0.0589	18.71	65.49	4.63	84.90
	0.00043	0.0019	0.12	0.67 (0.91)		
900	0.00368	0.00320	17.05	65.49	7.54	93.63
	0.00033	0.00032	0.11	0.55 (0.82)		

950	0.00361	0.0793	16.92	65.03	7.48	93.69
	0.0003	0.0027	0.12	0.55 (0.82)		
1000	0.0502	0.04774	17.51	65.76	5.85	91.53
	0.0002	0.00095	0.13	0.54 (0.82)		
1050	0.01805	0.0774	21.78	67.4	0.92	75.51
	0.00076	0.0017	0.76	3.2 (3.2)		
1100	0.05421	0.168	40.2	98.2	0.24	60.12
	0.00072	0.014	2.4	9.7 (9.7)		
1150	0.1015	1.382	48.5	76.0	0.17	38.14
	0.0024	0.021	3.3	13 (13)		
1200	0.265	1.02	87.2	36.0	0.14	10.11
	0.011	0.33	4.6	23 (23)		
Integrated Values	0.009001	0.15533	19.036	67.15	100.0	86.03
	0.000073	0.00076	0.039	0.17 (0.65)		

The age spectra along with isotope correlation plots for all four samples are shown in Figures 4.1 - 4.4. The plateau ages along with percent ^{39}Ar included for the plateaus; isochron ages and inverse isochron ages of plateau steps along with ratios of trapped argon and MSWD values; and integrated (total) ages are summarized in Table 4.5. Errors quoted in all the values are at 2σ level. Two alkaline rocks (AD-16 and AD-45) and the phlogopite separate from a carbonatite (AD-46) yielded good plateaus in the age spectra (Figs.4.1a, 4.2a and 4.3a) giving ages of 64.8±0.6 Ma, 64.7±0.5 Ma, and 65.5±0.8 Ma, respectively. The third alkaline rock (AD-47) yielded a 10 step high temperatures plateau (from 600°C to 1050°C) with an age of 65.3±0.6 Ma (Fig.4.4a). The three low temperature steps of AD-47 (Fig.4.4a) showed higher apparent ages, perhaps due to recoil effect. The one or more initial and final temperature steps (Figs. 4.1a, 4.2a, 4.3a and 4.4a), which are not included in the plateaus, showed large errors in their apparent ages due to the very small amount of ^{39}Ar-release in these steps. For all the four samples, there is an excellent agreement between plateau and isochron ages indicating that these samples have not lost any significant amount

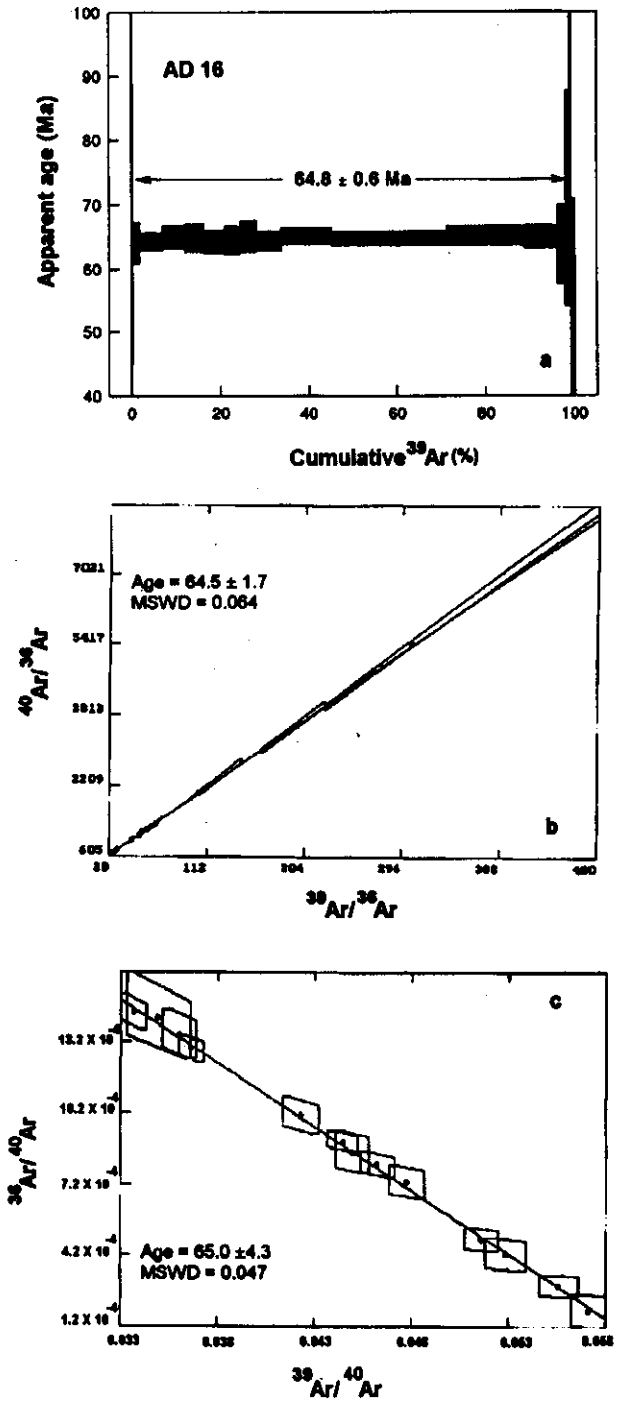

Fig. 4.1. *(a) Step heating of $^{40}Ar/^{39}Ar$ apparent age spectrum for AD-16 (Amba Dongar Nephelinite). The age shown is plateau age, which includes 2σ error on J but the vertical width of plateau boxes indicate 2σ errors calculated without error on J. (b) $^{40}Ar/^{36}Ar$ vs. $^{39}Ar/^{36}Ar$ correlation diagram of AD-16 showing 2σ error envelopes and regression line. Error on isochron age is at 2σ. (c) $^{36}Ar/^{40}Ar$ vs. $^{39}Ar/^{40}Ar$ correlation diagram of AD-16 showing 2σ error envelopes and regression line. Error on inverse isochron age is at 2σ.*

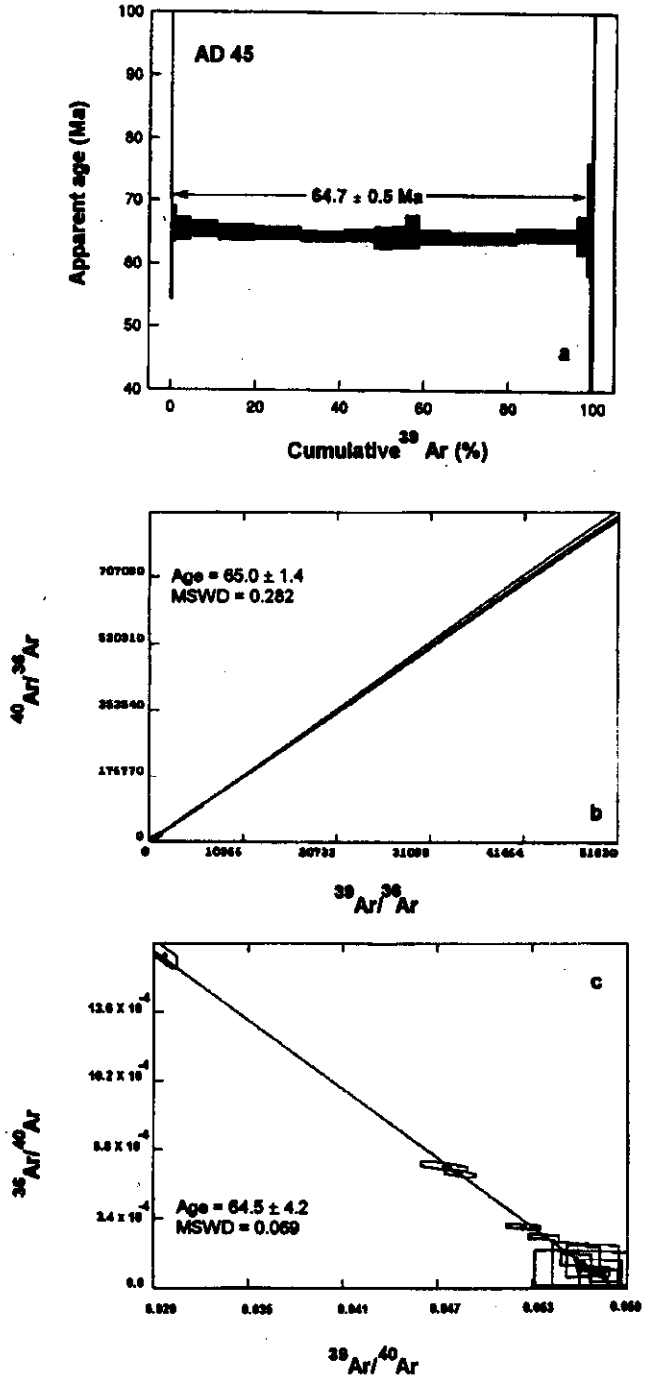

Fig.4.2 *(a) Step heating $^{40}Ar/^{39}Ar$ apparent age spectrum for AD-45 (Amba Dongar Tinguaite)with plateau age.(b) $^{40}Ar/^{36}Ar$ vs. $^{39}Ar/^{36}Ar$ correlation diagram of AD-45 with isochron age and MSWD value. (c) $^{36}Ar/^{40}Ar$ vs. $^{39}Ar/^{40}Ar$ correlation diagram of AD-45 with inverse isochron age and MSWD value. Please also see the caption of Fig. 4.1.*

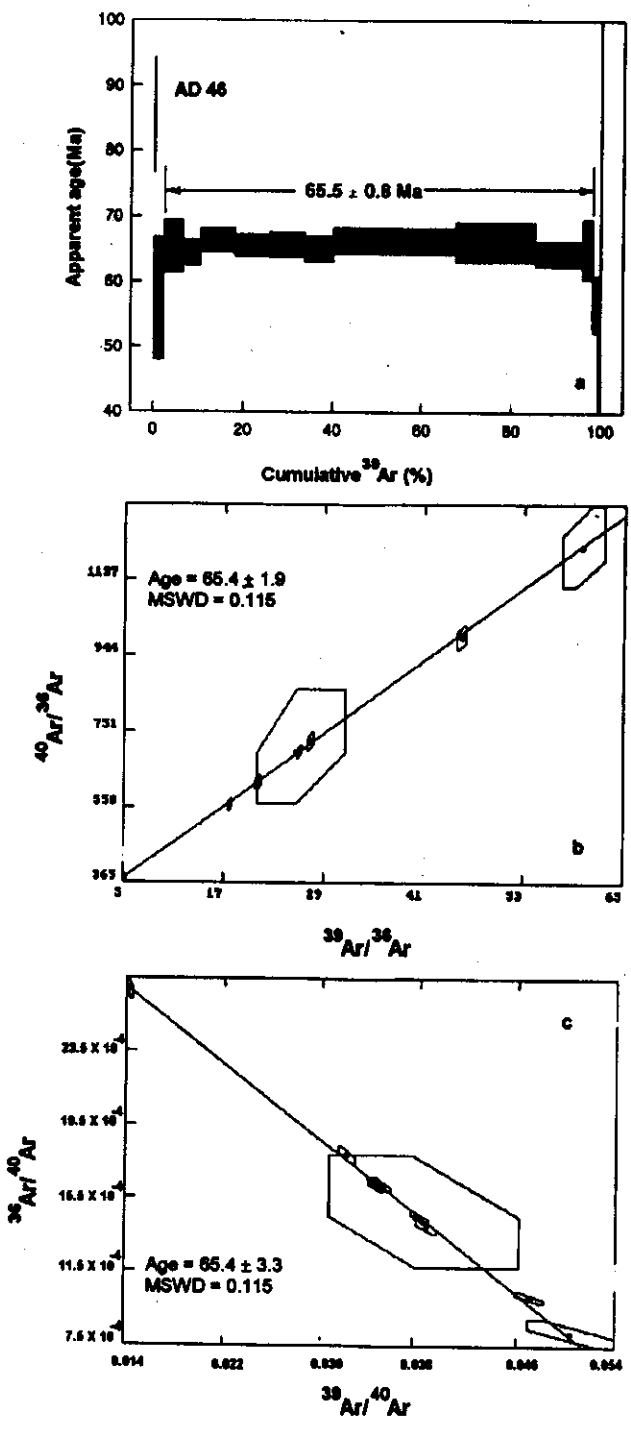

Fig. 4.3. (a) Step heating $^{40}Ar/^{39}Ar$ apparent age spectrum for AD-46 (Phlogopite separate from a carbonatite of Amba Dongar) with the plateau age. (b) $^{40}Ar/^{36}Ar$ vs. $^{39}Ar/^{36}Ar$ correlation diagram of AD-46 with isochron age and MSWD value. (c) $^{36}Ar/^{40}Ar$ vs. $^{39}Ar/^{40}Ar$ correlation diagram of AD-46 with inverse isochron age and MSWD value. Please also see the caption of Fig. 4.1.

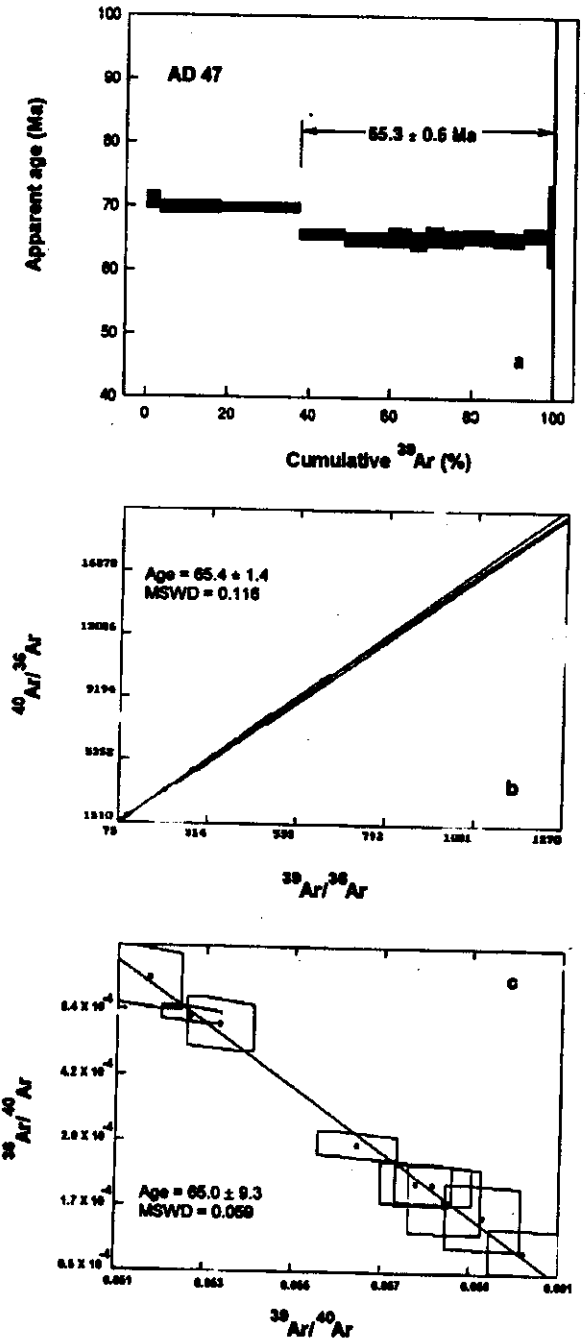

Fig. 4.4. *(a) Step heating $^{40}Ar/^{39}Ar$ apparent age spectrum for AD-47 (Amba Dongar Tinguaite) with the plateau age. First three steps of the spectrum are not included in the plateau (See text for discussion). (b) $^{40}Ar/^{36}Ar$ vs. $^{39}Ar/^{36}Ar$ correlation diagram of AD-47 with isochron age and MSWD value. (c) $^{36}Ar/^{40}Ar$ vs. $^{39}Ar/^{40}Ar$ correlation diagram of AD-47 with inverse isochron age and MSWD value. Please also see the caption of Fig. 4.1.*

of radiogenic argon since their crystallization. The undisturbed nature of these samples is also reflected in the total ages, which are indistinguishable from the plateau ages within the 2σ level of error. In the isotope correlation plots of the plateau steps of all these samples showed atmospheric trapped argon composition (i.e. $(^{40}Ar/^{36}Ar)_i = 295.5$) within the limits of uncertainties (2σ errors) implying that the plateau ages are true ages of the samples.

Table 4.5. Summary of results of ^{40}Ar-^{39}Ar dating of Amba Dongar samples.

Sample	Plateau			Isochron			Inverse Isochron			Integrated Age
	steps	% ^{39}Ar	Age (Ma)	Age (Ma)	Trap	MSWD	Age (Ma)	Trap	MSWD	(Ma)
AD-16	13	97.88	64.8 ±0.6	64.5 ±1.7	297.4 ±13.2	0.064	65.0 ±4.3	292.7 ±11.5	0.047	64.5 ±1.5
AD-45	14	98.27	64.7 ±0.5	65.0 ±1.4	297.7 ±12.8	0.282	64.5 ±4.2	306.7 ±13.2	0.069	65.5 ±1.4
AD-46	10	98.27	65.5 ±0.8	65.4 ±1.9	295.9 ±6.5	0.115	65.4 ±3.3	295.9 ±6.5	0.115	65.4 ±1.6
AD-47	9	61.05	65.3 ±0.6	65.4 ±1.4	296.9 ±23.4	0.116	65.0 ±9.3	310.6 ±29.9	0.059	67.2 ±1.4

Note: Trap: Initial $^{40}Ar/^{36}Ar$ (trapped argon); MSWD: Mean Square Weighted Deviate.
Errors are 2σ.

Indistinguishable ages of alkaline silicate rocks and carbonatites indicate that these two rock types of Amba Dongar complex are contemporaneous. The weighted mean (determined following Bevington (1969)'s procedures) of all plateau ages is 65.0±0.3 Ma, which is the age of emplacement of the Amba Dongar complex.

4.1.2. Discussion

The contemporanity of alkaline silicate rocks and carbonatites of Amba Dongar complex probably indicates a genetic relationship between these two. The 65.0±0.3 Ma age of this complex suggests that the complex got emplaced towards the end phase of Deccan Trap magmatism and it is ~2.0 Ma younger than the main pulse of Deccan (67.0 Ma, Pande et al, in preparation). As mentioned in Chapter-II, the Amba Dongar complex intrudes into the Deccan tholeiites of this region. Therefore, the Traps of this region are older than 65.0 Ma.

This age of Amba Dongar complex along with the two northern most 68.5 Ma old alkaline complexes at Sarnu-Dandali and Mundwara fits well in the plume theory for the generation of Deccan flood basalts and is consistent with the idea of 10-15 cm/year northward motion of the Indian plate over nascent Reunion hotspot (Basu et al., 1993). In this plume model, Amba Dongar complex would represent a late stage alkaline magmatism on the southern end side of the plume head.

Amba Dongar is part of the Chhota Udaipur carbonatite-alkaline district of Gujarat, which covers an area of ~1200 km^2 (Viladkar, 1996) and consists of several alkaline complexes. Phenai Mata carbonatite-alkaline complex (present to the northeast of Amba Dongar), which is also a part of this district, has been dated to 64.96±0.11 Ma by Basu et al. (1993). This probably indicates that the carbonatite-alkaline magmatism of this district occurred at 65.0 Ma, which happens to be just at the K/T boundary (Izett et al., 1991). This coincidence makes these carbonatite alkaline magmatisms very important in the ongoing debate on the K/T mass-extinctions. Alkaline and carbonatite magmatism are associated with the release of very high amount of CO_2 + CO + SO_2 gases (Bailey and Hampton, 1990). Owing to their very low viscosity and density these melts get emplaced/erupted very fast which obviously results in a lot of volatile input into the atmosphere in a very short interval of time. A conservative calculation shows that the total CO_2 flux from just carbonatites of Chhota Udaipur district was 2.67 x 10^{14} moles, which came out in a very short period of time (in a few years). Workers who believe in the internal cause (i.e. Deccan Volcanism) to be responsible for the mass-extinctions at K/T boundary suggest that the high amount of CO_2 released due to the Deccan volcanism (~5 x 10^{17} moles in ~1 Ma ; McLean et al., 1985) is one of the major reasons for the catastrophism. In this context the carbonatite-alkaline magmatism of Chhota Udaipur district would have enhanced the catastrophic effects due to addition of a very significant amount of CO_2 in a very short time into the already disturbed atmosphere.

4.1.3. Summary

The age of Amba Dongar carbonatite-alkaline complex is 65 Ma. This age is consistent with the plume hypothesis proposed for the origin of this complex (Sen, 1995) and also confirms the genetic relationship of Amba Dongar with the Deccan flood basalts. Being

emplaced just at the K/T boundary it could have enhanced the catastrophic effects leading to mass extinctions, by rapidly adding a substantial amount of CO_2 into the atmosphere.

4.2 Sr ISOTOPIC STUDIES OF AMBA DONGAR COMPLEX

4.2.1. Results

Sr isotope ratio and concentration were measured in samples of carbonatites, alkaline rocks and different country rocks from Amba Dongar complex. The aim of this study was to assess the role of different magmatic processes, particularly the crustal contamination, in the evolution of this complex and to characterize the isotopic composition of the source region. Table 4.6 summarizes the results of this study. It gives concentrations of Rb and Sr, measured $^{87}Sr/^{86}Sr$ and $^{87}Rb/^{86}Sr$ ratios with 2σ error and initial $^{87}Sr/^{86}Sr$ ratios calculated using the age of 65 Ma for Amba Dongar. As mentioned in Chapter-III, the 2σ errors in the $^{87}Sr/^{86}Sr$ measurements were higher in the samples analyzed at Physical Research Laboratory compared to the errors in the samples analyzed at National Geophysical Research Institute. The initial $^{87}Sr/^{86}Sr$ ratios of alkaline rocks and carbonatites are plotted against Sr concentration in Fig. 4.5.

Table 4.6. Results of Sr isotopic measurements in samples from Amba Dongar.

Sample	Rb (ppm)	Sr (ppm)	$(^{87}Sr/^{86}Sr)_m$ (atomic)	$(^{87}Rb/^{86}Sr)_m$ (atomic)	$(^{87}Sr/^{86}Sr)_i$
Alkaline Rocks					
AD-14	27	1998	0.7062±3	0.0391	0.7062
AD-16*	14	3511	0.70633±4	0.0115	0.70632
AD-17*	51	1854	0.70621±4	0.0796	0.70614
AD-18	80	1551	0.7069±2	0.1492	0.7068
AD-45*	103	1172	0.70678±4	0.2543	0.70655
AD-47*	95	93	0.71562±4	2.9579	0.71289
AD-65*	21	2535	0.70706±6	0.02397	0.70704
AD-66*	18	3278	0.70660±6	0.01589	0.70658

AD-67*	85	237	0.71154±3	1.03089	0.71058
Calcite Carbonatites					
AD-1	0.5	6176	0.7066±3	0.0023	0.7066
AD-10/1	0.7	5413	0.7059±3	0.00037	0.7059
AD-38	1.4	3710	0.7060±4	0.00109	0.7060
AD-49	bdl	3594	0.7055±2	bdl	0.7055
AD-52*	5.0	2705	0.7060±2	0.0053	0.70605
Ferro-carbonatites					
AD-19	0.8	3248	0.7065±2	0.0007	0.7065
AD-36	bdl	4920	0.7061±2	bdl	0.7061
AD-55	bdl	8477	0.7061±1	bdl	0.7061
Sandstone					
AD-6	56	68	0.7590±7	2.3947	0.7568
Limestones					
AD-59/1	bdl	676	0.7087±2	bdl	0.7087
AD-62	4	4558	0.7109±2	0.00254	0.7109

* = Samples analyzed at National Geophysical Research Institute, Hyderabad. 'm' stands for measured isotopic ratio and 'i' for initial ratio (at 65 Ma). bdl = below detection limit. Errors are 2σ.

The initial $^{87}Sr/^{86}Sr$ ratios of alkaline rocks are highly variable (0.70614-0.71289) compared to those of carbonatites (0.7055-0.7066). The Sr isotopic ratios of carbonatites fall within the range of values given by Deans and Powell (1968) and overlap with the range given by Simonetti et al. (1995). Sr concentration in carbonatites (2705-8477 ppm) are higher than the alkaline silicate rocks (93-3511 ppm) (Table 4.6 and Fig. 4.5). Initial $^{87}Sr/^{86}Sr$ and Sr concentrations of ferrocarbonatites are similar to those of calcite carbonatites.

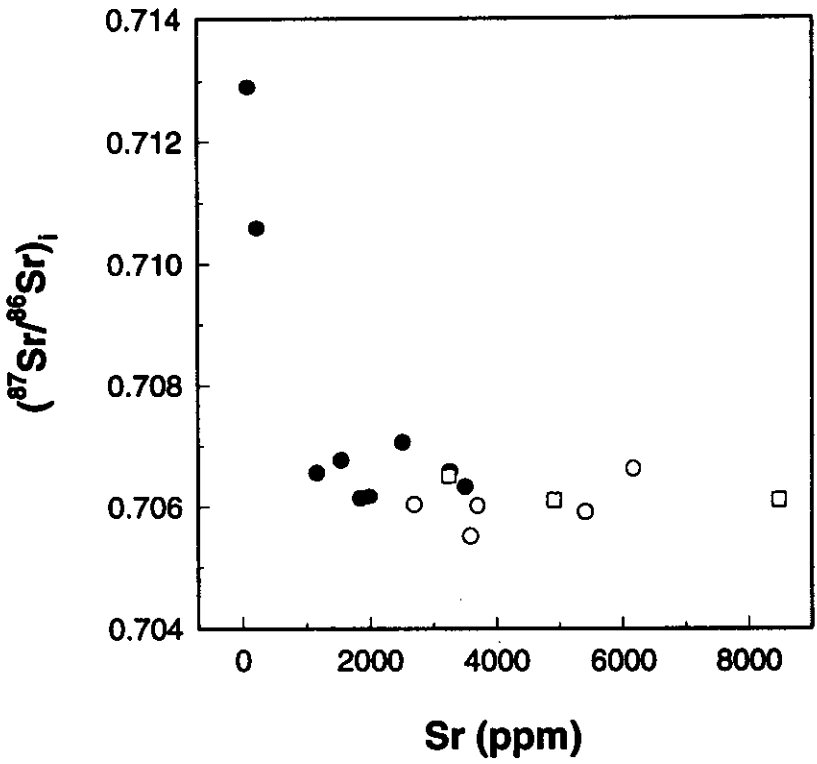

Fig. 4.5. *Plot of initial $^{87}Sr/^{86}Sr$ vs. Sr content for the whole-rock samples of Amba Dongar complex. Filled circle = alkaline rocks; open circles = calcite carbonatites; and open squares = ferrocarbonatites.*

4.2.2. Discussion

As seen in Fig.4.5, the alkaline rocks show higher initial $^{87}Sr/^{86}Sr$ ratios and lower Sr concentrations compared to the carbonatites. Whereas, the initial ratios of carbonatites are homogeneous within the experimental error. The trend of decreasing Sr concentration with increasing isotopic ratio shown by the alkaline rocks suggests that probably the rocks have been contaminated by some crustal material having high $^{87}Sr/^{86}Sr$ and lower Sr concentration during their crystallization. The country rocks, sandstone (Table 4.6) and Precambrian granitic gneiss (Gopalan et al., 1979) are likely candidates for contaminant. Limestones do not qualify to be the contaminant as the Sr ratios of these (0.7087 and 0.7109) are smaller than the highest initial ratio (0.71289) observed in alkaline rocks. Hence, to find out the contaminant and the amount of contamination simple binary mixing

and assimilation fractional crystallization (AFC) (DePaolo, 1981) models were applied to the observed data. The following section discusses the results of these models.

4.2.2a. Simple Binary Mixing and AFC for Alkaline Rocks

A simple binary mixing curve was generated (Fig.4.6) taking an unfenitized sandstone [$(^{87}Sr/^{86}Sr)_i$ = 0.7568 and Sr = 68 ppm] as one end-member and an alkaline rock [$(^{87}Sr/^{86}Sr)_i$ = 0.70632 and Sr = 3511 ppm] with highest Sr concentration as the second end-member. As seen in Fig.4.6, the binary mixing curve does not coincide with the observe alkaline rock trend.

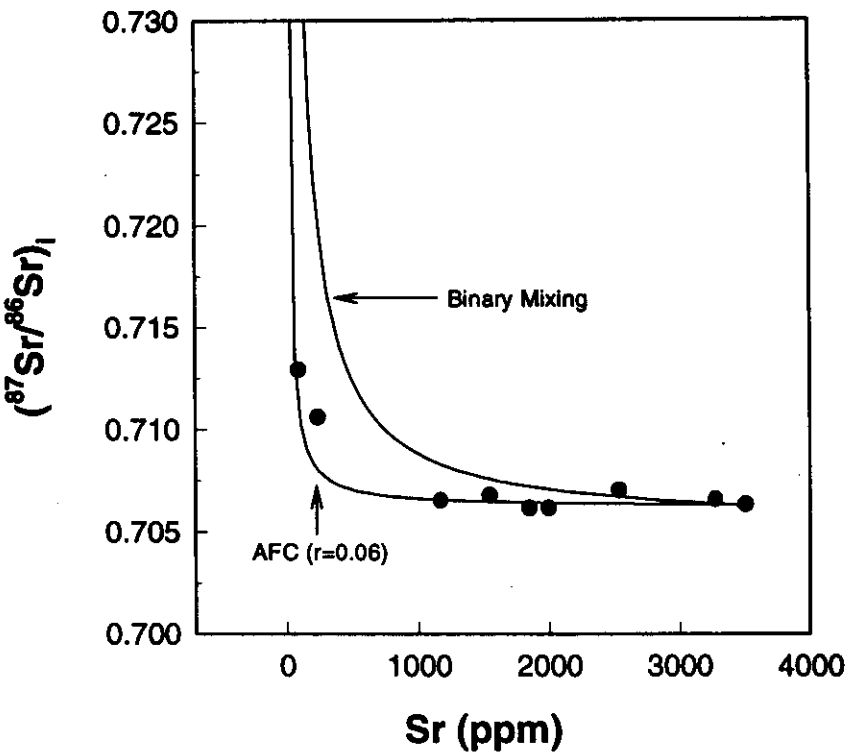

Fig. 4.6. *Plot of initial $^{87}Sr/^{86}Sr$ vs. Sr content for alkaline rocks of Amba Dongar complex. Binary mixing curve represents results of simple binary mixing between alkaline silicate magma with Bagh sandstone and the AFC curve represents results of AFC modelling (DePaolo, 1981), when Bagh sandstone gets assimilated in the alkaline silicate magma for a r (rate of assimilation/rate of crystallization) value of 0.06. See section 4.2.2a for discussion.*

The AFC model (DePaolo, 1981) was tried out with the above sandstone as the assimilant and the alkaline magma with Sr ratio of 0.70632 and concentration of 1951 ppm. The Sr concentration in the magma was determined assuming a rock-melt bulk distribution coefficient of 1.8. This distribution coefficient was calculated considering an average alkaline rock (nepheline = 25%, K-feldspar = 10%, aegirine augite = 12%, melanite = 5%, calcite = 7%, apatite = 4% and matrix = 37%) and mineral-alkaline melt partition coefficients K_d (neph.) = 2.7 [assumed to be same as K_d (K-spar-melt)], K_d (K-spar) = 2.7 [Long (1978)], K_d (aug.) = 0.1, K_d (melanite) = 0.001 [Jones (1995)], K_d (calcite) = 4.0 [assumed to be same as K_d (carbonate liquid-silicate liquid), Green et al., 1992] and K_d (apatite) = 14.5 [assumed to be same as K_d (apatite-basaltic melt), Nagasawa (1970)]. Using the above end-members AFC curves were generated for different r (rate of assimilation/rate of crystallization) values and it was found that the model curve with r = 0.06 (i.e. 6% assimilation) explained the observed alkaline rock trend (Fig.4.6).

A similar exercise was carried out taking the Precambrian basement gneisses, which are exposed near Chhota Udaipur, as the assimilant. The Sr isotopic composition and concentration of gneiss (0.7690, 145 ppm) were taken from Gopalan et al. (1979). Like sandstone, in this case the binary mixing hyperbola did not explain the observed trend (Fig.4.7), whereas the AFC curve for r = 0.03 (i.e. 3% assimilation) explained the observed variation.

In summary, combined wall-rock assimilation fractional crystallization process is probably the cause of observed isotopic and concentration variation in alkaline rocks. However, as both sandstone and gneiss assimilation explain this, it is difficult to find out the true assimilant/contaminant unequivocally.

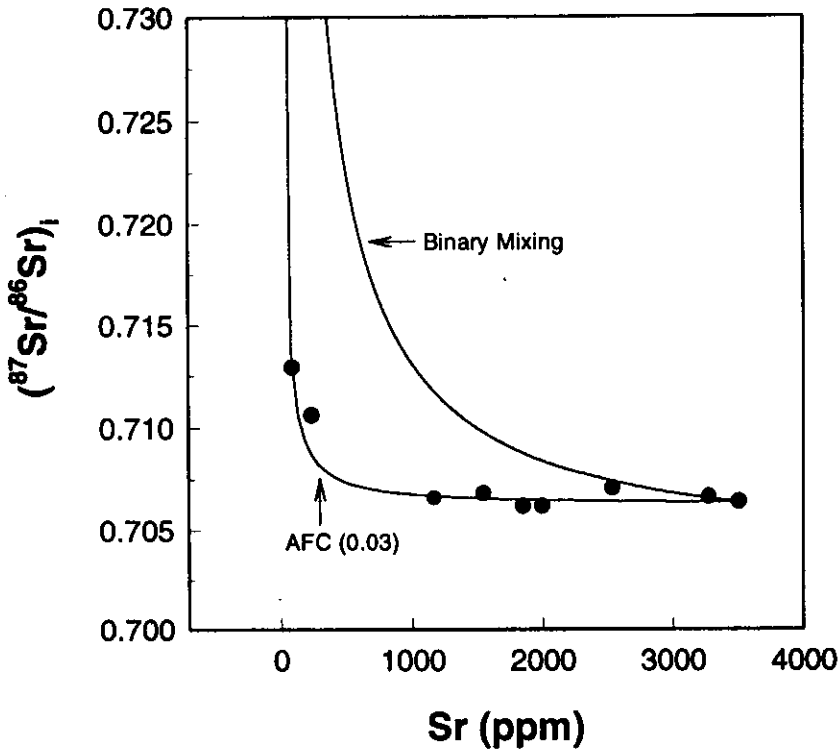

Fig. 4.7. *Plot of initial $^{87}Sr/^{86}Sr$ vs. Sr content for alkaline rocks of Amba Dongar complex. Binary mixing curve represents results of simple binary mixing between alkaline silicate magma with a Precambrian gneiss (basement rock) from Chhota Udaipur (Gopalan et al., 1979) and the AFC curve represents results of AFC modelling (DePaolo, 1981), when the above gneiss gets assimilated in the alkaline silicate magma for a r value of 0.03 (see section 4.2.2a for details).*

4.2.2b. An Alternative Explanation

Liquid immiscibility has been proposed to be the underlying process in the formation of alkaline silicates and carbonatites (LeBas, 1977; Kjarsgaard and Hamilton, 1989). In Amba Dongar, these two types of rocks are temporally and spatially related, which indicates a possible involvement of liquid immiscibility in their generation. Secondly, the alkaline rocks, as discussed in the above section, show crustal contamination. Hence, an attempt was made to include liquid immiscibility in the AFC process. For this a model was developed for trace element and isotopic effects by modifying the AFC model of DePaolo (1981) and then the model was applied to the observed data. In the following paragraphs, I discuss the model in general and its application to Sr-isotope systematics alkaline rocks of Amba Dongar.

A. Assimilation Fractional Crystallization coupled with Liquid Immiscibility (AFCLI).

In this model it is assumed that the wall-rock assimilation, fractional crystallization of alkaline rock and the separation of immiscible carbonate melt occur simultaneously and the immiscibility is a fractional process like crystallization. Other assumptions are same as those considered by DePaolo (1981) for the simple AFC model.

(i) *Element Concentrations*

Consider a parent magma body, whose mass is M_m at any time t, which is assimilating wall rock at a rate dM_a/dt, removing carbonate liquid at a rate dM_l/dt and crystallizing silicate phases at a rate dM_c/dt. dM_a, dM_l and dM_c stand for mass at any instant of assimilated material, carbonate melt and crystallized solids, respectively. Let us define $D_c = C_c/C_m$, the silicate rock-melt distribution coefficient of a particular element and $D_l = C_l/C_m$, the carbonate melt-silicate melt distribution coefficient of the same element, where C_c, C_l and C_m, respectively stand for concentrations in crystallizing phase, carbonate melt and parent magma. Now the change of mass of the magma can be written (following the procedure given by DePaolo (1981)) as:

$$d(C_m M_m) = C_a\, dM_a - D_l\, C_m\, dM_l - D_c\, C_m\, dM_c \quad (1)$$

$$\text{or, } dC_m = \frac{dM_a}{M_m}(C_a - C_m) - \frac{dM_l}{M_m}(D_l - 1)C_m - \frac{dM_c}{M_m}(D_c - 1)C_m \quad (2)$$

Defining the parameters $a = dM_a/dM_c$ (rate of assimilation/rate of crystallization) and $b = dM_l/dM_c$ (rate of carbonate immiscibility/rate of crystallization) and replacing dM_a and dM_l by $(a.dM_c)$ and $(b.dM_c)$ in equation (2) we have:

$$dC_m = \frac{dM_c}{M_m}[a(C_a - C_m) - b(D_l - 1)C_m - (D_l - 1)C_m]$$

$$= \frac{dM_c}{M_m}[aC_a - C_m(a + bD_l - b + D_c - 1)] \quad (3)$$

If $F = M_m/M_m^o$ (fraction of remaining parent magma where M_m^o is the initial mass of the parent magma) then

$$\frac{dF}{F} = \frac{dM_c}{M_m}(a - b - 1) \quad (4)$$

$$\text{or, } \frac{dM_c}{M_m} = \frac{dF}{F}\left(\frac{1}{a - b - 1}\right) \quad (5)$$

Now substituting the value of dM_c/M_m in equation (3), we have

$$\frac{dC_m}{dF/F} = \left(\frac{a}{a-b-1}\right)C_a - \left(\frac{a-b+bD_l+D_c-1}{a-b-1}\right)C_m \quad (6)$$

$$\text{or, } \frac{dC_m}{dF/F} = \left(\frac{a}{a-b-1}\right)C_a - zC_m \quad (7)$$

where $z = (a - b + bD_l + D_c - 1) / (a - b - 1)$ (8)

The transformation (7) is valid only when $(a - b) \neq 1$, that means when $dM_a \neq dM_c + dM_l$. This is the most general case of the equation (7). Rearranging equation (7) we get

$$\frac{dC_m}{\left(\frac{a}{a-b-1}\right)C_a - zC_m} = \frac{dF}{F} \quad (9)$$

Now integrating equation (9) with the initial conditions; at $t = 0$, $F=1$ and $C_m = C_m^\circ$ (initial concentration of the element in magma to start with), we get the equation for concentration variation in the parent magma:

$$C_m = C_m^\circ F^{-z} + \left(\frac{a}{a-b-1}\right)\frac{C_a}{z}(1-F^{-z}) \quad (10)$$

which is similar to equation (6a) of DePaolo (1981). Equation (10) is the most general case of concentration variation in AFCLI model. When there is no liquid immiscibility ($b=0$) then equation (10) reduces to simple AFC equation (6a) of DePaolo (1981): $C_m = C_m^\circ F^{-z} + \left(\frac{a}{a-1}\right)\frac{C_a}{z}(1-F^{-z})$, where $z = (a + D_c-1)/(a-1)$ and a is r of DePaolo (1981).

(ii) *Isotopic Ratios*

For heavier isotopes, there is no isotopic fractionation during any of the magmatic processes, hence the isotopic ratios E_m, E_c and E_l are equal at any instant during AFCLI. The differential equation involving isotopic ratios in this model can be written as:

$$d(M_mC_mE_m) = C_aE_adM_a - C_cE_cdM_c - C_lE_ldM_l \quad (11)$$

Now expanding this equation and substituting the value of dCm from equation (3), we get:

$$C_mE_m(dM_a - dM_c - dM_l) + M_mC_mdE_m + M_mE_m[(dM_c/M_m)\{a(C_a - C_m) - b(D_l - 1)C_m\}] = C_aE_adM_a - C_cE_cdM_c - C_lE_ldM_l \quad (12)$$

Simplifying equation (12) we get:

$$dE_m = \frac{dM_aC_a}{M_mC_m}(E_a - E_m) \quad (13)$$

for the most general case ($dM_a \neq dM_l + dM_c$) equation (13) will be:

$$\frac{dE_m}{(\frac{a}{a-b-1})\frac{C_a}{C_m}(E_a - E_m)} = \frac{dF}{F} \qquad (14)$$

Integrating equation (14) we get the isotopic ratio evolution equation:

$$\frac{E_m - E_m^o}{Ea - E_m^o} = 1 - (\frac{C_m^o}{C_m})F^{-z} \qquad (15)$$

Where E_m^o is the initial ratio of the parent magma. This equation is same as the evolution equation (15b) of DePaolo (1981), but here z is different (see equation (8)).

The AFCLI model equations (10) and (15) may be applied to situations where both wall-rock assimilation and liquid immiscibility are important. Like any other model this model also has certain limitations, which arise from the basic assumption of simultaneity of fractional crystallization and liquid immiscibility. The application of this model is also limited to magmas in which liquid immiscibility occurs within the crust so that the contamination effects are readily observed in the final products. In the case of alkaline rocks and carbonatites this model probably is the best model to explain isotopic variations resulted from wall rock assimilation as the silicate-carbonate liquid immiscibility has been experimentally observed to occur within the crust (Wyllie, 1989).

Fig.4.8 shows the application of AFCLI model to Sr isotope systematics and the model curves are compared with the simple binary mixing curve. In this figure the model calculations are done when a magma with initial $^{87}Sr/^{86}Sr$ of 0.705 and Sr concentration of 400 ppm assimilates a wall rock having ratio 0.72 and concentration 200 ppm. The model curves are generated for different D_c (rock-melt distribution coefficient of Sr) at a constant D_l of 4.0 (carbonate-silicate distribution coefficient of Sr). Fig.4.8a shows the model evolution curves for a=0.2 and b=0.2 and Fig.4.8b shows these for a=1.0 and b=0.02.

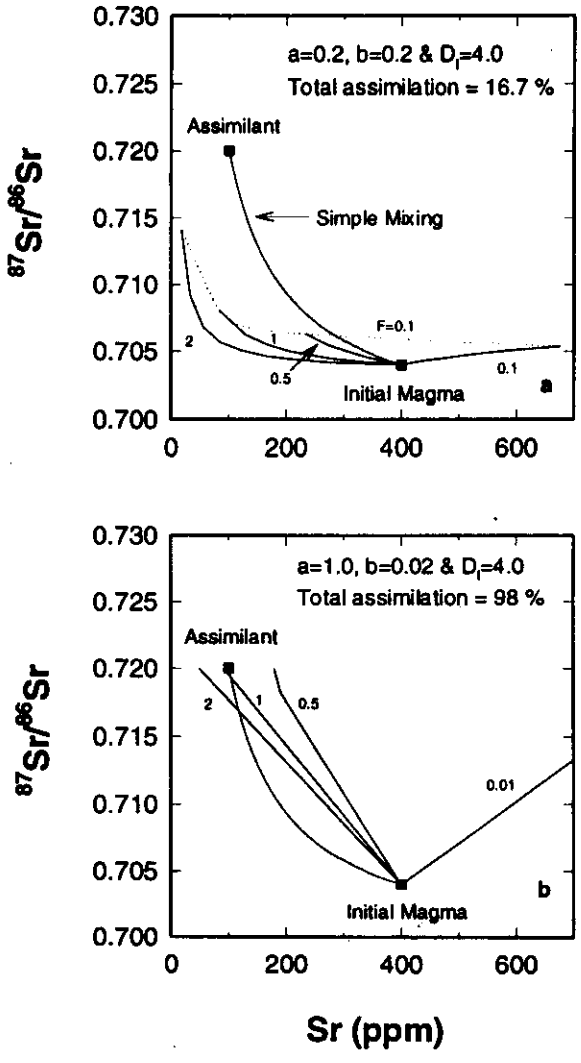

Fig. 4.8. *$^{87}Sr/^{86}Sr$ and Sr concentration evolution in a carbonated silicate magma affected by simultaneous wall rock assimilation, fractional crystallization of alkaline silicate rocks and separation of a carbonate magma by liquid immiscibility for different values of a (rate of assimilation/rate of crystallization) and b (rate of immiscibility/rate of crystallization). Numbers on model curves represent D_c (bulk distribution coefficient for Sr between alkaline rock and magma). In plot (a) evolution is done up to F (fraction of remaining magma) = 0.1 and in (b) up to F= 1.0. The total assimilation percent was calculated using equation (16). The D_i (bulk distribution coefficient for Sr between carbonate melt and silicate melt) is taken as 4.0 in both the cases. See section 4.2.2b for discussion.*

In Fig.4.8a, calculations are done up to F=0.1, whereas in Fig.4.8b, calculations are done up to F=0 (i.e., process completed). Most of the properties of AFCLI model curves are very similar to AFC curves (Fig.3 of DePaolo (1981)), however, the most striking

difference of this model is that even for a small amount of contamination a significant change in the isotopic ratio and concentration can be achieved in a short time (i.e. for a larger F) compared to AFC model.

(iii) ***Amount of Assimilation***

The amount of assimilation in AFCLI model, expressed in percentage is :

% assimilation = [mass of assimilated material/(mass of alkaline rock + mass of carbonatite)] $\times 100$

$$= [M_a/(M_c+M_l)] \times 100$$

$$= [(M_a/M_c)/(1+(M_l/M_c)] \times 100$$

$$= [a/(1+b)] \times 100 \qquad (16)$$

(iv) ***Composition of the Carbonate Melt***

As the crystallization temperatures of carbonates are lower than the silicates, carbonate melt is expected not to crystallize during AFCLI process. Most likely the carbonate melt which fractionally gets removed from the parent melt slowly accumulates and after the liquid immiscibility is over it comes out of the system and travels up ward as a single homogeneous melt before it crystallizes. In such a situation the concentration of an element and isotopic ratio of the carbonate melt will be averages of those of all the fractional melts separated out during AFCLI. If $\bar{C}_c$ and $\bar{C}_m$ are average concentrations in the crystallized phase and carbonate magma, respectively then we can write a mass balance equation:

$$C_a M_a + C_m^o M_m^o = \bar{C}_c M_c + \bar{C}_l M_l \qquad (17)$$

Equation (17) can be rewritten as

$$C_a M_a + C_m^o M_m^o = D_c \bar{C}_m M_c + D_l \bar{C}_m M_l \qquad (18)$$

where $\bar{C}_m$ is the time average concentration of the element in the evolving parent magma. Simplifying (18) we get

$$\bar{C}_m = \frac{C_a M_a + C_m^o M_m^o}{D_c M_c + D_l M_l} \qquad (19)$$

Hence,

$$\bar{C}_l = D_l \bar{C}_m = D_l \left[\frac{C_a M_a + C_m^o M_m^o}{D_c M_c + D_l M_l}\right] \qquad (20)$$

$$\text{or, } \bar{C}_l = D_l\left[\frac{aC_a + (1+b-a)C_m^o}{D_c + bD_l}\right] \quad (21)$$

Equation (21) gives the required concentration of the element in the accumulated carbonate melt. Doing similar mass balance for isotopic ratio we get:

$$\bar{E}_l = \bar{E}_m = E_m^0\left(\frac{C_m^o M_m^0}{C_a M_a + C_m^o M_m^o}\right) + \left(\frac{E_a C_a M_a}{C_a M_a + C_m^o M_m^o}\right) \quad (22)$$

Alkaline and carbonate melts get emplaced very rapidly owing to their low viscosity and density, which may lead to a very small amount of contamination/assimilation of wall-rocks in such melts (i.e. $M_a << M_m^o$). In the case of Sr isotopic ratio and concentrations, most of the crustal rocks, which are likely candidates for assimilant have very low concentrations of Sr (i.e. $C_a << C_m^o$). So for Sr systematics, one can safely make the following approximations:

$$\frac{C_m^o M_m^o}{C_a M_a + C_m^o M_m^o} \approx 1 \quad (23)$$

and

$$\frac{E_a C_a M_a}{C_a M_a + C_m^o M_m^o} \approx 0 \quad (24)$$

Hence, equation (22) becomes:

$$\bar{E}_l = \bar{E}_m = E_m^o \quad (25)$$

This essentially means that even if there is a crustal contamination of the parent magma, due to very high content of Sr in this melt, the $^{87}Sr/^{86}Sr$ of the carbonate melt (which is an average of evolving E_m values) formed by liquid immiscibility retains the initial value of the parent magma (i.e. $= E_m^o$).

B. Application of AFCLI model to Amba Dongar Complex

In Amba Dongar, out of all the country rocks only the Precambrian gneiss qualifies to be an assimilant for the parent magma, as other rocks such as sandstone, limestone and basalt are surficial rocks, which probably do not occur at depths, where liquid immiscibility takes place. Hence, considering gneisses ($^{87}Sr/^{86}Sr = 0.7690$ and Sr = 145 ppm) as an assimilant AFCLI model curves were generated using $D_c = 1.8$ (assumed, see section 4.2.2a) and $D_l = 4.0$ (from Green et al., 1992). It was found that the evolution curve with a = 0.05 and b = 0.15 (Fig.4.9) explained the observed alkaline rock trend which suggests that the parent

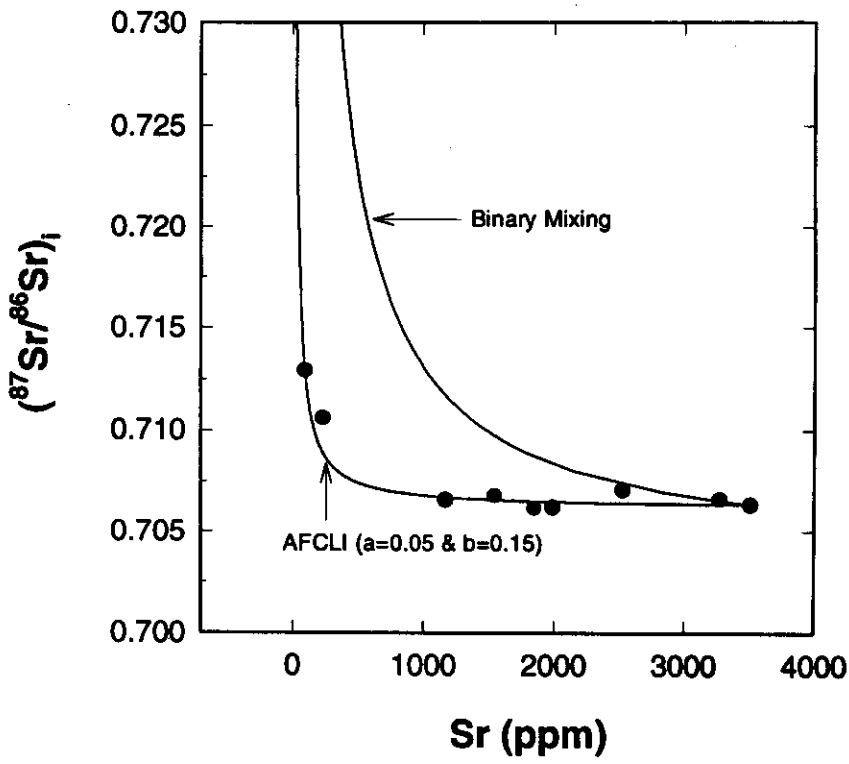

Fig. 4.9. *Plot of initial $^{87}Sr/^{86}Sr$ vs. Sr concentration for alkaline rocks of Amba Dongar complex. Top curve represents results of binary mixing between an alkaline silicate magma and Precambrian gneiss. Bottom curve represents results of AFCLI modelling (see section 4.2.2b.) with a carbonated silicate magma and the gneiss as two end-members at a = 0.05 and b = 0.15. For the model the bulk distribution coefficients for Sr, D_c and D_l are taken to be 1.8 and 4.0, respectively. Please see the caption of Fig. 4.8 and text in section 4.2.2b for discussion.*

magma of this complex have evolved through AFCLI by assimilating ~4% of basement gneisses. In such a case the carbonate magma generated by means of liquid immiscibility will have initial $^{87}Sr/^{86}Sr$ of 0.70632 (same as the parent magma) and Sr concentration of 4306 ppm (calculated using equation (21)). However, the lowest initial $^{87}Sr/^{86}Sr$ of carbonatites of Amba Dongar (Table 4.6) is 0.7055±2. This discrepancy may be due to the lack of data of the most primitive or uncontaminated alkaline rock, which could be used as the magmatic end-member in the AFCLI model.

The Sr isotopic evolution of Amba Dongar alkaline rocks are explained by both the AFC and the AFCLI model. This is because the distribution coefficient of Sr for alkaline rock is assumed to be more than 1.0, which masks the effects of liquid immiscibility in a simple AFC model. If the above distribution coefficient is less than 1.0 then the AFC model cannot explain the observed alkaline rock trend of Amba Dongar complex (Fig.4.5), whereas AFCLI can explain (this is evident in Fig.4.8a). Hence, the AFCLI process is believed to be the most probable magmatic process that have generated the alkaline rocks and carbonatites of Amba Dongar.

4.2.3. Sr Isotopic Evolution of Carbonatites of Amba Dongar

After its removal from the parent magma, carbonate magma rises rapidly within the crust and crystallizes on or close the surface. During its ascent, like the parent magma, it may get contaminated by the wall-rocks. However, because of its rapid ascent and very different composition, carbonate melt may not be able to assimilate silicate wall-rocks but can get contaminated by compositionaly similar rocks such as limestones. In Amba Dongar complex, to check for such contamination Sr isotopes were used.

Fig.4.10 shows the binary mixing curve for Amba Dongar limestone ($^{87}Sr/^{86}Sr$) = 0.7087 and Sr = 676 ppm) and carbonatite ($^{87}Sr/^{86}Sr$ = 0.70549 and Sr = 6810 ppm, taken from Simonetti et al., (1995)). The figure 4.10 also shows AFC evolution curves for different D values. As one can see neither the simple binary mixing nor the AFC of limestones explains the observed variations of $^{87}Sr/^{86}Sr$ and Sr concentration in carbonatites. Hence, carbonatites are not contaminated by any of the country rocks. The probable explanation for the Sr concentration variation in carbonatites is the fractional crystallization of the carbonate parent magma. Considering the high errors associated with the $^{87}Sr/^{86}Sr$ measurements in the carbonatites (measured at Physical Research Laboratory, see section 3.4.5 of Chapter-III), the variation in initial $^{87}Sr/^{86}Sr$ is too small to be a result of any magmatic or secondary process.

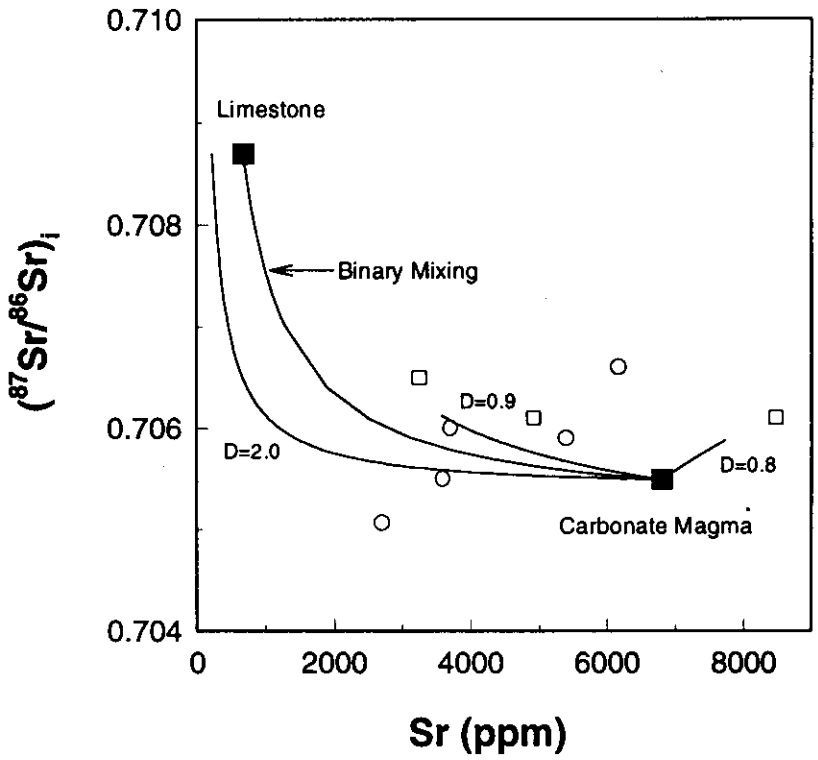

Fig. 4.10. *Plot of initial $^{87}Sr/^{86}Sr$ vs. Sr content for Amba Dongar carbonatites. Open circles = calcite carbonatites,; open squares = ferrocarbonatites. Binary mixing curve represents results of simple binary mixing between carbonate magma and Bagh limestone. Other curves are AFC curves generated with the same end end-members for different values of D (bulk distribution coefficient for Sr between carbonatite and carbonate magma). See section 4.2.3 for discussion.*

4.2.4. Mantle Source Regions

The range of initial strontium isotopic ratios of Amba Dongar carbonatites observed in the present study and those observed by other workers (Deans et al., 1968; Simonetti et al., 1995) overlap with the observed range of Mundwara complex (0.7038 - 0.7055; Rathore et al., 1996). The only available initial Sr ratio from Sarnu-Dandali complex (0.70449; Basu et al., 1993) also falls within the range of Mundwara. This observation probably suggests a similarity in the mantle source regions of these complexes. Although the Sr ratios of Mundwara and Sarnu-Dandali complexes are higher than that of the Reunion-basalts (0.7033 - 0.7044; White et al., 1990), He-isotopic evidence (Basu et al., 1993) suggests a plume origin for these complexes. As the carbonatites and the least contaminated alkaline

rocks from Amba Dongar have similar Sr ratios like those of rocks from Mundwara , I believe that Amba Dongar too was derived from a plume source. The difference in the ratios in the alkaline complexes and the present day basalts from Reunion island can be attributed either to the involvement of enriched subcontinental lithosphere in the generation of these complexes (mixing of plume material with the material from subcontinental lithosphere) or to the complex evolutionary history of the Reunion hotspot (White et al., 1990).

4.2.5. Summary

Strontium isotopic study of Amba Dongar revealed that the silicate rocks and carbonatite of this complex ware generated by liquid immiscibility and the parent magma of this complex was contaminated by the basement gneisses (up to ~4%). The model which gives the above results also suggests that the carbonate melt does not retain any isotopic signature of this contamination process rather retains the isotopic ratio of the primary magma if it does not get contaminated during its later evolution after immiscibility, which is true for Amba Dongar carbonatites. The overlapping of initial strontium isotopic ratios of Amba Dongar, Mundwara and Sarnu-Dandali probably suggests a similarity of their source regions and possibly all these complexes were derived from the Reunion plume.

4.3. TRACE-ELEMENT STUDIES ON AMBA DONGAR COMPLEX

Trace element variations were studied in carbonatites and alkaline rocks of Amba Dongar complex to understand the major magmatic processes involved in the evolution of this complex. The abundances of Zr, Ba, Hf and nine rare earth elements (REE) (La, Ce, Sm, Eu, Gd, Tb, Yb, and Lu) were measured in samples of calcite carbonatites, ferrocarbonatites and alkaline rocks by INAA following the procedures described in Chapter-III.

4.3.1. Results

The REE, Zr, Ba and Hf concentrations of four calcite carbonatites, three ferrocarbonatites and three alkaline rocks are given in Table 4.7. Chondrite normalized REE concentrations are plotted in Fig. 4.11 and chondrite normalized concentrations of some selective trace elements (which also includes Sr concentrations taken from the previous section) are shown

in Fig. 4.12. In both the figures the concentration patterns are grouped according to the rock types. As seen in Fig. 4.11, carbonatites are enriched in lighter REE compared to the alkaline rocks and within carbonatites, ferrocarbonatites are enriched in these elements compared to calcite carbonatites. Heavier REE abundance patterns of both types of carbonatites overlap (Fig. 4.11). Enrichment of other incompatible trace elements also follows the same trend; i.e., ferrocarbonatites > calcite carbonatites > alkaline silicate rocks (Fig. 4.12).

Table 4.7. Trace element abundances in the whole-rock samples from Amba Dongar.

Sample Conc. (ppm)	AD 10	AD 12	AD 17	AD 19	AD 31	AD 36	AD 38	AD 43	AD 45	AD 47
Zr	258	448	741	1165	905	472	216	446	683	197
Ba	1736	114630	552	8553	8779	28684	2663	8974	1623	573
La	325	3464	161	2084	1372	5620	356	971	139	34
Ce	581	5528	227	4276	2465	6241	615	1794	264	61
Nd	209	778	69	1583	938	935	215	640	120	25
Sm	26.4	82.2	10.4	180	137.5	95.1	16.4	63.0	18.4	4.6
Eu	7.0	17.0	2.8	42.3	29.5	19.9	7.0	17.1	5.0	1.1
Gd	14.6	61.7	9.5	96.1	110.5	72.7	17.5	51.8	13.4	4.0
Tb	1.6	3.6	1.2	10.2	7.9	5.0	2.1	4.1	1.9	0.6
Yb	3.1	13.1	3.5	10.2	23.2	20.5	4.3	6.9	4.8	2.5
Lu	0.44	0.84	0.51	0.96	1.64	1.2	0.55	0.54	0.65	0.40
Hf	0.25	0.47	10.2	0.64	0.77	0.32	0.34	0.62	9.4	3.0

Note: AD-10, AD-31, AD-38 and AD-43 are calcite carbonatites. AD-12, AD-19 and AD-36 are ferrocarbonatites. AD-17, AD-45 and AD-47 are alkaline rocks.

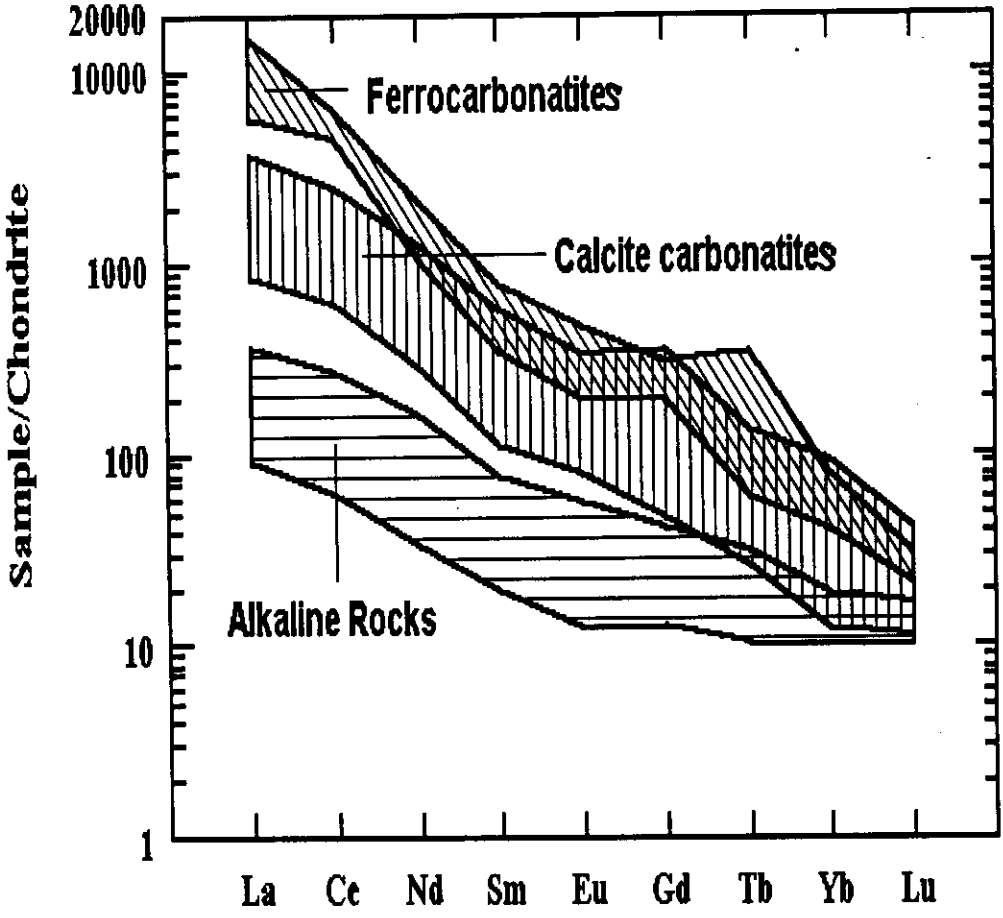

Fig. 4.11. *Chondrite normalized concentrations of nine rare earth elements in different lithological units of Amba Dongar complex are shown in groups. Chondrite values are those of Taylor and McLennan (1985).*

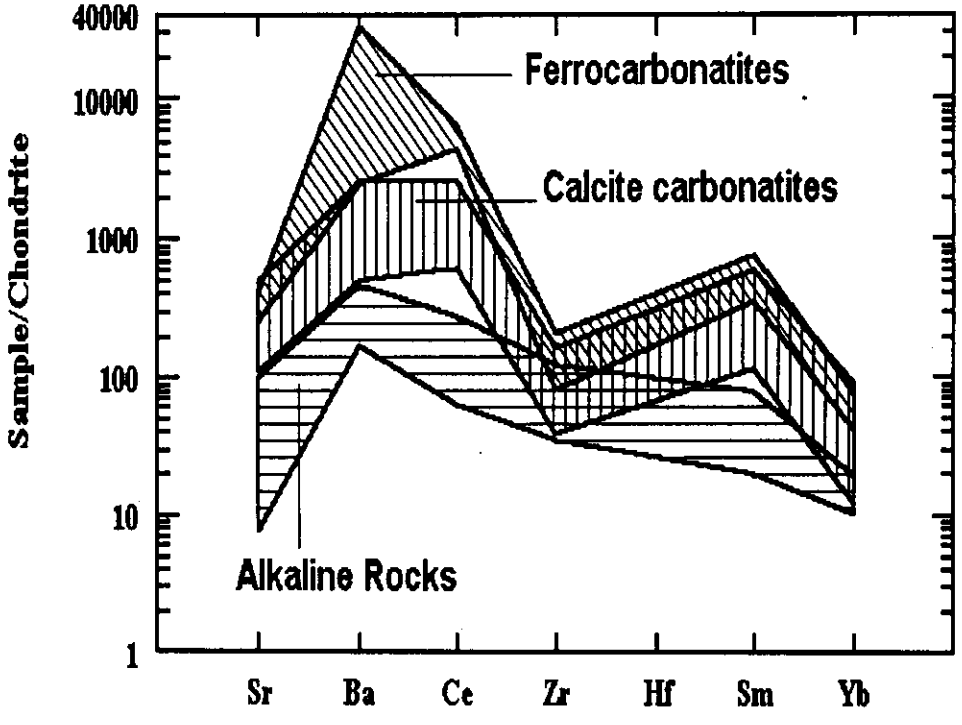

Fig. 4.12. *Trace-element abundances in different lithological units of Amba Dongar Complex normalized to Chondrite abundances. Chondrite values are from Taylor and McLennan (1985).*

4.3.2. Discussion

Amba Dongar carbonatites, like most of the carbonatites of the world, are highly enriched in LREE, a feature usually attributed to the generation of the parent magma of these rocks by extremely low degree of partial melting of a carbonated peridotite or eclogitic source (Nelson et al., 1988). The higher abundance of these elements in carbonatites compared to the alkaline rocks probably is a result of fractional crystallization or liquid immiscibility process involved in the formation of these rocks. Similarly the higher LREE and Ba content in ferrocarbonatites compared to calcite carbonatites indicates their derivation from a carbonate parent magma at a later stage by fractional crystallization. The negative anomalies of Zr in carbonatites (Fig. 4.12) may be attributed to the early removal of zircon from the parent magma.

The main purpose of the present trace element studies in Amba Dongar complex is to establish whether alkaline silicate rocks and carbonatites of this complex have a common genetic link through liquid immiscibility or not. For this a simple conservative calculation is done assuming that the carbonatites of Amba Dongar have crystallized fractionally from a carbonate magma after its separation from a carbonated silicate parent magma through liquid immiscibility. In a fractional crystallization process concentration of a particular element in the crystallizing solid (C_s) evolves as:

$$C_s = C_o D f^{(D-1)} \quad (26)$$

where C_o is the original concentration in the carbonate magma, D is the rock-magma distribution coefficient of the element under consideration and f is the fraction of remaining parent melt. To find out the concentration of the element in the silicate melt, we need to know C_o. For this, it was assumed that the observed minimum and maximum concentrations of different elements represent the carbonatites formed from the carbonate parent melt at f = 1 and f = 0.001, we get two simultaneous equations for two unknowns C_o and D.

$$C_s^i = C_o D \quad (27)$$

$$C_s^f = C_o D (0.001)^{D-1} \quad (28)$$

where C_s^i and C_s^f stand for minimum and maximum concentration of the element in carbonatites, respectively. Then solving for D and C_o, we get:

$$D = 1 + [\ln(C_s^f / C_s^i)] / [\ln(0.001)] \quad (29)$$

and

$$C_o = C_s^i / D \quad (30)$$

Using equations (29) and (30), the D and C_o values for different rare earth elements (La, Ce, Sm, Eu, Yb and Lu) were calculated. Table 4.8 summarizes these values. As the measured concentrations (C_s^i and C_s^f) have some analytical errors and also the rocks analyzed for this work do not represent the whole carbonatite intrusion, a conservative error of 10 % was assigned to the estimated C_o values. Then using nephelinitic melt-carbonate melt partition coefficients (at 1150° C and 6 Kb) of Hamilton et al. (1989), the expected concentrations in the silicate melt (C_{sm}) were calculated from the relation;

$$C_{sm} = C_o K_d \quad (31)$$

The error in this estimated concentration was calculated using the equation:

$$\sigma_{sm} = C_{sm}\sqrt{(\frac{\sigma_{K_d}}{K_d})^2 + (\frac{\sigma_{C_o}}{C_o})^2} \quad (32)$$

where σ_{K_d} and σ_{C_o} represent the errors in the K_d values and C_o values (10 %), respectively. The estimated concentration with their errors are given in Table 4.9. the chondrite normalized pattern of these estimated concentrations (with their errors) are plotted in Fig. 4.13 (silicate melt-1) and compared with the alkaline rock field. The alkaline rock field of Fig. 4.13 also includes data from Viladkar and Dulski (1986) apart from the data from the present study. The estimated concentration in the carbonate melt (C_o) is also shown in this figure. The estimated concentration field for silicate magma overlaps with the observed field. Similar estimations were made using the carbonate melt-silicate melt partition coefficients given by Wendlandt and Harrison (1979) for Ce and Sm (silicate melt-2 and silicate melt-3 of Fig. 4.13) and it was found that these model melts fell well within the observed alkaline rock field of Amba Dongar. The above observations, though have many limitations which arise from the choice of K_d values and initial melt compositions, suggest that the carbonatites and alkaline rocks of Amba Dongar were derived by liquid immiscibility.

Table 4.8. Modelled Distribution coefficients (Carbonatite-Carbonate Melt) of some REE and their estimated concentrations in the carbonate melt.

Elements	$D_{rock\text{-}melt}$	C_o (ppm)
La	0.59	551
Ce	0.66	880
Sm	0.72	37
Eu	0.74	9.5
Yb	0.71	4.4
Lu	0.81	0.54

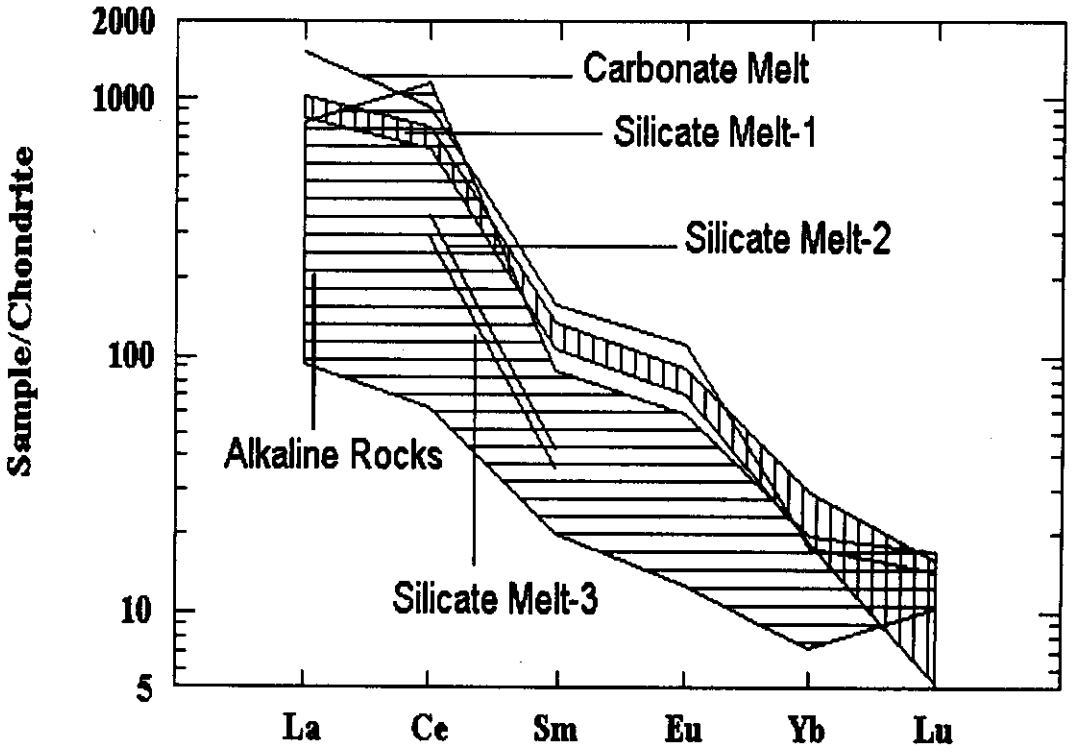

Fig. 4.13. Chondrite normalized REE diagram, illustrating potential silicate parent melts for the Amba Dongar carbonate melt, calculated on the basis of available experimental carbonate melt-silicate melt partition coefficients (K_d values). Silicate melt-1 field is calculated using K_d values from Hamilton et al. (1989). Silicate melt-2 and 3 are calculated using K_d values respectively for 20 kbar & 1200°C and 5 kbar & 1200°C from Wendlandt and Harrison (1979). The alkaline rock field is the observed data, which also includes data from Viladkar & Dulski (1986). See section 4.3.2 for discussion.

Table 4.9. Estimated concentrations of some REE in the silicate melt with their errors.

Elements	C_{SM} (ppm)	1σ (ppm)
La	342	33.5
Ce	678	62.2
Sm	28.5	3.4
Eu	6.9	0.8
Yb	5.9	1.4
Lu	0.4	0.2

SM stands for silicate melt

4.3.3. Summary

The rare earth elemental abundances in different rocks of Amba Dongar complex show an enrichment pattern in the order; alkaline rocks < calcite carbonatites < ferrocarbonatites. Ferrocarbonatites were probably generated from the magma at a later stage by fractional crystallization. Model calculations suggest that the carbonate magma of this complex was derived by liquid immiscibility from the silicate magma.

4.4. STABLE CARBON AND OXYGEN ISOTOPES

Study of stable carbon isotopic variations in carbonatites may provide important clues to the nature of carbon in the mantle, in particular to the carbon isotopic heterogeneity and possibly to the fate of recycled carbon. The combined study of carbon and oxygen isotopes in carbonatites and associated alkaline rocks helps in characterizing their source regions, understanding the processes involved in their formation and the isotopic evolution during and after their emplacement. Stable carbon and oxygen isotopes were analyzed in samples from the three carbonatite-alkaline complexes of Deccan province in order to understand the isotopic evolution of these complexes and to characterize the stable isotopic compositions of their mantle source regions. Before discussing the results of the present work, at this juncture, it will be appropriate to discuss briefly the earlier stable isotopic studies on carbonatites in general.

4.4.1. Stable Carbon and Oxygen Isotopic Variations in Carbonatites: A Brief Review

In one of the earliest stable isotopic studies on carbonatites, Taylor et al. (1967) suggested that the carbon and oxygen isotopic compositions of carbonatites were homogeneous and defined a field (Taylor Box) for carbonatites in a $\delta^{13}C$ versus $\delta^{18}O$ plot (Fig.4.14). But later studies (Pineau et al., 1973; Deines and Gold, 1973; Nelson et al., 1988; Deines, 1989) showed a considerable range of $\delta^{13}C$ and $\delta^{18}O$ compositions

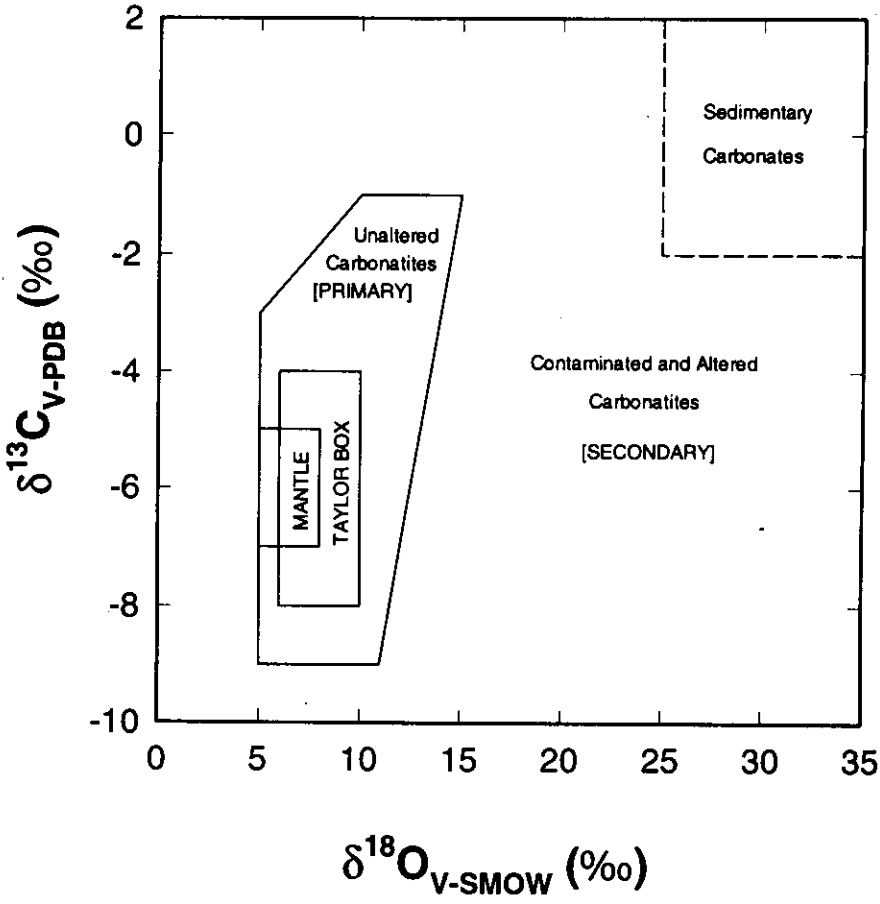

Fig. 4.14. *Plot of $\delta^{13}C$ vs. $\delta^{18}O$ showing different carbonatite and sedimentary carbonate fields. Mantle box is after Nelson et al. (1988), Taylor box represents the primary carbonatites studied by Taylor et al. (1967) and the unaltered (primary) carbonatite field is inferred from studies of Plyusnin et al. (1980) and Deines (1989). Crustally contaminated and altered carbonatites (secondary) plot between the primary carbonatite and the sedimentary carbonate fields.*

which partly overlap with the mantle compositions inferred from studies of mid-oceanic ridge basalts and meteorites. The variations in $\delta^{13}C$ and $\delta^{18}O$ in carbonatites have been interpreted in different ways by earlier workers. Deines and Gold (1973) related these variations to the emplacement levels of carbonatites and suggested that the deep-seated complexes have narrower ranges of isotopic compositions (primary variations) compared to the shallower ones, which they attributed to secondary near-surface processes. Pineau et al. (1973) observed three different groups of $\delta^{13}C$ and

$\delta^{18}O$ variations. The first group showed typical mantle values; the second showed correlated variation of $\delta^{13}C$ and $\delta^{18}O$, which they attributed to Rayleigh fractionation during late stage carbonatite crystallization and the third showed no correlation of $\delta^{13}C$ and $\delta^{18}O$, which was explained by fluid related secondary processes. In another study, Deines (1989) suggested that the correlated variation could be explained by simultaneous crystallization of carbonates and silicates from a parent magma.

In general, carbonatites can be grouped into two: (1) those which are not affected by secondary processes and show either mantle values or some kind of correlated variation of $\delta^{13}C$ and $\delta^{18}O$ (Primary variations) (2) those which show extreme variations, probably as a result of alteration by secondary processes (Secondary variations). Considering $\delta^{13}C$ and $\delta^{18}O$ variations of carbonatites of the world (Plyusnin et al., 1980; Deines 1989), it is possible to define two different fields for the above described groups of carbonatites in a $\delta^{13}C$ versus $\delta^{18}O$ diagram. Group-1 variety (Fig. 4.14) encompasses the fields of mantle rocks (Nelson et al., 1988) and the primary carbonatite field defined by Taylor (1967). Group-2 variety of carbonatites generally fall outside the Group-1 field (Fig.4.14). In order to evaluate the isotopic compositions of the mantle source regions, for a given complex, it is important to distinguish the primary variation (which bears the magmatic signatures) from the secondary.

4.4.1a. Primary Carbonatites

Primary carbonatites, according to the general belief, are purely magmatic and whose $\delta^{13}C$ and $\delta^{18}O$ variations overlap with the mantle values. These are unaltered rocks (belong to Group-1, as defined above), whose isotopic variations are either results of magmatic isotope fractionation processes or reflect the source heterogeneity (Deines,1989). In the following paragraphs, I briefly discuss different models which have been proposed by different workers to explain these variations.

The magmatic processes which are expected to cause $\delta^{13}C$ and $\delta^{18}O$ variations in carbonatites include, extraction of carbonatite melt from the mantle, liquid immiscibility, crustal contamination and fractional crystallization. Deines (1989)

suggested that $\delta^{13}C$ and $\delta^{18}O$ variations in carbonatites could be related partly to the extraction of carbonate melt from a heterogeneous source region. Liquid immiscibility has been suggested as an important process in the formation of carbonatites (Wyllie, 1989; Kjarsgaard and Hamilton, 1989). Mattey et al. (1990) found from experimental studies that the carbon isotopic fractionation between carbonate melt and silicate melt is very small (0.4‰) in the temperature pressure range of 1200-1400°C and 5-30 kbars, which led them to suggest that carbon isotopes do not fractionate during liquid immiscibility. However, such an inference may not be correct, if fractionation of ^{13}C during liquid immiscibility is of Rayleigh type. Isotopic fractionation during liquid immiscibility will be discussed in detail in the next section.

Contamination of carbonate magma by crustal rocks is another magmatic process which can affect their isotopic composition. Carbon being a trace element in most of the crustal rocks, except limestones, contamination of these rocks may not generate large variations in $\delta^{13}C$ composition of carbonatites. $\delta^{18}O$ value of crustal rocks (excluding limestones) are not very different from the carbonatites, hence, contamination effects may not be detected. Contamination due to limestones can generate isotopic compositions which are likely fall between mantle field and sedimentary carbonate field in a $\delta^{13}C$ vs. $\delta^{18}O$ plot (Fig. 4.14). In such a case it is difficult to extract information about the source regions. Therefore, in such situations it is important to assess the extent of contamination using other isotope systematics (e.g., Sr).

Fractional crystallization of carbonatite from a carbonate melt is another magmatic process which may generate variations in $\delta^{13}C$ and $\delta^{18}O$. Lack of knowledge about the fractionation factors between the minerals and the carbonate melt makes the modelling of isotopic variations during fractional crystallization difficult. With certain assumptions and considering the involvement of magmatic fluids and silicate phases, earlier workers (Pineau et al., 1973; Deines, 1989) modelled the effects of fractional crystallization. Pineau et al. (1973) gave an approximate equation for isotopic fractionation from a two component source and suggested that the late stage calcite (calcite carbonatite) crystallization from a CO_2 enriched, H_2O bearing magmatic fluid

at 700°C could explain the correlated variation of $\delta^{13}C$ and $\delta^{18}O$ in some primary carbonatites. To explain the observed slope (of 0.4) of the $\delta^{13}C$ - $\delta^{18}O$ plot, they restricted the oxygen contribution from H_2O and silicates present in the magma to less than 30%. Later this was challenged by Deines (1989) on the ground of their unrealistic assumption. Deines (1989) proposed a Rayleigh isotopic fractionation model to treat simultaneous fractional crystallization of carbonates and silicates (or carbonate-silicate immiscibility) from a parent melt and suggested that probably such a process could explain the observed slope of $\delta^{13}C$ versus $\delta^{18}O$ plot. However, the model required unrealistic fractionation factors ($\alpha^{18}O$(silicate rock-magma) = 0.9978, which is too low and $\alpha^{13}C$(carbonatite-magma) = 0.9993, which in fact should be more than 1.0) and unrealistic molar ratios of carbon between carbonatite and silicates (=1000, which is too high considering the fact that the volume of carbonatites is much smaller than the volume of silicate rocks in a given complex).

4.4.1b. Altered Carbonatites

Altered carbonatites generally do not fall in the primary carbonatite box of Fig.4.14 because of their higher $\delta^{18}O$ values. These rocks sometimes also show widely different $\delta^{13}C$ values compared to primary carbonatites. Many models have been proposed (Deines, 1989; Santos and Clayton, 1995) to explain these variations. These models propose different fluid related processes as responsible mechanisms for alteration of magmatic isotopic signatures of carbonatites. As fluid activity during and after the carbonatite magmatism is very common in carbonatite complexes (this is evident from the fenitization of host rocks, formation of hydrothermal mineral deposits, presence of alteration products in carbonatites, recrystallization textures and above all the extreme variation of $\delta^{13}C$ and $\delta^{18}O$ of carbonatites and the host rocks affected by fluid activities), it is likely that isotopic compositions of some of the carbonatites are likely to get affected by this.

Fluids can be magmatic, hydrothermal or meteoric water of varying isotopic compositions. The $\delta^{13}C$ variations in altered carbonatites (though smaller compared to $\delta^{18}O$) suggest for a CO_2 bearing aqueous fluid activity being responsible for the isotopic alteration. To understand the effect of such fluid activity on the C and O

isotopic composition of carbonatites, a simple closed system fluid-rock interaction model was developed by Santos and Clayton (1995). However, this model had some flaws in the derivations, which have been rectified in this work (this will be discussed in the section 4.4.3).

4.4.2. Results

The carbon and oxygen isotopic compositions of carbonates from carbonatites, alkaline rocks and metasomatic rocks from Amba Dongar, Mundwara and Sarnu-Dandali complexes were measured following the procedures described in Chapter-III. Isotopic compositions of coexisting calcites and ankerites were measured following the selective CO_2 extraction procedures developed by me (see Section 3.2.2b of Chapter-III). Table 4.10 summarizes the results. $\delta^{13}C$ and $\delta^{18}O$ of calcites of samples from Amba Dongar, Mundwara and Sarnu-Dandali are plotted in Fig.4.15a, b and c, respectively. Some calcite carbonatites of Mundwara and Sarnu-Dandali fall within the mantle box defined by Nelson et al. (1988) (Figures 4.15b and 4.15c). But most of the calcite carbonatites do not show mantle values and have higher $\delta^{13}C$ and $\delta^{18}O$ values compared to those of the mantle. The $\delta^{13}C$ and $\delta^{18}O$ ranges of calcites from different rocks are very similar in all the three complexes. The highest $\delta^{18}O$ values in each complex are observed in calcites from metasomatic rocks and ferrocarbonatites. Calcites from alkaline rocks of Amba Dongar show two groups in a $\delta^{13}C$ vs $\delta^{18}O$ plot (Fig.4.15a).

Table 4.10. Carbon and Oxygen isotopic compositions of samples from carbonatite-alkaline complexes of Deccan Province.

Sample	$\delta^{13}C_{calcite}$ (‰)	$\delta^{18}O_{calcite}$ (‰)	$\delta^{13}C_{ankerite}$ (‰)	$\delta^{18}O_{ankerite}$ (‰)
Amba Dongar				
AD-1	-2.9	7.4		
AD-2/x	-3.3	14.9		
AD-2/y	-3.1	14.3		
AD-3	-3.3	20.8		
AD-4	0.1	10.5		
AD-8	-3.6	6.1		

AD9/2	-2.4	10.9		
AD-10/1x	-4.4	8.6		
AD-10/1y	-4.2	9.2		
AD-10/2x	-3.9	11.1		
AD-10/2y	-4.4	9.6		
AD-12	-4.3	25.8	-1.8	15.2
AD-13/1	-3.7	17.3		
AD-14	-3.8	11.3		
AD-17/1	-6.3	13.9		
AD-18	-5.9	13.0		
AD-19	-2.7	12.1	-4.7	7.3
AD-20	-3.4	15.7		
AD-24	-1.5	29.0		
AD-25	---	---	-4.2	8.6
AD-26	-2.6	29.5		
AD-27	-3.5	8.0		
AD-28	-3.4	28.6		
AD-29	-4.0	18.7		
AD-30	-6.9	22.3		
AD-31	-2.9	12.1		
AD-32	-3.4	10.4		
AD-33	-5.4	27.4	-2.3	13.0
AD-34	---	---	-1.8	16.3
AD-35	-3.3	27.2	-2.7	15.5
AD-38	-4.4	10.2		
AD-39	-3.6	12.7		
AD-40	-3.2	12.1		
AD-41	-3.2	14.7		
AD-43	-1.9	13.0		
AD-44/1	-4.8	18.2		
AD-45	-6.3	10.9		
AD-47	-5.7	10.7		
AD-49	-3.1	9.0		
AD-51	-4.3	15.0		
AD-52	-4.8	13.1		
AD-54	-3.6	11.2		
AD-55	-3.8	27.6	-1.1	18.2
AD-58	-6.7	25.9		

AD-59/1	0.1	10.6
AD-60	-0.1	14.2
AD-62	0.9	24.6
AD-63	-4.2	10.2
AD-64	-4.0	10.5
NS-2	-3.3	12.2
NS-3	-3.5	11.3
NS-20/2	-4.5	9.9
NS-20/O/2	-4.8	9.2
NS-20/O/3	-4.5	10.6
NS-20/O/4	-4.2	10.2
NS-20/6	-4.3	9.6
NS-20/8	-4.6	9.5
NS-20/9	-4.2	10.6
NS-20/10	-3.8	10.2
NS-20/11	-3.8	7.6
NS-20/13	-5.1	9.5
Mundwara		
M-1	-5.2	7.9
M-2	-6.4	6.1
M-3	-3.8	21.6
M-15	-3.7	9.4
M-39	-3.9	10.1
M-40	1.1	16.7
M-121	-1.2	16.2
Sarnu-Dandali		
C-94	-2.7	18.7
C-119	-4.9	9.3
C-142	-2.0	16.7
C-143	-5.4	8.2
C-149	-5.3	25.2
C-177	-1.4	28.2
C-254	-4.4	10.9
C-255	-3.6	16.3
C-290	-5.9	13.9
C-291	-6.1	22.9
A-18	-3.6	24.3
A-161	-1.6	21.2

A-800	-2.1	24.6
A-805	-1.6	25.4
A-807	-1.1	27.5
A-808	-4.5	23.5
A-841	-1.6	17.0

Note: x and y are two different parts of a single whole rock sample (were taken out by drilling). $\delta^{13}C$ is expressed with respect to V-PDB and $\delta^{18}O$ with respect to V-SMOW.

Fig. 4.15a shows carbon and oxygen isotopic composition of calcites from different types of carbonatites and metasomatic rocks from Amba Dongar complex. It was found that the two major variety of calcite carbonatites show two different kind of isotopic variations in Fig.4.15a. The first variety (massive, coarse to medium grained and unaltered calcite carbonatites) shows some kind of correlated variation of $\delta^{13}C$ and $\delta^{18}O$ (open circles in Fig. 4.15a) starting from inside the primary carbonatite box (modified after Taylor, (1967); Keller and Hoefs, (1995)). The second variety of calcite carbonatite (fine grained, brown coloured and altered late stage calcite carbonatite veins) shows higher $\delta^{18}O$ values but similar $\delta^{13}C$ values (open triangles in Fig.4.15a) compared to the first variety. Some of the massive calcite carbonatites, which are found to be altered have also been included with the second variety. The altered nature of calcite carbonatites was detected by the presence of secondary microcrystalline silica, recrystallization texture hematization of magnetites and fluorite mineralization in these. Calcites from metasomatic rocks and ferrocarbonatites clearly plot as a separate group with very high $\delta^{18}O$ (~28 ‰) in Fig. 4.15a. Fig. 4.16 shows the $\delta^{13}C$ and $\delta^{18}O$ values of coexisting calcite and ankerites of ferrocarbonatites from Amba Dongar. In all ferrocarbonatites $\delta^{18}O$ of calcite is substantially higher compared to that of the coexisting ankerite. $\delta^{13}C$ of ankerites are higher compared to calcites as well, except in one case. A hydrothermal vein calcite associated with fluorite deposit was also analyzed; $\delta^{13}C$ and $\delta^{18}O$ compositions were -6.7 ‰ and 25.9 ‰, respectively.

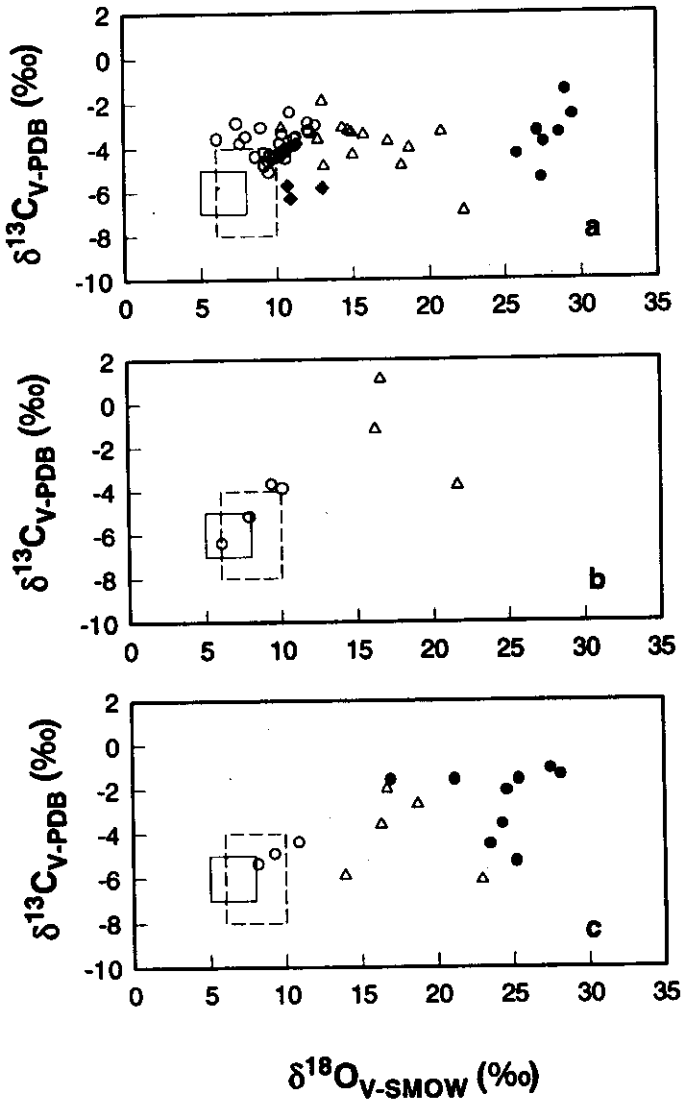

Fig. 4.15. *(a) $\delta^{13}C$ and $\delta^{18}O$ compositions of calcite from carbonatites, alkaline rocks and metasomatic rocks of Amba Dongar. (b) $\delta^{13}C$ and $\delta^{18}O$ of calcite from calcite carbonatites of Mundwara. (c) $\delta^{13}C$ and $\delta^{18}O$ of calcite from calcite carbonatites, ferrocarbonatites and metasomatic rocks of Sarnu-Dandali. Symbols: ○ = unaltered calcite carbonatites; △ = altered calcite carbonatites and late stage calcite carbonatite veins; ● = ferrocarbonatites and metasomatic rocks; ◆ = alkaline rocks. The small box with solid outline is the mantle box of Nelson et al. (1988) and the large box with dashed outline is for primary carbonatites (modified after Taylor, 1967 and Keller and Hoefs, 1995).*

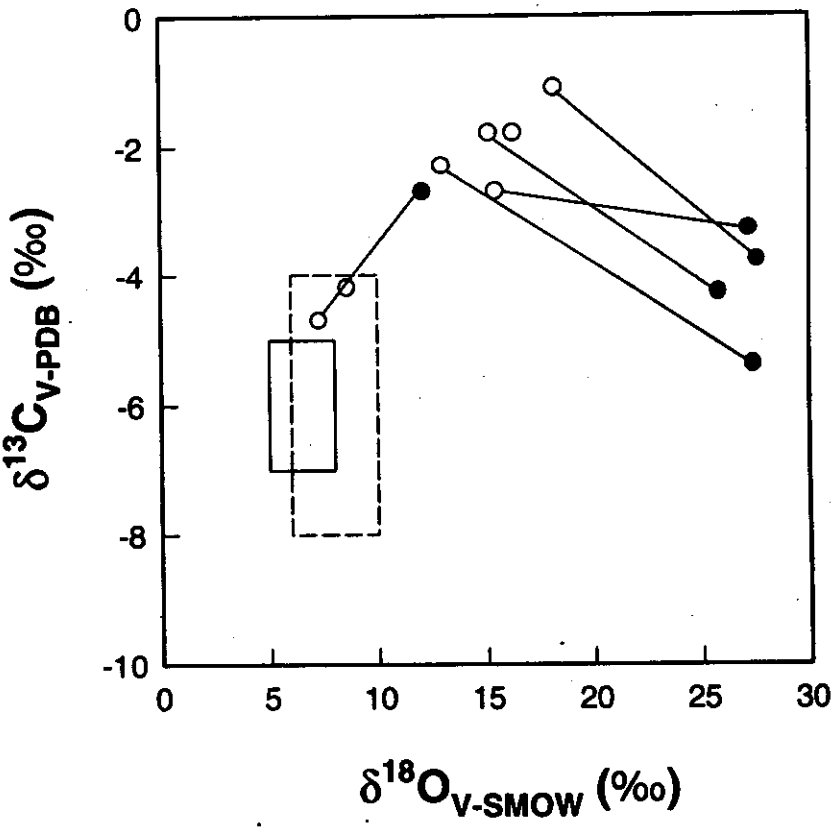

Fig. 4.16. *$\delta^{13}C$ and $\delta^{18}O$ of coexisting calcites (filled circles) and ankerite (open circles) joined by tie lines, from ferrocarbonatites of Amba Dongar. Boxes are mantle box (solid outline) and primary carbonatite box (dashed outline) as defined in Fig. 4.15.*

Calcite carbonatites from Mundwara show the widest range of $\delta^{13}C$ compared to those of calcite carbonatites from other two complexes. $\delta^{13}C$ of calcites from calcite carbonatites varies from -6.4 ‰ to 1.0 ‰ (Fig. 4.15b). Four of these samples show correlated variation of $\delta^{13}C$ and $\delta^{18}O$. Other samples plot away from the mantle and primary carbonatite box with very high $\delta^{18}O$ values.

In Sarnu-Dandali, $\delta^{13}C$ values of calcite from calcite carbonatites vary from -6.1 ‰ to -2.0 ‰, and $\delta^{18}O$ from 8.0 ‰ to 22.9 ‰ (Fig. 4.15c). Three calcite carbonatite samples show correlated variation of $\delta^{13}C$ and $\delta^{18}O$ and all others in this complex, which are found to be altered, show high $\delta^{18}O$ values. Metasomatic rocks and ferrocarbonatites also show higher $\delta^{18}O$ values compared to that of the calcite carbonatites.

4.4.3. Discussion

As described above, the isotopic compositions of calcite carbonatites from all the three complexes clearly form two groups in $\delta^{13}C$ versus $\delta^{18}O$ covariation diagrams (unaltered calcite carbonatites and altered calcite carbonatites). Ferrocarbonatites and metasomatic rocks from all the complexes, generally fall in the altered carbonatite field of such diagrams with very high $\delta^{18}O$ values. The $\delta^{13}C$ and $\delta^{18}O$ of unaltered calcite carbonatites from all three complexes (Fig.4.15) clearly show some kind of correlated variation, which is likely to a be result of one/more magmatic processes involved in the formation of carbonatites. As the limestone-contamination is already ruled out in the case of Amba Dongar (from Sr isotopic study) and there is no limestone in the vicinity of carbonatites in other two complexes, it is unlikely that crustal contamination could have contributed towards the observed isotopic variations in carbonatites in all the three complexes. Hence, the magmatic processes such as liquid immiscibility and fractional crystallization are probably responsible for the $\delta^{13}C$ and $\delta^{18}O$ variation in unaltered calcite carbonatites of the complexes. In the following sub-section (4.4.3a). I discuss the isotopic effects that could be generated by the silicate-carbonate liquid immiscibility. In the sub-section (4.4.3b) the isotopic effects generated by fractional crystallization are modelled and the results of unaltered rocks from the complexes under consideration are interpreted. As discussed in the section 4.4.1, the extreme $\delta^{13}C$ and $\delta^{18}O$ variations (shown by altered calcite carbonatites, calcite from ferrocarbonatites and metasomatic rocks) are probably results of fluid activities in these complexes. In sub-section 4.4.3c a model developed for fluid-rock interaction is given and the observed isotopic variation are interpreted using this model.

4.4.3a. Liquid Immiscibility

It is generally believed that carbonate-silicate immiscibility has insignificant effect on the isotope distributions in these melts (Mattey et al., 1990; Santos and Clayton, 1995). However such an inference is valid only when the immiscibility process is an equilibrium process. It has been suggested that carbonate-silicate liquid immiscibility is a very rapid process (Wyllie, 1989) and after their separation, these two liquids are unlikely to interact (Kjarsgaard and Hamilton, 1989). In such a process the isotopic fractionation is likely to be of Rayleigh type. If the parent magma (PM) is a carbonated silicate magma from which carbonate melt separates out continuously then the carbon isotopic composition in the remaining silicate melt (SM) is be given by

$$\delta^{13}C_{SM} = (1000+\delta^{13}C^{i}_{PM})f^{\alpha-1} - 1000 \quad (33)$$

where f is the fraction of the source melt remaining; and the average carbon composition of the carbonate melt (CM) separated out after the completion of liquid immiscibility is given by

$$(\delta^{13}C_{CM})_{avg} = \frac{\delta^{13}C^{i}_{PM} - f\delta^{13}C_{SM}}{1-f} \quad (34)$$

where α stands for carbon isotope fractionation factor between carbonate melt and silicate melt (=1.0004; Mattey et al., 1990) and $\delta^{13}C^{i}_{PM}$ denotes the initial primary magma composition. With decreasing f, $\delta^{13}C_{SM}$ goes on depleting; however, the accumulated carbonate magma which comes out of the magma chamber upon completion of liquid immiscibility has an average $\delta^{13}C$ composition given by equation (34). The final value of f can be determined independently for a give complex using

$$f = 1/(1+N_{CM}/N_{SM}) \quad (35)$$

where N_{CM}/N_{SM} is the molar ratio of carbon in the carbonate melt (CM) to the silicate melt (SM). In one example, for f = 0.308 (a conservative value) and $\delta^{13}C^{i}_{PM}$ = -5.5‰, we find $\delta^{13}C_{SM}$ = -6‰ and ($\delta^{13}C_{CM})_{avg}$ = -5.3‰. Clearly a Rayleigh carbon isotopic fractionation during liquid immiscibility enhances the $\delta^{13}C$ of the carbonate melt relative to the parent melt. If carbonate melt comes out of the magma chamber in batches during immiscibility, contrary to what is assumed in the above model, then it may generate a series of isotopically heterogeneous melts and which in turn can generate the observed isotopic variations upon crystallization. However, Sr isotopic studies do not support this batch separation (as discussed in Section 4.3, carbonatites

do not show $^{87}Sr/^{86}Sr$ ratio heterogeneity even when the parent magma gets contaminated during liquid immiscibility). A similar evaluation can also be made for oxygen isotopes with the knowledge of oxygen isotope fractionation factor between silicate and carbonate melt.

In summary, liquid immiscibility can only decide the initial isotopic composition of the primary carbonate melt prior to its crystallization, not the variation observed in the ultimate product (i.e. the carbonatites). Hence, the only process which probably can explain the correlated variation observed in unaltered calcite carbonatites is fractional crystallization. In the next section, I discuss a model developed to treat fractional crystallization of carbonatites.

4.4.3b. Fractional Crystallization

To model the isotopic effects generated during fractional crystallization of a carbonate magma Rayleigh isotopic fractionation process was assumed. Carbonatite magmas are rich in CO_2 and H_2O fluids, which are likely to affect the isotopic composition of the rock during crystallization. If calcite represents the crystallizing primary carbonatite (which is mainly calcite carbonatite) then its oxygen isotopic evolution will be controlled by three source components (i.e. melt, CO_2 and H_2O), whereas carbon isotopic evolution will be controlled by two source components (melt and CO_2). To treat isotopic fractionation in such cases where the isotopic evolution of the product depends on multiple source components, a model (called Rayleigh isotopic fractionation from a multicomponent source) was developed. In the following subsection I discuss the model in general and next I apply this model to explain the carbon and oxygen isotopic variations in some primary carbonatites.

A. Rayleigh Isotopic Fractionation from a Multicomponent Source

Here a Rayleigh fractionation equation is derived to evaluate the isotopic evolution of a reservoir which has many discrete components, with distinctly different isotopic ratios, each contributing isotopes of an element to a phase forming and separating out of the reservoir. For this we assume that (a) the different components of the source are in isotopic equilibrium with each other always (i.e., the isotopic composition of the

source reservoir at any time can be expressed as a product of isotopic composition of the most abundant component of the source and a linear combination of the fractionation factors between the rest of the components with the major one), (b) the product that forms is in instant isotopic equilibrium with the source before being removed, (c) the process is isothermal, and (d) the abundance of the heavier isotope is much smaller than that of the lighter isotope of the element under consideration (e.g. $[^{12}C] >> [^{13}C]$).

(i) ***Notations***

n, n_o	Number of atoms of the element under consideration in the whole source reservoir at the time $t > 0$ and at $t = 0$ respectively.
N, N_o	Number of molecules of the i^{th} component of the source at $t > 0$ and at $t = 0$, respectively.
r_{j1}	Ratio of the initial number of moles of the j^{th} component to the 1^{st} component (N_j/N_1). The latter is chosen to be the biggest component so that $r_{j1} \leq 1$ for all j.
L	Total number of components in the reservoir at $t = 0$.
p_i	Number of atoms contributed by the i^{th} source component to the phase(s) formed (e.g. in the case of calcite precipitation from CO_2 and H_2O mixture, CO_2 contributes 2 atoms of oxygen and H_2O, one).
P	A constant for given L; $P = \sum_1^L p_i$
R	Isotopic ratio of the element under consideration; subscripts s, c, i denote the source reservoir, phase formed and the i^{th} source component; o denotes the value at $t = 0$.
α_{ij}	Fractionation factor between the i^{th} and j^{th} component ($=R/R_j$). Note that $\alpha_{ii} = 1$ for all the values of i.
A	Overall fractionation factor between the phase(s) formed and the multicomponent source reservoir ($= R_c / R_s$).
f	Fraction of atoms of the element under consideration left in the source ($= n / n_o$).
f_j	j^{th} critical value of f, when the j^{th} reservoir gets exhausted.
δ	Isotopic composition expressed in permil [$(R / R_{std} - 1) .10^3$].

Δ Deviation of isotopic composition from its initial value (δ-δ_o).

In addition to these variables g, a and b are defined below.

(ii) *Equations*

By definition we have

$$n_o = \sum_1^L p_j N_{oj} \tag{36}$$

$$n = \sum_1^L p_j N_j \tag{37}$$

and

$$R_s = \frac{\sum_1^L p_j N_j R_j}{\sum_1^L p_j N_j} \tag{38}$$

Using $\alpha_{j1} = R_j/R_1$ and $f = n/n_o$ we get

$$R_s = \frac{R_1 \sum_1^L p_j N_j \alpha_{j1}}{n_o f} \tag{39}$$

Also, the number of atoms removed from the j^{th} component and the total number of atoms removed from the reservoir are related by

$$p_j N_{oj} - p_j N_j = \frac{p_j}{P} n_o (1-f) \tag{40}$$

Therefore,

$$p_j N_j = \frac{p_j}{P}[n_o f - n_o (1 - \frac{PN_{oj}}{n_o})] \tag{41}$$

or,

$$p_j N_j = \frac{p_j}{P}[n_o f - n_o (1 - \frac{Pr_{j1}}{\sum_1^L p_i r_{i1}})] \tag{42}$$

By defining f_j, the j^{th} critical value of f, when the j^{th} source component exhausts (i.e., $N_j = 0$). This is given by (from equation 42):

$$f_j = 1 - \frac{Pr_{j1}}{\sum_1^L p_i r_{i1}} \tag{43}$$

Defining

$$a = \frac{1}{P} \sum_1^L p_j \alpha_{j1} \tag{44}$$

and

$$b = \frac{1}{P}\sum_{1}^{L} p_j \alpha_{j1} f_j \tag{45}$$

And using equations (41) to (45) in (39) we obtain

$$R_s = R_1 (a - \frac{b}{f}) \tag{46}$$

The physical significance of the variables a and b is that they are weighted mean values of the equilibrium fractionation factors between the different source components and the major (first) component. In the case of a, the weights are the numbers of atoms of the element under consideration contributed by various source components. In the case of b, besides this, the weight factor includes the critical values of f (i.e., the values of f when each of the source component exhausts).

Treating the mixed reservoir as a single unit, the Rayleigh fractionation equation in differential form can be written as:

$$\frac{dR_s}{R_s} = (A - 1)\frac{df}{f} \tag{47}$$

where

$$A = \frac{R_c}{R_s} = \frac{\alpha_{c1}}{(a - b/f)} \tag{48}$$

using (46).

Hence,

$$A - 1 = \frac{(\alpha_{c1} - a + b/f)}{(a - b/f)} \tag{49}$$

Defining $g = \alpha_{c1} - a$, we have

$$\frac{dR_s}{R_s} = (\frac{g + b/f}{a - b/f})\frac{df}{f} \tag{50}$$

or

$$\frac{dR_s}{R_s} = g(\frac{df}{af - b}) + b(\frac{df}{af^2 - bf}) \tag{51}$$

Expanding the second term into partial fractions we obtain,

$$\frac{dR_s}{R_s} = (\frac{g}{a})[\frac{d(af - b)}{(af - b)}] + [\frac{d(af - b)}{(af - b)}] - [\frac{df}{f}] \tag{52}$$

Integrating and applying the initial condition that at f= 1, $R_s = R_{os}$, we get

$$\ln(\frac{R_s}{R_{os}}) = (\frac{g}{a}+1)\ln[\frac{d(af-b)}{(af-b)}] - \ln f \quad (53)$$

$\ln(R/R_{os})$ can be approximated to $(\delta-\delta_o)10^{-3}$ for small values of δ.

Therefore,

$$(\delta-\delta_o) = 10^3(\frac{\alpha_{c1}}{a})\ln(\frac{af-b}{a-b}) - \ln f \quad (54)$$

Equation (54) describes the isotopic evolution of the multicomponent source reservoir. As the product and the source are related by A (eq. 48) the isotopic composition of the product as a function of f will be:

$$(\delta-\delta_o)_{product} = (\frac{\alpha_{c1}}{a-b/f})\delta_{source} - (\frac{\alpha_{c1}}{a-b})(\delta_o)_{source} + 10^3[(\frac{\alpha_{c1}}{a-b/f}) - (\frac{\alpha_{c1}}{a-b})] \quad (55)$$

I now show that equation (54) can be reduced to a single component Rayleigh equation ($P = p_1$ and $\alpha_{11} = 1$; $r_{11} = 1$ and $r_{21} = 0$; $f_1 = 0$). Now, $a = 1$ and $b = 0$; therefore, $\delta-\delta_o = 10^3(\alpha_{c1}-1)\ln(f)$. In the case of initial molar quantities of different source components being equal (i.e., $N_1 = N_2 = N_3 \ldots N_L$), r_{j1} is unity for all value of j (=1 to L) and $f_j = 0$ for all j. From (45) we see that $b = 0$ and (54) reduces to $(\delta-\delta_o) = 10^3[(\alpha_{c1}/a)-1]\ln(f)$, similar to the equation for a single component case, but with an effective fractionation factor given by (α_{c1}/a). For a two component case (calcite precipitation: $Ca^{2+} + CO_2 + H_2O \rightarrow CaCO_3 + 2H^+$) Pineau et al. (1973) had derived an approximate equation:

$$\delta-\delta_o = 10^3\{[(\alpha_{c1}-1)-\frac{(\alpha_{21}-1)}{3}]\ln f + \frac{2}{3}[(\frac{1-r_{21}}{2+r_{21}})(\alpha_{21}-1)(1-\frac{1}{f})]\} \quad (56)$$

where the subscripts c, 1 and 2 denote $CaCO_3$, CO_2 and H_2O, respectively. Under some approximations, the above described multicomponent Rayleigh equation (54) reduces to this equation. This can be readily seen by doing the integration (52) with an approximated value of A in equation (48): $A \sim (\alpha_{c1}/a)(1+b/f) \sim (\alpha_{c1}/a)+(b/f)$, as both α_{c1} and a are close to unity. Therefore, equation (51) becomes:

$$\frac{dR_s}{R_s} = (\frac{\alpha_{c1}}{a}-1)\frac{df}{f} + b(\frac{df}{f^2}) \quad (57)$$

and the solution yields:

$$\delta-\delta_o = 10^3[(\frac{\alpha_{c1}}{a}-1)\ln f + b(1-\frac{1}{f}) \quad (58)$$

For the two component case, $a = (1/3)(2+\alpha_{21})$ from (44) , $b = (1/3)(2f_1+\alpha_{21}f_2)$ from (45) and $f_1 = 1-[3/(2+r_{21})]$; $f_2 = 1-[3r_21/(2+r_{21})]$. Hence $b = (2/3)(2f_1+\alpha_{21}f_2)[(1-r_{21})/(2+r_{21})]$. Again $[(\alpha_{c1}/a)-1]$ can be approximated to be $(\alpha_{c1}-1)$ as $a\sim1$. Using this, and the relation for b in (57), I obtain Pineau et al's approximate equation (56).

However, when the initial molar quantities of different source components are different, the least of them will get exhausted first (this is why we chose index 1 for the largest source component). This happens when $f = f_j$, the j^{th} critical value of f when j^{th} source component gets exhausted. Subsequent isotopic evolution of the system can be still obtained from equation (54) by redefining P, a, b for the remaining L-1 components, δ_o taken as the δ value of the reservoir at the point when $f = f_j$, and replacing f by f/f_j . Similar calculations can be made as more and more components get exhausted. Finally, when all but the largest reservoir get exhausted, the isotopic evolution will be given by: $(\delta'-\delta_o) = 10^3(\alpha_{c1}-1) \ln f'$, where δ' is the δ value of the source at the point when L-1 reservoirs got exhausted, and $f' = f / f_{L-1}$. The above arguments show that there will be L-1 discontinuities in the δ versus f plot.

The above described model is a closed system generalized model which treats Rayleigh isotopic fractionation from a multicomponent source. This model can be applied to many geological processes like calcite precipitation from a fluid, hydrothermal graphite formation, metamorphic decarbonation, serpentinization etc., to understand the isotopic evolution of the source during such processes. In the present work, only the application of this model to the formation of carbonatites is discussed.

(iii) *Primary carbonatites*

Unaltered carbonatites whose carbon and oxygen isotopic composition is considered to be primary are generally calcite carbonatites. In calcite carbonatites it is the calcite which is the major mineral. Hence, isotopic composition of calcite can be treated as that of the calcite carbonatite. Probably the C and O isotopic fractionation behaviours of a carbonate melt and calcite are very similar (Deines, 1989), hence, it is safe to assume the fractionation factors of C and O between calcite and the carbonate melt as unity. Which means that the crystallization of calcite from a pure carbonate melt may

not cause any isotopic fractionation. However, if calcite crystallizes in equilibrium with the associated magmatic fluids then fractionation will occur. It is known that carbonate magmas carry a large amount of CO_2-H_2O fluids along with them. If calcite fractionally crystallizes from such a melt-fluid system then its formation reaction will probably be:

$Ca^{2+} + CO_2 + H_2O \rightarrow CaCO_3 + 2H^+$

as proposed by Pineau et al. (1973). Isotopically, CO_2 is the only source of carbon for calcite, while oxygen is contributed by CO_2 and H_2O. So the carbon isotopic evolution will follow a single component Rayleigh fractionation process, whereas, that of oxygen will follow a two component Rayleigh process.

Carbon isotopic evolution of the source and carbonatite then will be given by :

$$\delta^{13}C_s = (1000+\delta^{13}C_s^i)f_c^{(\alpha^c-1)} - 1000 \qquad (59)$$

and

$$\delta^{13}C_{cal} = \alpha^c(1000+\delta^{13}C_s^i)f_c^{(\alpha^c-1)} - 1000 \qquad (60)$$

where α^c is the fractionation factor of carbon between calcite and CO_2, f_c is the fraction of remaining carbon in the source and $\delta^{13}C_s^i$ is the initial carbon isotopic composition of the source. For oxygen isotope evolution of the source and the carbonatite, the multicomponent Rayleigh fractionation model for a two component case was used. In such a case oxygen isotopic evolution equation for calcite of carbonatite derived from (55), will be :

$$\delta^{18}O_{cal} = 10^3\left(\frac{\alpha_{c1}^o}{a-b/f_o} - 1\right) + \left(\frac{\alpha_{c1}^o}{a-b/f_o}\right)\delta^{18}O_s \qquad (61)$$

where α_{c1}^o is the fractionation factor of oxygen between calcite and the largest source component. f_o is the fraction of remaining oxygen in the reservoir. a, b and $\delta^{18}O_s$ are to be determined from equations (44), (45) and (54) respectively. To determine these parameters we need the values of p_j, s, P, α_{j1}, r_{i1} and f_j. In this calcite crystallization process, $p_1 = 2$, $p_2 = 1$, $P = 3$, α_{j1} is either $\alpha_{H_2O-CO_2}$ or $\alpha_{CO_2-H_2O}$ depending on which one of the two source components is the largest. f_j value, the j^{th} critical value of f_o, will depend on the smallest component. r_{i1} is the initial molar ratio of the i^{th} source component and the major (or first) source component. Here I discuss the isotopic

evolution of the source and calcite in two different cases: (I) when CO_2 is the largest source component, (II) H_2O is the largest source component.

Case-I

First I consider a case when CO_2 is the largest source component. Hence, subscript 1 will be used for CO_2 and 2 for H_2O. The initial molar ratio r_{i1} is r_{21} (i.e. H_2O/CO_2). The value of f_o at which H_2O will be completely used up in the calcite formation is given by:

$$f_{H_2O} = 1 - \frac{3r_{21}}{2 + r_{21}} \tag{62}$$

The other parameters are :

$$a = \frac{1}{3}(2 + \alpha_{21}) \tag{63}$$

$$b = \frac{2}{3}(\alpha_{21} - 1)(\frac{1 - r_{21}}{2 + r_{21}}) \tag{64}$$

To calculate $\delta^{13}C$ and $\delta^{18}O$ of calcite at the same time of formation, I relate f_c and f_o by:

$$f_c = (\frac{1 - r_{21}}{3}) + f_o(\frac{2 + r_{21}}{3}) \tag{65}$$

The carbon and oxygen isotope composition of the source can then be calculated putting the values of above parameters for appropriate r_{21} values in equations (56) and (54), respectively. Fig. 4.17 shows the evolution of ($\delta^{18}O$-$\delta^{18}O_o$) of the source as a function of f_o for different r_{21} values and Fig. 4.18 shows the covariation of ($\delta^{13}C$-$\delta^{13}C_o$) and ($\delta^{18}O$-$\delta^{18}O_o$) of the source for different r_{21} values. The end of each evolution curve marks the exhaustion of the smallest source component (i.e., H_2O). Similarly the carbon and oxygen isotope composition of the calcite can be found out from equations (60) and (61), respectively as a function of fraction of remaining source. Fig. 4.19a shows isotopic evolution curves of calcite, in a $\delta^{13}C$ vs. $\delta^{18}O$ space, for different r_{21} values. In this example the temperature of calcite formation is taken to be 700°C and the initial source $\delta^{13}C$ and $\delta^{18}O$ values are -5.5 ‰ and 8.5 ‰, respectively. Here the fractionation factors used are taken from Ritchet et al. (1977) and Chacko et al. (1991).

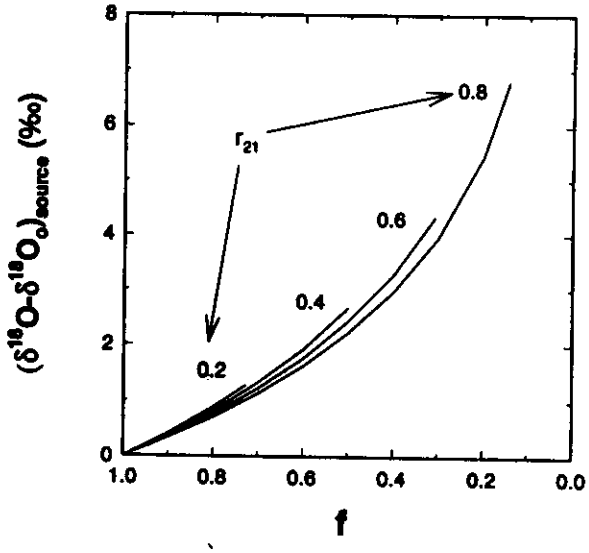

Fig. 4.17. Oxygen isotopic evolution curves of a two component source (CO_2+H_2O), relative to the initial source composition, from which calcite is fractionally crystallizing as a function of f (fraction of remaining oxygen atoms in the source) for different r_{21} (initial molar ratio of H_2O to CO_2) values. End of each curve marks the exhaustion of H_2O reservoir (Case-I of the multicomponent Rayleigh fractionation model for carbonatites). See section 4.4.3b for discussion.

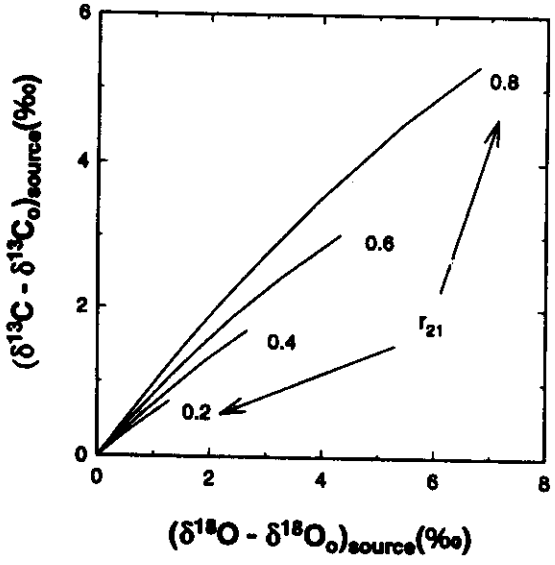

Fig. 4.18. Covariation of oxygen and carbon isotopic compositions of the source relative to the initial values in the same cases as in Fig. 4.17.

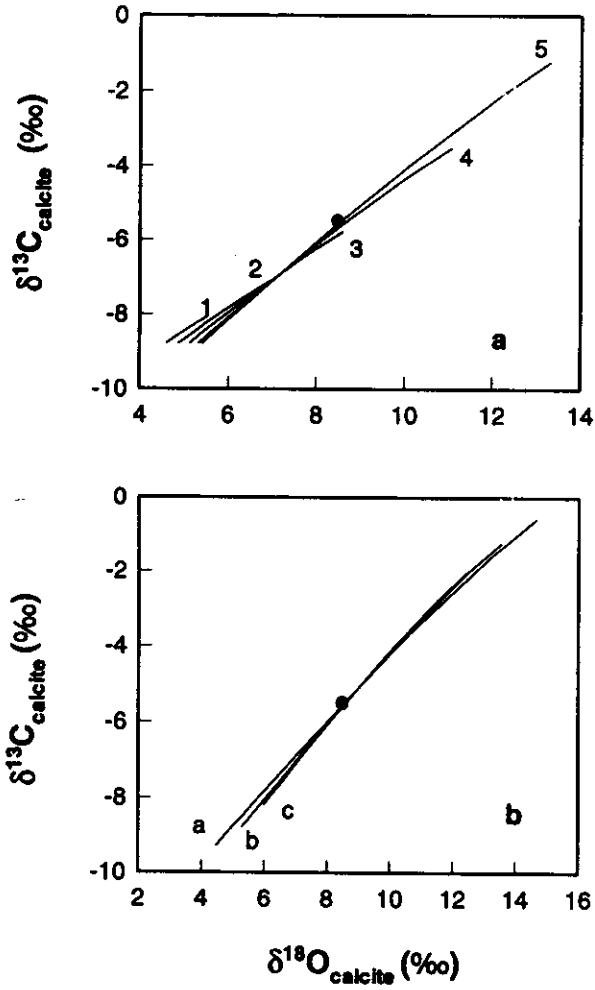

Fig. 4.19 (a) Plot of $\delta^{13}C$ vs. $\delta^{18}O$ showing isotopic evolution curves for the calcite (at 700°C) generated by the multicomponent Rayleigh fractionation model in Case-I (CO_2 is the largest source component). Filled circle represents the initial composition of the carbonate magma. Curves 1 to 5 are for r_{2l} values of 0.2, 0.4, 0.6, 0.8 and 0.9, respectively. (b) Isotopic evolution curves for calcite at r_{2l} = 0.95 at three different temperatures a = 500°C, b = 700°C and c = 900°C. Filled circles = initial magma. See section 4.4.3b (Case-I) for discussion.

The most striking feature of isotopic evolution curves (Fig. 4.19a) is that at the beginning of crystallization, isotopic compositions of calcite are lower than those of the initial source and then as the crystallization proceeds calcite becomes more and

more enriched and its isotopic compositions become higher than the initial source. Model calculations also showed that the slope of the isotopic evolution curves is not very sensitive to the temperature variation (Fig. 4.19b), however, it is sensitive to r_{21} values (Fig. 4.19a.). In fact, a particular range of variation of $\delta^{13}C$ and $\delta^{18}O$ of calcite can be explained by fractional crystallization at different temperatures. Hence, the isotopic evolution of fractionally crystallizing calcites in such a case is mainly controlled by the initial source compositions and the initial molar ratio of H_2O to CO_2.

Case-II

In the second case, I consider H_2O to be the largest source component. Then subscript 1 will be used for H_2O and 2 for CO_2 in all the equations. Here the value of f_o at which CO_2 finished is:

$$f_{CO_2} = (1 - r_{21}) / (1 + 2r_{21}) \tag{66}$$

and other parameter are:

$$a = 1 + \frac{2}{3}(\alpha_{21} - 1) \tag{67}$$

$$b = \frac{2}{3}(\alpha_{21} - 1)\left(\frac{1 - r_{21}}{1 + 2r_{21}}\right) \tag{68}$$

f_o and f_c are related by

$$f_c = \frac{1}{3}\left(1 - \frac{1}{r_{21}}\right) + \frac{1}{3}\left(2 + \frac{1}{r_{21}}\right) f_o \tag{69}$$

Using these parameters, $\delta^{13}C$ and $\delta^{18}O$ values at different f_o were calculated from equations (60) and (61), respectively for similar source compositions as used in Case-I. Fig. 4.20 shows the isotopic evolution curves at 700°C for different r_{21} values. Calculations were done up to $f_c = 0.001$ and at these points $f_o > f_{critical}$ ($=f_{CO_2}$). That is why the end points of all evolution curves have same $\delta^{13}C$ value. In this example the effect of change in r_{21} is much larger on the slope of the evolution curve compared to the Case-I. However, the variation in $\delta^{18}O$ generated by the model, here, is much smaller than what is observed when CO_2 is the largest source component (Case-I).

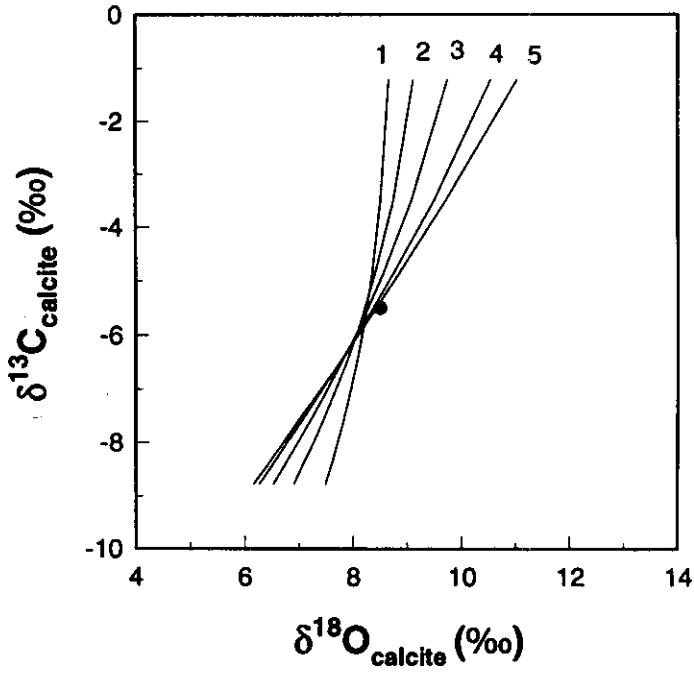

Fig. 4.20. Plot of $\delta^{13}C$ vs. $\delta^{18}O$ showing isotopic evolution curves for calcite generated by Case-II (H_2O is the largest source component) of the multicomponent Rayleigh fractionation model at 700°C. Different curves (numbered) are for different r_{21} values (same as in Fig. 4.19a). Filled circle = initial magma. Here the calculations are done up to f_c (fraction of remaining carbon in the source) of 0.001. See section 4.4.3b (Case-II) for discussion.

The above proposed multicomponent Rayleigh fractionation model probably can explain the $\delta^{13}C$ and $\delta^{18}O$ variations observed in primary carbonatites of different complexes of the world. It has been observed in many complexes that the observed correlated variation of $\delta^{13}C$ and $\delta^{18}O$, if fitted with straight lines give slopes whose values are less than 1 (Pineau et al., 1973; Deines, 1989). This can be explained if we consider Case-I of our model as slopes of evolution curves in this case are less than 1. It has been suggested that CO_2 is probably the major fluid associated with primary carbonate magmas (Kjarsgaard and Hamilton, 1989), which again supports the isotopic evolution of carbonatites following Case-I. If water were considered to be the major fluid component in the primary magma, then also Case-I of the model can be applied if

it is assumed that most of this water rich fluids go out of the magma as fenitizing fluids before the crystallization starts making the remaining fluid CO_2 enriched.

Primary carbonatites (mainly calcite carbonatites) also contain other minerals like magnetite, apatite, phlogopite, fluorite and other silicates and oxides. Although abundance of these minerals is very small compared to calcite, their crystallization may affect the oxygen isotope composition of the source magma. However, non-availability of fractionation factors between these minerals and melt creates difficulty in evaluating the exact isotopic effects. Using Chiba et al. (1989)'s fractionation factor for calcite-magnetite and calcite-water (Friedman and O'Neil, 1977) fractionation factors, it was found that fractional crystallization (Rayleigh type) enriches the $\delta^{18}O$ (by ~1‰) of the melt. The crystallization of apatite probably depletes the $\delta^{18}O$ of the melt at magmatic temperatures [this was found out assuming that $\alpha^{18}O$ (apatite-water) = $\alpha^{18}O$ (calcite-water)]. In all these calculations it was assumed that the carbonate melt and calcite have similar oxygen fractionation properties. Hence, in our model curves a range of ±1‰ in initial $\delta^{18}O$ composition of the source can be considered to accommodate the possible variation from crystallization of minerals other than calcite.

B. Unaltered Calcite Carbonatites from Carbonatite complexes of Deccan Province

(i) *Amba Dongar Complex*

Very coarse to medium grained unaltered calcite carbonatites of Amba Dongar show correlated variation of $\delta^{13}C$ and $\delta^{18}O$ values (Fig.4.15a). It was found that there are two such correlation trends, separated by at least 3‰ in $\delta^{18}O$. From field relations, it was found that the group having lower $\delta^{18}O$ values (Group-II) are relatively finer grained calcite carbonatites (alvikites of Viladkar, 1981) and these intrude into the coarse grained variety, which have higher $\delta^{18}O$ values (Group-I). The study Sr isotopes in these rocks and limestones (Section 4.2) revealed that these rocks were not contaminated by limestones. Hence, the observed slope of $\delta^{13}C$- $\delta^{18}O$ plot cannot be due to contamination from country rocks (limestones). As discussed earlier this kind of isotopic variation is a result of fractional crystallization and can be explained by Rayleigh fractionation from a CO_2 rich fluid-magma system (Case-I of the

multicomponent Rayleigh fractionation model). In such a case the $\delta^{13}C$ and $\delta^{18}O$ evolution of the calcite (of calcite carbonatite) can be calculated using equations (60) and (61), respectively, with proper substitution of the parameters a and b (equations 63 and 64). However, to apply this model, we need the initial $\delta^{13}C$ and $\delta^{18}O$ values of the parent carbonate magma. These can be assumed in different ways so that the model evolution curves fit the observed data. However, there is an independent way of estimating these for Amba Dongar complex, particularly the initial $\delta^{13}C$ value, with the help of liquid immiscibility model described in the section 4.4.3a, which is discussed in the following paragraph.

Many of the alkaline rocks of Amba Dongar contains calcite as an accessory phase. Calcites from unaltered alkaline rocks show two groups in $\delta^{13}C$ vs $\delta^{18}O$ plot (Fig.4.15a), which probably indicate that there are two different generations of alkaline rocks, though mineralogically these two groups are not very different. The average $\delta^{13}C$ of Group-I is -6‰, while of Group-II is -4‰. Assuming that these two groups were derived from two isotopically different primary carbonated silicate magmas by liquid immiscibility, the $\delta^{13}C$ compositions of corresponding two carbonate magmas were determined using equation (34) of section 4.4.3a. For this calculation the value of the fraction of remaining carbon in the source is taken as 0.238 [equation (35)], which is derived using carbon atom ratio in carbonatite to silicate rocks of 3.2 (in Amba Dongar, calcite carbonatites comprise 20% of the complex and average carbonate amount in these is 90%, while silicates have around 7% carbonate in them). The calculations yielded two different initial $\delta^{13}C$ compositions for two different carbonate magmas, one having $\delta^{13}C$ of -5.3‰ and the other -3.2‰. It is likely that these two isotopically different carbonate magmas have crystallized to give the two groups of calcite carbonatites observed in this complex. As the fractionation factor for oxygen between carbonate melt and silicate melt is not known, it is not possible to evaluate the $\delta^{18}O$ composition of the carbonate magma using liquid immiscibility model. However, it can be assumed to be in the range of 7 ‰ to 9 ‰, 2 ‰ enriched than the mantle peridotites (Deines, 1989). Using the above initial values of $\delta^{13}C$ and $\delta^{18}O$, the model calculations were done and it was found that the model curve at 800°C crystallization temperature and r_{21} value (initial H_2O/CO_2) of 0.9 explained the observed enrichment

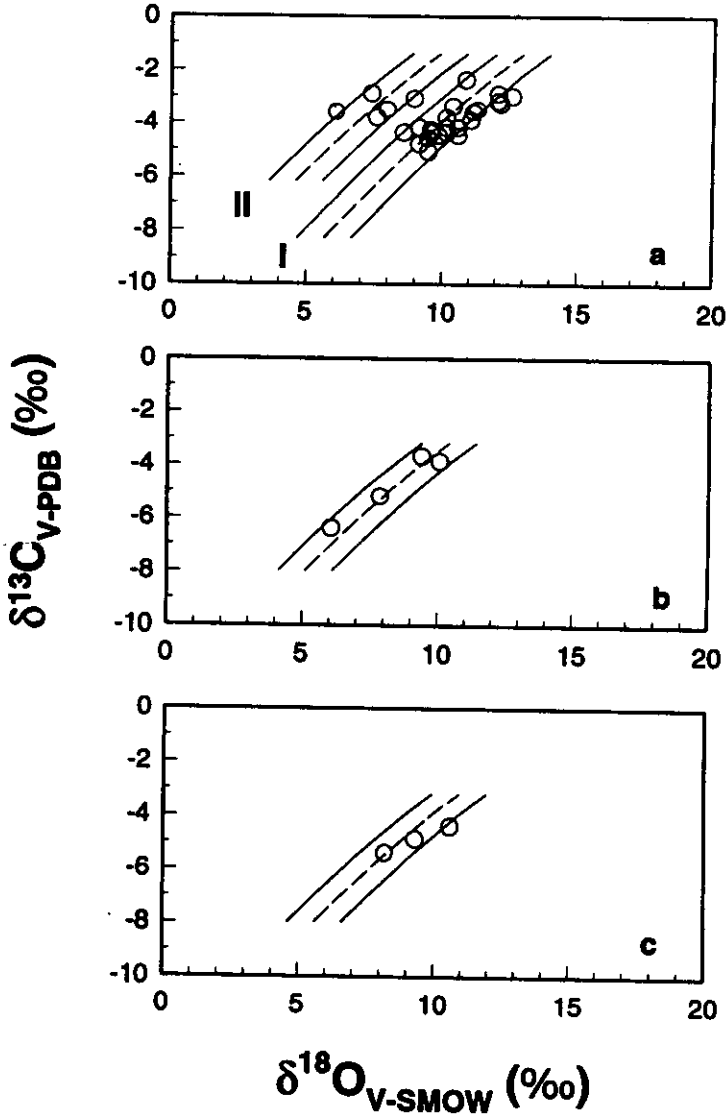

Fig. 4.21. *Observed data (open circles) for unaltered calcite carbonatites and two component Rayleigh fractionation model curves (dashed) for Amba Dongar (a), Mundwara (b) and Sarnu-Dandali (c). The solid curves represent model curves, which encompasses the ±1 ‰ variation of the initial $\delta^{18}O$ of the magma. In Fig. 4.21a, I and II represent the two groups of calcite carbonatites from Amba Dongar. See section 4.4.3b (B) for discussion.*

trend of Group-I calcite carbonatites when the initial $\delta^{18}O$ of magma was 8.5 ‰ (Fig.4.21a). However, the entire variation of $\delta^{13}C$ and $\delta^{18}O$ of these rocks could be explained by the model curves when the initial $\delta^{18}O$ of the carbonate magma varied from 7.5 ‰ to 9.5 ‰. This ±1 ‰ variation in initial $\delta^{18}O$ takes care of other factors,

particularly the crystallization of accessory minerals, which affect only the $\delta^{18}O$ of the crystallizing carbonate magma. Similar calculations for Group-II showed (Fig.4.21a) that their isotopic variations could be explained by their crystallization from a carbonate magma having r_{21} value of 0.8 and a smaller $\delta^{18}O$ initial value of 7.5 ‰. The two component Rayleigh fractionation model also generates $\delta^{13}C$ and $\delta^{18}O$ values which are beyond the range of observed values. Most likely, the rocks falling in the lower range of values are present below the present level of erosion and these were crystallized at an early stage. Similarly, the model generated values which fall in a higher range than the observed values either have been altered by secondary processes or the rocks which had them have been eroded out. In summary, uncontaminated and unaltered calcite carbonatites of Amba Dongar were found to have crystallized from two isotopically different primary carbonate melts (with $\delta^{13}C$ values of -5.3 ‰ and -3.2 ‰) which were enriched in CO_2 compared to H_2O.

It is usually believed that the carbon isotopic composition of a primary carbonate melt reflects its mantle source composition. The initial $\delta^{13}C$ of the primary melt of Group-I calcite carbonatites (-5.3 ‰) falls within the mantle $\delta^{13}C$ range suggested by Nelson et al. (1988), whereas the initial $\delta^{13}C$ of primary melt for Group-II calcite carbonatites (-3.2 ‰) is higher by at least 1.8 ‰ than the highest $\delta^{13}C$ values suggested for an average mantle (i.e. -5 ‰) (Nelson et al., 1988). This carbon isotopic enrichment in Group-II melt could be due to its generation from an isotopically different source than Group-I which essentially means that the source region of Amba Dongar complex was isotopically heterogeneous. However, it is difficult to explain the generation of compositionally similar magmas of a given complex from different source regions. But, if such a process was possible in Amba Dongar then the $\delta^{13}C$ enrichment of the source region for Group-II calcite carbonatites probably reflects mixing its juvenile carbon ($\delta^{13}C$ = -5 ‰) with the enriched recycled crustal carbon ($\delta^{13}C$ = 0-2 ‰) (Nelson et al., 1988). This means that the Group-II calcite carbonatites of Amba Dongar bear signatures of recycled crustal carbon. Alternatively, the $\delta^{13}C$ enrichment of the primary melt of Group-II can as well be explained by its removal from Group-I melt some time late in the crystallization history and subsequent mixing with water rich magmatic fluids of lower $\delta^{18}O$. We propose this late stage mixing with magmatic water in order

to maintain the required H_2O/CO_2 ratio of the magma for fractional crystallization and to bring down the $\delta^{18}O$ value from ≥10 ‰ to 7.5 ‰. However, such a mechanism does not explain the presence of the Group-II variety of alkaline rocks in this complex. Hence, the most appropriate explanation for the ^{13}C enrichment of Group-II melt is the incorporation of recycled carbon, which probably can be attributed to the metasomatic fluid activity in the source region.

Mundwara Complex

The unaltered calcite carbonatites of Mundwara also showed correlated $\delta^{13}C$ and $\delta^{18}O$ variations (Fig. 4.15b). Application of the two component Rayleigh fractionation model revealed that these rocks ere crystallized at 800°C from a primary carbonate magma whose initial $\delta^{13}C$ and $\delta^{18}O$ were -5 ‰ and 8 ‰, respectively and H_2O/CO_2 ratio in the magma was 0.8 (Fig.4.21b). Like Amba Dongar, here also we needed ±1 ‰ variation of initial $\delta^{18}O$ variation to explain the entire observed values (Fig. 4.21b), which suggests that the crystallization minerals other than carbonates had affected the $\delta^{13}C$ and $\delta^{18}O$ evolution of these rocks.

Sarnu-Dandali Complex

Like other two complexes, unaltered calcite carbonatites of Sarnu-Dandali also showed correlated $\delta^{13}C$ and $\delta^{18}O$ variation (Fig. 4.15c) indicating the involvement of fractional crystallization in their formation. We applied the two component Rayleigh model and found that the fractional crystallization of calcite at 800°C from a magma having H_2O/CO_2 ratio of 0.8 and initial values of $\delta^{13}C$ and $\delta^{18}O$, -5 ‰ and 8.5 ‰, respectively, could explain the observed variation (Fig. 4.21c).

In summary, the primary carbonate melts of all the three completed show average mantle $\delta^{13}C$ compositions and $\delta^{18}O$ compositions in the range of 7-9 ‰. These isotopic compositions are consistent with their origin from the mantle (Nelson et al., 1988 and Deines, 1989). The enrichment trend shown by the unaltered calcite carbonatites from these complexes in $\delta^{13}C$ vs $\delta^{18}O$ plot are interpreted here as product of fractional crystallization of these rocks from CO_2 rich carbonate melts. A two

component Rayleigh fractionation model successfully explains the correlated variation of $\delta^{13}C$ and $\delta^{18}O$ of these calcite carbonatites.

4.4.3c. A Fluid-Rock Interaction Model to Explain Secondary Isotopic Effects

A. The Model

To explain the $\delta^{13}C$ and $\delta^{18}O$ variations in altered rocks (altered calcite carbonatites, ferrocarbonatites and metasomatic rocks) a fluid-rock interaction model was developed by modifying an earlier model proposed by Santos and Clayton (1995). In a closed system condition the fluid-rock isotopic exchange of carbon and oxygen can be written as following to simple mass balance equations:

$$F_c\delta^{13}C^{i}_{fluid} + R_c\delta^{13}C^{i}_{rock} = F_c\delta^{13}C^{f}_{fluid} + R_c\delta^{13}C^{f}_{rock} \quad (70)$$

$$F_o\delta^{18}O^{i}_{fluid} + R_o\delta^{18}O^{i}_{rock} = F_o\delta^{18}O^{f}_{fluid} + R_o\delta^{18}O^{f}_{rock} \quad (71)$$

where F_c and F_o are amounts of carbon and oxygen, respectively; in the fluid expressed in moles. R_c and R_o are those for the rock. Superscripts i and f stand for initial and final, respectively. From these two equations final rock compositions can be found out. The relations for the final rock compositions are:

$$\delta^{13}C^{f}_{rock} = \frac{(F_c / R_c)(\delta^{13}C^{i}_{fluid} + \Delta^{c}_{rock-fluid}) + \delta^{13}C^{i}_{rock}}{1 + (F_c / R_c)} \quad (72)$$

$$\delta^{18}O^{f}_{rock} = \frac{(F_o / R_o)(\delta^{18}O^{i}_{fluid} + \Delta^{o}_{rock-fluid}) + \delta^{18}O^{i}_{rock}}{1 + (F_o / R_o)} \quad (73)$$

where $\Delta^{c}_{rock\text{-}fluid}$ and $\Delta^{o}_{rock\text{-}fluid}$ stand for the isotopic fractionation of oxygen and carbon, respectively, between rock and fluid. As the fluids are CO_2 containing aqueous fluids, the oxygen fractionation between the rock (i.e., calcite) and the fluid will depend on CO_2/H_2O ratio in the fluid. Defining r as the molar ratio of CO_2 to H_2O in the fluid, it was found the relation for $\Delta^{o}_{rock\text{-}fluid}$:

$$\Delta^{o}_{rock-fluid} = 10^3 \ln\alpha^{18}O_{cal-CO_2} + 10^3 \ln(1+2r) - 10^3(2r + \alpha^{18}O_{H2O-CO2}) \quad (74)$$

where $\alpha^{18}O_{cal\text{-}CO2}$ and $\alpha^{18}O_{H2O\text{-}CO2}$ are oxygen fractionation factors between calcite and CO_2 and H_2O and CO_2 respectively. For a covariance ($\delta^{13}C$-$\delta^{18}O$) plot, we require values corresponding to same time of formation/interaction. Therefore we relate F_o/R_o and F_c/R_c as:

$$F_o/R_o = [(2r+1)/3r][F_c/R_c] \quad (75)$$

Hence, in the final form the fluid-rock interaction equations are:

$$\delta^{13}C^{f}_{rock} = \frac{(F_c / R_c)(\delta^{13}C^{i}_{fluid} + \Delta^{c}_{rock-fluid}) + \delta^{13}C^{i}_{rock}}{1 + (F_c / R_c)} \quad (76)$$

$$\delta^{18}O^{f}_{rock} = \frac{(\frac{2r+1}{3r})(F_c / R_c)(\delta^{18}O^{i}_{fluid} + \Delta^{o}_{rock-fluid}) + \delta^{18}O^{i}_{rock}}{1 + (\frac{2r+1}{3r})(F_o / R_o)} \quad (77)$$

The value of $\Delta^{o}_{rock-fluid}$ is substituted from equation (74).

This model again is a simple closed system fluid-rock interaction model which assumes that the isotopic behaviour of CO_2-H_2O fluid is the same as a separate mixture of CO_2 and H_2O and it does not consider the isotopic effects generated by other carbon bearing species (like H_2CO_3, CO_3^{2-} and HCO_3^-) which are likely to be present in such fluids. However, such a simple model is reasonably a good model to interpret the extreme variations of $\delta^{13}C$ and $\delta^{18}O$ in altered carbonatites.

Fig. 4.22a illustrates the model and shows the evolution of the isotopic compositions of calcite with initial $\delta^{13}C$ and $\delta^{18}O$ values -6 ‰ and 6 ‰, respectively, which interacts with a fluid having similar initial compositions and CO_2/H_2O ratio of 0.001. Fig. 4.22b shows similar evolution when calcite interacts with a fluid having CO_2/H_2O ratio of 10. The calculations are done for F_c/R_c values ranging from 0 to infinity and temperatures varying from 100°C to 400°C. Fractionation factors are taken from Ritchet et al. (1977) and Chacko et al. (1991). It can be seen in these two figures that, CO_2 rich fluids do not generate very high enrichment in $\delta^{18}O$. Hence, to get extreme enrichments in $\delta^{18}O$, the interacting fluids have to be H_2O rich. This effect of CO_2/H_2O ratio of the fluid on the isotopic evolution is clearly demonstrated in Fig. 4.23. Physically the F_c/R_c characterizes the extent of fluid-rock interaction (e.g., $F_c/R_c = \infty$ implies that the fluid has completely altered the rock).

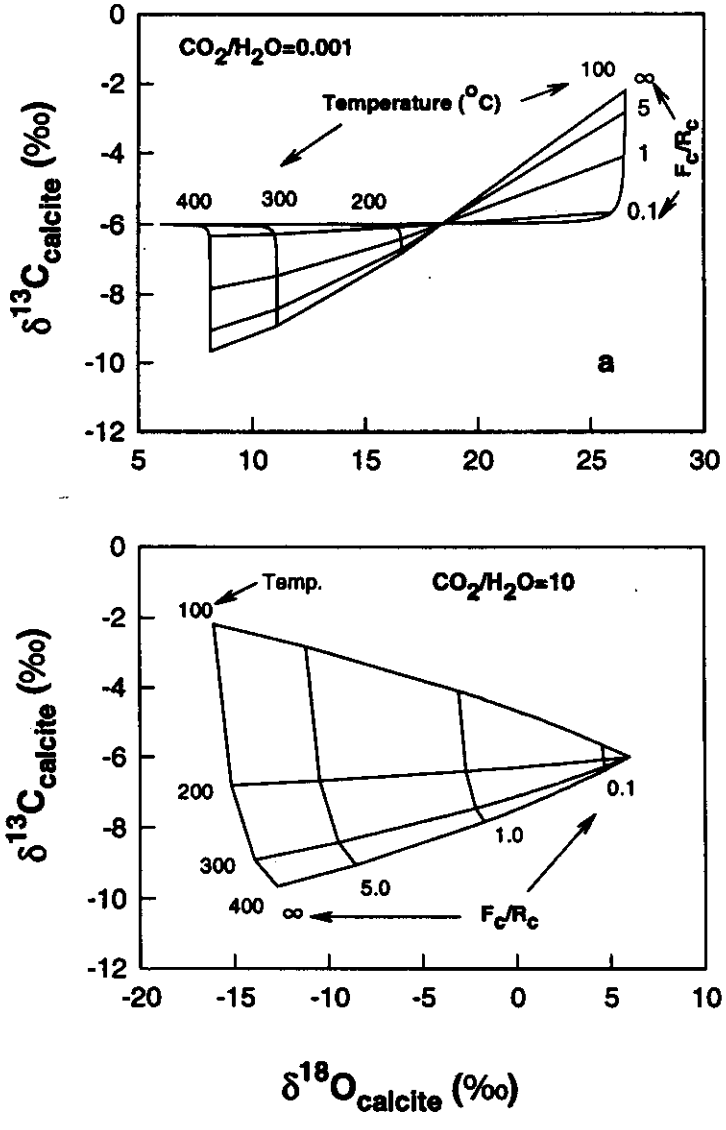

Fig. 4.22. (a) Evolution of carbon and oxygen isotopic compositions of calcite (initial $\delta^{13}C$ = -6 ‰ and $\delta^{18}O$ = 6 ‰) which interacts with a H_2O-CO_2 fluid (initial $\delta^{13}C$ = -6 ‰ and $\delta^{18}O$ = 6 ‰) having CO_2/H_2O = 0.001. The fluid/rock ratios (F_c/R_c) varies from 1 to infinity and temperature from 100°C to 400°C. (b) In this figure the fluid CO_2/H_2O ratio is 10, whereas other parameters are same as in (a).

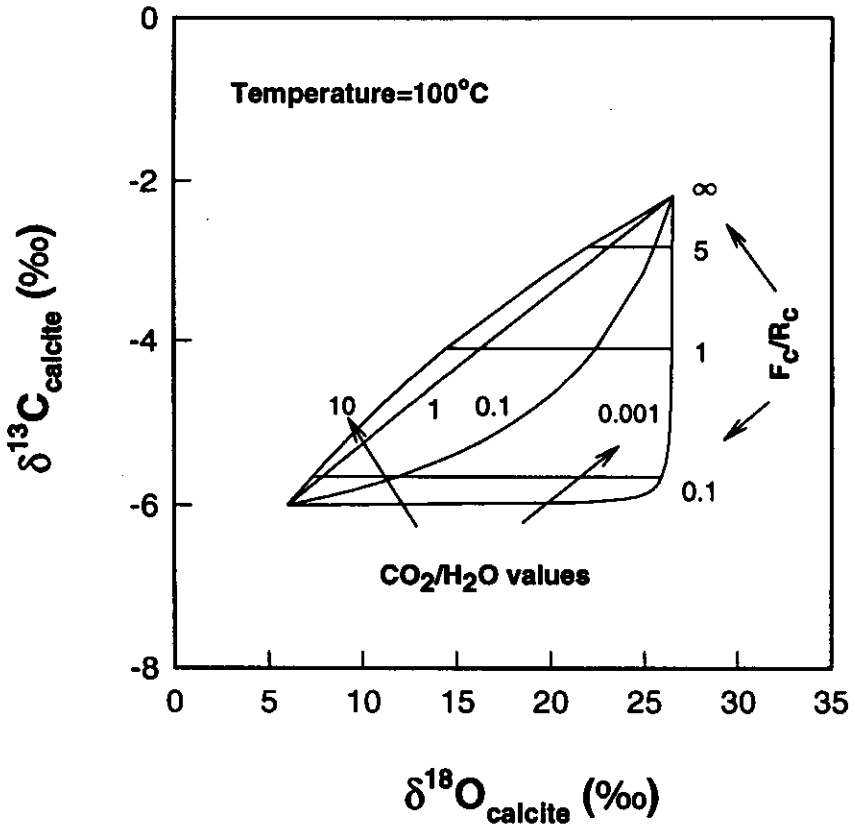

Fig. 4.23. Evolution of carbon and oxygen isotopic compositions of the same calcite as in Fig. 4.22 through fluid-rock interaction at a constant temperature of 100°C and varying fluid CO_2/H_2O ratio from 0.001 to 10. Fluid initial compositions are same as in Fig. 4.22.

B. Altered Rocks from Carbonatite Complexes of Deccan Province

$\delta^{13}C$ and $\delta^{18}O$ compositions of calcites of altered carbonatites and metasomatic rocks from all the three complexes show extreme variations and they neither plot in the mantle box nor show any kind of correlation as observed in the case of unaltered calcite carbonatites. As discussed earlier such isotopic variation is a result of secondary processes, particularly those related to post-crystallization fluid activities. In the following discussion, I explain the observed isotopic variations in these rocks using the fluid-rock interaction model described above.

(i) *Amba Dongar Complex*

The altered calcite carbonatites, late stage calcite carbonatite veins, calcites from ferrocarbonatites and metasomatic rocks from Amba Dongar show wide range of $\delta^{13}C$ and $\delta^{18}O$ values (Fig.4.15a). As Amba Dongar is a shallow seated complex, one would expect a lot of fluid action in this complex. In addition to its shallow emplacement level, the carbonatites of this complex hosts a massive fluorite deposit which is known to be a hydrothermal deposit (Simonetti and Bell, 1995). This suggests that a large scale fluid activity took place in this complex after the carbonatite emplacement and probably this was responsible for wide spread alteration observed. The carbon isotopic variations in altered carbonatites indicate that the fluids which were responsible for the alteration were CO_2 bearing aqueous fluids. Fluid inclusion study of Roedder (1973) also suggests similar post magmatic fluid activity in this complex.

To understand the nature of alteration and the kind of fluids involved in the alteration process, the fluid-rock interaction model was applied. For the model calculations, the initial $\delta^{13}C$ and $\delta^{18}O$ compositions of the calcite carbonatites were taken to be -2.5 ‰ and 12 ‰, respectively (representative of a late stage calcite carbonatite) and for ferrocarbonatites and metasomatic rocks the initial values of $\delta^{13}C$ = -2 ‰ and $\delta^{18}O$ = 13 ‰ were taken. Three different initial fluid compositions were considered for the model (1) $\delta^{13}C$ = -7.7 ‰ and $\delta^{18}O$ = 10.7 ‰ (a hydrothermal fluid, whose compositions were derived using those of the hydrothermally precipitated pure calcites associated with fluorite deposits and assuming an equilibrium precipitation of these calcites from the fluid at 150°C), (2) $\delta^{13}C$ = -4 ‰ and $\delta^{18}O$ = 0 ‰ (a meteoric fluid), and (3) $\delta^{13}C$ = -6 ‰ and $\delta^{18}O$ = 7 ‰ (a pure magmatic fluid). Model calculations were done for fluid CO_2/H_2O ratio of 0.001 and 0.1. Figures 4.24, 4.25 and 4.26 show the model calculations with the observed data for altered calcite carbonatites and late stage calcite carbonatite veins, while figures 4.27, 4.28 and 4.29 are for ferrocarbonatite and metasomatic rocks. It was found that the variations in calcite carbonatites could either be explained by interaction with the hydrothermal fluid (Fig. 4.24) or with the magmatic fluid (Fig. 4.26), but ferrocarbonatites and metasomatic rocks show alteration by the hydrothermal fluid alone (Fig. 4.27a) and have not been affected by magmatic waters like calcite carbonatites (Fig. 4.29).

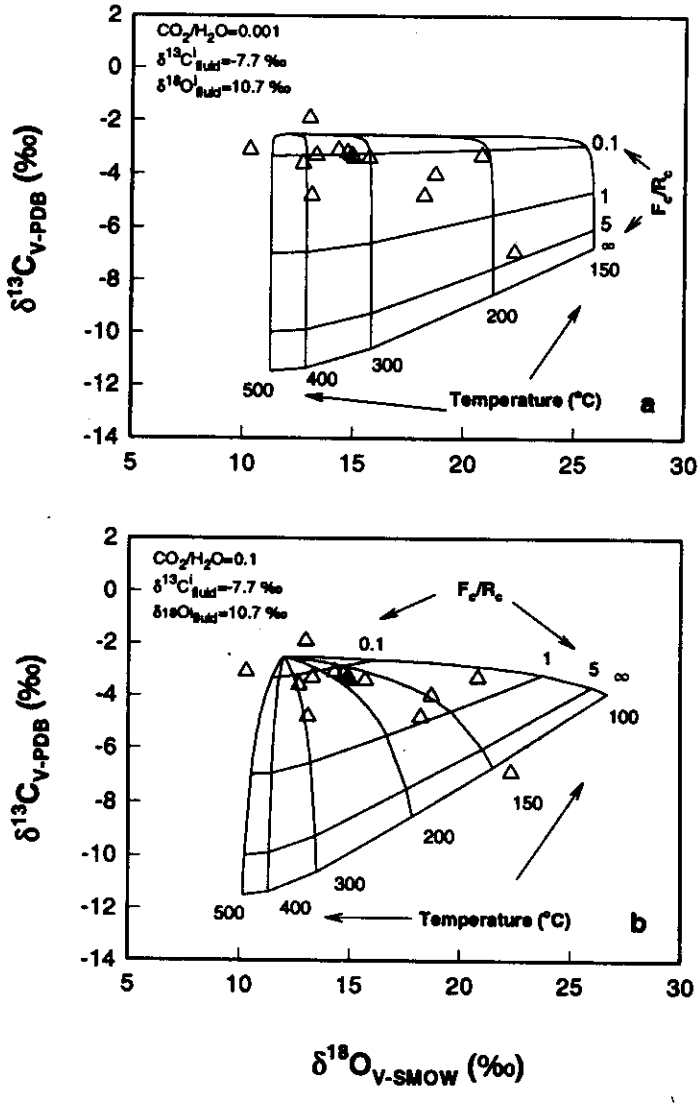

Fig. 4.24. Comparison of $\delta^{13}C$ and $\delta^{18}O$ values of altered calcite carbonatites from Amba Dongar with the fluid-rock interaction model curves for two different conditions (a) CO_2/H_2O of the fluid = 0.001 and (b) CO_2/H_2O of fluid = 0.1, for a hydrothermal fluid having initial $\delta^{13}C$ and $\delta^{18}O$ of -7.7‰ and 10.7‰, respectively. The initial values for the rock: $\delta^{13}C$ = -2.5‰ and $\delta^{18}O$ = 12.0‰.

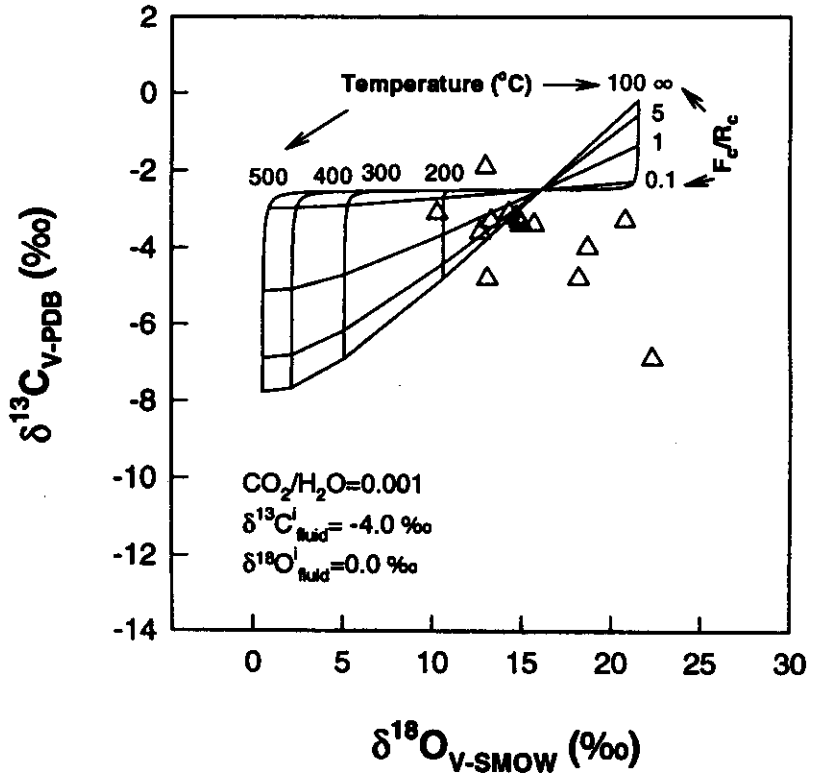

Fig. 4.25. Comparison of observed data of Amba Dongar altered calcite carbonatites with a fluid-rock interaction model curves when the fluid has $\delta^{13}C^i$ = -4‰, $\delta^{18}O^i$ = 0‰ (meteoric-hydrothermal) and CO_2/H_2O = 0.001.

None of the rocks seemed to have been affected by meteoric water alteration (Figs. 4.25 and 4.28). It was also found that the fluids having CO_2/H_2O ratio of 0.001 and 0.1 both could explain the variation in case of calcite carbonatites at temperatures between 100 and 400°C (Fig. 4.24a and b) whereas ferrocarbonatites and metasomatic rocks seemed to have interacted with fluid having CO_2/H_2O ratio of 0.001 at lower temperatures between 100 and 200°C (Fig. 4.27a). In summary, it is inferred that the isotopic composition of some calcite carbonatites (massive and veins) of Amba Dongar have been affected by a magmatic fluid and a hydrothermal fluid (which was responsible for fluorite mineralization) at different temperatures, whereas ferrocarbonatites and metasomatic rocks show alteration at lower temperature by the fluorite mineralizing hydrothermal fluid. However, it should be noted that the observed

isotopic variation may not be a result of one stage interaction process rather it could be a result of superimposed alteration effects generated by interaction of different fluids having different isotopic compositions and CO_2/H_2O ratios at different temperatures.

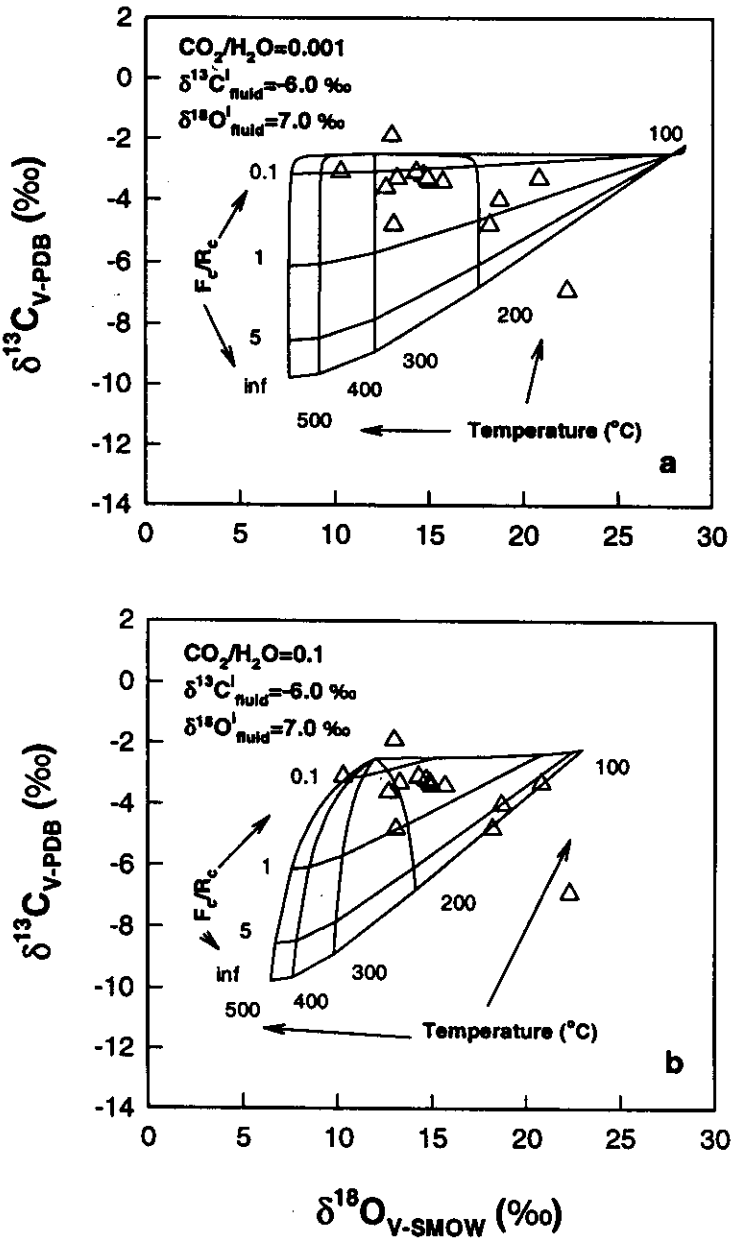

Fig. 4.26. Comparison of $\delta^{13}C$ and $\delta^{18}O$ values of altered calcite carbonatites from Amba Dongar with fluid-rock interaction model curves when the fluid is a magmatic fluid with (a) CO_2/H_2O = 0.001 and (b) CO_2/H_2O = 0.1.

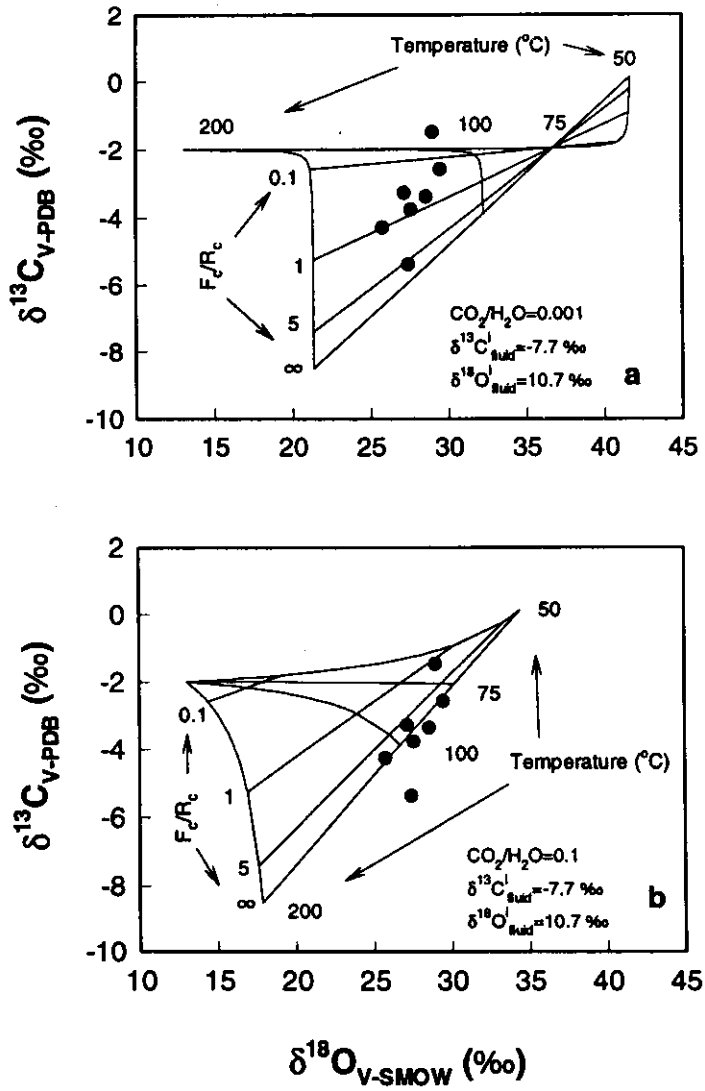

Fig. 4.27. Comparison of $\delta^{13}C$ and $\delta^{18}O$ values of the ferrocarbonatites and metasomatic rocks from Amba Dongar with the fluid-rock interaction model curves when the fluid (hydrothermal) has (a) CO_2/H_2O = 0.001 and (b) CO_2/H_2O = 0.1. The initial rock: $\delta^{13}C$ = -2.0‰ and $\delta^{18}O$ = 13‰

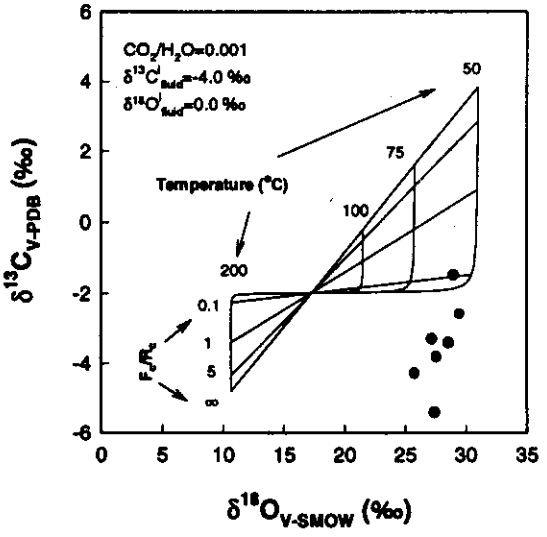

Fig. 4.28. Comparison of the $\delta^{13}C$ and $\delta^{18}O$ ferrocarbonatites and metasomatic rocks of Amba Dongar complex with the fluid-rock interaction model curves when the fluid is meteoric. Initial rock compositions are same as in Fig. 4.27.

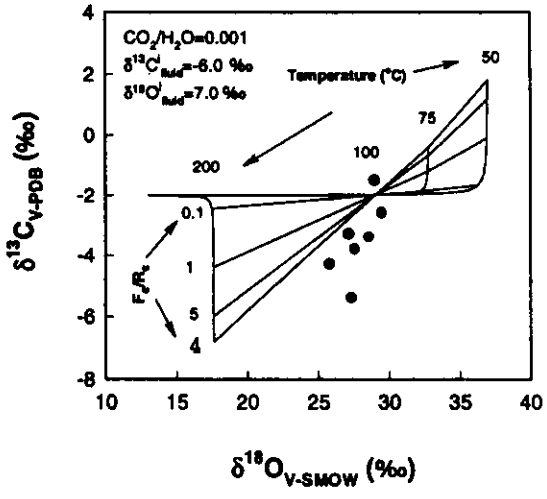

Fig. 4.29. Comparison of $\delta^{13}C$ and $\delta^{18}O$ of ferrocarbonatites and metasomatic rocks of Amba Dongar with the fluid-rock interaction model curves when the fluid is magmatic. Initial rock compositions are same as in Fig. 4.27.

Mundwara Complex

Application of fluid-rock interaction model to altered calcite carbonatites of Mundwara complex revealed that these rocks were altered by a low temperature meteoric-

hydrothermal fluid (Fig. 4.30). The fluid was found to be a CO_2 bearing aqueous fluid with initial $\delta^{13}C$ and $\delta^{18}O$ isotopic compositions of -1 ‰ and -4 ‰, respectively and having CO_2/H_2O ratio of 0.001. The $\delta^{13}C$ and $\delta^{18}O$ compositions of the rock was assumed to be -5 ‰ and 8 ‰, respectively. The temperature of fluid-rock interaction was found to be between 75°C to 150°C.

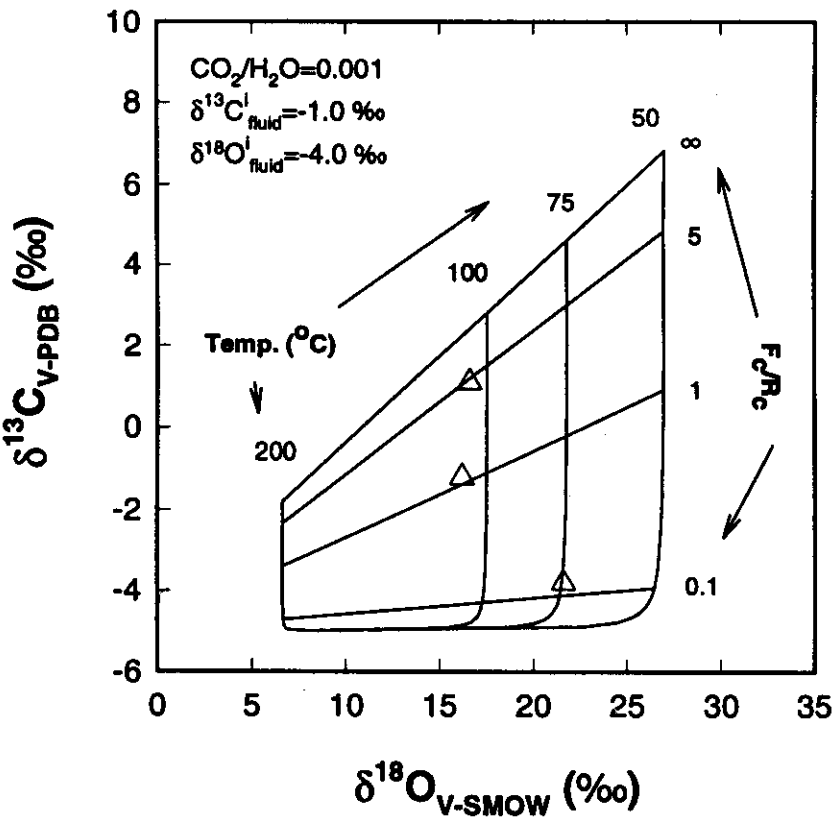

Fig. 4.30. *Comparison of $\delta^{13}C$ and $\delta^{18}O$ of altered calcite carbonatites of Mundwara complex with the fluid-rock interaction model curves when the fluid is meteoric-hydrothermal. The initial rock compositions are assumed to be: $\delta^{13}C$ = -5.0 ‰ and $\delta^{18}O$ = 8.0 ‰.*

Sarnu-Dandali Complex

Like, Mundwara, the extreme isotopic variation shown by altered calcite carbonatites, calcites from ferrocarbonatites and metasomatic rocks of Sarnu-Dandali complex was found to be a result of low temperature (50-150°C) fluid-rock interactions involving a

meteoric-hydrothermal fluid (Fig. 4.31). The fluid initial $\delta^{13}C$ and $\delta^{18}O$ compositions of -1.0 ‰ and -3 ‰, respectively, were used for the model calculations.

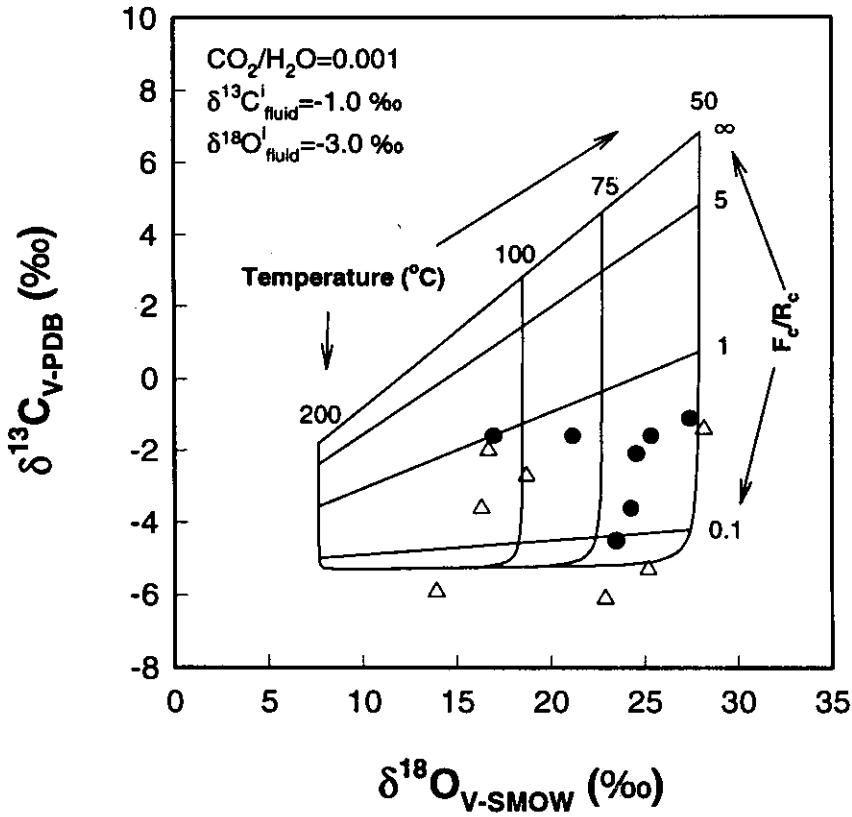

Fig. 4.31. *Comparison of the observed $\delta^{13}C$ and $\delta^{18}O$ variation of altered calcite carbonatites, ferrocarbonatites and metasomatic rocks of Sarnu-Dandali with the fluid-rock interaction model curves when the fluid is meteoric-hydrothermal. Initial rock compositions: $\delta^{13}C$ = -5.0 ‰ and $\delta^{18}O$ = 8.0 ‰*

In summary, the extreme variations of $\delta^{13}C$ and $\delta^{18}O$ in carbonatites and metasomatic rocks from Amba Dongar, Mundwara and Sarnu-Dandali are found to have been generated by interaction of CO_2 bearing aqueous fluids with the rocks at temperatures between 50° and 400°C. In the case of Amba Dongar the calcite carbonatites have probably been affected by both magmatic and fluorite mineralizing hydrothermal fluids, whereas ferrocarbonatites and metasomatic rocks by only the fluorite mineralizing

fluid. In the case of Mundwara and Sarnu-Dandali, low temperature alteration by meteoric-hydrothermal fluid is observed.

4.4.3d. Ferrocarbonatites from Amba Dongar

Fig. 4.16 shows the $\delta^{13}C$ and $\delta^{18}O$ values of coexisting calcite and ankerite from different ferrocarbonatite samples of Amba Dongar complex. Calcites are depleted in $\delta^{13}C$ but highly enriched in $\delta^{18}O$ compared to the coexisting ankerites, except in one sample, in which calcite shows higher $\delta^{13}C$ and $\delta^{18}O$ values. Except for this sample, in all other samples there is a clear indication of disequilibrium between calcites and ankerites (inferred from the negative value of $\Delta^{18}O_{dol\text{-}cal}$, Northrop and Clayton, (1966)). The sample which showed isotopic equilibrium gave a temperature of equilibration of ~380°C, which was calculated based on the carbon isotope fractionation equation of Sheppard and Schwartz (1970). The temperature of equilibration of 380°C indicates that the crystallization temperature of these rocks was ≥380°C. The higher values of $\delta^{18}O$ of calcites are due to hydrothermal alteration, this has already been discussed in the previous section.

4.4.4. Summary

The carbon and oxygen isotopic compositions of the carbonatites of Deccan Province show mantle signatures. All the three complexes studied here show similar isotopic variations. The correlated $\delta^{13}C$ and $\delta^{18}O$ variations observed in unaltered calcite carbonatites of these complexes are successfully explained here by a multicomponent Rayleigh fractionation model (Section 4.4.3b) which reveals that the variations are results of fractional crystallization of these carbonatites from CO_2 rich carbonate magmas. Model calculations also indicate that the carbon isotopic composition of the primary melts for these complexes essentially show average mantle values, except a particular batch of primary melt at Amba Dongar. This batch of primary melt has higher $\delta^{13}C$ composition (by at least 1.8‰) than the average mantle. Such an enrichment probably indicates the incorporation of recycled crustal carbon into this batch of carbonate magma.

Most of the extreme variations of $\delta^{13}C$ and $\delta^{18}O$ in carbonatites and metasomatic rocks studied here are explained by a fluid-rock interaction model (section 4.4.3c). Application of this model reveals that some Amba Dongar rocks have been altered by magmatic and fluorite mineralizing hydrothermal fluids, whereas in other two complexes, evidence of low temperature meteoric-hydrothermal alteration is found. In most of the ferrocarbonatites studied here, coexisting calcites and ankerites show isotopic disequilibrium and calcites are highly altered compared to ankerites. A temperature estimation in Amba Dongar based on carbon isotopes reveals that the crystallization temperature of ferrocarbonatites was >380°C.

PART-B: CARBONATITE-ALKALINE COMPLEXES OF ASSAM-MEGHALAYA PLATEAU

In this part, the results of different isotopic studies of three carbonatites-alkaline complexes (Sung Valley, Samchampi and Swangkre) are presented and discussed. This part is divided into three sections, discussing the results of ^{40}Ar-^{39}Ar chronology and strontium isotopic study of Sung Valley complex and stable isotopic study of all the three complexes, respectively.

4.5. ^{40}Ar-^{39}Ar CHRONOLOGY OF SUNG VALLEY COMPLEX

The formation of a large igneous province during Early Cretaceous at the continental margins of eastern Antarctica, western Australia and eastern India is generally believed to be related to the Kerguelen plume activity (Storey et al., 1992). This activity started around 116 Ma ago with the extrusion of Rajmahal Traps on the Indian subcontinent (Baksi, 1986; Ghose et al., 1996). Other magmatic activities of eastern India, which are considered to be members of the above large igneous province include Sylhet Traps; lamprophyres, dolerites and basalts of Bengal basin; and carbonatite-alkaline complexes of Assam-Meghalaya plateau (Ghose et al., 1996). The available geochronological data on Sung Valley complex give ages varying from 90 Ma to 150 Ma (Chattopadhay and Hashimi, 1984; Krishna et al., 1991; Kent et al., 1992). Hence, to precisely determine the age of these carbonatite-alkaline activities and to establish their temporal relationship with the Rajmahal Traps, precise ^{40}Ar-^{39}Ar dating of

samples from Sung Valley complex was undertaken in this work following the procedures described in Chapter-III.

4.5.1. Results

Three samples, one whole rock sample of alkali pyroxenite (SV-4) and two phlogopite mineral separates from carbonatites (SV-7 and SV-12) were dated. The argon isotopic compositions, fraction of ^{39}Ar released, apparent ages and percent radiogenic argon ($^{40}Ar^*$) released, for each temperature step are given in Tables 4.11-4.13. Modified J factors are also given in these tables. The age spectra along with isotope correlation diagrams are shown in Figures 4.11-4.13. The plateau ages along with percent ^{39}Ar included in the plateaus; isochron and inverse isochron ages of plateau steps along with ratios of trapped argon and MSWD values; and integrated (total) ages are summarized in Table 4.14. The two phlogopite separates (SV-7 and SV-12) yielded good plateaus in the age spectra (Fig. 4.32a and Fig. 4.33a) giving ages of 106.4±1.3 (2σ) Ma and 107.5±1.4 (2σ) Ma respectively, which are indistinguishable within the assigned errors. The pyroxenite (SV-4), a monomineralic rock yielded a four high temperature steps (1000°C 1150°C) plateau (Fig. 4.34a) with an age of 108.0±2.0 (2σ) Ma, agreeing with the phlogopite ages within 2σ level of error. However, the saddle shaped age spectrum (Fig.4.34a) and non-atmospheric trapped argon component (i.e., y-intercept >295.5; Table 4.14) of this sample suggest the presence of a small amount of inherited argon. Therefore, only the phlogopite ages are considered for the age calculation and the weighted mean of these, 106.9±0.9 (2σ) Ma, is the age of emplacement of Sung Valley complex.

Table 4.11. Step heating argon isotopic compositions and apparent ages of sample SV-4 (Sung Valley Pyroxenite). Errors on age are without and with (bracketed) error on J. Errors quoted are at 1σ .

(J = 0.00220 ± 0.00004)

Temp. (°C)	$^{36}Ar/^{39}Ar$ ±1σ	$^{37}Ar/^{39}Ar$ ±1σ	$^{40}Ar/^{39}Ar$ ±1σ	AGE (Ma) ±1σ	^{39}Ar (%)	$^{40}Ar^*$ (%)
500	3.53	10.06	2288.0	2380	0.01	54.43
	0.51	0.27	203.0	166 (168)		
600	2.04	3.33	1692.0	2208	0.02	64.45
	0.19	0.69	76.0	61 (65)		
650	0.815	10.23	489.8	788	0.10	50.84
	0.026	0.20	4.3	22 (25)		
700	0.991	35.67	664.3	1078	0.06	55.92
	0.043	0.35	6.7	31 (34)		
750	2.276	26.70	1039.0	1066	0.12	35.25
	0.028	0.51	11.0	21 (25)		
800	0.305	2.78	233.5	495	0.37	61.42
	0.034	0.18	2.1	31 (32)		
850	0.080	0.420	80.7	214	0.71	70.76
	0.022	0.075	1.0	23 (24)		
900	0.0497	0.439	50.65	137.5	1.35	71.0
	0.0019	0.017	0.58	2.9 (3.7)		
950	0.02279	0.4942	41.39	132.6	2.69	83.73
	0.00095	0.0089	0.99	3.8 (4.4)		
1000	0.01382	1.648	32.69	110.2	4.14	87.51
	0.00049	0.023	0.37	1.4 (2.4)		
1050	0.00275	2.977	29.04	108.73	17.72	97.20
	0.00022	0.023	0.21	0.62 (1.96)		

1100	0.000884	3.0930	28.17	107.58	57.37	99.07
	0.000062	0.0062	0.16	0.53 (1.91)		
1150	0.00661	6.127	30.29	109.17	12.61	93.55
	0.00022	0.012	0.22	0.78 (2.02)		
1200	0.0253	129.4	70.9	236	0.97	89.44
	0.0049	2.1	2.7	10 (11)		
1250	0.0176	101.76	60.1	205.6	0.77	91.34
	0.0049	0.24	1.3	7.8 (8.5)		
1300	0.039	69.39	69.6	217	0.45	83.47
	0.011	0.33	2.3	14 (15)		
1400	0.071	33.15	73.0	196	0.54	71.25
	0.015	0.11	3.2	20 (20)		
Integrated Values	0.01117	5.776	34.23	118.82	100.0	90.35
	0.00025	0.021	0.12	0.47 (2.08)		

Table 4.12. Step heating argon isotopic compositions and apparent ages of sample SV-7 (Phlogopite from Sung Valley Carbonatite). Errors on age are without and with (bracketed) error on J. Errors quoted are at 1σ .

(J = 0.00230 ± 0.00004)

Temp. (°C)	$^{36}Ar/^{39}Ar$ ±1 σ	$^{37}Ar/^{39}Ar$ ±1 σ	$^{40}Ar/^{39}Ar$ ±1 σ	AGE (Ma) ±1 σ	^{39}Ar (%)	$^{40}Ar^*$ (%)
600	0.1429	3.0	98.9	222	0.07	57.33
	0.0088	1.1	1.7	11 (11)		
650	0.0775	1.53	63.0	159.5	0.14	63.66
	0.0042	0.12	1.1	6.3 (6.9)		
700	0.0650	1.17	48.27	116.9	0.32	60.18
	0.0019	0.12	0.79	3.7 (4.2)		
750	0.0321	0.0946	37.36	112.3	1.56	74.60

	0.0010	0.0082	0.98	2.8 (3.4)		
800	0.0057	0.1591	28.21	107.04	3.56	94.03
	0.00018	0.0082	0.18	0.67 (1.95)		
850	0.0072	0.00924	28.44	106.18	5.71	92.50
	0.00016	0.00098	0.17	0.61 (1.91)		
900	0.005458	0.001	27.88	106.02	13.53	94.22
	0.000095	0.00087	0.16	0.56 (1.90)		
950	0.00209	0.0185	26.81	105.71	10.79	97.69
	0.00015	0.0016	0.15	0.56 (1.89)		
1000	0.00313	0.02065	27.22	106.11	11.68	96.60
	0.00012	0.00074	0.16	0.56 (1.90)		
1050	0.00424	0.02548	27.71	106.75	22.87	95.48
	0.000051	0.0004	0.20	0.59 (1.92)		
1100	0.003	0.02241	27.25	106.38	18.53	96.75
	0.00091	0.00043	0.16	0.55 (1.90)		
1150	0.00363	0.04049	27.47	106.50	9.03	96.09
	0.00014	0.00015	0.18	0.58 (1.91)		
1200	0.00682	0.614	28.56	107.1	1.57	92.94
	0.00076	0.011	0.34	1.6 (2.4)		
1250	0.0097	10.688	39.06	144.5	0.45	92.67
	0.0027	0.048	0.84	4.5 (5.1)		
1300	0.044	31.02	83.7	272.0	0.13	84.50
	0.011	0.11	3.3	16 (17)		
1400	0.718	26.18	217.0	18	0.04	2.01
	0.059	0.15	22.0	114 (114)		
Integrated Values	0.005223	0.13884	28.063	107.0	100.00	94.50
	0.000052	0.00096	0.069	0.23 (1.84)		

Table 4.13. Step heating argon isotopic compositions and apparent ages of sample SV-12 (Phlogopite from Sung Valley Carbonatite). Errors on age are without and with (bracketed) error on J. Errors quoted are at 1σ .

(J = 0.00229 ± 0.00004)

Temp. (°C)	$^{36}Ar/^{39}Ar$ ±1σ	$^{37}Ar/^{39}Ar$ ±1σ	$^{40}Ar/^{39}Ar$ ±1σ	AGE (Ma) ±1σ	^{39}Ar (%)	$^{40}Ar^*$ (%)
650	0.364	3.47	205.3	365	0.06	47.58
	0.017	0.38	4.6	18 (19)		
700	0.1215	7.005	107.0	272.4	0.18	66.43
	0.0079	0.060	5.2	6.4 (7.8)		
750	0.06182	1.0109	55.89	149.3	1.0	67.31
	0.00098	0.0097	0.40	1.8 (3.1)		
800	0.01761	0.0358	31.95	107.4	2.35	83.71
	0.00053	0.0094	0.27	1.2 (2.2)		
850	0.01265	0.00008	30.61	107.91	4.16	87.79
	0.00026	0.0000002	0.22	0.84 (2.02)		
900	0.01133	0	30.17	107.71	12.35	88.90
	0.00016	0	0.18	0.63 (1.94)		
950	0.00473	0.0093	28.31	108.08	10.66	95.06
	0.00024	0.00035	0.17	0.64 (1.95)		
1000	0.00617	0.0058	28.58	107.47	13.0	93.62
	0.00015	0.0019	0.17	0.60 (1.93)		
1050	0.00426	0.00701	28.02	107.48	28.43	95.51
	0.0001	0.00013	0.32	0.56 (1.92)		
1100	0.00220	0.01209	27.35	107.26	15.32	97.63
	0.00016	0.00013	0.16	0.59 (1.92)		
1150	0.00171	0.0273	27.13	106.95	10.88	98.14
	0.00026	0.0011	0.17	0.66 (1.94)		
1200	0.0068	0.8105	28.39	106.0	1.22	92.92
	0.0016	0.0038	0.61	2.9 (3.5)		
1250	0.0171	12.757	38.1	132	0.31	86.76
	0.0074	0.050	1.9	11 (11)		

1300	0.018	56.37	66.6	238	0.10	92.16
	0.023	0.11	6.6	35 (35)		
Integrated Values	0.06582	0.14037	28.99	108.58	100.00	93.29
	0.000077	0.00049	0.11	0.25 (1.87)		

Table 4.14. Summary of results of ^{40}Ar-^{39}Ar dating of Sung Valley samples.

Sample	Plateau			Isochron			Inverse Isochron			Integrated Age
	steps	% ^{39}Ar	Age (Ma)	Age (Ma)	Trap	MSWD	Age (Ma)	Trap	MSWD	(Ma)
SV-4	4	91.84	108.8 ±2.0	108.0 ±3.9	342.0 ±60.0	0.108	107.7 ±27.0	352.0 ±62.0	0.078	118.8 ±4.2
SV-7	9	97.27	106.4 ±1.3	106.6 ±3.9	284.0 ±71.0	0.128	105.9 ±34.5	319.0 ±73.0	0.088	107.0 ±3.7
SV-12	9	98.37	107.5 ±1.4	107.5 ±3.8	299.0 ±30.0	0.068	107.3 ±16.0	304.9 ±31.0	0.057	108.6 ±3.7

Note: Trap: Initial $^{40}Ar/^{36}Ar$ (trapped argon); MSWD: Mean Square Weighted Deviate.
Errors are 2σ.

4.5.2. Discussion

The contemporanity of alkali pyroxenite and carbonatites of Sung Valley complex probably indicates a genetic relationship between these two. The 106.9±0.9 Ma age of this complex suggests that this complex is much younger than most of the dates reported earlier and is younger than Rajmahal Traps by ~10 Ma. This age of Sung Valley also suggests that this alkaline activity is coeval with Kerguelen plume related magmatisms such as Damodar Valley and Darjeeling Lamprophyres (121-105 Ma; Sarkar et al., 1980), Prince Charles Mountains Lamprophyres (108-110 Ma; Walker and Mond, 1971) and Bundbury Basalt (88-105 Ma, McDougall and Wellman, 1976). Hence the age along with the location of Sung Valley carbonatite-alkaline complex (present within the Kerguelen plume affected region) can be put forward as a circumstantial evidence for Kerguelen plume origin for this complex.

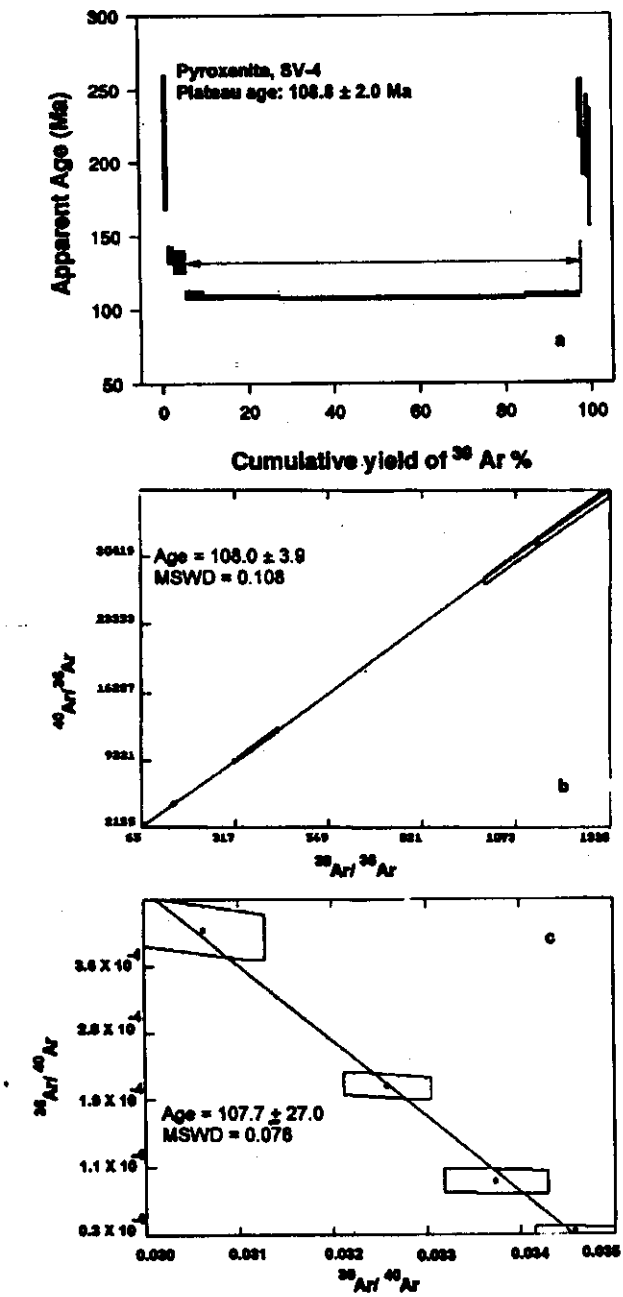

Fig. 4.32. (a) Step heating $^{40}Ar/^{39}Ar$ apparent age spectrum for SV-4 (Sung Valley Pyroxenite) with plateau age. The spectrum shows a saddle shaped pattern with a four temperature steps plateau (see text for discussion). (b) $^{40}Ar/^{36}Ar$ vs. $^{39}Ar/^{36}Ar$ correlation diagram of SV-4 showing 2σ error envelopes and regression line. Isochron age and MSWD value are also shown. (c) $^{36}Ar/^{40}Ar$ vs. $^{39}Ar/^{40}Ar$ correlation diagram of SV-4 showing 2σ error envelopes and regression line. Inverse isochron age and MSWD value are also shown. Please also see the caption of Fig. 4.1.

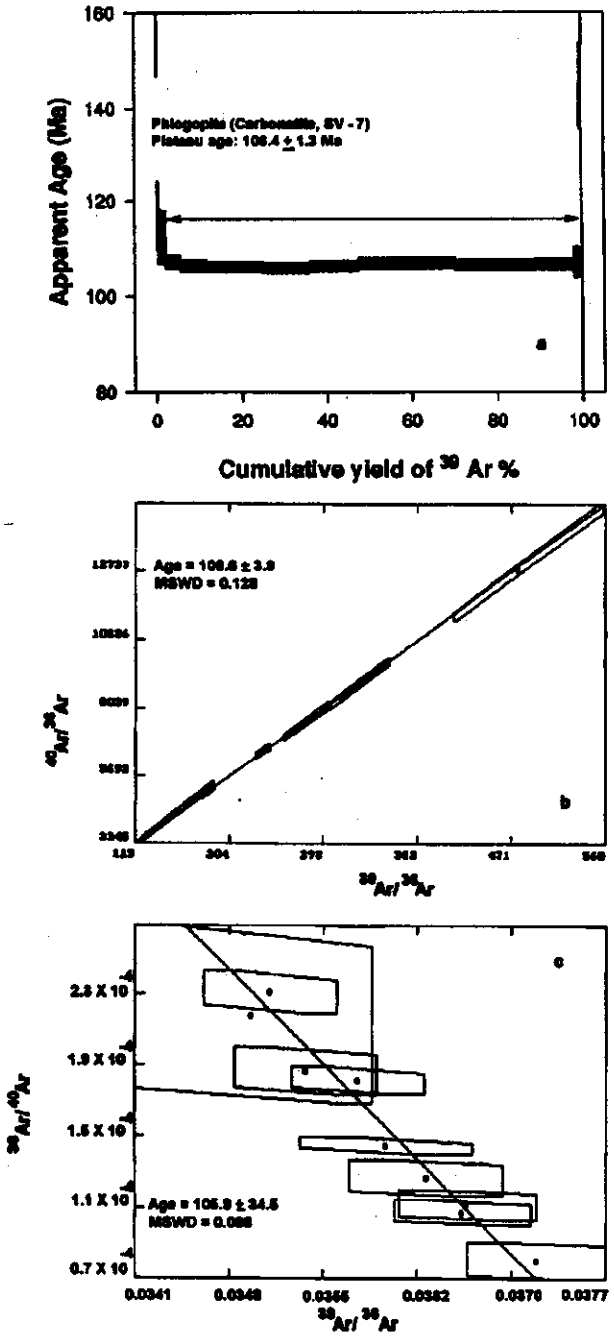

Fig.4.33. (a) Step heating of $^{40}Ar/^{39}Ar$ apparent age spectrum for SV-4(phlogopite separate from a carbonatite of Sung Valley) with the plateau age. (b) $^{40}Ar/^{36}Ar$ vs. $^{39}Ar/^{36}Ar$ correlation diagram of SV-7 with isochron age and MSWD value. (c) $^{36}Ar/^{40}Ar$ vs. $^{39}Ar/^{40}Ar$ correlation diagram of SV-7 with inverse isochron age and MSWD value. Please also see the caption of Fig.4.1 and Fig. 4.32.

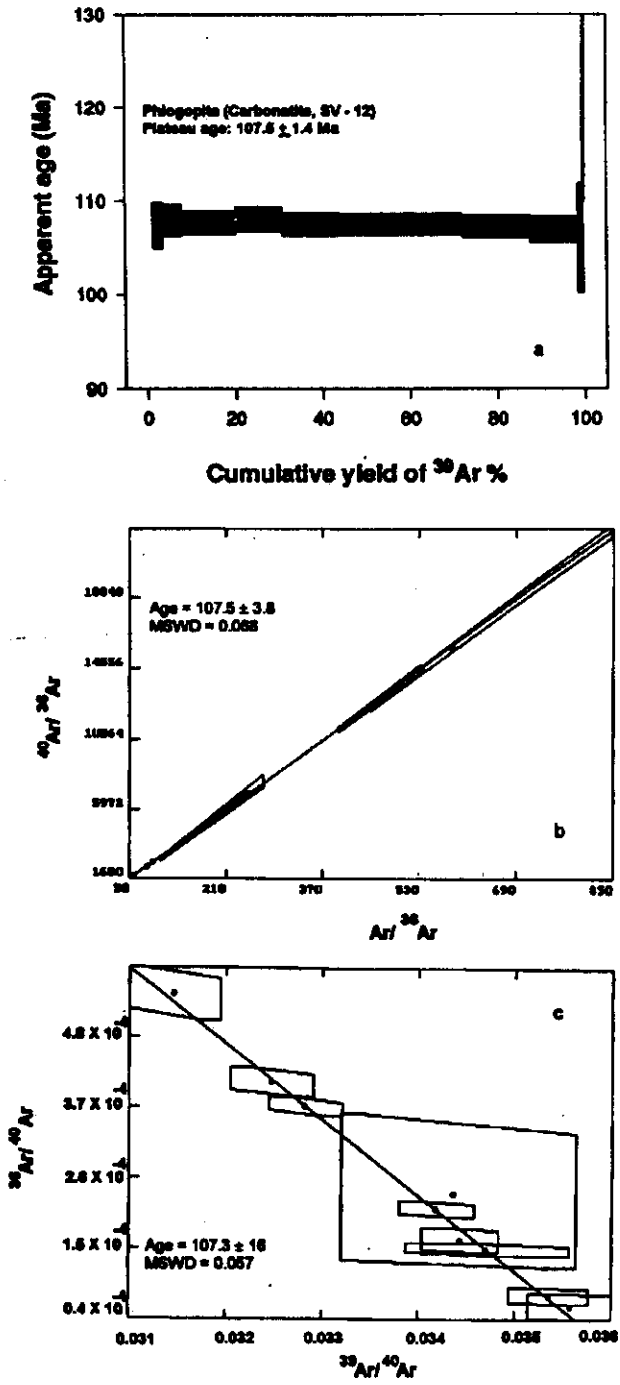

Fig. 4.34. (a) Step heating of $^{40}Ar/^{39}Ar$ apparent age spectrum for SV-12 (phlogopite separate from a carbonatite of Sung Valley) with plateau age. (b) $^{40}Ar/^{36}Ar$ vs. $^{39}Ar/^{36}Ar$ correlation diagram of SV-12 with isochron age and MSWD value. (c) $^{36}Ar/^{40}Ar$ vs. $^{39}Ar/^{40}Ar$ correlation diagram of SV-12 with inverse isochron age and MSWD value. Please also see the captions of Fig. 4.1 and Fig. 4.32.

4.5.3. Summary

The Sung Valley carbonatite-alkaline complex is 107 Ma old. The pyroxenites and carbonatites of this complex are coeval and hence, are probably genetically related. The temporal and spatial relation of this complex with Rajmahal Traps, Bengal basin magmatisms and other Kerguelen related activities suggest that this complex was generated by the Kerguelen plume.

4.6 Sr ISOTOPIC STUDIES IN SUNG VALLEY

4.6.1. Results

Sr isotope ratio and concentration were measured in samples of carbonatites, a phlogopite separate and a pyroxenite. The results are summarized in Table 4.15. The table also gives the initial $^{87}Sr/^{86}Sr$ ratios calculated using the age of 107 Ma for Sung Valley (^{40}Ar-^{39}Ar age). An attempt was made to date Sung Valley complex by Rb-Sr isochron method of dating and for this, two calcite carbonatite whole rocks (SV-11 and SV-12), and phlogopite separate (SV-12/P) from the calcite carbonatite and a pyroxenite whole rock (SV-4) were used. The Rb-Sr isochron age (using the method proposed by Provost, 1990) for this complex was found to be 106±11 (2σ) Ma (Fig. 4.35) and the y-intercept gave an initial ratio [$(^{87}Sr/^{86}Sr)_i$] for the complex of 0.70508±0.00004 (2σ). This isochron age matches well with the ^{40}Ar-^{39}Ar age for the complex within the error. The initial Sr ratios of carbonatites and the pyroxenite are essentially same as the initial ratio found from isochron diagram (Fig. 4.35) considering the errors associated with them. The average Sr concentration in carbonatites is ~4000 ppm.

Table 4.15. Results of Sr isotopic measurements in samples from Sung Valley complex.

Sample	Rb (ppm)	Sr (ppm)	$(^{87}Sr/^{86}Sr)_m$ (atomic)	$(^{87}Rb/^{86}Sr)_m$ (atomic)	$(^{87}Sr/^{86}Sr)_i$
Carbonatites					
SV-1	0.1	4076	0.7055±3	0.00007	0.7055

SV-5	0.12	4030	0.7049±2	0.00009	0.7049
SV-6	0.15	3859	0.7053±2	0.00011	0.7053
SV-10	0.1	4148	0.7046±5	0.00007	0.7046
SV-11	0.18	3831	0.7051±1	0.00014	0.7051
SV-12	0.22	3418	0.7053±3	0.00019	0.7053
SV-13	0.18	3956	0.7050±1	0.00013	0.7050
Phlogopite (carbonatite)					
SV-12/P	153	207	0.7083±3	2.1369	0.7050
Pyroxenite					
SV-4*	10	700	0.70514±4	0.04132	0.70508

Note: * = sample analyzed at NGRI; subscript 'm' stands for measured ratios and 'i' for initial ratio (at 107 Ma). The errors quoted on the measured Sr ratios are at 2σ.

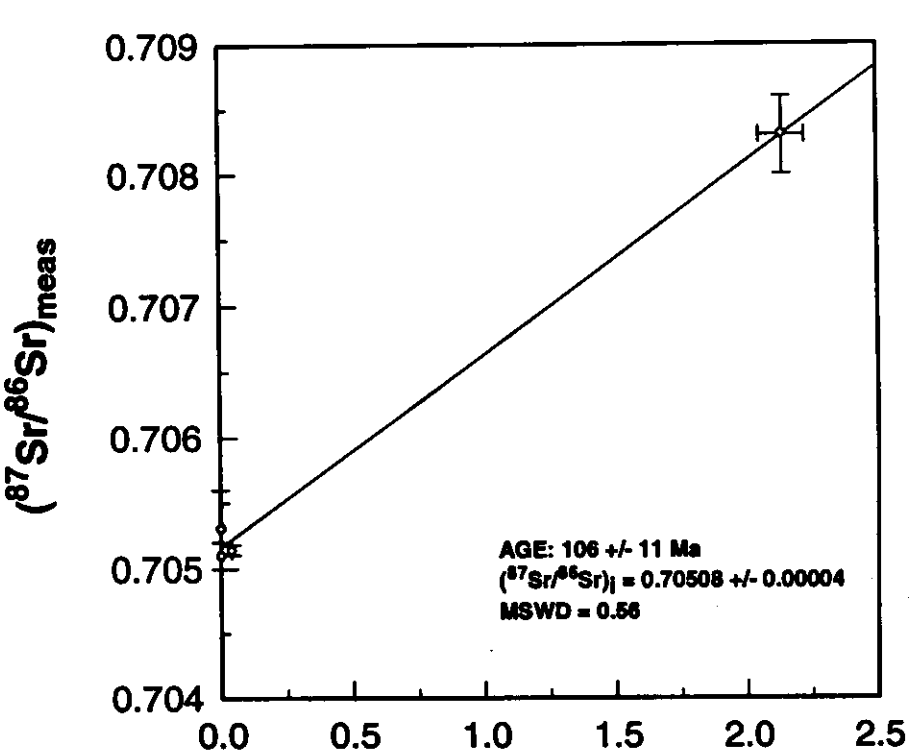

Fig. 4.35. Rb-Sr conventional isochron diagram for Sung Valley complex. Two whole rock carbonatites and one whole rock pyroxenite plot close to $^{87}Rb/^{86}Sr = 0$, whereas a phlogopite separate from carbonatite with very high $^{87}Rb/^{86}Sr$ (~2.14) and very high $^{87}Sr/^{86}Sr$ plots on the extreme right of the figure. Error bars are at 2σ.

4.6.2. Discussion

The consistency of Rb-Sr isochron age with the ^{40}Ar-^{39}Ar age and the homogeneous initial $^{87}Sr/^{86}Sr$ ratio in the rocks of Sung Valley suggests that the Sr reservoir of this complex has remained a closed system since the emplacement of the complex. The similarity of initial $^{87}Sr/^{86}Sr$ ratio of carbonatites and pyroxenites indicates that these rocks types were derived from similar sources and are genetically related.

The initial $^{87}Sr/^{86}Sr$ ratio of Sung Valley complex, i.e., 0.70508 (found from isochron diagram, Fig.4.35) falls within the initial ratio fields of Rajmahal tholeiites and the 105-115 Ma old basalts from Kerguelen plateau (Storey et al, 1992). This observation

along with the chronology clearly supports the generation of this complex by the Kerguelen plume activity.

4.6.3. Summary

The Rb-Sr isochron age a Sung Valley is 106±11 (2σ) Ma, which is same as the ^{40}Ar-^{39}Ar age of this complex. The homogenous initial Sr ratio in rocks of this complex suggests that the complex has remained a closed system since its formation. Similarity of the initial $^{87}Sr/^{86}Sr$ of Sung Valley with that of other Kerguelen plume generated rocks suggest a similar origin (i.e., generation from Kerguelen plume) for this complex.

4.7 STABLE CARBON AND OXYGEN ISOTOPES

4.7.1. Results

The carbon and oxygen isotopic compositions of carbonatites from all the three complexes (Sung Valley, Samchampi and Swangkre) were measured. Isotopic compositions of coexisting calcites and dolomites in samples of dolomite bearing calcite carbonatites from Sung Valley were measured following the selective CO_2 extraction produces discussed in section 3.2.2b of Chapter-III. Table 4.16 summarizes the results of these measurements. The $\delta^{13}C$ and $\delta^{18}O$ values of calcite from calcite carbonatites from all the three complexes are plotted in Fig. 4.36. The isotopic compositions of coexisting calcite and dolomite of Sung Valley samples are plotted in Fig. 4.37. These figures also show the primary carbonatite box, which is modified after Taylor (1967) and Keller and Hoefs (1995).

As seen in Fig.4.36, the carbonatites from Sung Valley, except two samples, from a cluster around $\delta^{13}C$ value of -3.0‰ and $\delta^{18}O$ value of 7.4‰. Similarly carbonatites from Samchampi form a cluster around $\delta^{13}C$ = -3.5‰ and $\delta^{18}O$ = 7.2‰ and the only sample from Swangkre plots at $\delta^{13}C$ = -3.7‰ and $\delta^{18}O$ = 9.6‰. All these complexes plot above the primary carbonatite box.

Table 4.16. Carbon and Oxygen isotopic compositions of samples from carbonatite-alkaline complexes of Assam-Meghalaya Plateau.

Sample	$\delta^{13}C_{calcite}$ (‰)	$\delta^{18}O_{calcite}$ (‰)	$\delta^{13}C_{dolomite}$ (‰)	$\delta^{18}O_{dolomite}$ (‰)
Sung Valley				
SV-1	-2.6	7.5	-2.2	6.8
SV-2	-1.8	15.3	-2.2	7.1
SV-5	-3.0	7.2	---	---
SV-6	-2.9	7.5		
SV-10	-2.9	7.1		
SV-11	-3.0	7.2		
SV-12	-3.0	7.2		
SV-15	-3.0	7.1		
SV-18	-2.8	7.2	-2.4	6.7
SV-19	-2.8	8.4	-3.1	8.8
SV-20	-2.8	7.3	-2.4	6.7
PKS-145	-3.0	7.6		
PKS-164	-3.1	7.8		
PKS-270	-2.9	7.5		
PKS-241	-3.1	15.3		
PKS-279	-3.1	7.1		
Samchampi				
71	-3.8	7.2		
C1/93	-3.7	7.5		
165	-3.0	7.3		
177	-3.7	7.0		
179	-3.5	7.1		
Swangkre				
WKS-1	-3.7	9.6		

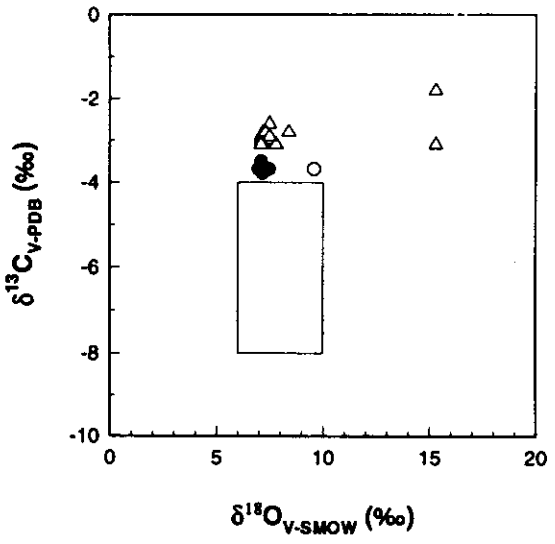

Fig. 4.36. Carbon and oxygen isotopic compositions of calcites from calcite carbonatites and dolomite bearing calcite carbonatites of all the three complexes of Assam-Meghalaya plateau. Open triangles = Sung Valley, filled circles = Samchampi, and open circles = Swangkre. The box is for primary carbonatites (modified after Taylor et al., 1967 and Keller and Hoefs, 1995).

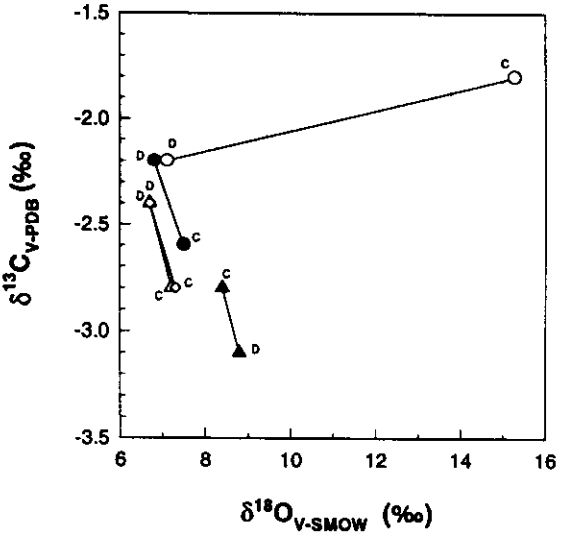

Fig. 4.37. $\delta^{13}C$ vs. $\delta^{18}O$ of coexisting calcites (marked as c) and dolomite (marked as d) joined by tie lines from dolomite bearing calcite carbonatites of Sung Valley complex.

4.7.2. Discussion

It has been postulated that the $\delta^{13}C$ and $\delta^{18}O$ variations of carbonatites depends on their emplacement levels (Deines and Gold,1973) and the isotopic compositions of deep-seated complexes are less variable than those of the shallow seated complexes. The carbonatites of Assam-Meghalaya plateau being the deepest complex (Section 2.8 of Chapter-II) of all the Mesozoic complexes studied in this work, shows less variable (in fact, homogeneous) isotopic composition, consistent with the observations made by Deines and Gold (1973). This is probably because these rocks have not been affected by any near surface alteration processes. Only the two samples (which are collected close to a river-cut section) from Sung Valley, which show higher $\delta^{18}O$ values than the rest but similar $\delta^{13}C$ values, possibly have been affected by meteoric water alteration.

4.7.2.a. Mantle Source Regions

All the samples from Sung Valley, Samchampi and Swangkre, except the two altered ones, show $\delta^{18}O$ value in the range of 7.0 to 9.6‰, consistent with the predictions made by Deines (1989) for the $\delta^{18}O$ of the primary carbonatites. However, the $\delta^{13}C$ values are higher than the generally observed $\delta^{13}C$ values for primary carbonatites (Deines, 1989; Keller and Hoefs, 1995). Homogeneous initial of Sr isotopic ratios (as discussed in the previous section) of Sung Valley rules out crustal contamination and the homogeneous nature of $\delta^{13}C$ and $\delta^{18}O$ values rules out the isotopic fractionation due to fractional crystallization in these complexes. In such a case the $\delta^{13}C$ and $\delta^{18}O$ values of the carbonatites directly reflect the isotopic composition of the parent magma. If so, then the parent magmas of these three complexes had higher $\delta^{13}C$ compositions (> 3.5%) than what is observed for most of the carbonatite complexes of the world. Deines (1989) suggested that during the formation of carbonate magma a fairly complete extraction of elemental carbon from the source takes place and hence the magma would simply inherit the carbon isotopic composition of the mantle source without fractionating it. Hence, the $\delta^{13}C$ of the primary magmas for the complexes under discussion are essentially the $\delta^{13}C$ values of their source regions which would mean that the mantle source regions of these complexes were enriched in carbon isotopes compared to an average mantle ($\delta^{13}C$ = -5.0‰, Nelson et al., 1988). If we assume that all the three complexes of Assam-Meghalaya plateau were derived from a

single source than the source had $\delta^{13}C$ values of -3.2‰ (average of all $\delta^{13}C$ values), which is 1.8‰ higher than an average mantle. This kind of carbon isotope enrichment of the mantle source is probably because of contamination of recycled crustal carbon with the juvenile carbon. Phanerozoic pelagic carbonates and secondary carbonates in altered oceanic crust generally have $\delta^{13}C$ values between 0-2‰ (Nelson et al., 1988); if such an oceanic crust got recycled into the mantle in the past, with a mixing of 26-36%, it could have generated higher $\delta^{13}C$ value in the carbonatite source region as observed. However, such an effect may not be detected in $\delta^{18}O$ of carbonatites as the reservoir for oxygen is much larger compared to that of carbon. As all these complexes were derived from Kerguelen plume, with the present findings, one would except that either the plume itself was enriched in carbon isotopes or it entrained subcontinental upper mantle material which was already enriched by mantle metasomatic processes. The latter explanation seems to be more reasonable as experiments (Yaxley and Green, 1994) have shown that calcite and dolomite can survive in the subducting oceanic crust as refractory phases up to 130-150 km depth, which can in turn provide the required carbon isotope enrichment upon dissociation of carbonates and subsequent metasomatism by the fluids (CO_2) removed from the oceanic crusts. It is not known yet whether the carbonates of subducting oceanic crust can survive up to core-mantle boundary in order to enrich the plume source regions. Hence, a plausible explanation for the generation of enriched carbonate magmas from the plume (like Sung Valley, Samchampi and Swangkre) would be melting of entrained carbon enriched subcontinental upper mantle material.

4.7.2b. Dolomite bearing calcite carbonatites from Sung Valley

Fig. 4.37 shows $\delta^{13}C$ and $\delta^{18}O$ values of coexisting calcite and dolomite from dolomite bearing calcite carbonatites. Calcites have lower $\delta^{13}C$ compared to dolomite and similar $\delta^{18}O$, except for two samples where calcites have higher $\delta^{13}C$ and $\delta^{18}O$ values compared to the dolomite. Except for these two samples, in all other samples (three of them) there is a clear indication of equilibrium between calcite and dolomite. The temperature of equilibration for these samples, calculated using the carbon isotopic fractionation equation of Sheppard and Schwartz (1970), is found to be ~600°C. This suggests that the carbonatites of Sung Valley complex were crystallized above 600°C.

3.7.3. Summary

Unlike carbonatites of Deccan Province, the carbonatites from Assam-Meghalaya plateau show homogeneous $\delta^{13}C$ (also $\delta^{18}O$) compositions. Except for two samples from Sung Valley (which are altered by meteoric water), others seem not to have experienced fractional crystallization or secondary alteration. The oxygen isotopic composition of these carbonatites suggest their magmatic nature. The carbon isotopic composition of these rocks suggest that the mantle source regions of these carbonatites were enriched compared to a isotopically normal mantle and this enrichment has been attributed to the incorporation of recycled crustal carbon.

CHAPTER V

CONCLUDING COMMENTS

In this work, I presented the findings of stable and radioisotopic studies on six Mesozoic carbonatite-alkaline complexes of India (Amba Dongar, Mundwara and Sarnu-Dandali from Deccan Flood Basalt Province and Sung Valley, Samchampi and Swangkre from Assam-Meghalaya Plateau). Summaries of different studies are provided in the closing notes of each of the respective investigations in the Chapter-IV. The intention of this final chapter is to bring out the ideas developed from this work on the formation and evolution of carbonatites and associated alkaline rocks in general and the Mesozoic Indian complexes in particular and to recommend the areas for future study.

An attempt has been made to understand the source regions of carbonatites and the magmatic and post magmatic process involved in their evolution using different geochemical tracers such as Sr-isotopes, trace and rare earth elements and stable isotopes in these rocks and the associated alkaline rocks with the available experimental facilities. Theoretical models were developed in order to track down the effects generated by different geological processes such as liquid immiscibility, crustal contamination, fractional crystallization and secondary alteration. Although the findings of this work are based on a small database, nevertheless, these provide interesting information on the evolution of carbonatites and form a foundation for future investigations on Indian carbonatites. From this study I make the following general conclusions for the evolution of carbonatites.

5.1. GENERAL CONCLUSIONS

5.1.1. Recycled Carbon

Carbonatites incorporate recycled carbon. Though many earlier workers have suggested this but there has been no direct conclusive evidence as the stable carbon isotopes in carbonatites of most of the complexes in the world showed large variations. The homogeneous nature of $\delta^{13}C$ value of carbonatites from Assam-Meghalaya plateau (average value = -3.2‰) suggests an incorporation of recycled crustal carbon ($\delta^{13}C$ =

0 - 2%, Nelson et al., 1988) in the primary melt, which is supposed to carry an average mantle like $\delta^{13}C$ value (-5.0‰, considering the highest value) under normal circumstances. As there is no other evidence for alteration of the primary carbonatite $\delta^{13}C$ value (inferred from Sr and O isotope results) by any magmatic (fractional crystallization or crustal contamination) or secondary (fluid related alteration) processes, I am inclined to believe that the primary magmas for these complexes did carry recycled carbon. In most of the carbonates of the world this kind of evidence is not found because of the fractionation of ^{13}C during their evolutionary processes. However, proper modelling of these fractionating processes can help the identification of recycled component (if present). Doing such an exercise in Amba Dongar complex of Deccan province, I found an evidence of recycled carbon in a particular batch of parent melt. However, the evidence from Amba Dongar is not as conclusive as that from the three complexes of Assam-Meghalaya plateau.

5.1.2. Plume Origin

The temporal, spatial relationship of the Mesozoic carbonatite-alkaline complexes of India with the plume derived flood basalts (Deccan and Rajmahal) and the initial strontium isotopic ratios suggest that these complexes were derived from plumes (Reunion & Kerguelen). They represent either early or late magmatic activity relative to the flood basalts, a finding that fits well with the proposed models for plume related carbonatite-alkaline magmatism (Wyllie, 1988; Sen, 1995). The above results also substantiate the findings of Basu et al. (1993). It is possible that carbonatites in general are related to plume activities. Evidence is mounting in favour of such a hypothesis, particularly with the help of multiple radioisotopic studies.

5.1.3. Common Parentage for Carbonatites and Associated Alkaline Rocks

There has been a lot of controversy over the linking of carbonatites with the associated alkaline silicate rocks. The coeval nature of these two rock types and the similarity of their minimum initial Sr isotopic ratios in Amba Dongar and Sung Valley complexes suggest a genetic link and most likely they have a common parentage. Such a finding along with the results from many other complexes of the world suggests that

carbonatites and associated silicates represent a single magmatic event and are derived from a common parent magma.

5.1.4. Assimilation Fractional Crystallization Coupled with Liquid Immiscibility

One of the major contributions of this work is a model that treats elemental and isotopic evolution of a carbonated-silicate magma (parent magma for carbonatite-alkaline complexes) which undergoes simultaneous assimilation of country rocks, fractional crystallization of silicates and separation of carbonate melt. I have applied this model only to Sr-isotopes in this work but it can be applied to other systematics as well. Using the model, I showed that even if there is a crustal contamination of the parent carbonated silicate magma (which is usually small owing to its fast ascent) the effect of contamination will be negligible (particularly for Sr isotopes) in the separated carbonate magma provided the carbonate melt does not get contaminated during its emplacement after liquid immiscibility. However, the alkaline rock will record the contamination effects. Hence, in order to establish crustal contamination in a given complex, the study of both the carbonatites and alkaline rocks are needed.

5.1.5. Stable Carbon and Oxygen Isotopes

Contrary to general belief, I found that magmatic processes like liquid immiscibility and fractional crystallization of carbonate melt can fractionate carbon and oxygen isotopes. The measured carbon isotope fractionation factor between a carbonate melt and a silicate melt is too small (Mattey et al., 1990) to cause any equilibrium isotopic fractionation; however, if the fractionation process is of Rayleigh type during immiscible separation (which is likely, considering the fast separation of carbonate and silicate melts as observed by Wyllie, 1989) then the heavier carbon isotope can get incorporated into the carbonate melt and increase the $\delta^{13}C$ of the carbonate melt with respect to the original mantle value. Fractional crystallization of carbonate magma can generate $\delta^{13}C$ and $\delta^{18}O$ variations if the crystallization process occurs in presence of magmatic fluids (CO_2 + H_2O). A model developed by me to treat such a process (called Rayleigh isotopic fractionation from a multicomponent source), which successfully explains the $\delta^{13}C$ and $\delta^{18}O$ variations in primary carbonatites of Amba

Dongar, Mundwara and Sarnu-Dandali complexes, can be applied to many other complexes of the world where fluid-associated fractional crystallization is suspected.

5.1.6. Evolution of carbonatite-alkaline complexes

From the present work, a general scheme for the evolution of carbonatite-alkaline complexes has evolved. I believe that the evolution of such complexes is a two stage process. Separation of a carbonate melt and simultaneous fractional crystallization of silicate rocks take place from the parent melt at stage one, probably within the crust. After immiscibility is complete, the carbonate melt moves up and crystallizes fractionally, at stage two, to generate different types of carbonatite. Crustal contamination may take place at both the evolutionary stages. At stage one, it is the parent magma which gets contaminated, whereas at stage two, the carbonate magma gets contaminated.

5.2. SITE SPECIFIC CONCLUSIONS

Of the six Mesozoic complexes studied in this work, Amba Dongar and Sung-Valley complexes were studied in detail, whereas only the stable isotopic studies were done in the rest of the complexes. As mentioned earlier, summary of each method of investigation has been provided at the end of each section in Chapter-IV. Here, I will be presenting the important findings of this work on different individual complexes in light of my observations.

5.2.1. Carbonatite-Alkaline Complexes of Deccan Province

Amba Dongar complex has been dated to 65.0 Ma. This is the first reliable age for this complex. The age, spatial relationship with the Deccan flood basalts and the minimum strontium isotope ratios of the three complexes studied from Deccan Province support the hypothesis of Reunion plume origin of these complexes. Amba Dongar carbonatites and other such complexes of Chhota Udaipur subdivision of Baroda District, Gujarat (covers an area of ~1200 km^2), being emplaced just at the K/T boundary (this work and Basu et al., 1993) could have enhanced the catastrophic effects leading to mass extinctions, by rapidly pumping a substantial amount of CO_2 into the already disturbed atmosphere.

The strontium isotopic study on carbonatites, associated alkaline rocks and country rocks of Amba Dongar complex suggests that the liquid immiscibility had played a major role in the formation of this complex. It was also found that the parent magma of this complex had assimilated basement gneisses (up to ~4%). This contamination effects are readily observed in the strontium ratios of the alkaline rocks, and not in carbonatites. The rare earth element abundances in carbonatites and alkaline rocks of Amba Dongar also support their generation by liquid immiscibility.

The stable carbon and oxygen isotopic compositions of primary melts of Amba Dongar, Mundwara and Sarnu-Dandali complexes show average mantle values except for a particular batch of melt at Amba Dongar which bears a signature of recycled crustal carbon. Fractional crystallization of fluid rich carbonate melts is found to be the main process responsible for the correlated variation of $\delta^{13}C$ and $\delta^{18}O$ in unaltered calcite carbonatites from these complexes. Extreme variations of $\delta^{13}C$ and $\delta^{18}O$ compositions shown by some carbonatites in all these complexes are found to be a result of fluid related (CO_2 bearing magmatic or hydrothermal or meteoric) secondary alteration processes.

5.2.2 Carbonatite-Alkaline Complexes of Assam-Meghalaya Plateau

Sung Valley complex has been dated to 107 Ma. This is the first reliable age data for this complex. The age, spatial relationship with Rajmahal Traps, Sylhet Traps and Bengal Basin magmatisms and the initial strontium isotopic ratio of this complex suggest its generation from Kerguelen plume.

Sung Valley carbonatite-alkaline complex is found to be an unique complex as it showed a closed system behaviour for strontium as well as stable isotopes. The Rb-Sr isochron age (which includes samples of carbonatites and an alkali pyroxenite) 106±11 Ma of this complex is same as the more reliable ^{40}Ar-^{39}Ar age of 107 Ma. The rocks of this complex also show homogeneous initial $^{87}Sr/^{86}Sr$ ratio and which is same as the intercept value in the Rb-Sr isochron diagram. The stable C and O isotopic compositions (except two samples, which are altered by meteoric water) are also found

to be homogeneous in the entire complex. These observations rule out the possibility of any crustal contamination.

The $\delta^{13}C$ values of the primary carbonate melts for all the three complexes (Sung Valley, Samchampi and Swangkre) were found to be higher than that of an average mantle (by 1.8‰). This has been attributed to the contamination of the source regions by recycled crustal carbon. A conservative calculation shows that the primary melts for these complexes incorporated around 26-36% of the recycled crustal carbon.

5.3 RECOMMENDATIONS

Though most of the carbonatites in India were discovered in nineteen sixties and seventies, not much work has been done to understand the formation and evolution of these complexes. Except for a few complexes isotopic studies are absent in these. There are many interesting complexes such as Newania (which is a dolomitic carbonatite complex) of Rajasthan and many metamorphosed Precambrian carbonatite complexes of Southern India, which can be taken up for isotopic studies in order to understand many magmatic and post magmatic processes in these complexes. However, in the ongoing discussion about the Mesozoic (Cretaceous, as indicated by my work) complexes, I recommend some important aspects, which should be taken up for study to establish many of the hypotheses presented in this work and elsewhere:

1. To establish whether plume material carries recycled carbon or not, carbon and oxygen isotopic studies are required on carbonates found in mantle xenoliths from many present day hot spot rocks (e.g. Kerguelen hot spot, Schiano et al., 1994).
2. A combined Sr, Nd and Pb isotopic study is required in the carbonatite-alkaline complexes of Assam-Meghalaya plateau, in order to characterize their source regions and their relationship with Kerguelen plume activity during early Cretaceous.
3. To confirm the plume origin for Amba Dongar and carbonatite complexes of Assam-Meghalaya plateau, He-isotopic study is needed.
4. Stable oxygen isotopic studies in silicate fractions of the associated silicate rocks are required to understand clearly the processes such as liquid immiscibility and crustal contamination in the Indian complexes, particularly in Amba Dongar.

5. For a better understanding of stable isotope fractionation during fractional crystallization, a theoretical model should be developed, which should treat isotopic evolution of a multicomponent source from which multiple phases crystallize at different temperatures.

REFERENCES

Al-aasm, I.S., B.E. Taylor, and B. South, Stable isotope analysis of multiple carbonate samples using selective acid extraction, Chem. Geol. (Isot. Geosci.), 80, 119-125, 1990.

Bailey, D.K., and C.M. Hampton, Volatiles in alkaline magmatism, Lithos, 26, 156-165, 1990.

Baksi, A.K., $^{40}Ar/^{39}Ar$ incremental heating study of whole-rock samples from the Rajmahal and Bengal Traps, eastern India, Terra Cognita, 6, 161, 1986.

Balakrishnan, P., S. Bhattachraya, and A. Kumar, Carbonatite body near Khambammettu, Tamil Nadu, Jour. Geol. Soc. India, 26, 418-421, 1985.

Barker, D.S., Consequences of recycled carbon in carbonatites, Can. Mineral., 34, 373-387, 1996.

Barreiro, B.A., and A.F. Cooper, A Sr, Nd and Pb isotope study of alkaline lamprophyres and related rocks from West land and Otago, South Island, New Zealand, Geol. Soc. Am. Special. Paper, 338, 415-418, 1987.

Basu, A.R., P.R. Renne, D.K., Das Gupta, F. Teichman, and R.J. Poreda, Early and late alkali igneous pulses and a high ^{3}He plume origin for the Deccan flood basalts, Science, 261, 902-906, 1993.

Bell, K., J. Blenkinsop, T.J.S. Cole and D.P. Menagh, Evidence from Sr isotopes for long-lived heterogeneities in the upper mantle, Nature, 298, 251-253, 1982.

Bell, K., and J. Blenkinsop, Archean depleted mantle : evidence from Nd and Sr initial isotopic ratios of carbonatites, Geochim. Cosmochim. Acta, 51, 291-298, 1987.

Bell, K., and J. Blenkinsop, Neodymium and strontium isotope geochemistry of carbonatites, In: Carbonatites: Genesis and Evolution, (ed: K. Bell), Unwin Hyman, London, 278-300, 1989.

Bevington, P.R., Data reduction and error analysis for the physical sciences, McGraw Hill Co., New York, 1969.

Bose, M.K., and D.K. Das Gupta, Petrology of alkali syenites of Mundwara magmatic suite, Sirohi, Rajasthan, Geol. Mag., 110, 457-466, 1973.

Bose, M.K., K. Randle, and A.G. Roy, Carbonatites from Kunavaram and Elchuru alkaline complexes, Andhra Pradesh (Abstract). Group diss. on Carb. Kimb. Complexes of India, Geol. Soc. India, Bangalore, 1976.

Brereton, N.R., Corrections for interfering isotopes in the $^{40}Ar/^{39}Ar$ dating method, Earth Planet Sci. Lett., 8, 427-433, 1970.

Chacko, T., T.K. Mayeda, R.N. Clayton, and J.R. Goldsmith, Oxygen and carbon isotope fractionation between CO_2 and calcite, Geochim. Cosmochim. Acta, 55, 2867-2882, 1991.

Chakraborty, M.K. and M.K. Bose, Theralite-melteigite-carbonatite association in Mer ring of Mundwara Suite, Sirohi district, Rajasthan, Jour. Geol. Soc. India., 19, 454-463, 1978.

Chandrasekaran, V., Geochemistry of basic, acid and alkaline intrusives and extrusives of Sarnu-Dandali area, Barmer district, Rajasthan, Unpub. Ph.D. Thesis, Univ. of Rajasthan, Jaipur, p 108, 1987.

Chandrasekaran, V., R.K. Srivastava, and M.P. Chawada, Geochemistry of the alkali rocks of Sarnu-Dandali area, District Barmer, Rajasthan, India, J. Geol. Soc. India, 36, 365-382, 1990.

Chandrasekaran, V., and R.K. Srivastava, Geochemistry of Sarnu-Dandali carbonatites, District Barmer, Rajasthan, India, J. Geol. Soc. India, 39, 321-238, 1992.

Chattopadhyay, B., and S. Hashimi, The Sung Valley alkaline-ultramafic-carbonatite complex, East Khasi and Jaintia Hill district, Meghalaya, Rec. Geol. Surv. India, 113, 24-33, 1984.

Chiba, H., T. Chacko, R.N. Clayton, and J.R. Goldsmith, Oxygen isotope fractionation involving diopside, fosterite, magnetite and calcite: application to geothermometry. Geochim. Cosmochim. Acta, 53, 2985-2995, 1989.

Coffin, M.F., and O. Eldholm, Large igneous provinces : JOI/USSAC Workshop Report, University of Texas at Austin Tech. Rep., No.114, 79, 1991.

Craig, H., Isotopic standards for carbon and oxygen and correction factors for mass spectrometric analysis of carbon dioxide, Geochim. Cosmochim. Acta, 12, 133, 1957.

Crawford, A.R., India, Ceylon and Pakistan : New age data and comparison with Australia, Nature, 223, 380-384, 1969.

Dalrymple, G.B., and M.A. Lanphere, $^{40}Ar/^{39}Ar$ technique of K-Ar dating : A comparison with the conventional technique, Earth Planet. Sci. Lett., 12, 300-308, 1971.

Dalrymple, G.B., E.C. Alexander Jr., M.A. Lanphere, and G.P. Kraker, Irradiation of samples for $^{40}Ar/^{39}Ar$ dating using the Geological Survey of TRIGA reactor. U.S. Geol. Surv., Prof. Paper, 1176, 1981.

Dalton, J.A., and B.J. Wood, The compositions of primary carbonate melts and their evolution through wallrock reaction in the mantle, Earth Planet Sci. Lett., 119, 511-525, 1993.

Damon, P.E., A theory of `real' K-Ar clocks, Ecolgae Geol. Helv., 63, 69-76, 1970.

Das Gupta, D.K., Mundwara alkalic suite and Deccan Volcanicity, Bull. Indian Geol. Assoc, 7, 137-144, 1974.

Das Gupta, D.K., On the alkaline gabbroic rocks and syenites from Musala hill, Mer Mundwara, Sirohi district, Rajasthan, Quart. Jour. Min. Met. Soc. India, 47, 117-124, 1975.

Deans, T., and J.L. Powell, Trace elements and strontium isotopes in carbonatites, fluorites and limestone from India and Pakistan, Nature, 218, 750-752, 1968.

Deans, T., R.N. Sukheshwala, and S.G. Viladkar, Discussions and contributions. Trans. Inst. Min. and Metall., 82, B33-B40, 1973.

Deines, P., and D.P. Gold, The isotopic composition of carbonatites and kimberlite carbonates and their bearing on the isotopic composition of the deep-seated carbon, Geochim. Cosmochim. Acta, 37, 1709-1733, 1973.

Deines, P., Stable isotope variations in carbonatites, In Carbonatites : Genesis and Evolution, (ed: K. Bell), 301-359, Unwin Hyman, 1989.

DePaolo, D.J., Trace element and isotopic effects of combined wall-rock assimilation and fractional crystallization, Earth Planet Sci. Lett., 53, 189-202, 1981.

Epstein, S., D.L. Graf, E.T. Degens, Oxygen isotope studies on the origin of dolomites. In : Isotopic and Cosmic Chemistry, Amsterdam, North-Holland, Pub. Co., 169-180, 1964.

Friedman, I., and J.L. O'Neil, Compilation of stable isotope fractionation factors of geochemical interest, in Data of Geochemistry, 6th edition, U.S. Geol. Surv. Pap., 440-KK, 1977.

Fritz, P., P.L. Binda, F.E. Folinsbee, and H.R. Krouse, Isotopic composition of diagenetic siderites from Cretaceous sediments in western Canada, Jour. Sediment. Petrol., 41-282-288, 1971.

Ghosh Roy, A.K., and P.R. Sengupta, Alkalic-carbonatitic magmatism and associated mineralisation along the Porapahar-Tamar lineament in the Proterozoics of Purulia district, West Bengal, Ind. Jour. of Earth Sci., 20, 193-200, 1993.

Ghose, N.C., S.P. Singh, R.N. Singh, and D. Mukherjee, Flow stratigraphy of selected sections of Rajmahal basalts, eastern India, Jour. South. As. Earth Sci., 13, 83-93, 1996.

Gittins, J., Origin and Evolution of Carbonatite Magmas, In: Carbonatites: Genesis and Evolution, (ed: K. Bell), Unwin Hyman, London, 580-600, 1989.

Gonfiantini, R., δ notation and mass spectrometric techniques, In: Stable Isotope Hydrology, Deuterium and Oxygen-18 in the water cycle, (eds: J.R. Gat & R. Gonfiantini) IAEA Techn. Rep. Series 210, IAEA, Viena, 35-84, 1981.

Gopalan, K., J.R. Trivedi, S.S. Merh, P.P. Patel and S.G. Patel, Rb-Sr age of Godhra and related granites, Gujarat, India, Proc. Ind. Acad. Sci., 4(II), 7-17, 1979.

Green, D.H., and M.E. Wallace, Mantle metasomatism by ephimeral carbonatite melts, Nature, 336, 459-462, 1988.

Green, T.H., J. Adam, and S.H. Sie, Trace element partitioning between silicate minerals and carbonatite at 25 kbar and application to mantle metasomatism, Min. Petrol., 46, 179-184, 1992.

Hamilton, D.L., P. Bedson, and J. Esson, The behaviour of trace elements in the evolution of carbonatites, In : Carbonatites : Genesis and Evolution, (ed: K. Bell), 405-427, 1989.

Hart, S.R., E.H. Hauri, L.S. Oschmann, and J.A. Whitehead, Mantle plumes and entrainment : Isotopic evidence, Science, 256, 517-520, 1992.

Hauri, E.H., N. Shimizu, J.T. Dieu and S.R. Hart, Evidence for hotspot-related carbonatite metasomatism in oceanic upper mantle, Nature, 365, 221-227, 1993.

Hunziker, J.C., Potassium argon dating, In : Lectures in Isotope Geology, (eds: E. Jager & J.C. Hunziker), Springer-Verlag, Berlin, 52-76, 1979.

Izett, G.A., G.B. Dalrymple, and L.W. Snee, ^{40}Ar-^{39}Ar age of Cretaceous-Tertiary boundary tektites from Haiti, Science, 252, 1539-1542, 1991.

Jones, J.H., Experimental Trace Element Partitioning, In: Rock Physics and Phase Relations, A hand Book of Physical Constants, AGU ref. self 3, 73-104,1995.

Keller, J., and J. Hoefs, Stable isotope characteristics of recent natrocarbonatite from Oldoinyo Lengai, In: Carbonatite Volcanism : Oldoinyo Lengai and the Petrogenesis of Natrocarbonatites, (eds: K.Bell and J. Keller), IAVCE I, Proc. Volcanol., 4, 113-123, 1995.

Kent, R.W., M. Storey, and A.D. Saunders, Large igneous provinces : Site of plume impact or plume incubation?, Geology, 20, 891-894, 1992.

Kjarsgaard, B., and D.L. Hamilton, The genesis of carbonatites by immiscibility, In : Carbonatites, Gneisis and Evolution, (ed: K. Bell), 388-404, Unwin Hyman, 1989.

Kundsen, C., and B. Buchardt, Carbon and oxygen isotope composition of carbonates from the Qaqarssuk carbonatite complex, southern west Greenland, Chem. Geol. (Isot. Geosci.), 86, 263-274, 1991.

Krishna, V., B.K. Pandey, P. Krishnamurthy, T. Chabria, and J.N. Gupta, Sr and Nd isotopic data and Rb-Sr age on the Amba Dongar-Siriwasan carbonatite complex and its relation to the Deccan Trap volcanism, 6th Ntl. Symp. on Mass Spectrometry, 515-517, 1993.

Krishnamurthy, P., Petrology of carbonatites and associated rocks of Sung Valley, Jaintia Hills District, Meghalaya, India, Jour. Geol. Soc. India, 26, 361-379, 1985.

Krishnamurthy, P., Carbonatites of India, Explor. Res. At. Mineral, 1, 81-115, 1988.

Kumar, D., R. Mamallan, B. Saravanan, S. K. Jain, and P. Krishnamurthy, Explor. Res. At. Mineral, 2, 183-199, 1989.

Kumar, A., and K. Gopalan, Precise Rb-Sr age and enriched mantle source of Sevattur carbonatites, Tamil Nadu, South India, Curr. Sci., 60, 653-654, 1991.

Kwon, S.T., G.R. Tilton, and M.H. Grunenfelder, Pb isotope relationships in carbonatites and alkaline complexes : An overview, In: Carbonatites: Gneisis and Evolution, (ed: K. Bell), Unwin Hyman, 360-387, 1989.

Laul, J.C., Neutron activation analysis of geological materials, At. Energy Rev., 17, 603-195, 1979.

LeBas, J.M., Carbonatite-nephelinite volcanism, Wiley, London, 347pp., 1977.

LeBas, J.M., Oceanic carbonatites, In : Kimberlites. I : Kimberlites and Related Rocks, (ed: J. Kornprobst), Elsevier, 169-178, 1984.

LeBas, M.J., and R.K. Srivastava, The mineralogy and geochemistry of the Mundwara carbonatite dykes, Sirohi district, Rajasthan, India, Neus. Jah. Min. Abh., 160, 207-227, 1989.

Long, L.F., Isotope dilution analysis of common and radiogenic strontium using ^{84}Sr-enriched spike, Earth Planet Sci. Lett., 1, 289-292, 1966.

Long, P.E., Experimental determination of partition coefficients for Rb, Sr and Ba between alkali feldspar and silicate liquid, Geochim. Cosmochim. Acta., 42, 833-846, 1978.

Mattey, D.P., W.R. Taylor, D.H. Green, and C.T. Pillinger, Carbon isotopic fractionation between CO_2 vapour, silicate and carbonate melts, an experimental study at 20 kbars, Contrib. Mineral. Petrol., 104, 492-505, 1990.

McCrea, J.M., On the isotope chemistry of carbonates and a paleotemperature scale. J. Chem. Phys., 18, 849-857, 1950.

McDougall, I., Precise methods of potassium-argon isotope age determination on young rocks, In: Methods and techniques in geophysics, Wiley Interscience, 2, 279-304, 1966.

McDougall, I., and P. Wellman, Potassium-argon ages for some Australian Mesozoic igneous rocks, Jour. Geol. Soc. Austr., 23, 1-9, 1976.

McDougall, I, and T.M. Harrison, eds., Geochronology and Thermochronology by the $^{40}Ar/^{39}Ar$ Method, 120-126, Oxford Univ. Press, New York, 1988.

McLean, D.M., Deccan Traps mantle degassing in the terminal Cretaceous marine extinction. Cretaceous Research, 6, 235-259, 1985.

Mitchell, J.G., The argon-40/argon-39 method for potassium-argon age determination, Geochim. Cosmochim. Acta, 32, 781-790, 1968.

Molarev, V.M., S.V. Voronovski, and L.S. Borodin, New findings about the age of carbonatites and syenites from Southern India, USSR Acad. Sci., 222, 1975.

Nagasawa, H., Rare earth concentrations in zircons and apatites and their host dacites and granites. Earth Planet Sci. Lett., 35, 953-968, 1970.

Nambiar, A.R., and P.R. Golani, A new find of carbonatite from Meghalaya, Curr. Sci., 54, 281-282, 1985.

Natarajan, M., B.B. Rao, R. Parthasarathy, A. Kumar, and K. Gopalan, 2.0 Ga old pyroxenite-carbonatite complex of Hogenakal, Tamil Nadu, South India, Precamb. Res., 65, 167-181, 1994.

Nelson, D.R., A.R. Chivas, B.W. Chappel, and M.T. McCulloch, Geochemical and isotopic systematics in carbonatites and implications for the evolution of oceanic-island sources, Geochim. Cosmochim. Acta, 52, 1-17, 1988.

Northrop, D.A., and R.N. Clayton, Oxygen-isotope fractionations in systems containing dolomite, J. Geol., 74(2), 174-196, 1966.

Pande, K., T.R. Venkatesan, K. Gopalan, P. Krishnamurthy, and J.D. McDougall, ^{40}Ar-^{39}Ar ages of alkali basalts from Kutch, Deccan Volcanic Province, India, Mem. Geol. Soc. India, 10, 145-150, 1988.

Pineau, F., M. Javoy, and C.J. Allegre, Etude systematique des isotopes de l'oxygene, du carbone et du strontium dans les carbonatites, Geochim. Cosmochim. Acta, 37, 2363-2377, 1973.

Plyusnin, G.S., V.S. Samoylov, and S.I. Gol'shev, The $\delta^{13}C$, $\delta^{18}O$ isotope pair method and temperature facies of carbonatites. Doklady Akademi Nank USSSR, Seriya Geologiya, 254, 1241-1245, 1980.

Raman, P.K., and T.V. Viswanathan, Carbonatite complex near Borra, Visakhapatanam district, Andhra Pradesh, Jour. Geol., Soc. India, 18, 605-610, 1977.

Ramaswamy, R., Carbonatite dykes from Kudangulam area, near Cape Comorin, Tamil Nadu, Jour. Geol. Soc. India, 48, 221-226, 1996.

Rathore, S.S., T.R. Venkatesan, and R.K. Srivastava, Mundwara Alkali Igneous Complex, Rajasthan, India : Chronology and Sr isotope systematics, Jour. Geol. Soc. India, 48, 517-528, 1996.

Richardson, S.H., A.J. Erlank, A.R. Duncan, and D.L. Reid, Correlated Nd, Sr and Pb isotope variation in Walvis Ridge basalts and implications for the evolution of their mantle source, Earth Planet Sci. Lett., 59, 327-342, 1982.

Ritchet, P., Y. Bottinga, and M. Javoy, A review of hydrogen, carbon, nitrogen, oxygen, sulfur, and chlorine stable isotope fractionation among gaseous molecules, Ann. Rev. Earth Planet. Sci., 5, 65-110, 1977.

Rock, N.M.S., L.G. Gwalani, and B.J. Griffin, Alkaline rocks and carbonatites of Amba Dongar and adjacent areas, Deccan Alkaline Province, Gujarat, India. 2. Complexly zoned clinopyroxene phenocrysts, Mineral. Petrol., 51, 113-135, 1994.

Roedder, E., Fluid inclusions from the fluorite deposits associated with the carbonatite of Amba Dongar, India and Okorushu, South west Africa, Trans. Inst. Min. Metal., 82, B35-39, 1973.

Rollinson, H., Using Geochemical Data : Evaluation, Presentation, Interpretation, Longman, UK, P-235, 1993.

Rosenbaum, J., and S.M.F. Sheppard, An isotopic study of siderites, dolomites and ankerites at high temperatures, Geochim. Cosmochim. Acta, 50, 1147-1150, 1986.

Samson, S.D., and E.C. Allexander Jr., Calibration of the interlaboratory ^{40}Ar-^{39}Ar dating standard MMhb-1, Chem. Geol. (Isot. Geosci.), 66, 27-34, 1987.

Santos, R.V., and R.N. Clayton, Variations of oxygen and carbon isotopes in carbonatites : A study of Brazilian alkaline complexes, Geochim. Cosmochim. Acta, 59, 1339-1352, 1995.

Santosh, M., P.K. Thampi, S.S. Iyer, and M.B.A. Vasconcell, Os, Rare earth element geochemistry of the Munnar carbonatite, Central Kerala, Jour. Geol. Soc. India, 29, 335-343, 1987.

Sarkar, A., D.K. Paul, M.N. Balasubrahmanyam, and N.R. Sengupta, Lamprophyres from the Indian Gondwanas - K-Ar ages and Chemistry, Jour. Geol. Soc. India, 21, 188-193, 1980.

Sarkar, A., and S.K. Bhattacharya, Carbonatites from Rajasthan indicate mantle carbon and oxygen isotope composition, Curr. Sci., 62, 368-370, 1992.

Sarin. M.M., D.V. Borole, S. Krishnaswami, Geochemistry and geochronology of sediments from Bay of Bengal and equatorial Indian ocean, Proc. Ind. Acad. Sci., 88 (II), 131-154, 1979.

Schiano, P., R. Clocchiatti, N. Shimizu, D. Weis, and N. Mattielli, Cogenetic silica-rich and carbonate-rich melts trapped in mantle minerals in Kerguelen ultramafic xenoliths: Implications for metasomatism in the oceanic upper mantle, Earth Planet Sci. Lett., 123, 168-178, 1994.

Sen, S.N., and R. Rao, Igneous activity in Cuddapah basin and adjacent areas and suggestion on the paleogeography of the basin (Abstract), Proc. Symp Upp. Mantle, Project Press, V, p 85, 1967.

Sen, G., A simple petrological model for the generation of Deccan Trap Magmas, Int. Geol. Rev., 37, 825-850, 1995.

Sengupta, S.K., J.S. Ray, S. Rahman, and N. Nag, Stable carbon and oxygen isotopic studies on carbonatites of Samchampi alkaline complex, Karbi Anglong District, Assam, India (Abstract), Abstract Vol. of the Conf. on Isot. in Solar Sys. (PRL, Ahmedabad), 1997.

Sharma, T.R., Petrochemistry of the Mundwara igneous complex, Sirohi district, Rajasthan, Jour. Ind. Geosci. Asso., 7, 35-45, 1967.

Sharma, N., Geochemistry and fluid inclusion studies on the carbonatites, associated alkaline rocks and fluorites of Amba Dongar, Guajrat India, Unpubl. Ph.D. Thesis, IIT Bombay, 1991.

Sheppard, S.M.F., and H.P. Schwarcz, Fractionation of carbon and oxygen isotopes and magnesium between coexisting metamorphic calcite and dolomite, Contrib. Mineral. Petrol., 26, 161-198, 1970.

Simonetti, A., K. Bell, and S.G. Viladkar, Isotopic data from the Amba Dongar Carbonatite complex west-central India : Evidence for an enriched mantle source, Chem. Geol. (Isot. Geosci.), 122, 185-198, 1995.

Simonetti, A., and K. Bell, Nd, Pb and Sr isotopic systematics of fluorite at Amba Dongar carbonatite complex, India : Evidence for hydrothermal and crustal fluid mixing, Econ. Geol., 90, 2018-2027, 1995.

Srinivasan, V., The carbonatite of Hogenakal, Tamil Nadu, South India, Jour. Geol. Soc. India, 18, 598-604, 1978.

Srivastava, R.K., Petrology, Petrochemistry and Genesis of the alkaline rocks associated with the Ambdungar carbonatite complex, Baroda district, Gujarat, India, Jour. Geol. Soc. India, 43, 23-39, 1994.

Storey, M. et al., Lower Cretaceous volcanic rocks on continental margins and their relationship to Kerguelen Plateau, Proc. Ocean. Drill. Prog., Sci. Res., 120 33-53, 1992.

Subrahmanyam, N.P., and G.V.U. Rao, Petrology, geochemistry and origin of the carbonatite veins of Mer pluton, Mundwara igneous complex, Rajasthan, Jour. Geol. Soc. India, 18, 306-322, 1977.

Subrahmanyam, N.P., and C. Leelanandam, Differentiation due to probable initial immiscibility in the Musala pluton of the Mundwara alkali igneous complex, Rajasthan, India, Mem. Geol. Soc. India, 15, 25-46, 1989.

Subrahmanyam, N.P., and C. Leelanandam, Geochemistry and Petrography of the cumulphyric layered suite of rocks from the Toa pluton of the Mundwara alkali igneous complex, Rajasthan, Jour. Geol. Soc. India, 38, 397-411, 1991.

Sukheswala, R.N., and G.R. Udas, Note on the carbonatite of Amba Dongar and its economic potentialities. Sci. and Cult., 29, 563-568, 1963.

Sukheswala, R.N., and S.G. Viladkar, The carbonatites of India, Proc. 1st Intl. Symp. on Carbonatites, Brazil, 277-293, 1978.

Sukheswala, R.N., and S.G. Viladkar, Fenitized sandstones in Amba Dongar carbonatites, Gujarat, India, Jour. Geol. Soc. India, 22, 368-374, 1981.

Sun, S.S., Lead isotopic study of young volcanic rocks from mid-oceanic ridges, ocean islands and island arcs, Phil. Trans. R. Soc., A297, 409-445, 1980.

Sweeney, R.J., Carbonatite melt compositions in the Earth's mantle, Earth Planet Sci. Lett., 128, 259-270, 1994.

Taylor, H.P., J. Frechen Jr., and F.T. Degens, Oxygen and carbon isotope studies of carbonatites from Laacher See District, West Germany and Alno district, Sweden, Geochim. Cosmochim. Acta, 31, 407-430, 1967.

Taylor, S.R., and S.M. McLennan, The continental crust : its composition and evolution, Blackwell, Oxford, 1985.

Tetley, N., I. McDougall, and M.R. Heydegger, Thermal neutron interferences in the $^{40}Ar/^{39}Ar$ dating technique, Jour. Geophys. Res., 85, 7201-7205, 1980.

Tilton, G.R., and K. Bell, Sr-Nd-Pb isotope relationship in Late Archean carbonatites and alkaline complexes : Applications to the geochemical evolution of Archean mantle, Geochim. Cosmochim. Acta, 58, 3145-3154, 1994.

Toyoda, K., H. Horiuchi, and M. Tokonami, Dupal anomaly of Brazilian carbonatites : geochemical correlations with hotspots in the South Atlantic and implications for mantle source, Earth Planet Sci. Lett., 126, 315-331, 1994.

Trivedi, J.R., K. Gopalan, K.K. Sharma, K.R. Gupta, and V.M. Choubey, Rb-Sr age of Gaik granite, Ladakh batholith, northwest Himalaya, Proc. Ind. Acad. Sci., 91, 65-73, 1982.

Turner, G., Argon-40/Argon-39 dating: the optimization of irradiation parameters, Earth Planet Sci. Lett., 10, 227-234, 1971.

Udas, G.R., G.R.N. Das, and C.V. Sharma, Carbonatites of India in relation to structural setting, proc. Intl. Sem. on Tect. and Melt. of SE Asia and Far East, Geol. Surv. Ind. Misc. Pub., 34, 77-92, 1974.

Venkatesan, T.R., K. Pande, and K. Gopalan, ^{40}Ar-^{39}Ar dating of Deccan Basalts, Jour. Geol. Soc. India, 27, 102-109,1986.

Viladkar, S.G., The carbonatites of Amba Dongar, Gujarat, India, Bull. Geol. Soc. Finland, 53, 17-28, 1981.

Viladkar, S.G., Alkaline rocks associated with the carbonatites of Amba Dongar, Gujarat, India, Ind. Mineral., (Sukheswala Vol.), 130-135, 1984.

Viladkar, S.G. and P. Dulski, Rare earth element abundances in carbonatites, alkaline rocks and fenites of the Amba Dongar complex, Gujarat, India, Neus. Jahr. Min. Mont., H-1, 37-48, 1986.

Viladkar, S.G., and W. Wimmenauer, Geochemical and petrological studies on the Amba Dongar carbonatites (Gujarat, India), Chem. Erde., 52, 277-291, 1992.

Viladkar, S.G., Geology of the carbonatite-alkalic diatreme of Amba Dongar, Gujarat, a monograph published by GMDC, Ahmedabad, 1996.

Viladkar, S.V. and R. Upendran, Carbonatite alkali complex of Samalpatti, Dharmapuri Distt., Tamil Nadu, Jour. Geol. Soc. India, 19, 206-216, 1978.

Wada, H., and K. Suzuki, Carbon isotope thermometry calibrated by dolomite-calcite solvus temperatures, Geochim. Cosmochim. Acta, 47, 697-706, 1983.

Walker, K.R., and A. Mond, Mica Lamprophyre (alonite) from Radok Lake, Prince Charles Mountains, Antarctica, BMR Rec., 108, 1971.

Walters, L.J., G.E. Claypool, and P. Choquette, Reaction rates and ^{18}O variation for carbonate-phosphoric acid preparation method, Geochim. Cosmochim. Acta, 36, 129-140, 1972.

White, W.M., M.M. Cheatham, and R.A. Duncan, Isotope geochemistry of leg 115 basalts and inferences on the history of the Reunion mantle plume, Proc. Ocean. Drill. Prog., Sci. Res., 115, 53-61, 1990.

Wijbrans, J.R., Geochronology of metamorphic terrains by the $^{40}Ar/^{39}Ar$ age spectrum method. Unpub. Ph.D. Thesis, Australian National Univ., Canberra, 1985.

Wendlandt, R.F., and W.J. Harrison Rare earth element partitioning between immiscible carbonate and silicate liquids and CO_2 vapour: Results and implications for the formation of light rare earth enriched rock. Contrib. Mineral. Petrol., 29, 242-254, 1979.

Wooley, A.R., and D.R.C. Kempe, Carbonatites: nomenclature, average chemical compositions, and element distribution, In : Carbonatites: Genesis and Evolution (ed : K. Bell), 1-13, 1989.

Wooley, A.R., The spatial and temporal distribution of carbonatites, In: Carbonatites: Genesis and Evolution (ed: K. Bell), 15-37, 1989.

Wyllie, P.J., Discussion of recent papers on carbonated peridotite, bearing on the mantle metasomatism and magmatism, Earth Planet Sci. Lett., 82, 391-397, 1987.

Wyllie, P.J., Solidus curves, Mantle Plumes, and magma generation beneath Hawaii, Jour. Geophys. Res., 93, 4171-4181, 1988.

Wyllie, P.J., Origin of carbonatites: evidence from phase equilibrium studies, In: Carbonatites: Genesis and Evolution (ed: K.Bell), Unwin Hyman, 500-540, 1989.

Yaxley, G.M., and D.H. Green, Experimental demonstration of refractory carbonate-bearing eclogite and siliceous melt in subduction regime. Earth Planet. Sci. Lett., 128, 313-325, 1994.

York, D., Least square fitting of a straight line with correlated errors. Earth Planet Sci. Lett., 5, 320-324, 1969.